AL/CF-TR-1996-0026

ARMSTRONG LABORATORY

ADVANCED DEVELOPMENT OF NEW ACTUATORS FOR HUMAN SENSORY FEEDBACK

**Owen D. Brimhall, Jeffrey Brown, Allen P. Hilton, Kristofer J. James,
H. Roy Curtin, Charles R. Galway, Robert R. Goodwin**

TECHNICAL RESEARCH ASSOCIATES, INC.
2257 SOUTH 1100 EAST
SALT LAKE CITY, UT 84106-2379

OCTOBER 1995

FINAL REPORT FOR THE PERIOD JULY 1993 TO OCTOBER 1995

AIR FORCE MATERIEL COMMAND
WRIGHT-PATTERSON AIR FORCE BASE, OHIO 45433-6573

NOTICES

When US Government drawings, specifications, or other data are used for any purpose other than a definitely related Government procurement operation, the Government thereby incurs no responsibility nor any obligation whatsoever, and the fact that the Government may have formulated, furnished, or in any way supplied the said drawings, specifications, or other data, is not to be regarded by implication or otherwise, as in any manner, licensing the holder or any other person or corporation, or conveying any rights or permission to manufacture, use or sell any patented invention that may in any way be related thereto.

Please do not request copies of this report from the Armstrong Laboratory. Additional copies may be purchased from:

National Technical Information Service
5285 Port Royal Road
Springfield VA 22161

Federal Government agencies and their contractors registered with Defense Technical Information Center should direct requests for copies of this report to:

Defense Technical Information Center
8725 John J. Kingman Rd., STE 0944
Ft Belvoir VA 22060-6218

TECHNICAL REVIEW AND APPROVAL
AL/CF-TR-1996-0026

DISCLAIMER

This Technical Report is published as received and has not been edited by the technical editing staff of the Armstrong Laboratory.

This report has been reviewed by the Office of Public Affairs (PA) and is releasable to the National Technical Information Service (NTIS). At NTIS, it will be available to the general public, including foreign nations.

This technical report has been reviewed and is approved for publication.

FOR THE COMMANDER

Thomas J. Moore

THOMAS J. MOORE, Chief
Biodynamics and Biocommunications Division
Crew Systems Directorate
Armstrong Laboratory

DISCLAIMER NOTICE

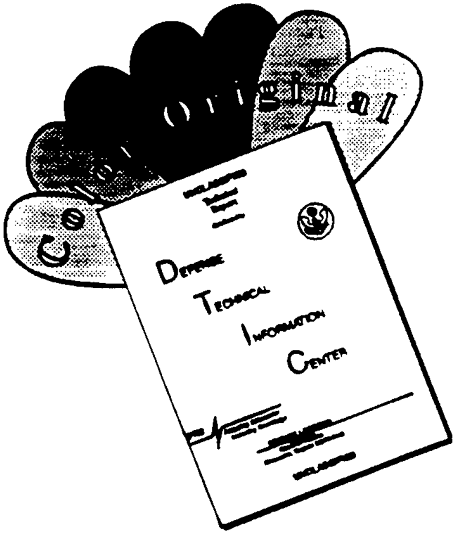

REPORT DOCUMENTATION PAGE

Form Approved
OMB No. 0704-0188

1. AGENCY USE ONLY *(Leave blank)*

2. REPORT DATE
October 1995

3. REPORT TYPE AND DATES COVERED
Final - July 1993 to October 1995

4. TITLE AND SUBTITLE
Advanced Development of New Actuators for Human Sensory Feedback

5. FUNDING NUMBERS
C - F41624-93-C-6016
PE - 65502F
PR - 3005
TA - CB
WU - 32

6. AUTHOR(S)
Owen D. Brimhall, Jeffrey Brown, Allen P. Hilton, Kristofer J. James, H. Roy Curtin, Charles R. Galway, Robert R. Goodwin

7. PERFORMING ORGANIZATION NAME(S) AND ADDRESS(ES)
Technical Research Associates, Inc.
2257 South 1100 East
Salt Lake City UT 84106-2379

8. PERFORMING ORGANIZATION REPORT NUMBER
TRABE950

9. SPONSORING/MONITORING AGENCY NAME(S) AND ADDRESS(ES)
Armstrong Laboratory, Crew Systems Directorate
Biodynamics and Biocommunications Division
Human Systems Center
Air Force Materiel Command
Wright-Patterson AFB OH 45433-7901

10. SPONSORING/MONITORING AGENCY REPORT NUMBER
AL/CF-TR-1996-0026

11. SUPPLEMENTARY NOTES

12a. DISTRIBUTION/AVAILABILITY STATEMENT
Approved for public release; distribution is unlimited

12b. DISTRIBUTION CODE

13. ABSTRACT *(Maximum 200 words)*

The objective of this SBIR Phase II project was to develop a small magnetostrictive actuator using Terfenol-D. The device was configured to be applicable to dexterous force feedback. Several device configurations were studied. The final Terfenol-D actuator was configured as an inchworm motor. The device can be adjusted to be fully back-drivable. The motor is small (approx. 3cc), light weight (16 grams), and provides forces (10N max) and velocities (14.5 cm/sec max) appropriate to the task of dexterous force feedback. The motor driven at 5 KHz could be used for both force and tactile feedback. The device was shown to be highly controllable by means of pulse-width modulation and current control methods. The device was demonstrated in several modes: constant force on a stationary object, arbitrary force output, constant force on an arbitrarily moving object and arbitrary velocity control. Exoskeleton issues were explored and the motors are integrated into a rudimentary three degree of freedom, force-feedback finger with adjustable virtual axis joints. Each joint has a magnetostrictive motor, angle sensor and load cell. Electronic boards are controlled by simple software to demonstrate the motors and the force-feedback exoskeletal finger.

14. SUBJECT TERMS
Terfenol-D
Magnetostrictive
Inchworm motors
Force feedback
Exoskeleton

15. NUMBER OF PAGES
288

16. PRICE CODE

17. SECURITY CLASSIFICATION OF REPORT	**18. SECURITY CLASSIFICATION OF THIS PAGE**	**19. SECURITY CLASSIFICATION OF ABSTRACT**	**20. LIMITATION OF ABSTRACT**
UNCLASSIFIED	UNCLASSIFIED	UNCLASSIFIED	UNLIMITED

This page intentionally left blank.

Acknowledgments

This research was performed under an SBIR Phase II contract sponsored by the Human Sensory Feedback team at the Armstrong Laboratory, Human Systems Center, Air Force Material Command, Wright-Patterson, Air Force Base. The authors thank Capt. Christopher J. Hasser for his interest and support as technical monitor.

In addition to those noted as authors the P.I. wishes to thank, Mike Peterson for assistance in device fabrication.

◆ Table of Contents ◆

LIST OF FIGURES

LIST OF FIGURES (cont.)

LIST OF FIGURES (cont.)

LIST OF FIGURES (cont.)

Advanced Development of New Actuators for Human Sensory Feedback

SBIR Phase II - Final Report

◆ ◆

◆ Introduction & Background ◆

The purpose of this Phase II SBIR contract was to develop new actuator mechanisms, utilizing a magnetostrictive material (Terfenol-D). The new actuators are applied to human sensory feedback in the form of dexterous exoskeletal control for telerobotics or virtual reality applications. While the new motor technology is still in its infancy we have demonstrated that the new motors can be made fast, strong, small and have a bandwidth high enough to model both force and tactile response with a single actuator within a reasonable human range.

Terfenol-D is a magnetostrictive material developed by scientists at the Naval Ordnance Laboratory, (now the Naval Surface Weapons Center), in Silver Spring, Maryland, and the Ames Laboratory, (located at Iowa State), of the U.S. Department of Energy. It is an alloy of terbium, dysprosium, and iron. The name "Terfenol-D" is representative of the composition of the material and the original name for the Navy laboratory where the work was begun. The breakdown is as follows[Butler]: *Ter* (terbium), *fe (*iron), *nol (*Naval Ordnance Laboratory), *D (*dysprosium). Magnetostrictive materials are materials which change shape when exposed to magnetic fields. Magnetostrictive materials have been available for over a century since their discovery by James Joule in 1842. They came into common use in the 1950's with the use of nickel-based alloys for ultrasonic applications. These alloys were limited to strains (change in length) on the order of 50 parts per million (ppm). The discovery of piezoceramics improved this with strains of approximately 250 ppm. Discovery of Terfenol-D, a relatively new magnetostrictive material, improved on the magnitude of the achievable strains by a factor of at least 40 times or an order of magnitude greater than piezoceramics such as lead titinate zirconate (LTZ). Thus Terfenol-D has also been referred to as a giant magnetostrictive material.

Actuators based on Terfenol-D have been shown to transmit large amounts of energy in a small volume and are highly efficient. The Terfenol-D actuators, compared to piezoceramics, can operate at low voltages and require relatively low intensity magnetic fields. The new alloy is being applied to many applications which have been previously accomplished by piezoceramics or traditional electric motors. The Terfenol-D material demonstrates a high Young's modulus and can withstand compressive stresses on the order of to 780 N/mm2. The material has a rapid response time. Devices have been demonstrated operational frequencies over 40 KHz. This is a great advantage over shape memory alloys such as Nitinol. The functional characteristics of the Terfenol-D magnetostrictive technology provides the basis for innovative new actuator designs of interest in this proposal. Other systems have benefited from the use of the Terfenol-D material and include active vibration suppression systems in industrial and in military and space environments. New actuators based on the new material have been proposed and are under investigation for many varied applications such as; servovalves, sonar, machine tool chucks, linear motors, rotary motors, hydraulic pistons, active vibration control, fuel injection, smart control surfaces and structures for spacecraft, aircraft and marine vehicles [Fanson,Wada,Takahara, Goodfriend].

Actuators made from Terfenol-D have been used for micro-actuators with high precision and micro displacements, and as acoustical drivers. Schemes using magnetostrictive materials as macro-actuators normally involve designs that rectify the tiny oscillatory motions of the material to produce large displacements. In general, magnetostrictive linear motors take the form of inchworm motors. In a simple form, an inchworm motor consists of three actuators, namely: two brake actuators and one push actuator. Linear motion is obtained by activating the three actuators in a phased cyclic manner.

The primary objective of this research was to develop an actuator that could be used as a small, linear motor in dexterous exoskeletal feedback. The motor concept in mind was an *inchworm* motor. An inchworm motor generally utilizes both active and passive actuation. One such configuration consists of two brakes and a mover. One brake locks the motor position onto a shaft and the mover then advances (stretches) the motor forward. While the motor is stretched forward, the other brake clamps down on the shaft and the first brake releases. The process is then repeated many times over. In this manner the motor will *inch* forward in a method somewhat similar to an inchworm in nature.

The integration of human control and robots has a number of demonstrated advantages. For example combining cognitive capabilities of the human with the strength and durability of robots facilitates remote operation in hazardous and lethal condition. Significant effort has been expended in developing robotic end effectors, sensors and exoskeleton to control the motions of the robotic arms and hands. Human size robotic hands have been developed which can effect fine manipulations. While advances are impressive much room for improvement is available. Concepts for force feedback are not new but the implementation of actual physical systems is definitely an area which needs continued development. For intuitive control and fine manipulation, high capability, small, light weight exoskeletons and or virtual objects with force feedback actuators are needed. The development of anthropomorphic dexterous force feedback systems has naturally lagged behind the development of anthropomorphic robotic hands. And both technologies need better actuators. In addition to the application for robotic control the explosion of virtual reality software has increased need for realistic force feedback. Demand for dexterous force feedback systems is no longer limited by the lack of a good slave robotic hand since many software applications are begging for a good anthropomorphic tactile and force feedback interfaces.

The quality of actuation systems has been recognized as the bottleneck of control in dexterous telemanipulation where force feedback is required [Burdea]. The three types of actuators typically used include pneumatic, electromagnetic and hydraulic. Each has its own set of merits and limitations. Pneumatic actuators can be compact and lightweight, but possess relatively low bandwidth properties, low actuation stiffness and low power production capabilities. Electromagnetic actuators, on the other hand, have good stiffness properties, and high bandwidth, but are relatively sizable and heavy. Hydraulic actuators have traditionally been considered the most appropriate, because their properties lie somewhere between the other two systems. If the size and weight limitations of electromagnetic actuators can be overcome, then their other properties will make them the obvious choice.

As telerobotic and virtual reality systems gain popularity in industrial and technical settings, the need for improvements in the science of haptic sensing has become increasingly important. Haptic science is composed of two parts: "tactile perception, or the awareness of stimulation at the skin, and kinesthesis, or the sense of joint positions, movements and torques"[Chang]. Important to this science is the need to improve on commercially available dexterous exoskeletons used to measure motions of the hand and reflect object shape, compliance, impact, contact, sliding, slipping, and kinematic constraints. This actuator will eventually be used to provide force feedback in dexterous exoskeletons for use in telerobotics and virtual reality systems.

Virtual reality is defined as a "computer generated immersive environment with which users have real-time, multisensorial interactions"[Burdea]. The participant enters the virtual world by donning special equipment which provides feedback between the two realities. This equipment often includes a visual element whose purpose is to provide the visual perception of the virtual world. Another key piece of hardware used is some type of glove or exoskeleton which measures the movements of the hand and uses this information to control a virtual hand in the virtual world. Since it is this virtual hand that is used to manipulate objects within the virtual world, the dexterous exoskeleton must be able to accurately reflect the virtual forces experienced by the virtual hand. "The key to virtual reality is its interactivity - it's not a place where you go and watch, it's a place where you go to do things" [Delaney]. As virtual reality moves from the games environment to a simulation environment where real objectives are accomplished, the devices used to reflect the virtual forces "must match as many of the kinesthetic ... capabilities of the human hand ... as [the available] technology will allow" [Chang]. The less the wearer of the glove/exoskeleton is physically burdened by the device, the more realistic the virtual experience will be. Bulky and heavy attachments to the hand detract from the experience and contribute to the fatigue felt by the operator over time. Advances are incremental as improvements are made through reductions in size and mass. As the hardware becomes smaller and lighter, the performance of the virtual reality system will improve.

For telerobotics, "future strategies for environmental clean-up and hazardous waste removal will rely primarily on remote manipulation and sensing"[Long]. The integration of human control and robots has demonstrated advantages by combining the cognitive capabilities of the human with the strength and durability of robots. With teleoperation, the human is given the ability to operate real time in lethal and hazardous environments. The operation of telerobotic systems is not unlike the operation of a virtual reality environment. The principal difference is that in virtual reality, the operator interacts with a virtual world, where in teleoperation, the operator is actually controlling a remote device such as a robotic manipulator. Like virtual reality, the teleoperation of multifingered robots also requires the use of a dexterous master or exoskeleton which is a multi-DOF controller and is worn on the operator's hand [Burdea]. As the operator moves his hand, the system monitors the changes in position and orientation and reflects these changes back to the robotic manipulator. Force and tactile information is then fed back into the exoskeletal hand. For reasons similar to those with virtual reality, improvements in the size and mass of the exoskeletal dexterous master would improve overall operator performance.

Force feedback is often separated from tactile feedback which involves the ability to create the sensation of touching textures or distinguishing surfaces. This is due to the fact that, other than the motor discussed in this project, no force actuators were available which provided high frequency tactile forces and bulk forces simultaneously. In a study intended to improve the design of space suit gloves, Chodack and Spampinato reported the results of their "peg-board dexterity test". When four (4) subjects wore gloves, the time it took for these subjects to insert the pegs increased by 80% when compared to using their bare hands. This is an indication of how important force and tactile feedback are to dexterous manipulation. In telerobotics or virtual manipulation, if the operator were able to feel the forces as if he/she were actually present performing the work, productivity would increase.

Why is a better motor or actuator needed? There are many exoskeletal hands now available that provide a type of force feedback to the operator. The technologies used are many and varied and include: pneumatic, hydraulic, cable driven, and electric solutions.

A good reviews of existing devices were prepared by KB Shimoga and Hasser. Shimoga analyzed and compared at least 14 different devices designed for use in the telemanipulation environment. He arrived at six conclusions. They are:

1. Of the fourteen designs discussed [in his review], only six are capable of providing some force feedback.
2. None of the existing hand masters that are capable of finger force feedback are truly isomorphic to the human hand.
3. A few hand masters are portable while most are bulky.
4. An ideal hand master must function well up to at least 10,000 Hz.
5. An ideal hand master should be able to sustain forces of 4-7 Newtons, and exert forces up to 30-50 Newtons for short periods of time.
6. The hand master should have at least ten times the force sensitivity than that of the human hand. Human fingers can sense force steps of about 0.5 Newtons.

Based on the review by Shimoga, the existing force feedback devices are not adequate to provide realistic force reflection. A new device is needed that is small and lightweight, has a high force density, and can operate anywhere from 0 Hz to 10 KHz.

In a small Phase I project to identify the feasibility of Terfenol-D based actuators and motors several first generation concepts were tested. By the end of the Phase I we had demonstrated several working joint brake mechanism for resistive feedback. Two selected brake mechanism were fitted to a simple exoskeletal feedback structure for demonstration purposes. In addition to the brake mechanisms a fully functioning Terfenol-D motor was fabricated and tested. The Terfenol-D inchworm motor had adjustment means on each of the brake and pusher elements. This allowed the motor to be configured from an "always locked" to a "fully back-drivable" configuration. In the fully locked configuration the motor was capable of forces in excess of 50 lbf. The motor was about the size of a cigarette pack. It was operated from 0 to 300 Hz. The Phase I motor was two large for the longer range goal of putting the actuator mechanism directly on the finger joints but went a long way in elucidating the problems that needed to be overcome in the development of the smaller, higher speed devices. From that point a more advanced development project was outlined and resulted in this Phase II project to help direct the technology toward the goal of a small high force, high speed Terfenol-D motor for dexterous exoskelatal feedback.

◆ Proposed Phase II Tasks ◆

The following are the technical objectives as outlined in the Phase II proposal:

- **Task 1. System Review**
- **Task 2. Resistive Actuator Development**
- **Task 3. Linear Motor Development**
- **Task 4. Application Simulation**
- **Task 5. Documentation**

Since the use of Terfenol-D in motors is a relatively new effort the developments in this project were of a necessity iterative. In this report we briefly report on the efforts undertaken under each of the five project task but do not attempt to describe all the iterations and small lessons learned in detail. Actual progress was achieved during the course of the project in an iteravet and parallel manner . This final report reviews the progress by the **task** (as noted above) with no particular effort to show chronology.

◆ Phase II Progress ◆

Progress - Task 1. System Review.

In this project the "system" includes the human hand, fingers, finger joints, brake actuators, pusher actuators, inchworm force actuators, angle sensing, force sensing, exoskeletal structure, electrical controllers, computer, software and ergonomic issues. Each of these elements also have subsystems such as solenoid coils, Terfenol-D, etc.,. Each of which had to be studied and developed in order to complete the overall goal. The nature or of the project and its funding limitations sculpted the effort and the overall scope. The state of the art for Terfenol-D motors and anthropomorphic dexterous force feedback both show great promise but the technologies are still in their infancy. Therefore a significant portion of the project involved the study of both telerobotic and magnetostrictive technologies in an effort to establish resonable goals and requirements for design purposes. The telerobotic review targeted operation requirements as it related to dexterous force feedback. In the review of Task 1 in the project we report the ergonomic, physiological issues and then will detail design solutions under review of Task 4.

Dexterous Biomechanical Requirements.

The project began by establishing requirements of the exoskeletal hand interface. The hand related parameters studied were:

- Size
- Axis of joint rotation
- Range of joint motion
- Finger forces

Hand Sizing

The following data are averages for adult finger bone lengths (Poznanski, 1984). The sizes have been input into a generalized computer model of the hand (Fig. 1 and Fig. 2) in order to study relationships between the joint centers of rotation, segment lengths and the exoskeleton framework.

SEGMENT	#	MALE mm/std dev	FEMALE mm/std dev
Distal	5	18.7/1.3	16.2/1.2
	4	20.5/1.2	18.0/1.3
	3	20.1/1.2	17.7/1.3
	2	18.8/1.4	16.6/1.3
	1	25.2/1.4	22.1/1.6
Middle	5	21.6/1.6	18.7/1.7

	4	29.6/1.6	26.4/1.7
	3	31.1/1.8	27.9/1.7
	2	26.1/1.6	23.2/1.6
Proximal	5	36.3/2.0	32.5/1.9
	4	45.5/2.3	40.8/2.4
	3	48.5/2.6	44.0/2.3
	2	43.7/2.2	40.0/2.3
	1	35.0/1.9	31.4/2.0
Metacarpal	5	58.0/3.0	51.9/3.6
	4	62.1/3.5	56.0/3.5
	3	69.0/3.8	62.6/4.0
	2	73.7/3.8	66.9/4.3
	1	49.6/2.9	44.2/2.6

These sizes represent a sample size of 78 adults of unknown ethnic background, as measured from radiologic studies. Some variability has been reported in the literature in conjunction with ethnicity, but will be ignored at this iteration.

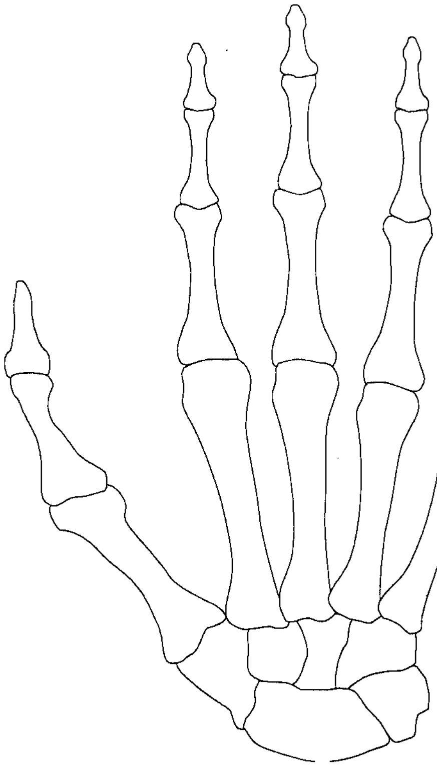

Figure 1.

Data regarding segment length variation, as well as center of rotation locations for the hand joints, have been shown to be linear with respect to hand size (Buchholz, 1992). The variability of the dimensions of the middle phalangeal segment is of particular importance to this study, since a fixed length rigid glove master may be sufficient to cover the majority of the population at that segment if the variance is small enough. The standard deviation of segment size at that level is between 1.6 mm and 1.8 mm for men and women.

Middle phalangeal segment length can be determined from hand size (Buchholz 1992):

Little finger (#5): 0.117 * hand length
Ring finger (#4): 0.165 * hand length
Middle finger (#3): 0.170 * hand length
Index finger (#2): 0.143 * hand length

Percentile hand sizes have been documented from 4000 male air force personnel (Hertzberg, 1959).

PERCENTILE	1	5	50	95	99
Hand Length (in)	6.7	6.9	7.5	8	8.3
Finger III dia (in)	0.77	0.79	0.85	0.93	0.96

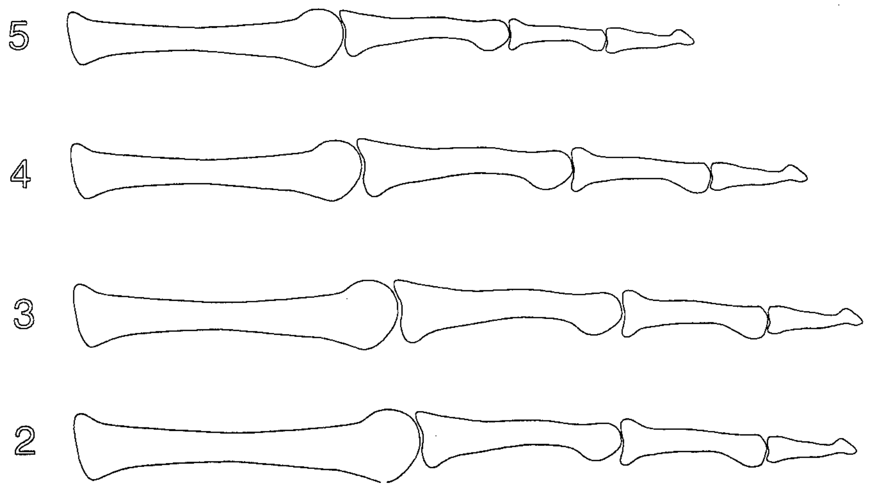

Figure 2.

In order to verify the fact that the model sizes derived from Poznanski are compatible with Air Force personnel, we can apply the linear model established by Buchholz to the percentile hand sizes from the Air Force study.

PERCENTILE	Hand Length (in) (Hertzberg)	Hand Length (mm) (converted from Hertzberg)	Digit II (index) mid phalange length (mm) HL*0.143 (Buchholz)	Segment Length (Poznanski)
1%	6.7	170	24.3	--
5%	6.9	175	25	--
50%	7.5	190	27.2	26.1
95%	8	203	29	--
99%	8.3	211	30.1	--

The segment length of the general male population, as measured by Poznanski, is approximately one millimeter shorter than that of the male Air Force Personnel when the model of Buchholz is applied to digit II. Results from other digit comparisons are similar. The approximation derived from Buchholz's model is relatively consistent (within 1 mm), and therefore both sets of data will be used in determining optimal hand sizes and variation in this study.

PHALANGE AXIS OF ROTATION

The axis of rotation of the phalangeal joints have been modeled as both fixed by some authors (Flatt et al. 1968, Youm 1978, Micks et al. 1978) and variable by others (Walker et al. 1975, Pagowski et al. 1977, Tamai et al. 1988). Where variability exist, they are small enough to ignore for many model applications (within 1.5 mm). In this application, it is not likely that glove stability and fit will hinder drift of an axis of rotation of that magnitude, and therefore a fixed axis model is adequate for these distal segments.

If the rigid mechanism is centered over the middle phalanges, then the variation over 90% of the population (+/- 2mm for digit II) will be distributed across two joints, and allow a fixed center of rotation to fall within a millimeter of its actual location. adjustability of this segment, therefore, would be on the order of one or two millimeters, and is not necessarily required. Variability of hand size is more a function of the proximal phalanges (+/- 4mm) as well as the metacarpals (+/- 7mm), and adjustability will be a key design feature at those locations. These two segments alone account for over 70% of hand size, and must be accommodated to achieve an accurate and effective fit. The remaining variation on hand size is accounted for by the distal phalanges, which will not need to be accounted for, providing an open-tip exoskeleton is designed.

The joint center can be estimated by a linear model, by multiplying the segment length by a constant, giving the joint center as a distance from the base of the bone.

JOINT CENTER CONSTANTS:

Digit	Joint 1*	Joint 2*	Joint 3*
I	--	0.832	0.85
II	0.9**	0.909	0.89
III	0.9**	0.91	0.89
IV	0.9**	0.91	0.9
V	0.9**	0.9	0.87
II-V	0.9**	0.91	0.89

* for digit I, joint 1 is CMC, joint 2 is MCP, and joint 3 is IP. For digits II-V, joint 1 is MCP, joint 2 is PIP, and joint 3 is DIP (Buchholz, 1992)

** (Youm et al. 1978)

MIDDLE PHALANGE EXOSKELETON

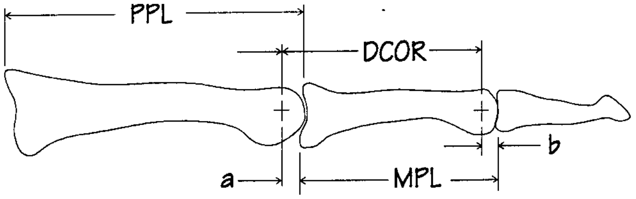

Figure 3.

A fixed length segment towards the distal end of the exoskeleton will accommodate both the PIP joint and the DIP joint. The length of this segment will be equal to the distance between the two centers of rotation. The centers of rotation can be found through a linear model (Buchholz, 1992) with the following results:

MALE:

Digit	MPL	PPL	PIPK	a	DIPK	b	DCOR
5	21.6	36.3	0.9	3.7	0.87	2.8	22.5
4	29.6	45.5	0.91	4.2	0.9	3.1	30.7
3	31.1	48.5	0.91	4.3	0.89	3.3	32.1
2	26.1	43.7	0.91	4	0.89	3	27.1

MPL = Middle Phalange Length

PPL = Proximal Phalange Length

PIPK = the PIP center of rotation constant (PIPK*PPL=PPL-a)

DIPK = the DIP center of rotation constant (DIPK*MPL=MPL-b)

DCOR = Distance between Centers of Rotation

FEMALE:

Digit	Mpl	Ppl	PIPK	a	DIPK	b	DCOR
5	18.7	32.5	0.9	3.3	0.87	2.4	19.6
4	26.4	40.8	0.91	3.8	0.9	2.8	27.4
3	27.9	44	0.91	3.9	0.89	3.0	28.8
2	23.2	40	0.91	3.6	0.89	2.6	24.2

Given the data on hand size and variability, it is conceivable to approach the design of the hand exoskeleton as adjustable at the proximal end (over the metacarpals and proximal phalange) and fixed-length at the distal end (over the middle and distal phalanges). The length of the fixed segment will correspond to DCOR.

RANGE OF MOTION

Although the ranges of motion of the joints in the hand are well documented, the question of functionality is usually left unaddressed. Information is available, however, which documents the actual range of the finger joints necessary to perform functional tasks (Hume, 1990).

ROM	Normal (deg)	Functional (deg)
Thumb MCP	56	22
Thumb IP	73	19
Finger MCP	100	62
Finger PIP	105	63
Finger DIP	85	39

The tasks requiring this functional range of motion were: Holding a telephone, holding a can, using a zipper, holding a toothbrush, turning a key, using a comb, printing with a pen, holding a fork, holding scissors, unscrewing a jar, and holding a hammer. These results imply that a full functional range of motion of the hand is possible without maximizing the range of motion of each segment.

Pinch forces have been extensively reported in the literature for the index finger and thumb pinch, reportedly the strongest of all the fingers. In a review of several studies, the range of male hand pinch is between 30 and 100 N, depending on the pinch geometry. The joint forces measured in the human hand are 4.1 to 8.8 times the pinch load, as a result of the configuration of the tendons and reaction surfaces (Weightman, 1982). It will not be necessary for the maximum values of force applied to the hand by the exoskeleton to exceed these values.

ACTUATOR SELECTION AND CONTROL:

Currently, there are two commercially available dexterous hand masters, neither of which provide a mechanism for force feedback. One system, the VPL DataGlove, is a compliant structure which uses optical sensors and fiber-optic cables to transduce finger angles, while the other system, the Exos, Inc. Dexterous Hand Master (DHM), relies on rigid, mechanical linkages to transduce finger joint position angles (Burdea 1, 1991). Exos does provide a force feedback hand master, but not one that includes position sensing of the finger digits. The DHM has a resolution and accuracy which is reportedly superior to that of the DataGlove (0.1 deg vs 0.5 deg), presumably as a result of the decreased compliance.

In an apparently objective review of the DataGlove for the purpose of semi-automated goniometric measurements for physical therapy applications, the accuracy and repeatability of the device was evaluated (Wise, 1990). In their study, the authors reported significant differences in repeatability between subjects, and attributed the differences to the fit of the glove on different subjects. The repeatability of measurements supplied by the manufacturer is +/- 5 degrees. Removing or keeping the glove on between measurements had little effect on the repeatability of the measurements, indicating the fact that any differences in fit of the glove are probably due to slipping and reorientation of the hand during the test, and not initial application of the glove itself. This is further substantiated by the fact that the gripping force had an effect on the transduced position of the joints as well, with angles varying by as much as 11 degrees with different force application at the same joint position. Additionally, it was found that wrist flexion and extension affected the measurements of the glove. The compliance offered by a flexible structure such as the DataGlove may provide significant advantages with regards to comfort and flexibility, but brings significant disadvantages as well, including the repeatability and accuracy of the transduced joint angles.

COMPLIANT	RIGID
Flexibility, various sizes	must be adjusted to fit
inaccurate force transmission	positive force transmission
lack of sensitivity	very sensitive
lack of resolution	high resolution
must be calibrated to user fit	possibility of no calibration
lightweight	lightweight given certain materials

The drawback of a rigid structure is the lack of adaptability to the various sizes of hands which will encounter it. A review of anthropometric hand sizes has shown that hand size variability is mostly accounted for at the proximal segments, where adjustability will be mandatory. It is conceivable that a *fixed length distal segment* interface may be able to accommodate 95% of the population without compromising the accuracy of the position transduction.

Another area of interest related to Force feedback is that of tactile feedback. It is the opionion of the author that the ideal force actuator would also becapable of providing the frequency response for both tactile and force feedback. The human is capable of discriminating vibrations up to about 300 Hz. And of sensing vibrations up to approximately 10KHz. There are no gear motors appriately scaled to the dexterous feedback which can provide 300 Hz vibrations. The inchworm motor developed in this project does have that capbility. Thus is could become important to provice means of measuring joint angle from 0 to 300 Hz at very small amplitudes.

Finger Forces

There continues to be some discussion among researchers as to what Force values should be used as design criteria for dexterous force feedback. The measurement of maximum joint forces has been conducted and is reported in the range of 40 N (9 lb) for the index and middle fingers. It is generally agreed that for most applications a force less than the maximum would be desirable to avoid possible damage to the joints and to reduce motor requirments. Recent review of the PHANToM by Hasser illicited favorable results with forces substainially (20%) lower than the maximums. Hasser has also begun an interesting comparison of actuator technologies by studing not only the force but the power (joint torque x joint velocity) required by the joints and the candidate actuators. His estimates show a requirment ranging from 1 watt at the lower end up to 21 watts for the maximum.

Task 2. Resistive Actuator Development

To accomplish the goal of force feedback, both active and resistive actuation are desirable. An example of an active actuator is one that actively drives a joint, and a resistive actuator is something that simply resists joint movement. The main objective of this project is to develop a device that utilizes Terfenol-D and that could be used as both an active and resistive force actuator. During the preceding Phase I project we had evaluated the concepts of resistive force feedback (brake only) as an independent concept from active (motor driven) feedback. In Phase II we began by joining these two concepts. A three element inchworm motor consists of two brakes and a pusher element. During this project to develop actuators applicable to telerobotic manipulation we broke the study down into the study of resistive elements (brakes) and active elements (moving shaft). In this case the brake is to activated by using the induced strain in Terfenol-D as the brake piston.

Terfenol-D is a magnetostrictive material. As the magnetic field increases, the induced strain in Terfenol-D increases up to a certain field strength. At that point, the Terfenol-D is saturated and any increase in magnetic field will not improve the strain. Apparent in Figure 4 is the effect of a prestress or preload on Terfenol-D. A higher strain is achieved when a preload is placed on the Terfenol-D rod. "These compressive loads serve to orient the magnetization perpendicular to the rod axis in zero field in order to achieve a full 90° rotation of the magnetization with fields applied along the rod axis" [Clark].

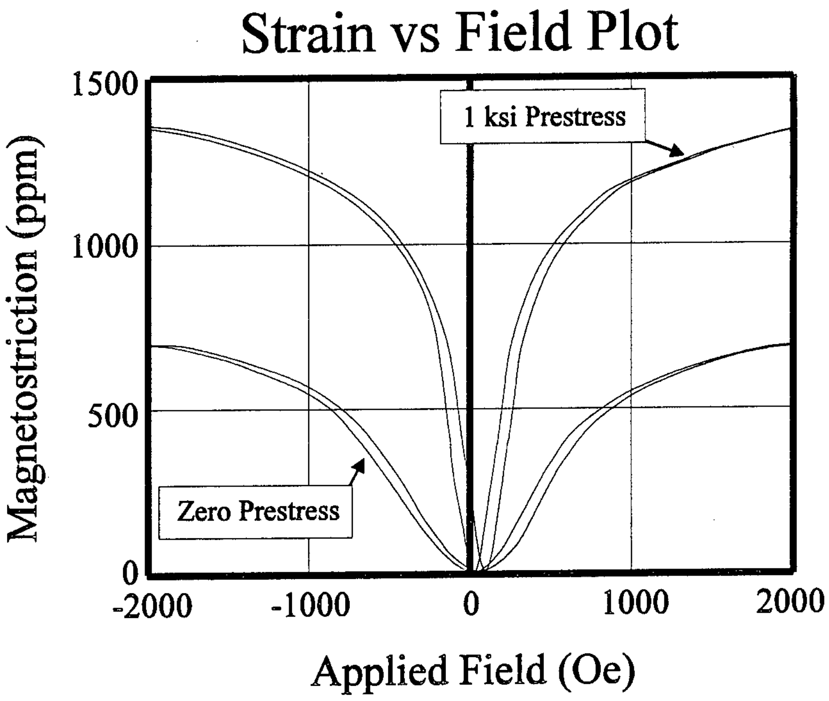

Figure 4.

Aside from its high strain, Terfenol-D lends itself quite well to use in linear actuators because of it mechanical properties. The following table lists some of the properties of Terfenol-D as established by ETREMA Products, Inc.

Properties of ETREMA Terfenol-D [Butler].

Property	Value
Bulk Modulus	9×10^{10} N/m^2
Tensile Strength	28 MPa
Compressive Strength	700 MPa
Magnetostriction	1500 - 2000 ppm
Energy Density	$14 \times 10^3 - 25 \times 10^3$ J/m^3
Curie Temperature	380°C
Magnetization	1.0 T

Brake Element Design Constraints:

There are specific design constraints inherent with both Terfenol-D and dexterous hand exoskeletons. Some of these constraints are as follows:

1. Size constraints of a hand exoskeleton.
2. Limited displacement of Terfenol-D rods.
3. Required preload for optimal Terfenol-D performance.
4. Provisions for magnetic return path.
5. Desired frequency response to match finger/hand velocities.
6. A flexure design that limited localized stress concentrations in Terfenol-D rod.
7. Infinite fatigue life.

1. Size constraints of a hand exoskeleton (i.e. a motor mounted on a joint).

The ideal exoskeleton would be a device where the motors that are controlling joint motion are located at the joints that they actuate. When motors are located away from the joint that they actuate, energy and precision losses due to friction and slack are introduced into the system. Frequency responses would also be limited with the addition of mechanical linkages. The ideal motor, then, would be small enough to be mounted effectively on a finger joint, yet have sufficient power to provide the necessary actuation.

2. Limited displacement of Terfenol-D rods.

Terfenol-D is magnetostrictive and undergoes a strain when exposed to a magnetic field. The relationship is:

Strain = (d constant)[(magnetic field)(1000)/(4)] [Butler]

As a example, a Terfenol-D rod that is 0.5 inches (1.27 cm) long and 0.1 inches (0.254 cm) in diameter, in a 1000 Oe magnetic field would undergo a strain of 1.60×10^{-3} ppm along it's axis.

Strain (S) = $(2.0106 \times 10^{-8})[(1000)(1000)/(4)] = 1.60 \times 10^{-3}$ ppm
This strain equates to a change in rod length of:
Delta Length = (Initial Length of Terfenol-D rod)(S)
Delta Length = (0.500 inches)(1.60×10^{-3}) = 0.0008 inches (0.002 cm)

3. Required preload for optimal Terfenol-D performance.

It has been shown that Terfenol-D's performance improves when an initial preloading or prestress is applied to the rod. When a preload (prestress) is applied, the Terfenol-D rod displays a much larger strain for a given magnetic field. In Figure 4, the strain at no preload and at a 1000 psi (6.895 MPa) preload is shown. It can be seen that with the added prestress, the strain for a given magnetic field is significantly larger than without the prestress.

"Magnetostriction is a result of the rotation of small magnetic domains which causes internal strains in the material. The strains result in a positive expansion of Terfenol-D in the direction of a magnetic field. As the field is increased, more domains rotate and become aligned until finally saturation is achieved, where nearly all domains are aligned in the direction of the field" [Butler]. A compressive load, or prestress, serves to "... orient the magnetization perpendicular to the rod axis in zero field in order to achieve a full 90° rotation of the magnetization with fields applied along the rod axis" [Clark]. In simpler terms, the magnetic domains are initially not all oriented perpendicular to the rod, but at some angle ϕ. The compressive load compresses the material and orients the magnetic domains perpendicular to the rod axis. This allows the magnetic domains to rotate over the full 90°, instead of $(90° - \phi)$, which produces a greater change in length (strain).

4. Magnetic Circuit.

The magnetic circuit was studied to enhance efficiency. Basically the most efficient magnetic solenoid circuit is achieved by trapping the magnetic flux lines in a permeable circuit and eliminating permeability through free space. For this purpose a small end cap is placed on the ends of the Terfenol-D and coil. Experiments to confirm effectiveness of the design are illustrated in the photographs.

5. Desired frequency response due to speeds of human hand.

To obtain the linear motor velocities that are needed to provide both active and resistive actuation of the human hand, the actuator must operate within the range of 5 Hz to 10 KHz. Shimoga suggested that the slave fingertip forces be presented to the human hand by the master device at 20 - 30 Hz. He also suggested that "... chattering could only be felt if signals are presented to the hand within the range of 300 - 400 Hz, while the corresponding bandwidth for fine vibrations is 5,000 - 10,000 Hz. The ideal hand master must be able to use all these bandwidths in accordance with the situation."

6. Preload string (flexure) designed such that undue local stress are not introduced to the Terfenol-D rod.

Another requirement in this design is that of maintaining the flexure surface parallel to the Terfenol-D rod. If the middle section of the flexure is distorted by the movement of the Terfenol-D rod, local high stress regions are introduced that could lead to metal fatigue and failure. This concept is illustrated in Figure 6. Here a Finite Element Model (FEA) of a flexure is being displaced by a rod and the mating surfaces are not parallel. This condition produces local high stress concentrations that could fracture the brittle Terfenol-D material.

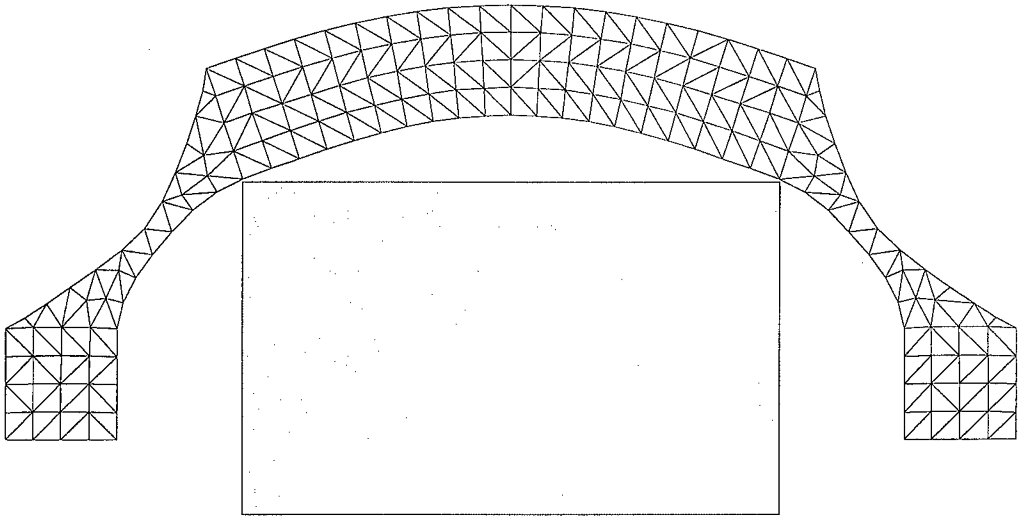

Figure 6: Finite Element Demonstration of Non-Parallel Surfaces

7. Designed for Infinite Fatigue Life.

One other important design consideration is that of designing for infinite fatigue life. The material selection and mechanical design must be such that allows for an infinite number of cycles without a fatigue failure. "Fatigue failures result from repeated plastic deformation. An example of this is the breaking of a wire by bending it back and forth. Fatigue failures typically occur after thousands or millions of cycles of minute yielding. It can occur at stress levels far below the conventionally determined yield point or elastic limit. The endurance limit of a material is defined as the highest level of alternating stress that can be withstood indefinitely without failure"[Juvinall]. S_n is the symbol used to designate endurance limit. A S-N curve, (stress - number life cycles), for steel can easily be approximated with a knowledge of the ultimate tensile strength. From this curve, the endurance limit can be obtained. The relationship is

$$S_n = 0.5S_u$$

where

S_n = endurance limit
S_u = ultimate tensile strength

Figure 7 illustrates an example of a generic endurance limit curve for steels. Any stress level below the endurance limit of $0.5S_u$ can theoretically cycle indefinitely without a fatigue related failure.

The stress component (value) to be considered in this analysis is the Von Mises stress. Von Mises stresses are related to the Maximum Distortion Energy Theory. This theory states that "... any elastically stressed material undergoes a slight change in shape and/or volume. The energy required to produce this change is stored in the material as elastic energy. It was recognized early on that engineering materials could withstand enormous hydrostatic pressures (i.e. $\sigma_1 = \sigma_2 = \sigma_3$ = large compression) without damage. It was therefore postulated that a given material has a finite capacity to absorb energy of distortion (i.e. energy tending to change shape but not size), and that attempts to subject the material to greater amounts of distortion energy result in yielding [Juvinall].

When using this failure theory, it is convenient to work with an equivalent stress or a Von Mises stress. This stress is defined as the value of uniaxial tensile stress that would produce the same level of distortion energy as the actual stresses involved. The equation for this Von Mises stress is as follows:

$$\sigma_{vm} = \sqrt{\sigma_1^2 + \sigma_2^2 + \sigma_3^2 - \sigma_1\sigma_2 - \sigma_2\sigma_3 - \sigma_3\sigma_1}$$

where $\sigma_1 > \sigma_2 > \sigma_3$

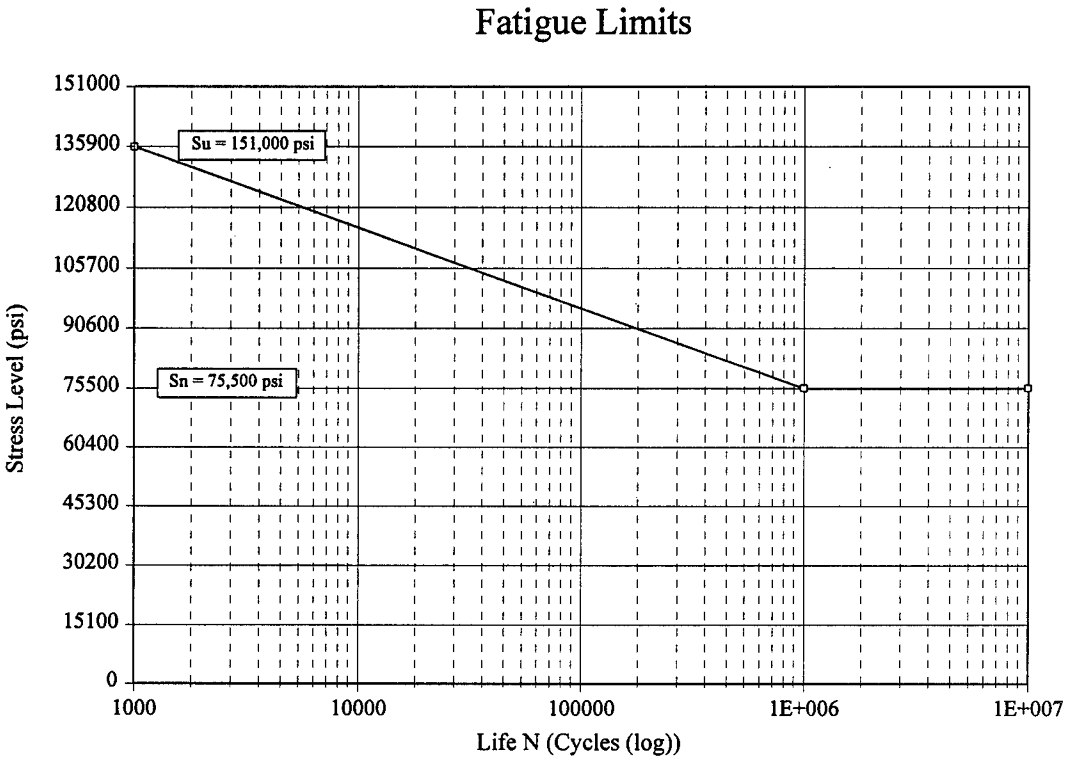

Note: Su = Ultimate Strength & Sn = Endurance Limit

Figure 7: Typical Endurance Limit Curve For Steel

Magnetic Coil Design Criteria

To maximize the performance of the Terfenol-D rods, the magnetic coil design needs to be optimized for size, current and voltage, and several potential failure related challenges need to be resolved. The basic objectives of the coil design are:

1. To achieve a 1000 Oe field through the Terfenol-D rod.
2. Have the coil geometry compatible with the actuator housing geometry.
3. Have the current and voltage requirements within an acceptable range (based primarily on available equipment to drive the coils).
4. Provide protection to the coil to prevent failures.

- thermal
- mechanical
- electrical

As can be seen in the Strain vs. Magnetic Field Plot in Figure 1.1, 90+ percent of the strain is achieved when the magnetic field is 1000 Oe. Above 1000 Oe, little improvement in strain is achieved. Additionally, stronger magnetic fields require more current through the coil which produces more heat.

The coil geometry must be such that it optimizes the available space in the actuator housing, yet can still be inserted and removed without damaging the windings.

The current and voltage required to drive the coil are dependent on the resistance of the coil, which is largely determined by the wire gauge used. The goal is to have a current less than 5 amps, and a voltage less than 10 volts.

Large amounts of heat will be generated because of inefficiencies in the coil and the Terfenol-D material. As the coil and Terfenol-D heat up, several things could happen. First and most likely is that the coil will burn up and no longer provide the needed magnetic field. Secondly, the magnetostrictive effect of the Terfenol-D rod falls off linearly as the temperature approaches the Curie point[4] which is approximately 715°F or 380°C [Goodfriend]. As the temperature of the rod approaches the Curie temperature, the efficiency of the rod drops off until it is no longer useful.

Mechanical failure could result if there is relative motion between the Terfenol-D rod and the magnetic coil. In order to miniaturize the actuator, the device must be extremely small with close tolerances. As the rod moves up and down at 5 KHz to 10 KHz, friction can wear the insulation off the coil and cause an electrical short. Early devices failed in this mode. The coil and Terfenol-D were insulated using a Teflon barrier both insulate and mechanically isolate the two components to ensure that the wearing is minimal and that no electrical shorts occur.

The design goal for this task was to develop a modular brake actuator that could also be used as the prime mover in a small, linear motor. The final motor concept in mind was an *inchworm* motor. One such configuration consists of two brakes and a mover. One brake locks the motor position onto a drive shaft and the mover then advances (stretches) the motor forward. While the motor is stretched forward, the other brake clamps down on the shaft and the first brake releases. The process is then again repeated many times over. In this manner the motor will *inch* forward in a method somewhat similar to an inchworm in nature.

As the movers in a small motor, this actuator must convert the electrical energy of the coil into a small motion, or change in length of a rod in this case. The motions that will be present are on the order of 0.001 - 0.002 cm (0.0004 - 0.0008 inches). These tiny motions require a device with extremely tight tolerances and an exceptionally efficient mechanical transfer of motion between components.

It was determined that the brake actuator would be based on a flexure configuration. As the Terfenol-D expands, the supporting mechanical structure (housing) must expand with it and then contract back with it as it contracts. This would be necessary to provide a good frequency response and preload. Other actuators that have been developed using Terfenol-D, used springs and plates to provide the preload and stiffness needed to reset the mechanical structure. These devices are relatively large and bulky and have a frequency response that is not suitable for operation on a finger or hand. They also would be prone to inefficiencies due to slack in the system and low energy transfers from mating parts.

A properly designed flexure would be constructed out of one continuous piece of metal and would not have slack, looseness, or low mechanical energy transfer. It would have the spring built into the housing which would allow better control of stiffness and ultimately frequency response. It would also provide the necessary preload to the Terfenol-D rod.

The design of the brake module, dubbed "motive cell", was broken into three (3) basic components: The flexure, the housing (housing, end cap, and magnetic return path) and the coil.

Flexure

The flexure design was initiated with a simple, 2-D (2 dimensional) baseline design. This design can be seen in Figure 8. What followed next was an iterative process of modification and analysis.

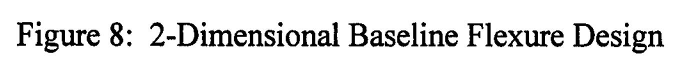

Figure 8: 2-Dimensional Baseline Flexure Design

COSMOS/M Explorer, a Finite Element Analysis (FEA) software package that was used for theoretical determination of stresses, strains, and resonant vibrations modes. The performance criteria used in this iterative design sequence were:

- To maintain the stress levels within a specified safety margin to ensure an infinite fatigue life.
- To create a motion that was stable and maintained a surface parallel to the Terfenol-D rod so as not to create undo stress concentrations. What was desired was essentially a button of metal that moved up and down with the expanding and contracting Terfenol-D rod.
- The flexure is designed to have a vibrational response up to 10 KHz to achieve the desired motor velocity. The following flow chart illustrates the sequence followed in this iterative design process.

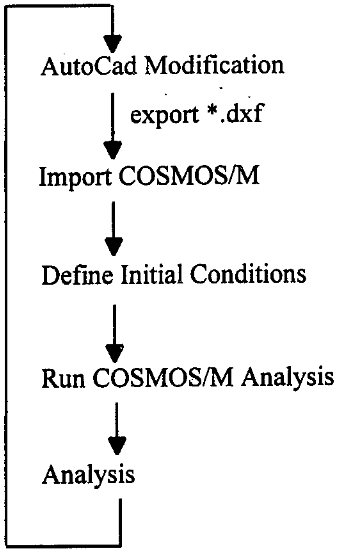

Figure 9: Analysis Flowchart

The following documents the process used in the development of the flexure.

1. AutoCad Modifications

The initial flexure design and each subsequent modification was made using AutoCad. The 2-D designs were then exported as *.dxf files.

2. Import into COSMOS/M
The *.dxf file was imported into COSMOS/M.

3. Define Initial Conditions

The initial conditions had to be defined with each revision. These initial conditions are:
Material Properties: Alloy Steel 4340 with elastic modulus (E) = 30,000,000 psi; ultimate strength (S_u) = 151,000 psi; yield strength (S_y) = 132,000 psi; and Poisson's ratio (ν) = 0.28.
Loading Conditions: Each flexure was loaded with a 1000 psi load and a 2000 psi load.
Boundary Constraints: The ends (outside edges) of the flexure, where the housing would attach, were constrained to not move. The flexure itself was allowed to move in all directions.
Element Type: 4 node tetrahedron

4. Perform COSMOS/M Analysis

Both the stress/strain and the frequency analysis were performed. The conditions that were looked for are:

- Stress within acceptable limits. (for infinite fatigue life)
- Strains within acceptable limits.
- Frequency of first and second harmonic.
- Was a surface maintained parallel to the Terfenol-D rod?

After many iterations, an acceptable 2-D design was obtained. This design can be seen in Figure 10. (Show both undeformed and deformed modes) This design was then modeled in three (3) dimensions to confirm the validity of the 2-D design, and to determine how to deal with hoop stresses in the flexure.

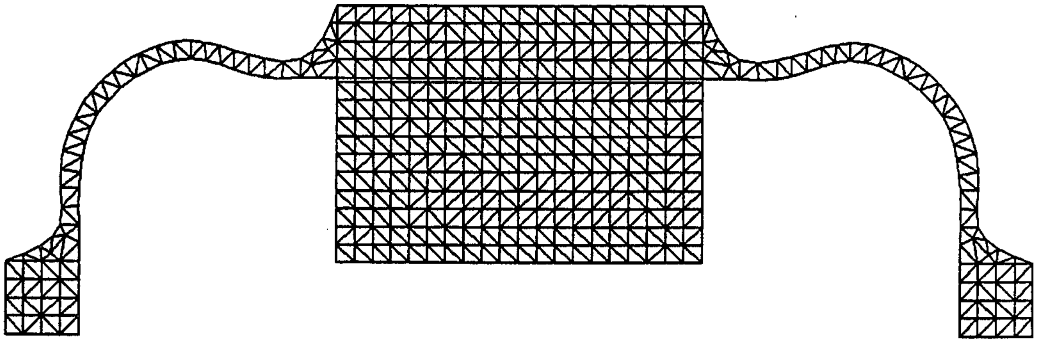

Figure 10: Final 2-D Flexure Model

Hoop stresses were a particular problem with this design. This was because of the motion of the flexure. As the flexure moved up, extreme stresses developed along the "S" portion of the flexure. To resolve this problem, slots were designed into the flexure that radiated out from the center disk every 35° and were 10° wide. This alleviated the severity of the hoop stress problem. A sketch of the final 3-D design with the slots can be seen in Figure 11.

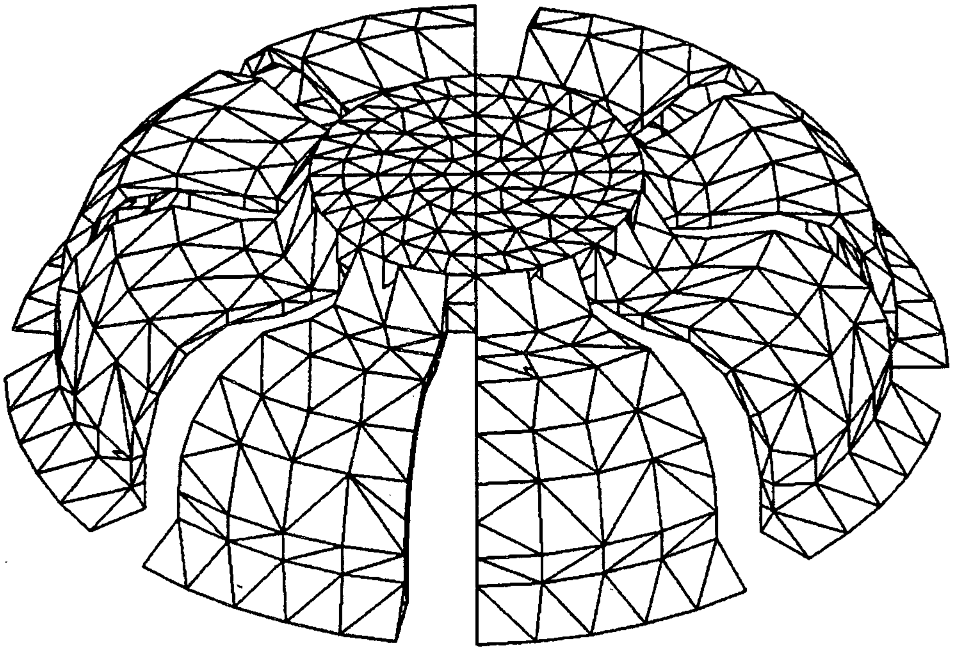

Figure 11: Final 3-D Flexure Model

The results from the final 3-D flexure FE analysis are as follows:

	Loading 1	Loading 2
Maximum stress (Von Mises) =	17,350 psi	34,701 psi
Maximum strain =	0.0002 inch	0.0004 inch

Analysis of Final Three Dimensional Design

As stated earlier, the Von Mises stress is an equivalent tensile stress for the material. A stress - strain curve for alloy steel 4340 is illustrated in Figure 12. It should be noted that the Von Mises stress levels for both loading conditions are well below the yield stress of the material. This indicates a safety factor of at least 2 for these conditions.

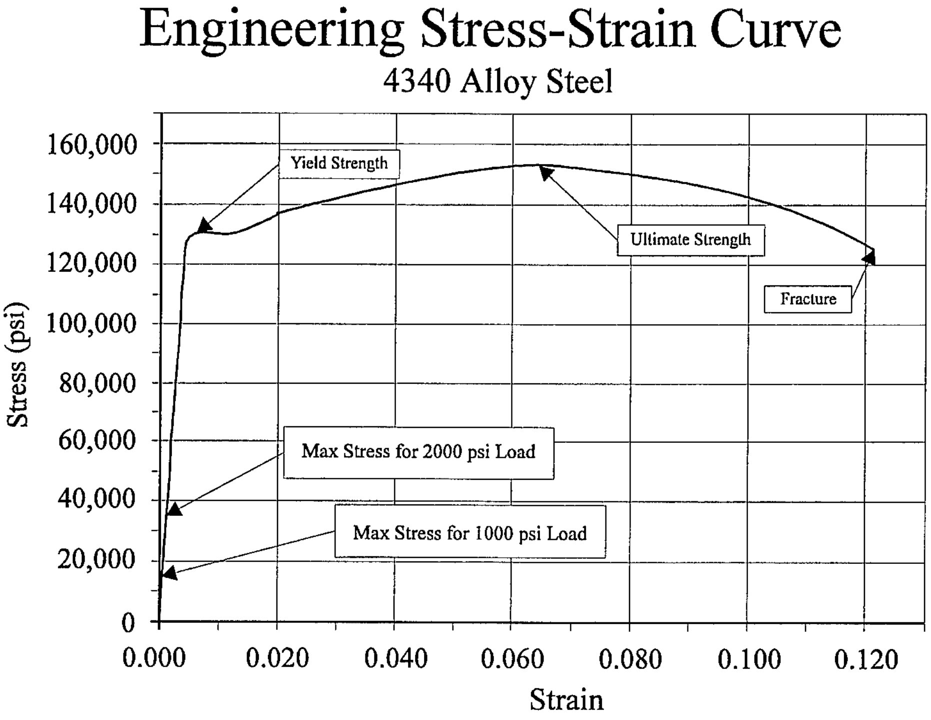

Figure 12: Stress-Strain Diagram for Alloy Steel 4340.

Figures 13 and 14 are the COSMOS/M results on screen. Figure 13 is a front view of the flexure displaying the Von Mises stress levels. Figure 14 is the back side displaying the same. It can be seen that there are specific regions of high stress. This is the region where the hoop stresses are still present, but are within acceptable ranges.

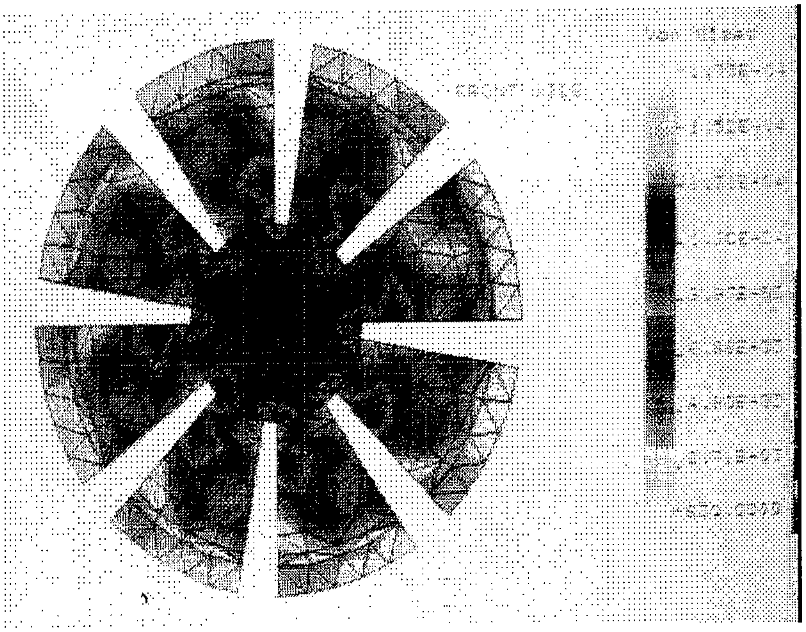

Figure 13: Front View of Flexure Displaying Von Mises Stress Levels.

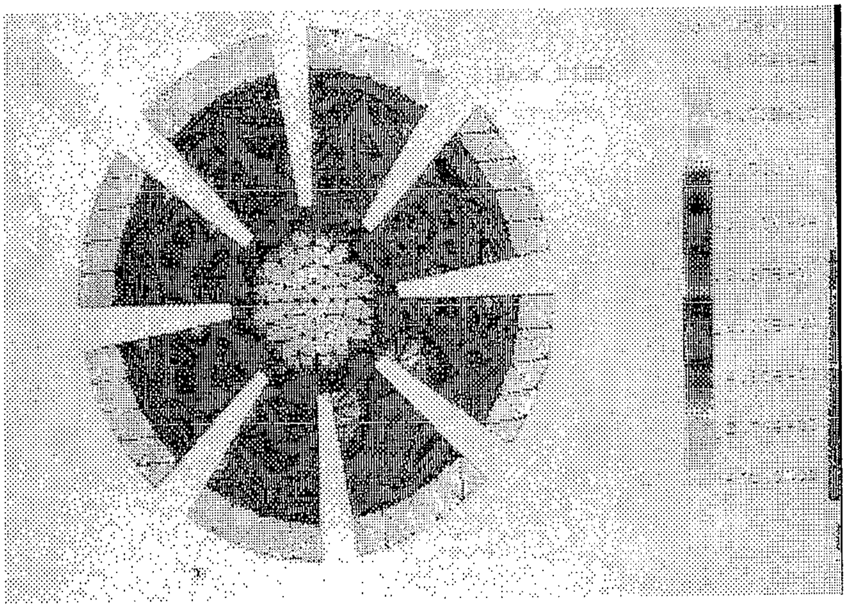

Figure 14: Back View of Flexure Displaying Von Mises Stress Levels.

Fatigue - Endurance Limit

The endurance limit of a material is defined as the highest level of alternating stress that can be withstood indefinitely without failure. For this material, the endurance limit (Sn) = 75,500 psi. This means that any stress condition below this level can theoretically cycle indefinitely without a fatigue related failure. This can be seen clearly in Figure 15, an endurance limit plot for alloy steel 4340.

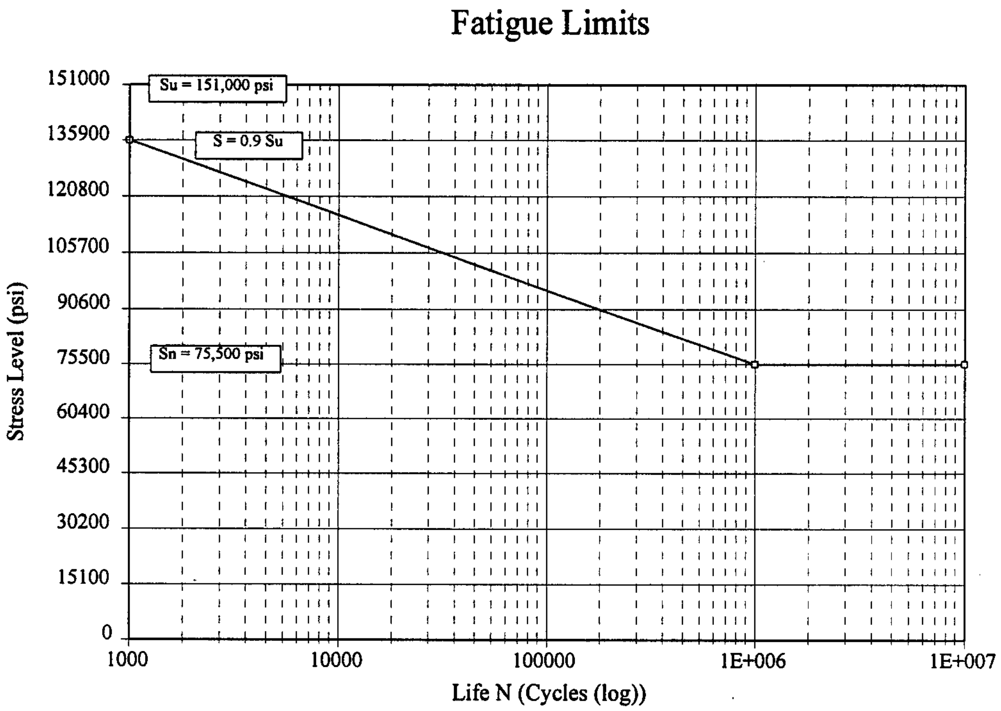

Note: Su = Ultimate Strength & Sn = Endurance Limit

Figure 15: Endurance Limit Plot for Alloy Steel 4340.

The flexure continued to be improved over the course of the project. The final flexure used in the motor had significantly reduced hoop stress due to the use of more radial slices.

Motive Cell Housing and Accessories

The housing for the motive cell plays an important role in the functionality of the device. It has to:

Provide an external housing to the Terfenol-D rod and the coil.
Provide a magnetic return path which encourages the flux lines back through the Terfenol-D.
Provide a preload to the Terfenol-D rod (in conjunction with the flexure).
Provide a means of securing the device to the structure upon which it will act.

A wall thickness of 0.030 inches for the external housing was chosen and tested using COSMOS/M. It was found to be adequate in that it did not deform significantly under the loading conditions. The wall thickness also provided adequate space for threading the diameter.

Several sizes were studied as we developed the final concepts. It was decided that two different size actuators would be developed for the final inchworm device. The only difference would be the length of the Terfenol-D rod. The two sizes chosen are:

1. A Terfenol-D rod that is 0.25 inches long and 0.10 inches in diameter.

2. A Terfenol-D rod that is 0.50 inches long and 0.10 inches in diameter.

The expected displacement of a Terfenol-D rod is proportional to the length of the rod. Therefore, a rod that is twice as long, with the same diameter, will produce twice the displacement.

Magnetic Return Path:

In order to insure that the electromagnetic coupling is not to lossy features had to be built into the device which forced these flux lines back through a more efficient circuit. On the end of the housing opposite the flexure, a threaded end cap was placed. This end cap screwed into the housing and would provide the magnetic return path on this end of the rod. It would also provide a means of adjusting the compressive preload on the Terfenol-D rod.

At the flexure end of the Terfenol-D rod, the flexure itself would act somewhat as a magnetic return path, but the cross-sectional surface area of the flexure was so small that it was not sufficient. Another piece of metal was added between the flexure and the Terfenol-D rod to provide the definitive magnetic return path. It would also act as a buffer/bearing between the brittle Terfenol-D rod and the flexing flexure.

Coil Design

The coil plays an important role in the function of this actuator because it provides the magnetic energy needed to induce the strain on the Terfenol-D rod. Even though the main criteria for the coil is that it needs to generate a 1000 Oe field through the Terfenol-D rod, there were several other challenges that presented more of a problem. Some of them are:

A coil winding apparatus must be developed for custom windings.
The coil geometry must be compatible with the motive cell;
The current and voltage requirements must be at reasonable levels;
The coil must be protected against thermal, mechanical and electrical failures.

Programs were written in software to help automate iterative calculation for coil configurations. The software is included in an appendix.

Coil Winding:

In early prototype actuators, the coils were wound around a small nylon spool that was machined on the lathe. A representation of this method can be seen in Figure 16. These prototypes, however, were considerably larger and were not optimized for size. The challenge here was to develop a method of winding extremely small coils that could be slipped on and off of a Terfenol-D rod, yet take up the least amount of space as possible. This meant that the coils had to maintain their physical integrity without a supporting structure like a nylon spool.

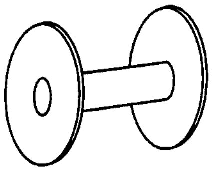

Figure 16: Nylon Spool Upon Which Coils Were Wound

Bondable Wire:

A solution to part of this problem was found in a bondable wire manufactured by MWS Wire (Westlake Village, CA). This bondable wire is copper magnet wire that is film coated with an insulation and has an additional coating of a thermoplastic adhesive. The thermoplastic adhesive is activated by either using a specific solvent, or by heating the wire beyond a specific temperature. This heat bonding can be accomplished by passing a current through the winding to achieve the desired bonding temperature. The specific insulation used was a polyurethane-nylon that has a temperature rating of 130°C. The bondable overcoat used was a polyvinyl butryal that has a heat activation temperature of 120°C. The maximum continuous operating temperature of the wire is 105°C.

By using this bondable wire, small coils were wound that did not require a special spool and could be slipped on and off the Terfenol-D rods.

Coil Winder:

To wind the coils, a small mandrel was machined that held the dimensions of the coil until the wire could be heat bonded. This mandrel was placed in a chuck which was driven by a variable speed DC motor. A counter was attached to the chuck to digitally count revolutions or coil windings. Bonding was accomplished by passing approximately 1 amp of current through the coil.

Visualization:

With the smaller coils, often it was difficult to visualize the winding process because of the size. A video camera with a macro zoom lens was placed above the coil being wound and the image displayed on a 25 inch screen television. This allowed the individual winding the coil to see close up what was happening.

Coil Geometry Compatible with Actuator Housing:

The coil should have to be as large as it possibly can, yet still slip in and out of the actuator housing. The inside diameter of the housing in 0.25 inches and the outside diameter of the Terfenol-D rod is 0.1 inches. Therefore, the coil outside diameter should be around 0.240 inches, and the coil inside diameter should be around 0.10 inches.

Current and Voltage Levels:

Wire Gauge Optimization

The next major challenge was choosing the optimum wire gauge for the coil. The desired magnetic field was 1000 Oe, and voltage, current, and resistance values had to be maintained within a manageable range.

An iterative software process was followed to determine which wire gauge size was optimum to meet the design objectives. Using the Terfenol-D rod that was 1.27 cm (1/2 inch) long and 0.254 cm (1/10 inch) in diameter as an example, a sample calculation follows. The maximum outer diameter of the coil was determined by the inside diameter of the motive cell, which was 0.635 cm (0.25 inch). This data limited the physical size of the coil. The desired magnetic field was 1000 Oe, which constrained the current and voltage inputs. Three (3) different wire gauge sizes were evaluated.

To determine the voltage and current inputs required to achieve a 1000 Oe field and calculate the expected response from the Terfenol-D rod.

Constraints:
Wire gauge = 30
Wire diameter = 0.011 inch
Coil length = 0.500 inch
Coil OD = 0.240 inch
Coil ID = 0.100 inch
Wire resistance = 0.1032 ohms/ft
Desired magnetic field = 1000 Oe

Number of Wire Turns: The first calculation made was to determine how many turns could fit within the geometrically constrained space of the actuator.

Terms Definition:

OD = outside diameter
ID = inside diameter
n_{len} = number of wire diameters that would fit in coil length
n_{dia} = number of wire diameters that would fit in coil diameter

n_{turns} = number of wire turns in coil
n = turns density (turns/length)
Res_{coil} = resistance of coil
S = strain
mag field = magnetic field
δ = change in rod length
L_{rod} = length of rod
ppm = parts per million = a change in length of 50 μ inch / 1 inch of material length[5]

The number of wire diameters that would fit along length of rod:

$n_{len} = (\text{length rod})/(OD_{wire})$
$n_{len} = (0.5\text{ inch})/(0.011\text{inch}) = 45.45 = 45$

The number of wire diameters that would fit between OD of the rod and OD of coil:
The number of wire turns in the coil:

$n_{dia} = ((OD_{coil} - (OD_{rod} + 0.01\text{ inch})) / 2) / dia_{wire}$
$n_{dia} = ((0.240\text{ inch} - (0.1\text{ inch} + 0.01\text{ inch})) / 2) / 0.011\text{ inch}) = 5.91 = 6$
$n_{turns} = n_{len} * n_{dia}$
$n_{turns} = (45)(6) = 270$ turns

Length of Wire:

The length per layer of wire in the coil:

$\text{Length(layer)} = ((OD_{rod} + 0.01\text{ inch}) + (\text{Layer}*2*OD_{wire}))\ (\pi*n_{len})$
$\text{Length}(1) = ((0.1\text{ inch} + 0.01\text{ inch}) + (1*2*0.011\text{ inch}) = 18.66$ inches
Length(2) = 21.77 inches
Length(3) = 24.88 inches
Length(4) = 27.99 inches
Length(5) = 31.10 inches
Length(6) = 34.21 inches

Total wire length = 158.61 inches

Coil Resistance:

Res_{coil} = (wire length)(resistance per ft)

$$Res_{coil} = \frac{(158.61\text{in}\ (\text{ft})(0.1032\text{ ohms})}{12\text{ in} \quad * \quad \text{ft}} = 1.364\text{ ohms}$$

Current Through Coil / Voltage Across Coil:

$n = \text{turns} / \text{length}_{coil}$

$n = 270 / 0.5 \text{ inch} = 540 \text{ turns/inch} = 21{,}259.84 \text{ turns/meter}$

$\text{Current} = I = (\text{Mag field} * 1000) / (n * 4 * \pi)$

$I = (1000 \text{ Oe} * 1000) / (21{,}259.84 * 4 * \pi) = 3.74 \text{ amps}$

$\text{Voltage} = V = I * \text{Res}_{coil}$

$V = (3.74 \text{ amps})(1.364 \text{ ohms}) = 5.11 \text{ volts}$

Expected Strain in Terfenol Rod:

$\text{Predicted Strain} = S = (\text{const})[(\text{mag field})(1000)/(4\pi)]$

$$S = (2.0106 \times 10^{-8})[(1000)(1000)/(4\pi)] = 1.60 \times 10^{-3} \text{ ppm}$$

$\text{Change in Rod Length} = \delta = L_{rod} * S$

$$\delta = (0.5 \text{ inch})(1.60 \times 10^{-3}) = 0.0008 \text{ inches}$$

This calculation was programmed into a simple basic program to simplify the repetitive calculations. A hard copy of the code can be found in the appendix.

Based on the results of these calculations, the following coil parameters were chosen:

- Magnetic field = 1000 Oe
- Wire gauge = 30 = 0.011 inch dia
- ID of coil = 0.110 inch
- OD of coil = 0.24 inch
- No. of turns = 270
- Resistance of coil = 1.36 ohms
- Current required to achieve magnetic field = 3.74 amps
- Voltage across coil to achieve desire current = 5.11 volts
- Predicted (δ), or change in length), in 0.5 inch long terfenol rod = 0.008 inches

Figure 17 displays in graphic form the results of these calculations. It can be seen that as the gauge size increases, the resistance and input voltage also increase.

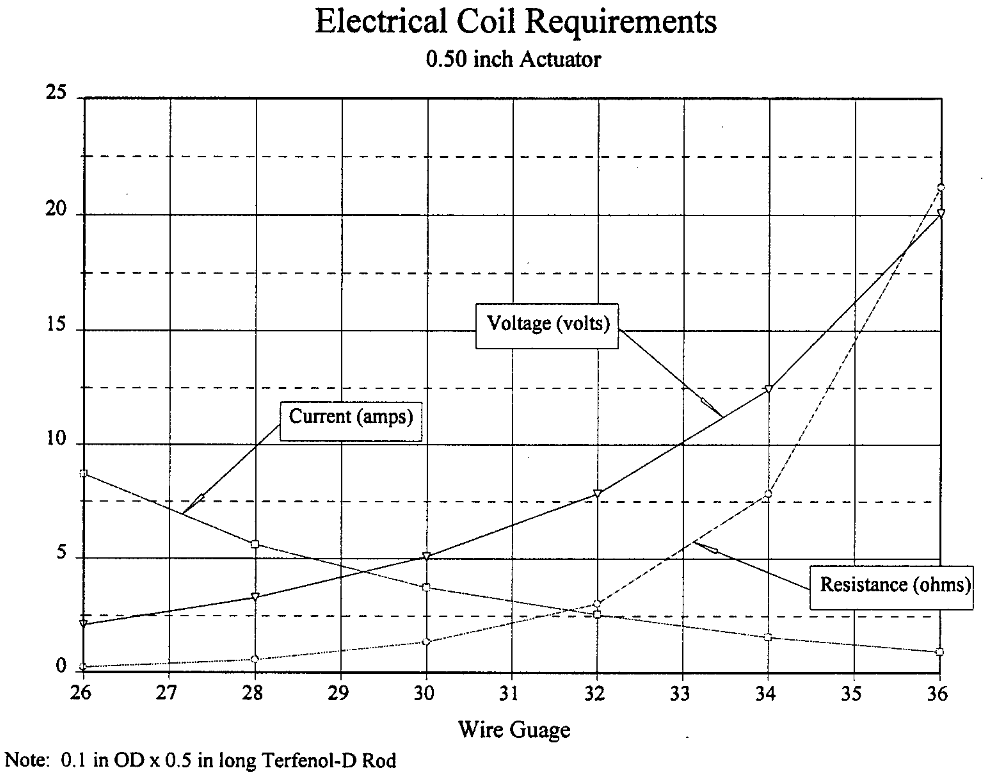

Figure 17: Electrical Coil Requirements - 1/2 inch Long Terfenol-D Rod

Failures:

After physical testing of the preliminary design was initialed we began to see failures of the coils due to rubbing at the ends of the Terfenol-D rods. This was expected. But occurred sooner than expected. A process of mechanically isolating the wires from the rods was developed using thin film Teflon.

Also means of potting the drive coils into the Motive Cell's was studied and would improve both the heat transfer and reduce possible solenoid bouncing within the housing.

Figure 18 illustrates the actuator design as it was at this stage of development.

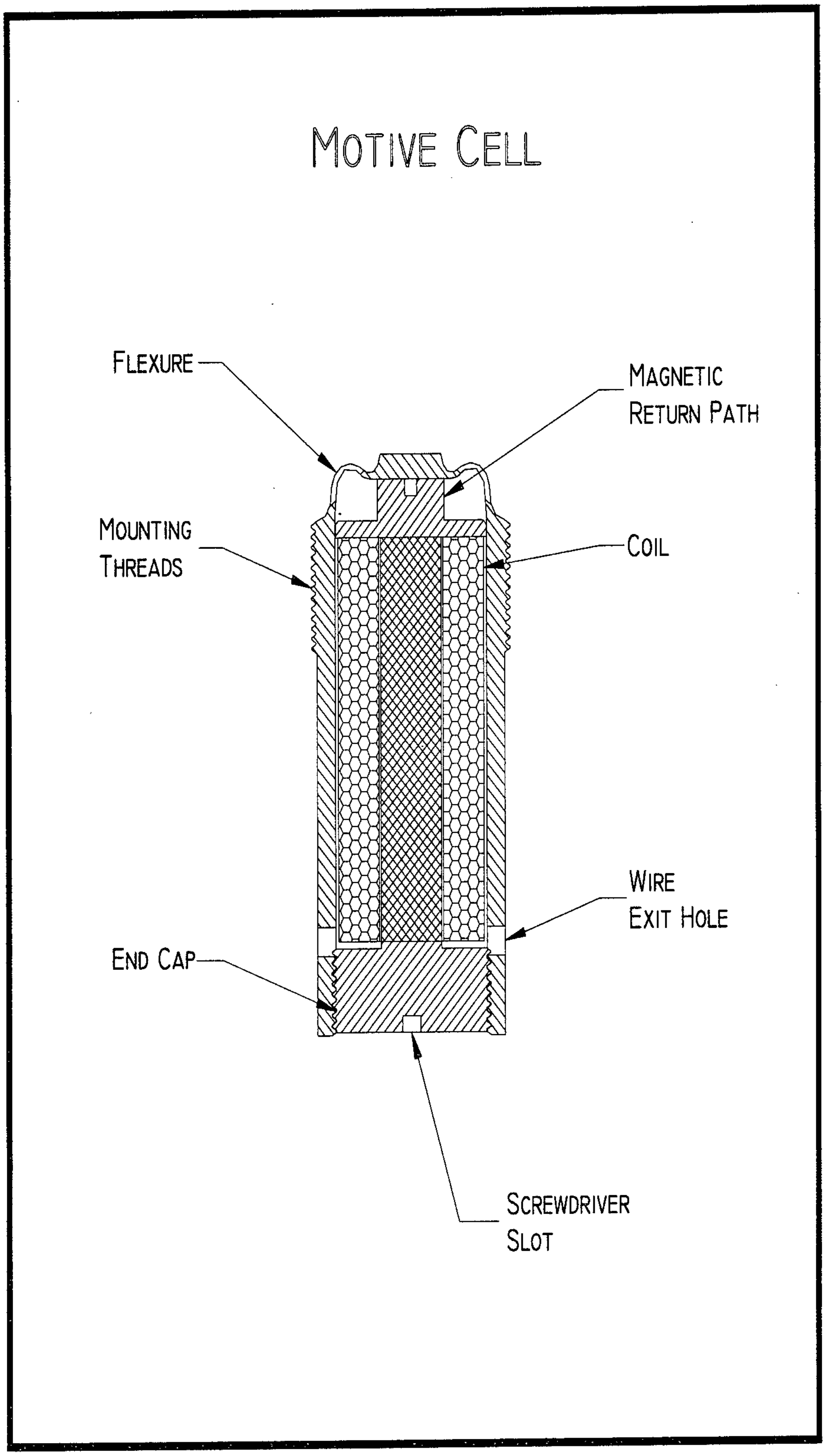

Figure 18: Initial Brake Module Actuator Design

Motive Cell Testing

As with any design/development project, one true test of success is how well the measured performance compares to the design or predicted performance. The motive cell must demonstrate sufficient displacement for use within an inchworm type motor and not fail mechanically.

Fatigue Life:

Determining the fatigue life of the motive cell is best determined through cycling the flexure through it's range of motion for many cycles. If the flexure fails, then it did not have an infinite fatigue life. There were several motive cells constructed. Some that utilized the 0.25 inch Terfenol-D rods and some that utilized the 0.50 inch Terfenol-D rods. For a conservative estimate of how many cycles each device had been subjected to, each motive cell was operated for 30 minutes each at an average frequency of 10 KHz. This equates to 1.8×10^7 cycles, with anything over 10^6 cycles indicating an infinite fatigue life. One of the early flexures failed in this fatigue test. Subsequent microscopic analysis indicates that the flexure cross-section was not close to the design specifications or dimensions. Photographs are included in this report. The other three motive cells, and subsequent ones that have been built, continue to function without signs of flexure wear.

Frequency Response and Deflection:

The other two criteria for success were a little more difficult to ascertain. A method and device were needed that could measure extremely small deflections, on the order of 0.0001 inches, over a broad range of frequencies, from 0 Hz to 50 KHz.

The initial testing was a static test that used a digital dial indicator. This device would indicate deflection of the flexure at 0 Hz, but did not function at higher frequencies.

A second attempt to measure deflection over this broad range of frequencies was to reflect a laser off the top button of the flexure and onto a distant screen. The up and down motion of the flexure would cause the reflected light on the screen to move as well. The displacements on the screen could be calibrated with the static dial indicator test to reflect motion of the flexure.

This method had several problems. First, to obtain a significant magnification of the motion of the flexure to the light reflected onto the screen, the screen needed to be located at quite a distance away from the motive cell (i.e. 20 - 30 feet). The light that was reflected off of the flexure scattered to the extent that resolution on the screen was extremely poor. Secondly, this method would not easily indicate the frequency of the flexure deflections with out developing an optical counter of some kind.

A system was then implemented using an LED / phototransistor pair. A photomicrosensor was found that provided the desired information. The chip was an OMRON EE-SG3 photomicrosensor. (Digi-Key) A sketch of it's configuration can be seen in Figure 19. In this device, the LED and the phototransistor are opposite each other and anything breaking the beam could be detected as a change in voltage.

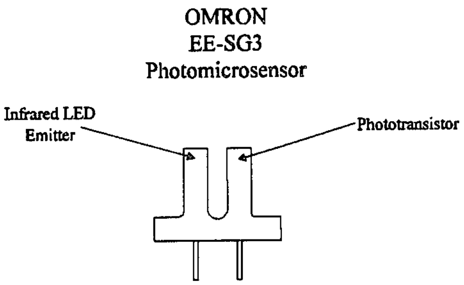

Figure 19. OMRON EE-SG3 Photomicrosensor

For this photomicrosensor to work, the motive cell needed to be modified slightly. A small, lightweight strip of aluminum was glued normal to the flexure button surface. This strip of aluminum was used to break the LED beam and register a voltage change from the phototransistor. A sketch of this arrangement can be seen in Figure 20.

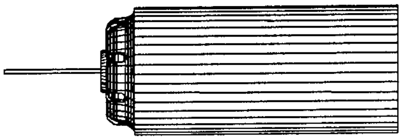

Figure 20. Motive Cell with Aluminum Strip Attached.

An electronic circuit with signal amplification was needed to control the OMRON EE-SG3. This circuit schematic can be seen in Figure 21.

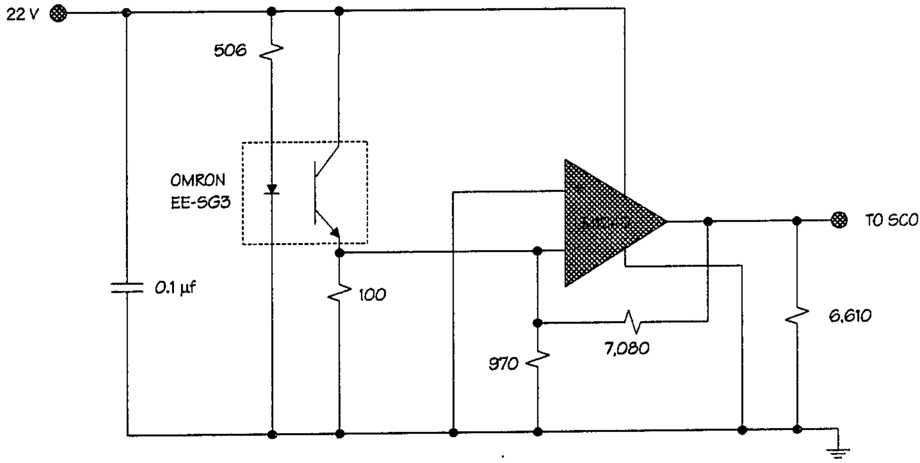

Figure 21: Driving Circuit for OMRON EE-SG3 with Signal Amplification.

Setup and Procedure for Measuring Deflection and Frequency

The setup, which can be seen in Figure , involved sending a square wave from a function generator through a 170 Watt audio amplifier and then to the coil. A meter was used to monitor the current through the coil so as not to overheat and destroy it. In most of the characterization experiments the current was limited to 1 ampere by controlling the output voltage from the function generator and the audio amplifier. The motion of the motive cell was detected by the OMRON EE-SG3 photomicrosensor and sent to an oscilloscope where the voltages were manually recorded as a function of the driving frequency.

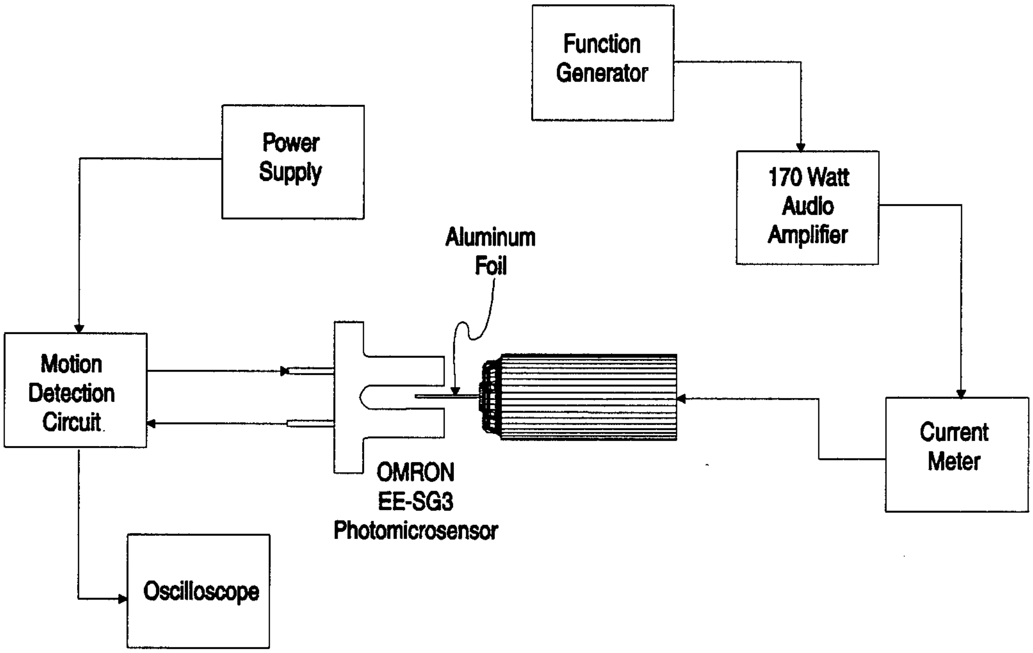

Figure 22. Setup and Apparatus

Procedure:

To measure the displacement of the motive cells, the measurement system had to be calibrated. The motive cell to be tested was placed in a vice, with substantial mass, that was bolted onto an x-y table, which was mounted on an optical bench. The optical bench was placed on a large granite block to help damp out surrounding vibrations. The tip of the aluminum strip that had been placed on the motive cell was brought up to the OMRON EE-SG3 photomicrosensor such that the aluminum strip just broke the beam of the detector. The motive cell was then moved a measured distance into the beam of the photomicrosensor by using the x-y table. The output of the photomicrosensor circuit was directed to an oscilloscope where the displacement was measured as a voltage change. By moving the motive cell with the x-y table a measured distance, the photomicrosensor was calibrated.

For the actual frequency response measurement, the current through the motive cell was held constant over the range of frequencies by adjusting the gain on the audio amplifier and the output voltage of the function generator. The current was held constant to ensure that the magnetic field strength was constant over the range of frequencies. The frequency was swept from 20 Hz up to where the motive cell no longer responded. The amplitude of the signal from the photomicrosensor circuit was manually recorded at each frequency increment. Both of the motive cell sizes were characterized using this method. The frequency responses can be seen in Figures 23 and 24.

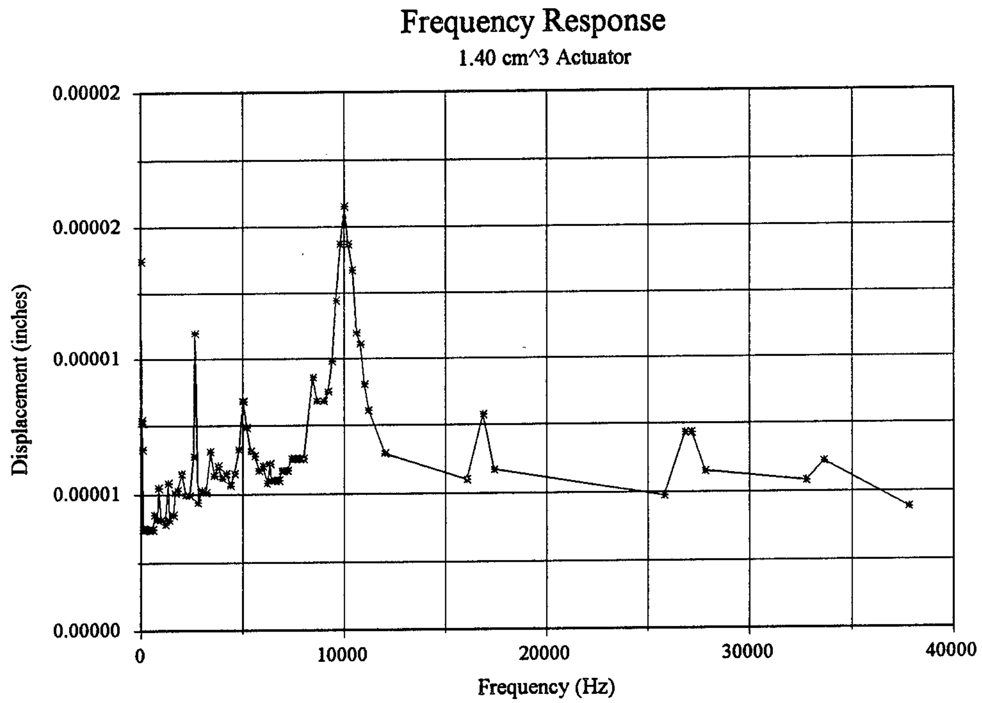

Note: Current = constant = 0.70 amps

Figure 23. Frequency Response - 1.40 cm^3 Motive Cell

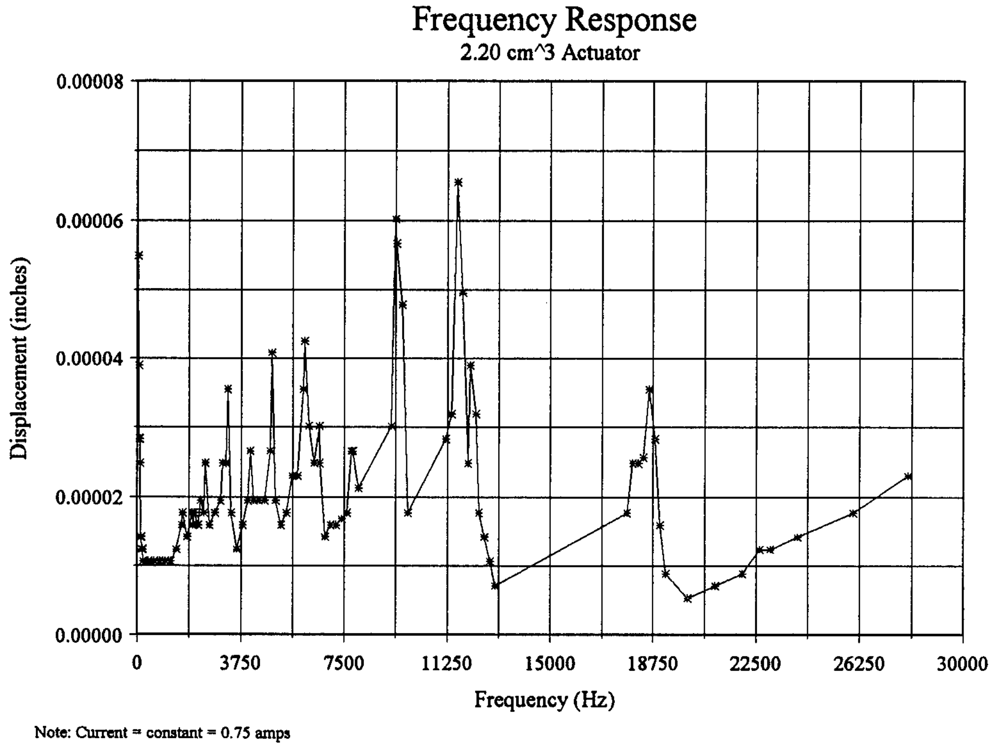

Figure 24. Frequency Response - 2.20 cm^3 Motive Cell

The graphs in Figures 23 and 24 show several resonant frequencies for each of the motive cell sizes. For the 1.40 cm^3 motive cell, the principal resonant frequency is right at 10 KHz. For the 2.20 cm^3 motive cell, there are a couple of resonant frequencies with one around 9 KHz and another around 13 KHz. This data indicates that the motive cells are capable of operating in the range of 5 KHz to 10 KHz as expected.

The measured displacements of the motive cells did not quite meet the predicted displacements. The results are as follows:

Table 2: Measured Displacements of Motive Cells

Motive Cell	Current	Predicted Displacement	Measured Displacement
1.40 cm3	0.70 amps	0.00007 inches	0.0000158 inches
2.20 cm3	0.75 amps	0.0001603 inches	0.000066 inches

There are many possible reasons why the predicted displacement was not achieved. First and foremost is the issue of tolerances. These motive cells were machined on a lathe by hand. It is difficult to maintain tight tolerances on any part, but especially difficult when dealing with parts that are extremely small. This problem is demonstrated by the motive cell flexure that failed after extensive use. Microscopic analysis of the fatigue fracture indicates that it was not built to specifications. Although the other three motive cells have not failed, it is reasonable to assume that they also do not meet exact specifications. The motive cells built for final implementation in inchworm motor wiere be machined by an EDM process to ensure a much tighter tolerance and improved performance.

Maximum Flexure Frequency

One question that needed to be answered dealt with the relationship of the frequency response of the flexure to the driving frequency of the function generator. The flexure is the limiting component in this design because of its limited frequency response. At some frequency it would no longer keep up with the Terfenol-D rod. To determine this parameter, a setup similar to the one used to determine the frequency response was used. The difference was that this time the frequency of the flexure was measured off the oscilloscope and compared to the driving frequency of the function generator. The results of this study for the 0.50 inch motive cell can be seen in Figure 25. It can be seen that the flexure frequency follows the driving frequency until up around 38 KHz. This number is not unrealistic in light of the fact that ETREMA markets an motive cell that runs up to 40 KHz. (reference)

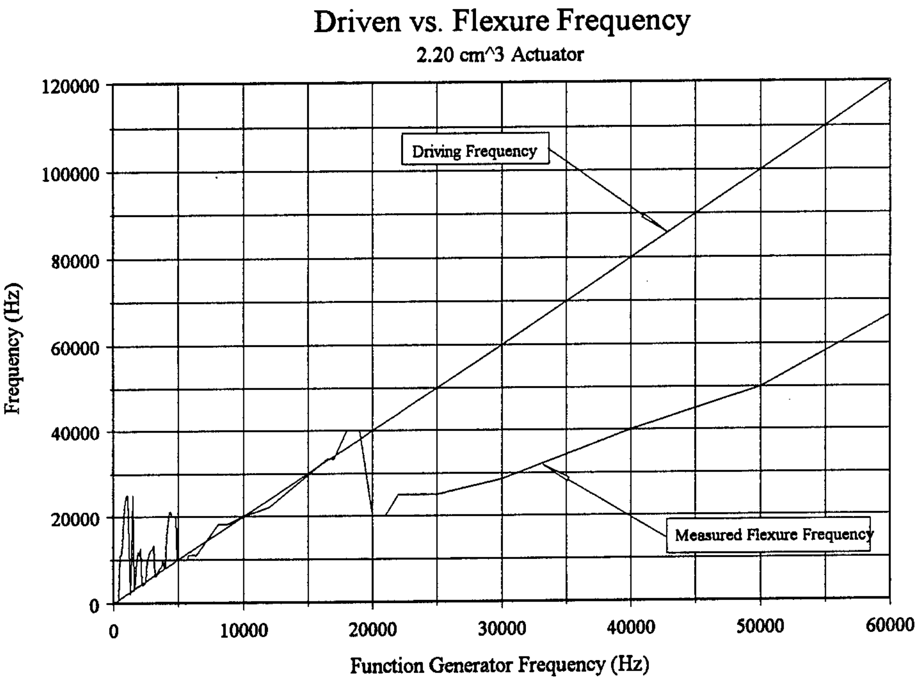

Figure 25. Measured Flexure Frequency vs. Driving Frequency

The overall concept of the Motive Cell was tested in these experiments. The data indicates that the device is a success. The device is small (about 0.375 inches long and 0.625 inches long). It provides the necessary preload to the Terfenol-D rod, and magnetic return path for the coil. The frequency response of the motive cell is within the range that would be usable for force feedback exoskeletons, and it meets the requirements set forth for an infinite fatigue life. The concept was successful but the implementation needed to be improved for the final motors. This was noted by the less than ideal motion of the Terfenol-D rods. Much of this was simply solved by using a higher precision manufacturing process. The final flexures used in the final motor have a much tighter tolerance and are machined by EDM processes. With this tighter control on geometry the predicted length excursion of the Terfenol-D rods is improved. Also we were able to reduce the hoop stresses future by modifying the slots on the flexure using the precission EDM machining.

Photographs 1 through 12 document aspects of the Motive Cell development.

Progress - **Task 3. Linear Motor Development**

As briefly noted in the background section of this report we ended the Phase I portion of the project by demonstrating a cigarette pack sized Terfenol-D Motor. The motor demonstrated several important features: modular design, low voltage drive, variable force output, backdrivability and digital control. Also we demonstrated that small high frequency micro movements of the motor felt similar to smooth forces. While others have demonstrated inchworm motors, most are made from piezoceramics, and are used for position control. To our knowledge no Terfenol-D inchworm motors had been demonstrated to provide a variable force. In the Phase I we demonstrated that velocity and force could be controlled either by controlling electrical current to the brake elements or varying the electrical pulsing. A combination of the two modes was possible. Variable force in pulse mode is made possible by allowing the drive shaft to move freely when no signal is applied. This allows a series of micro-pulses and non pulses to simulate a net force. Force in this sense is a combination of mass times acceleration effects and braking forces. Therefore in this application the finger tissues and exoskeletal structure integrate the many small positive and negative acceleration pulses into a sensation of a relatively smooth net force. As an alternate mode of control, if the finger is acting against a stationary object one could just lock the brakes with no pulses and just vary the amplitude of the braking force.

While Phase II was to continue and improve these preliminary studies the most fundamental questions to the project, in Phase II, were size related . No small Terfenol-D motors had been developed to our knowledge, therefore there was no preexisting knowledge base that could be tapped relative to Terfenol-D micro motors. There is quite a lot of preexisting data on piezoceramic based micro motor, but they do not have the complications of solenoid coils, magnetic return paths and various preload conditions, etc.. Also they are not backdrivable or force controllable. Conceptually the piezoceramic motors and the proposed magnetostrictive motors are similar, but their physical implementation must differ.

Clearly the device in Phase I was much to large and bulky for placement on human finger joints. Thus we began the Phase II project by evaluating several possible technologies that might facilitate making the motor smaller. There were both functional, materials science and manufacturing issues that had to be resolved. For example the smaller the structure of the motor the more important precise manufacturing technologies become an issue. Early in the project, before we had refined the concept of the motive cell we began investigating possible motor configurations and concepts. Several novel and useful concepts were designed and prototyped. Much was leaned from these devices. Photographs 13 & 14 illustrate two early working concept prototypes. These devices were used to test braking methods, driving coil parameters, heating, drive methods, and drive shaft concepts. Photograph 15 shows a different approach using only one brake element. It is configured as rotary joint. This device would make a smaller motor but would have an inherently narrower operational velocity and force. But it is a good concept and should be pursued further for related application.

After we had developed a general approach that we believed would be effective we began investigating the modular Motive Cell concepts noted in the previous section of this report. Various concepts were modeled in CAD and FEA. The selection of Terfenol-D magnetostrictive rod dimensions were made after completion of the ergonomic studies related to required forced and joint velocities. Figure 26 illustrates an iteration of the inchworm motor concept.

In Phase II we wanted a force motor which had a fairly high velocity. This velocity was determined from ergonomic data on joint velocities, etc. To accomplish the target velocity it was decided to design the motor with a pusher element twice as long as the brake elements. The geometric configuration of flexure structure was also used to increases the amplitude of the linear motion.

The Terfenol-D elements for the brakes and pusher cells were chosen to be of the same diameter. The pusher element is capable of pushing approximately 45 N (10 lbf). However, because of the mechanical amplification of motion force is traded for extension and the effective net force is reduced.

The brake elements are capable of the same forces as the pusher but they have a smaller stroke. The net output force, or holding force, of the brake is reduce by the friction coefficient between the brake pads and the drive shaft ribbon. A preliminary study was conducted of possible materials which could provide adequate stiffness and a high coefficient of friction. Several novel materials were proposed and a few concepts were tested. The two most promising concepts for future development are ceramic composites technologies. A custom ceramic brake pad was fabricated by a new rapid laser prototyping system and tested. The device fabricated for this project uses hardened steel alloys for both the brake pads and drive shaft ribbon. Increasing the coefficient of friction is an area of study which will facilitate enhanced motor performance for a give size Terfenol-D rod.

The final motor developed under this contract took the final form as illustrated in Figure 27. This design was chosen over the preceding concept in figure 26, because it provided a more symmetric oscillation. Detailed engineering drawings are included in an appendix. This motor is configured using two Motive Cell modules as brakes on either end of a scissors jack type pusher element. The pusher is configured as a double flexure Motive Cell. The better the symmetry the more effective the vibration modes and hence the more efficient the motor. The basic body of the device, which encompasses the brake and the pusher elements, is a single piece flexure based design. The use of flexures reduces motion losses due to pined type joints and also minimizes mechanical friction. The motor is fabricated using standard machining processes included surface grinding, milling, wire EDM and plunge EDM machining. The device could be relatively easily fabricated in quantity with few changes. Photographs 17 & 18 show the first finished Terfenol-D inchworm motor. The dime in the photograph is to demonstrate scale.

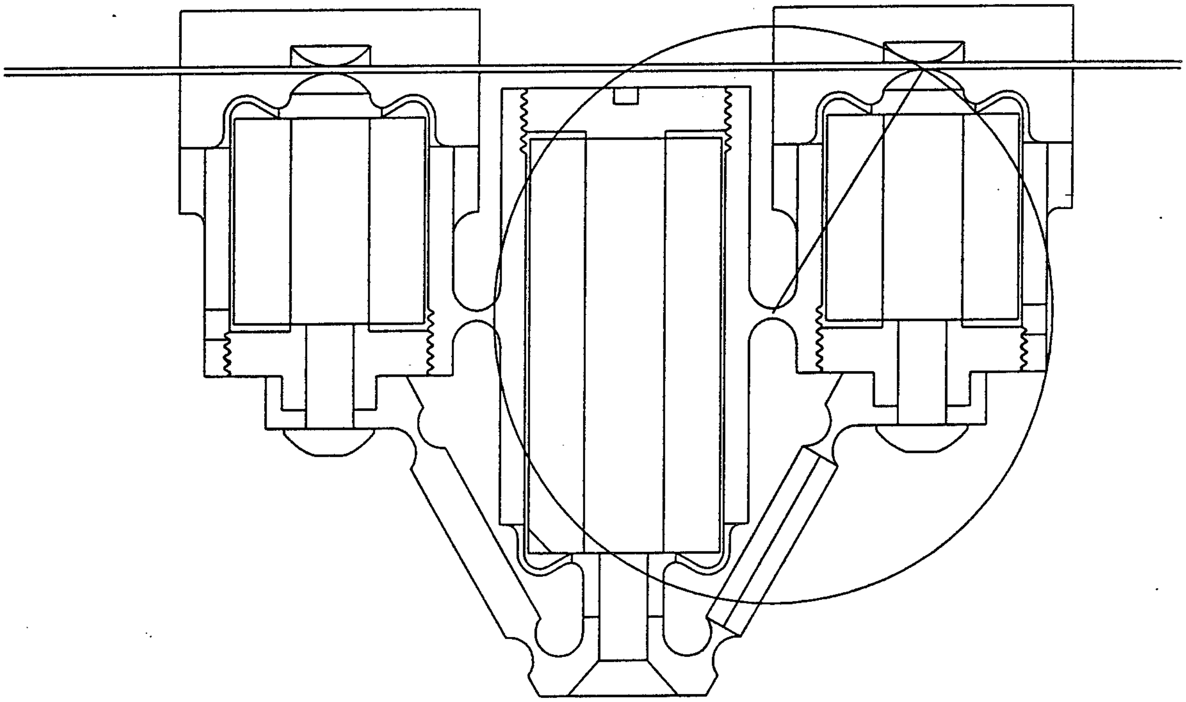

Figure 26. Inchworm concept iteration.

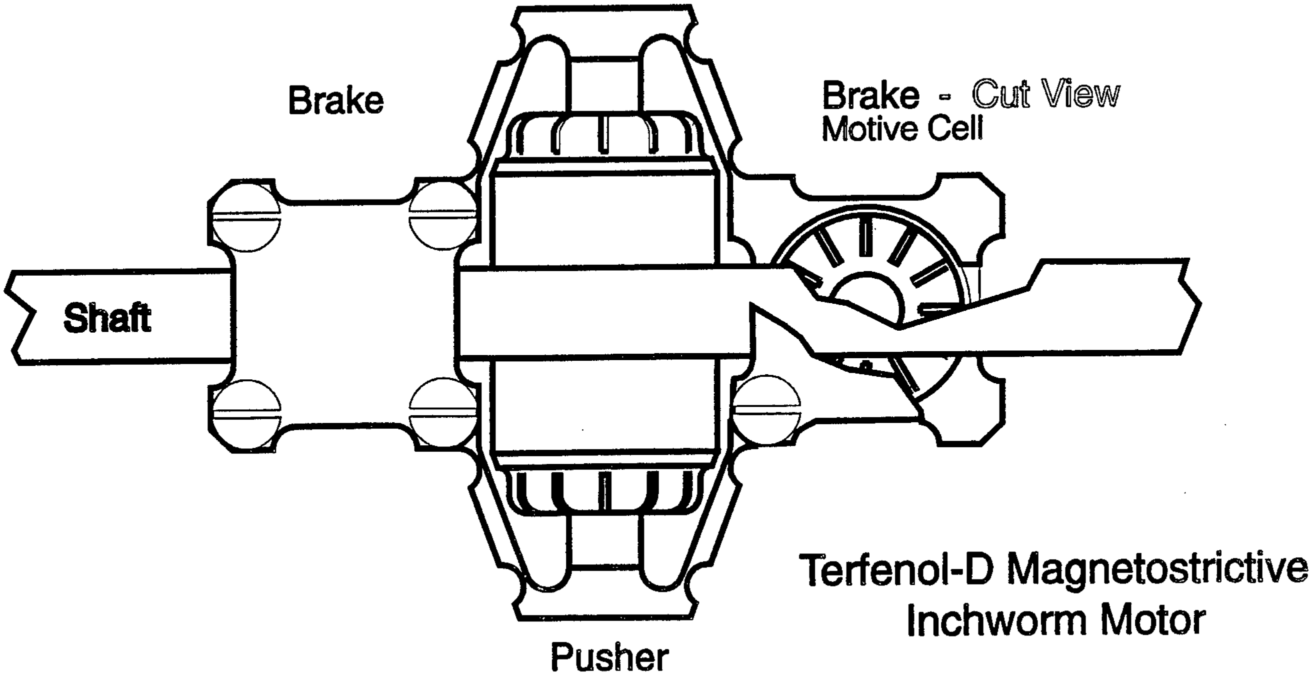

Figure 27. Final Phase II inchworm motor concept iteration.

Electronic Controller design

After completion of the inchworm motor we were ready to begin evaluation and testing the prototype. In order to test the device an electronic motor controller, to provide the needed phasing, needed to be designed and fabricated.

The electronic control board (ECB) has several functions including amplification of the load cell signal and virtual force signal, offset adjustments, onboard clocking, pulse-width modulation, and driver signals for the coil driving power board. The load cell selected has a signal range from 0 to 250 mV in amplitude with an excitation of 15 Vdc. To make this a useful signal an instrumentation amplifier was used to provide a gain of 20. The virtual force signal is connected through a similar amplifier but with a lower gain setting. The advantages to using an instrumentation amplifier includes decoupling the load cell resistor bridges from circuit ground, high impedance inputs, reduction of noise (specifically 60 Hz), and high gain. Each amplifier circuit is followed by a low-pass filter (3 dB pole of ~10 Hz) to help further reduce noise and signal spikes. The conditioned signals are compared to each other to determine if the load cell voltage is higher or lower than the virtual force signal. The resultant signal controls the pulse-width modulation.

The pulse-width modulation circuit is a 16 step, digital modulator. If the load cell signal is greater than virtual force signal the pulse-width is increased. If the load cell signal is less than the virtual force the pulse-width is decreased. If the two signals are matched then there is no change in the pulse-width signal. This digital pulse-width modulator is created by using a binary up counter, a binary up/down counter, and a 4-bit comparator. The counters are adjusted once per pulse-width cycle. The frequency for the pulse-width control is about 11 kHz. This was to ensure that the pulse-width control could change from full on to full off in about 1 msec. Hence, the limiting factor on control speed is either the motors or the input filters. There is some control logic on the board to control how the brakes and pusher elements work together. This logic sets the direction of the drive shaft, the speed of the motor elements (and therefore the drive shaft), and synchronizes the braking and pushing on the drive shaft. These logic signals are used by the power board to excite the coils surrounding the Terfenol-D rods.

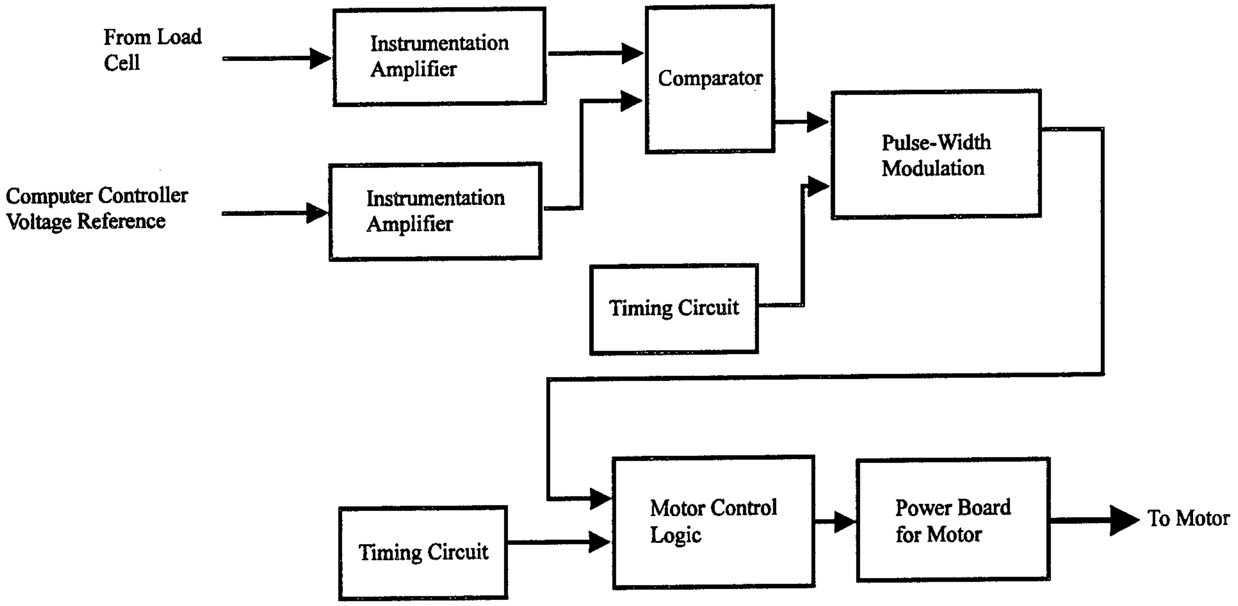

Figure 28.

Coil Driver - Power Board

The technology for driving the magnetostrictive inchworm motor is similar to driving a brushless DC motor. It is has low resistance, low voltage, and high current. The three windings are driven in a cyclic phased pattern. The inchworm motor driver is less complicated than the brushless motor drivers because we do not need to sense the position of winding relative to the magnets. In this case there is no rotor lag, the coil and the Terfenol-D are mechanical locked in position.

Several designs were considered for the power board. Initially, power modules designed for stepper motors were investigated. These modules had useful features such as combined logic and power components allowing a small package design, integrated heat sinks, and signal inputs which allowed it to be controlled from a computer. However, these modules typically could not provide a high enough current range, usually controlled only two elements, and did not allow for an adjustable time between phases. The second concept focused on using a multiple transistor power MOSFET package. This allowed for a smaller board footprint, use of logic level signals for control, and localization of heat. However, these transistor packages needed to bridge two transistors together to handle the power requirements. This meant a single chip package of four transistors could only run two drive elements. The single heat tab also proved too small of an area to allow heat sinks to effectively maintain the internal junction temperature below thermal shutdown limits. This design also prevent from using a current limiter on each individual coil. This tended to cause catastrophic failures when one coil would start to deteriorate. A custom made board was designed which allowed much easier and precise control of each coil.

Each driver element circuit contains a current limiter and a MOSFET transistor. The current limiter is to control the amount of current delivered through the wire and prevent burning out the coil. These are turned on and off by the MOSFETs. The power board uses power MOSFETs as switches for the excitation of the coils. The MOSFETs are logic level, hence they are full on with a 5 volt signal. The resistance, when the transistor is in the on state, is 0.3 ohms at 5 amps. The MOSFETs actually control the ground line. So the coils are left in a high floating state when not being used. This design allows for better control of the step response and helps keep the ground from having to much noise on it.

Feedback Control

A commercial software package was used to demonstrate the ability of the motors and controller board for providing force feedback. This was demonstrated by controlling force with a varying position load cell and applying a varying force to a stationary position load cell. The software, Notebook Pro, is a data capture and hardware controller package. We used this software with the PC-30D data interface board. The software has built in comparator functions and can output a varying signal based on conditioned input signals. This allowed to show both force and data measurements while providing a reference voltage signal.
This control board was used in collecting the initial arbitrary force control data which follows.

Setup for measuring speed versus
Pulse-Width Modualtion control

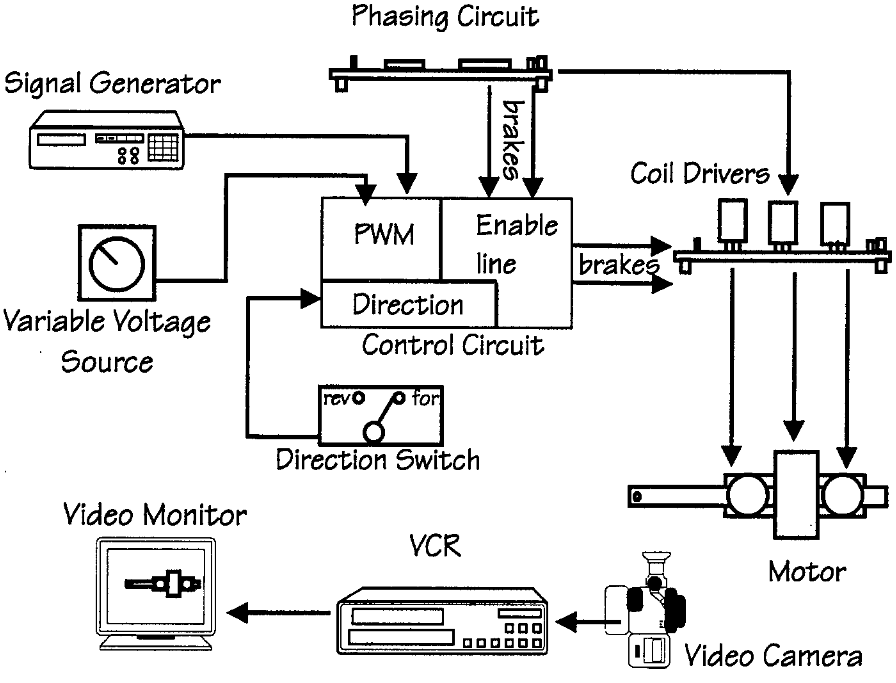

Figure 29.

Terfenol-D prototype inchworm motor - evaluation and testing.

Two Element Experiments - Inertial Drive Method

During this period of the project we also investigated several driving methods. Of particular interest were experiments conducted to evaluate the possibility of two element driving methods. This is an inertial drive system. In this method only one brake element is powered and the other is disconnected. Unlike the traditional inchworm method, the motor does not climb along the shaft. In the two element mode the motor effectively grabs the shaft and propels it forward. The drive shaft is grabbed thrown forward, released and re-grabbed 5000 times per second. The motor worked very well in this mode. It was demonstrated slightly lower force and velocity outputs. The advantage of this demonstrated inertial drive concept is that we can design a Terfenol-D motor with one third the volume and weight with a simple change to the design (take a hack saw and remove the unused brake motive cell). Because of the very limited scope of the project the concept was demonstrated but has been not pursed further at this time.

Three Element Experiments - Inch Worm Drive Method

Preliminary experiments to test frequency response and force output capabilities were conducted using calibrated spring scales. Velocities were measured by videotaping the motor motion under varying conditions and the velocities were measured from the TV screen.

The motor was found to be highly controllable. The output velocity was shown to be fundamentally a function of the number of steps per time. The inchworm motors velocity peaked at approximately 5 KHz. This was due to a resonant mode of the bulk motor frame. Above this frequency the motor continues to function but the velocity is degraded due to the non-resonant condition and perhaps an overlap of the mechanical and electrical phases.

Switching from forward to reverse was instantaneous and is accomplished by simply switching the pulse sequence to the motor. That is to say, the direction of motion is controlled by selecting which (Motive Cell brake) element leads in the pulse train.

Testing fixture.

In order to facilitate the measurement of motor force and arbitrary force control it became necessary to construct a special calibratable testing fixture. The test fixture needed to provide a known motion (velocity) output and an electrical feedback signal from a load cell to the controlling computer.

The test fixture was designed and constructed as shown in photographs 19 and 20. The apparatus provides a linear motion generator. The linear motion is sinusoidal and has a high mechanical impedance. The following figure illustrates the setup of the experiments.

Setup for applying a varying force to a stationary object &constant force to a moving object

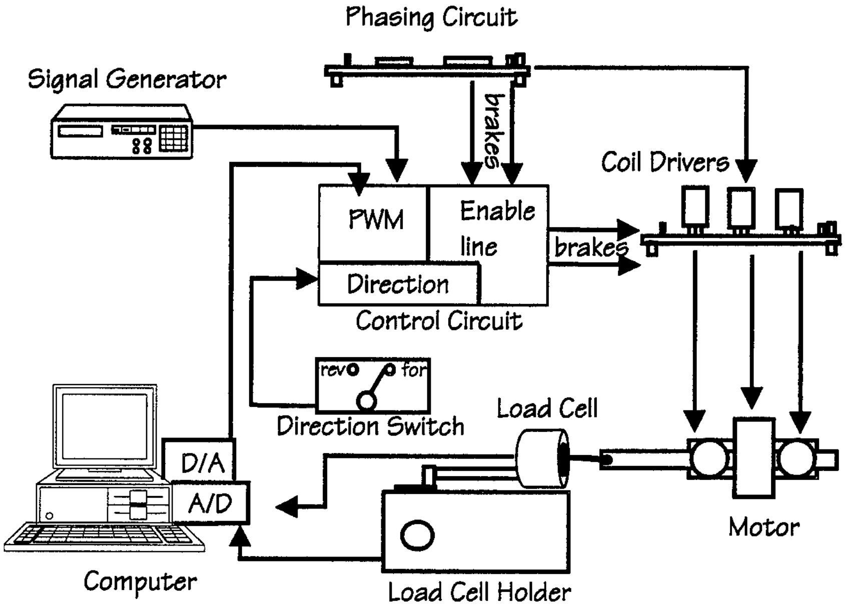

Figure 30.

The maximum force measured was 10 N (2.25 lbf). The maximum is obtained when the Motive Cell is adjusted intimately with the drive shaft. Because of a small variation in the original motor drive shaft ribbon thickness the velocity was improve when a small gap was allowed between the shaft and the brake. If the gap between the drive shaft of the motor and the Motive cell is opened to much it produces a reduced force output, since some of the energy is used to extend the Terfenol-D with no clamping. For most of the experiments we operated the motor at less than the maximum force condition.

The maximum velocity measured was 14.5 cm/sec at approximately 5 KHz. This corresponds to an average inchworm step of 0.029 mm.

As currently configured the range of motion is only limited by the length of the drive shaft selected. The motor was tested with a shaft 15 cm in length.

The following data is presented in graph form. As a matter of interest the first graph is a plot of a human finger being used to try and provide a constant force on the slowly moving load cell which is on the moving shaft of the test bed. In addition to the use of force sensing in the hand the human subject was also provided a visual feedback voltage on a CRT to aid in force tracking. The data is instructive when compared to the rudimentary control system used on the Terfenol-D inchworm motor.

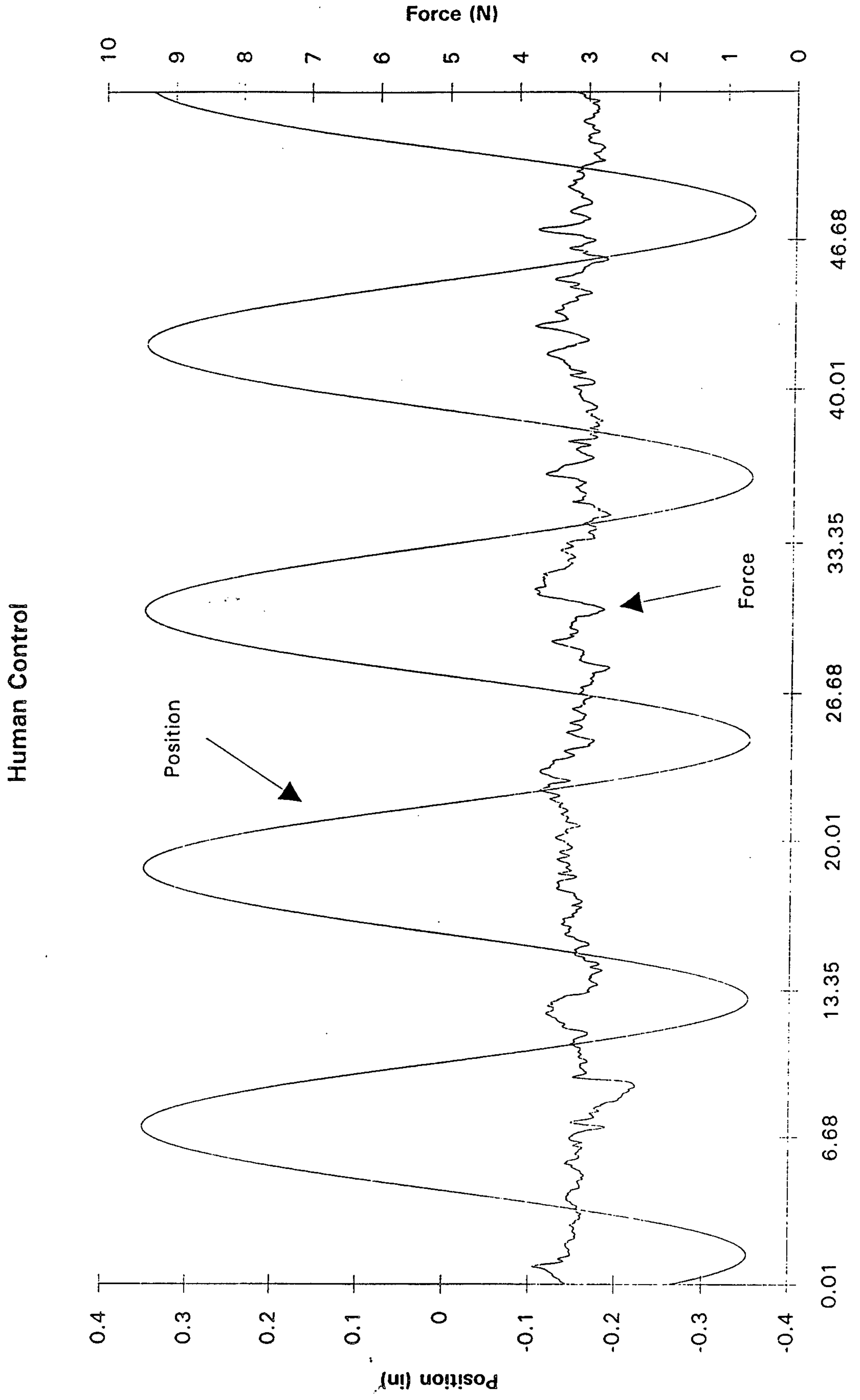

Figure 31. Human finger providing constant force tracking on a moving object.

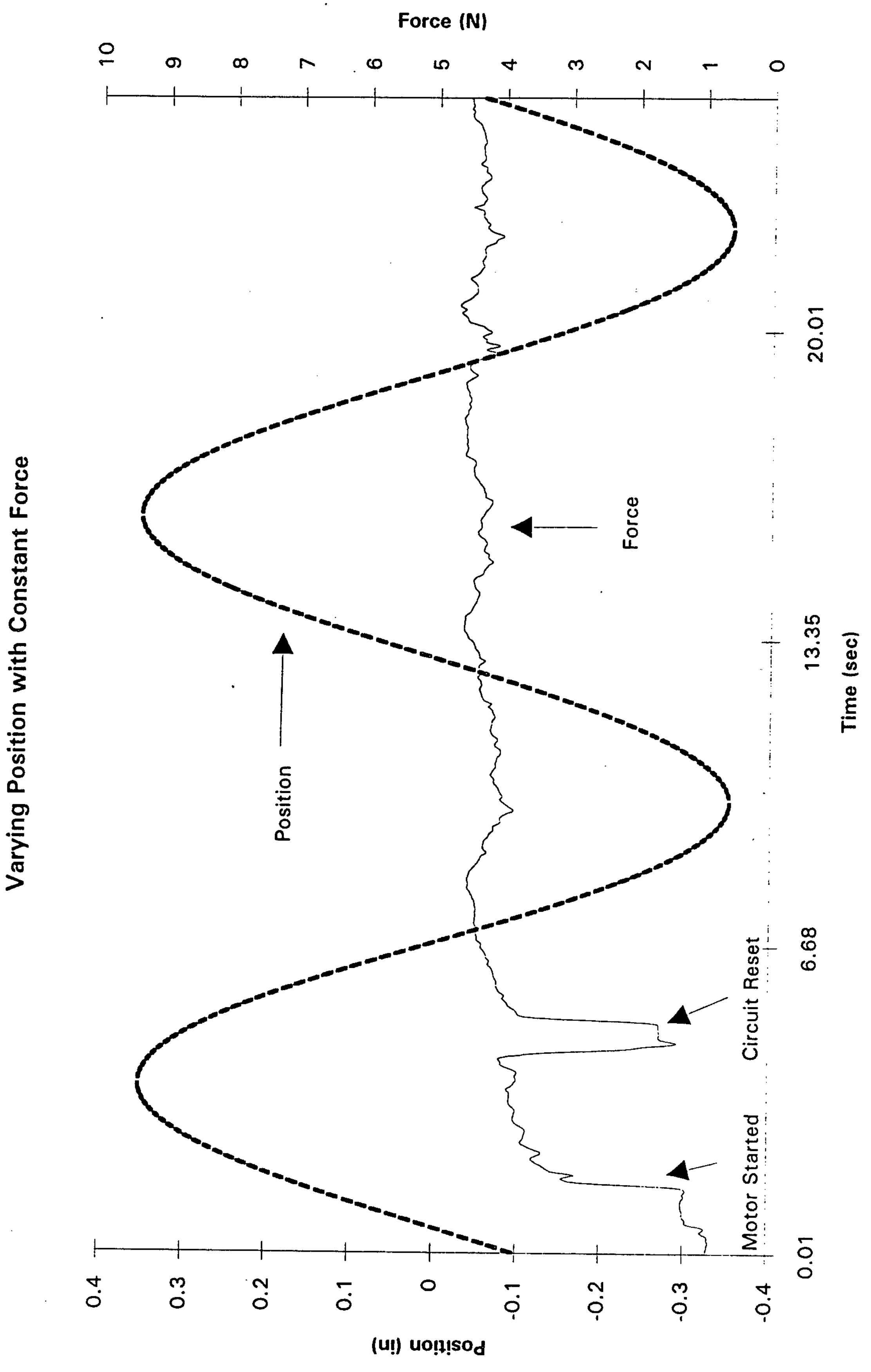

Figure 32. Terfenol-D motor providing constant force tracking on a moving object.

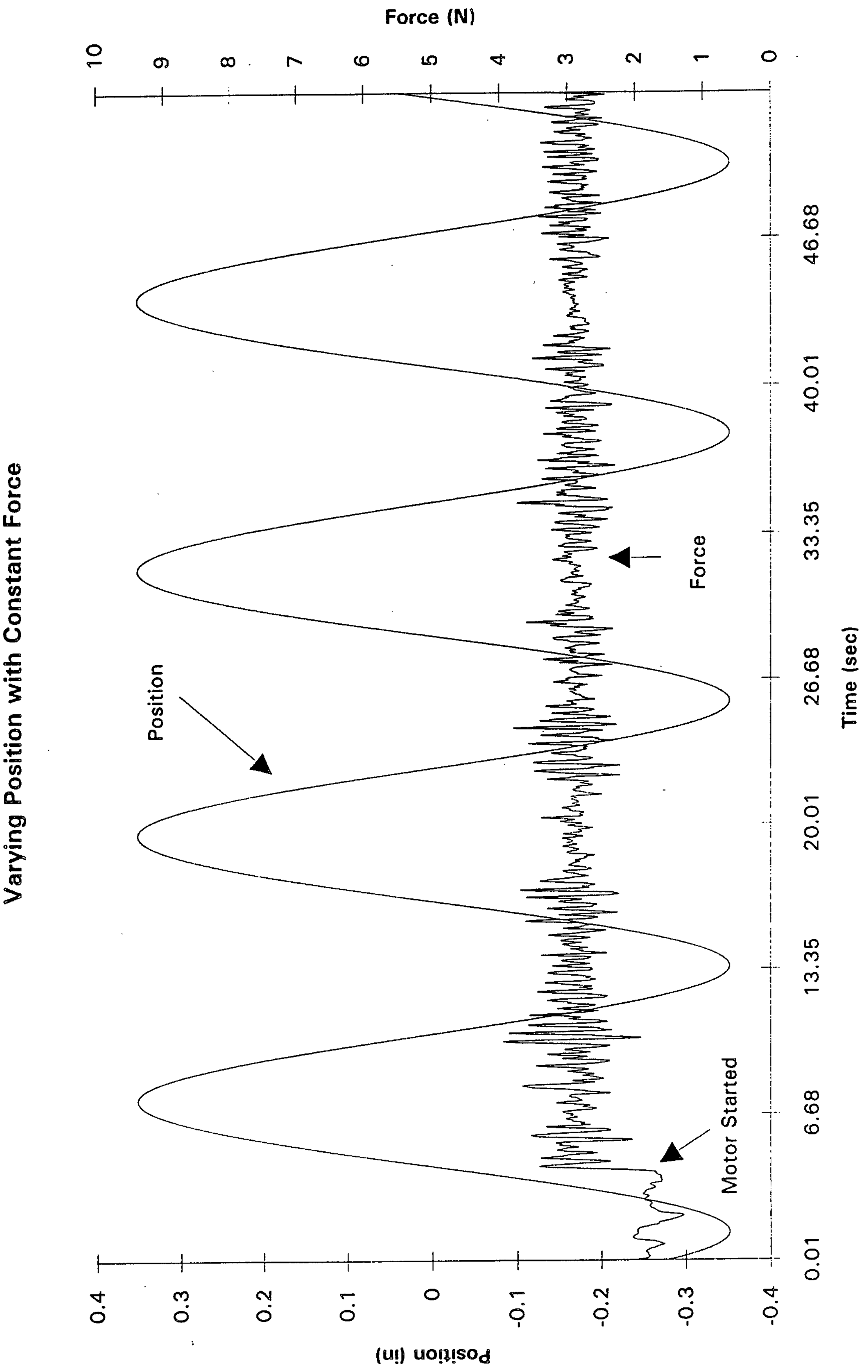

Figure 33. Terfenol-D motor providing constant force tracking on a moving object.

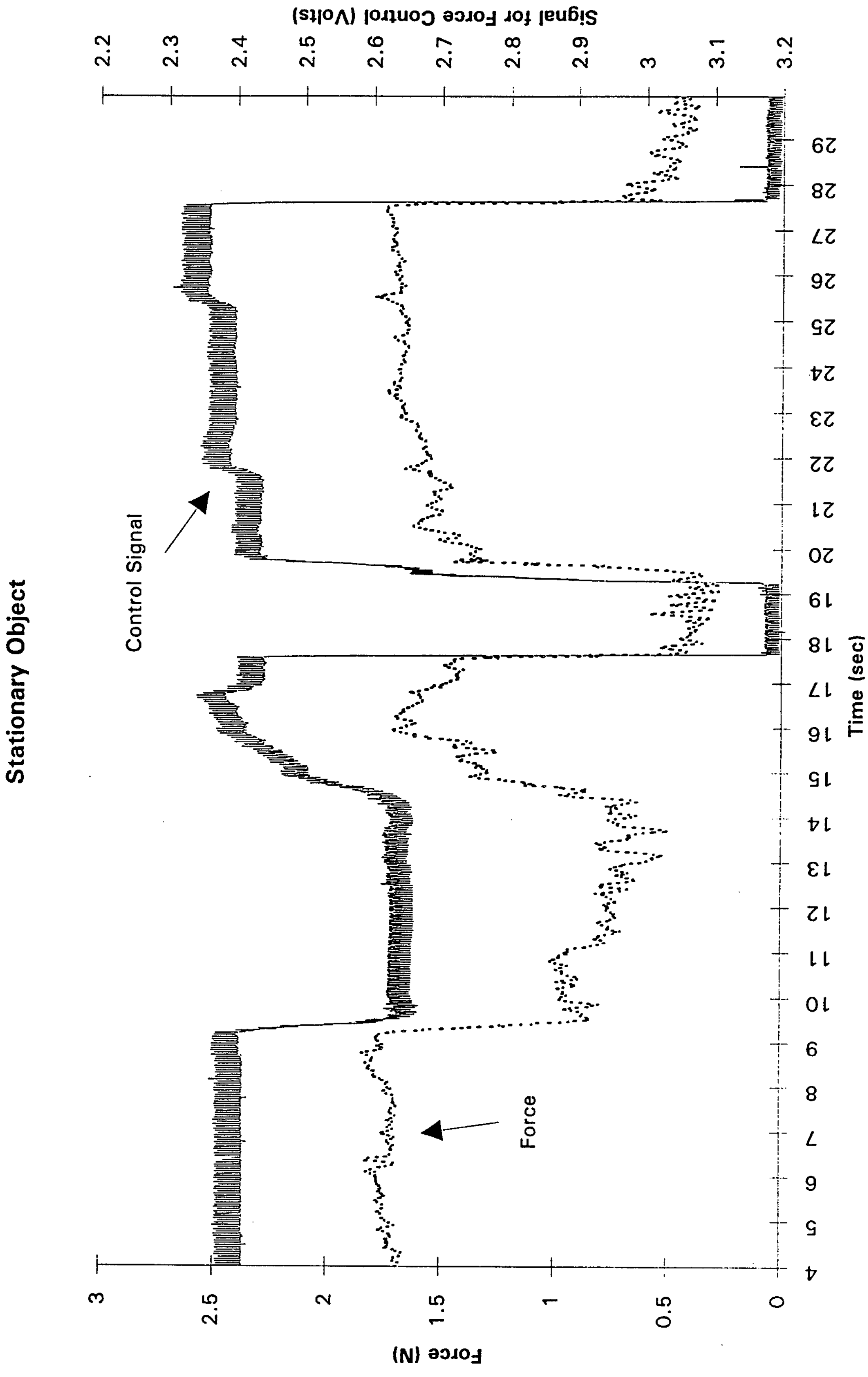

Figure 34. Terfenol-D motor providing varying force on a stationary object.

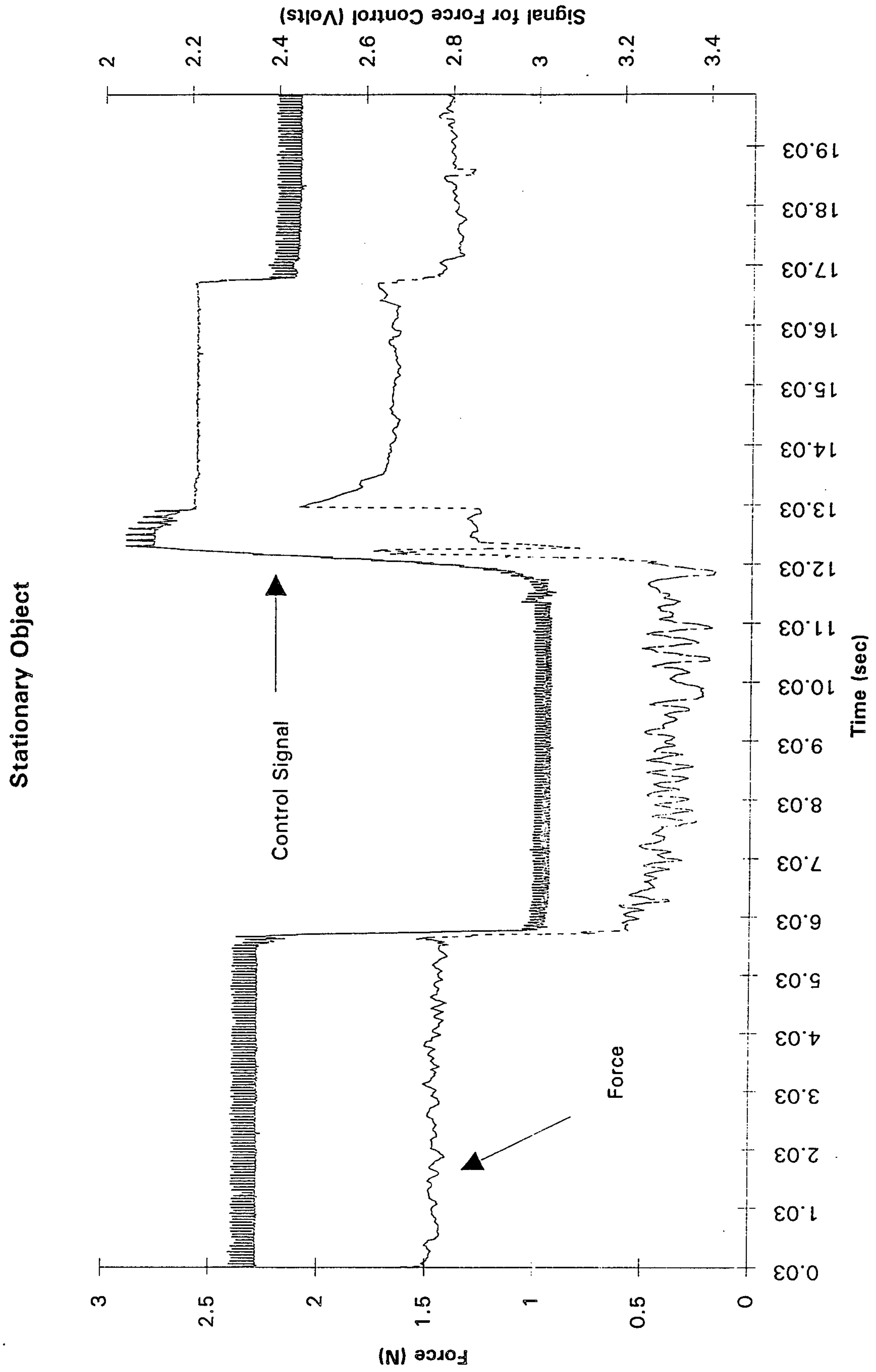

Figure 35. Terfenol-D motor providing varying force on a stationary object.

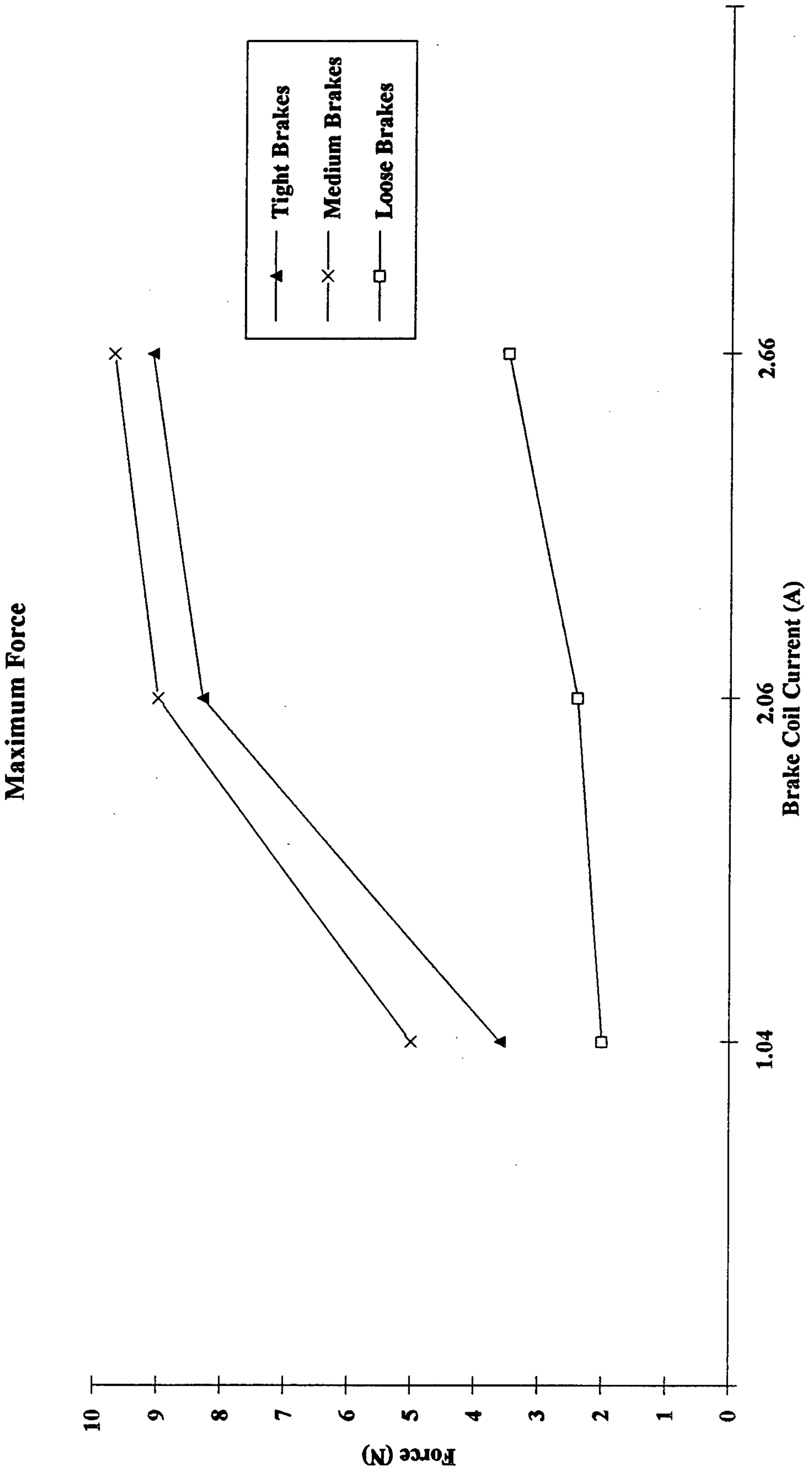

Figure 36. Maximum Force measurements as a function of current and brake adjustments.

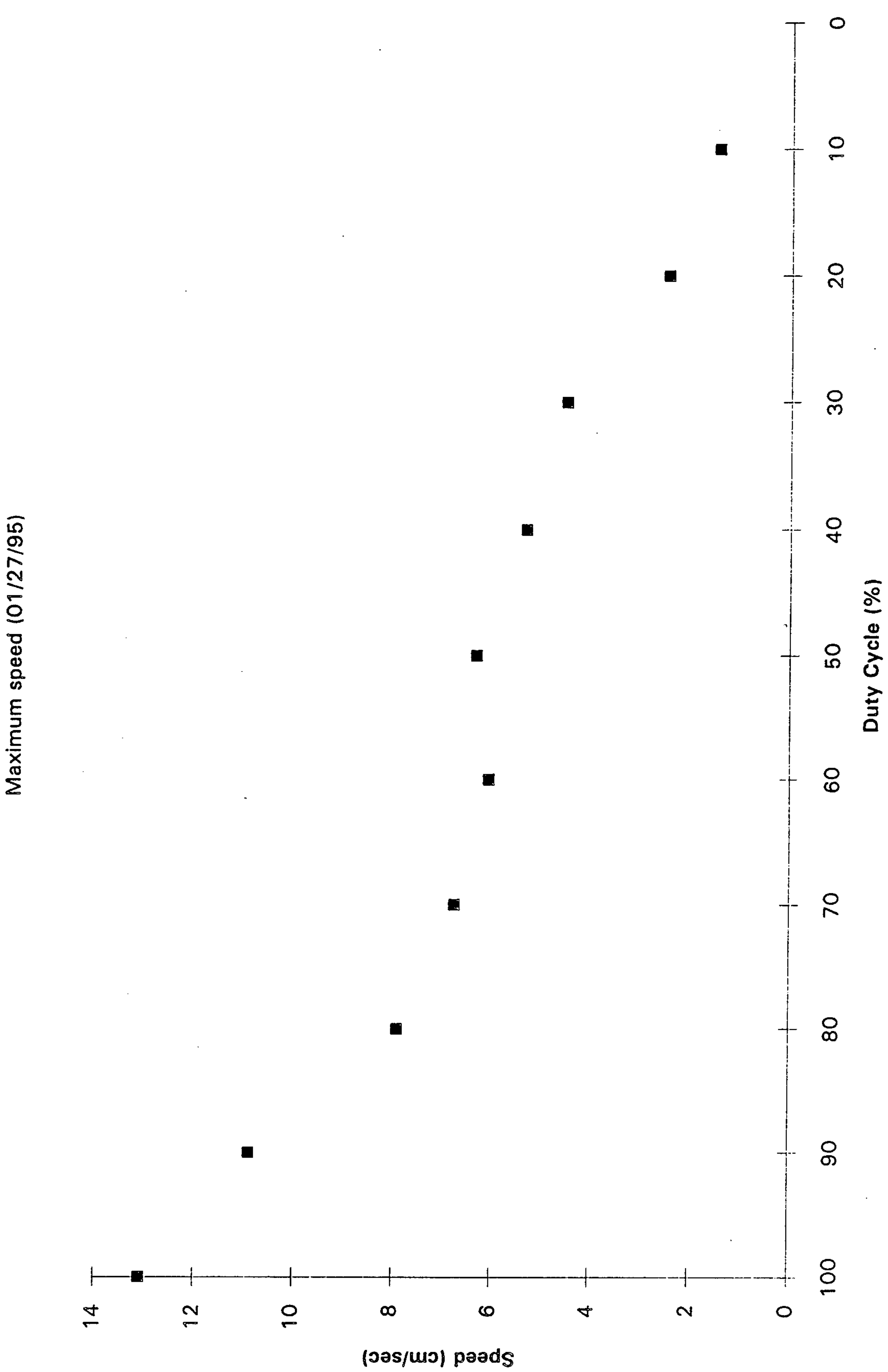

Figure 37. Speed versus pulse width modulation at 5 kHz.

Progress - **Task 4. Application Simulation**

The objective of task 4 was to explore methods for the application of the new actuator for dexterous force feedback. Or in other words, to integrate the actuator into a dexterous exoskeleton. It was understood from the beginning of the project that the motor developed in this project would be a beginning and that further improvements to the actuator would come as future funding was made available to this or other research teams. Thus, given that we are implementing a less than perfect actuator, the exoskeleton can certainly be improved as the motor improves. The integration of this actuator as it currently exists into an exoskeletal device is meant to be a demonstration of future possibilities rather than a demonstration of limitations. The limitations are however noted at the end of this section and serve a useful purpose in mapping out the direction of needed future development. The author believes that the obvious limitations of this system, such as noise, load sensors, etc., can be improved significantly given reasonable study and development.

During the course of the project we have studied an assortment of issues related to the ergonomic constraints for force feedback and exoskeletal attachment. We came to this task with certain blind spots and preconceived biases. The literature on the subject has also formed biases as to which ergonomic issues are of most critical concern. One of the most fundamental issues related to force feedback is whether this feedback is best given to the human interface in the form of, what we refer to as, "virtual object force feedback" or as an "exoskeletal feedback". Solutions for these types of mechanisms tend to evolve differently. Both concepts need new methods, actuators and concepts. The virtual type force feedback concepts are less concerned with the control of a slave telerobot and are therefore are potentially more simple to implement. The PHANToM device is a good example of a virtual object feedback. The P.I. has developed a theoretical bias towards the virtual type devices for most applications, but was contractually constraint to pursue the exoskeletal master slave type controller concepts. Clearly there is a need for exoskeletal configurations, but there may be a larger commercial demand for the virtual object systems. It has been anticipated that the need for force feedback exoskeletons is especially critical where the device is to be used as a controller for an anthropomorphic dexterous slave robot. As the technology now stands there is no one specific slave robot hand master in mind for this application, therefore the solutions for the exoskeleton master are general in nature.

During the project several discovery prototypes were fabricated to help us elucidate various design requirements for joint freedom, size and force application methods. One of the concerns which first shadowed our attention was that of the somewhat complex motion of the hand. Much of this concern is in fact unfounded if one begins to think properly about the concept of exoskeletal tracking. The concern grows from reading too much into the study of human joint motion. Much of the literature is concerned with replicating the exact motion of the bone joint with the goal of making prosthetic joints. We are concerned with a much simpler case of tracking the motion of the exterior hand positions and not the exact motion of the bones. We can not conveniently attach to the bones. The exoskeletal tracking case can be and is a much simpler case compared to bone tracking. There is much room for improvement in this area. This exoskeletal case is much simpler because we are constrained to interface not with the human bone, but with a significantly compliant human tissue bed surrounding the bones. If the tissue is used to absorb the small variations in movement in joint axes, it can be shown that simple pin joints can be used to model the hand motion inside the exoskeleton. In the short term it is unlikely that we will have slave robotic hands in a variety of sizes. The human hand (of various sizes) inside a master exoskeleton is used to position a (fixed size) slave. Therefore at this point we are designing an exoskeleton which is adjustable for many size hands with no particular need to match to any specific robot hand. It is reasonable to believe that slave hands can be designed with pinned joints and that the exoskeletons should have the same pined geometry. This is also true for the thumb joints. A good fit and tracking can be achieved with four axis per digit. There is also a move toward less degree's of freedom per digit such as in work on geared fingers by NASA, etc. The prototype devices shown in the photographs were used to convince ourselves about the adequacy of fixed axis pinned joints as an exoskeletal interface to all joints in the hand. In this project we have tested several different concepts to identify key issues. The following photographs and figures illustrate some of this devices.

The issue of hand size variation amongst potential users has also been given much consideration. The final device we have chosen to fabricate is adjustable for hand size in a multitude of ways. The device adjusts for finger thickness, joint length and joint position. The device is not perfect however and will not fit very small hands well. We have developed a highly adjustable device. This is however probably the wrong approach to take if one were developing a commercially viable system for average consumers. This is because adjustability leads to excessive complexity and cost. It is also likely that for a viable consumer product one might evolve towards a partially adjustable system. More simply, if volume were sufficient and cost was low enough, personal exoskeletons in small, medium and large might be practical. The concept of "one sizes fits all" usually equates to "one size fits almost no one well".

Another difficulty in the implementation of our final prototype was the size of the load cell. We did not have adequate time and funding to design and implement a new or custom small force sensor into the system. Thus the bottom of the finger rings are unnecessarily thick. This is not generally a problem except it can dramatically limit the curling of the fingers into a tight fisted position. This is especially true when the joints are adjusted close together for small hands.

Angle Sensing

Angle sensors adequately small were no located in our search of commercial supplies which would work in this application. Hall sensor devices such as used by the EXOS are small but have inadequate angle sensing range. Also we had some trepidation about the use of these devices because of possible magnetic interference from the yet undesigned magnetostrictive motors. Slotted type encoders were not felt to be precise enough for this device since they are not capable of measuring very fine motions such as tactile like responses. They are also significantly large. One of the significant problems with small profile tactile sensors using PVF2, is that they have a very poor low frequency response. We would like low frequency compatible devices in order to facilitate measurement of human frequency tactile signals, i.e. 0 to 300 Hz. Therefore we developed a new angle sensor for this project to give us fine resolution, small size, and wide frequency response (0 Hz to High - Mechanical limits).

TRA's technology utilizes a novel means of measuring angular position. It involves the optical polarization phenomena that occurs with transverse electromagnetic waves. Non polarized electromagnetic waves have multiple orientations. However, an electromagnetic wave having displacements in only one direction is said to be linearly polarized. Polarization of light is generally accomplished with the use of a polarizing filter. When two polarizers are used in series, the relative polarization angles of the films determine the intensity of the light transmitted. The amount of light transmitted through two polarizing films can be determined by the following relationship:

$$I = I_{\max}\cos^2\theta$$

where:

I_{max} = maximum intensity of light transmitted
θ = relative angle between two polarizing films
I = intensity of light transmitted at angle θ

With this relationship, when the polarization angles of the two films are parallel to each other, (i.e. θ =0), then the intensity of the light transmitted is equal to $I_{\max}$. When the polarization angles of the two films are perpendicular to each other, (i.e. θ = 90), then the intensity of the light transmitted is equal to zero. A graphic representation of this relationship can be seen in Figure 1. Here θ, or the relative polarization angles between the two films is represented along the "X" axis and the light intensity is represented along the "Y" axis. It can be seen that as the films are rotated 90° with respect to each other the intensity of light transmitted goes to zero.

To increase the usable angle of the sensor we can add a second pair of detectors at and use a simple mathematical manipulation to linearize and extend the useful sensing range.

TRA has built several prototypes (see photographs) based on this cross polarization principal. The technology is based on measuring the change in light amplitude relative to the motion of a simple polarize film. The concept was implemented in a very small geometry and was implemented in a stand alone configuration as in Photograph 26, and imbedded into a motorized finger joint, as in Photograph 27, and imbedded into the final demonstration device in Photograph 35.

Load Cell

During the course of the project we were not able to locate any off the shelf miniature load cells which would satisfy our needs. The two best devices evaluated were a strain gage, and a thin film device. We tested the Uniforce device and felt that it would make the better sensor for this application. None of the available configurations were of the appropriate geometry for the project, and were not easily modifiable. Therefore we opted to buy standard strain gauge modules. The strain gage load cells are much to bulky for the application, and the strain gauge technologies do not generally integration well in a commercial, cost sensitive applications.

Load cells for the final device were purchased from A.L. Design, Inc. 1411 Military Rd. Buffalo, New York. The Model ALD-SP-MICRO. The have a capacity of 10 lbs with a safe overload equal to 150% of the rated capacity, and a ultimate overload equal to 250% of rated capacity. The load cells are strain gage based devices.

Final Electronic Control Board

A revised board was developed for the final demonstration and added a few improvements over the initial design (noted in the previous section). A directional jumper was added to allow for changing the direction that the motor runs. A second comparator was added to provide a high and low force determination. This comparator compares a voltage reference, set with a potentiometer, with the compensated signal from the load cell. The output from the comparator is used by the power board to vary how hard the pusher element contracts. The instrumentation amplifier was modified to adjust for a different load cell. The new load cell signal ranges from 0 to 20 mV with an excitation of 10 Vdc. Hence, the amplifier gain was boosted to 200.

Final Power Board

The only revision to this circuit was the addition of a 5 Vdc relay and a second power resistor. The relay is controlled by the high/low force signal from the controller board. The relay places a second power resistor in parallel with one used by the current limiter in the pusher element circuit. This effectively provides a higher current to the coil, which causes the terfenol to push harder. This is possible with the pusher element since it is twice as large as the rods used in the braking elements.

Software Force Feedback Control

The commercial software package has been replaced with a custom designed, graphical interface control program. The code is written in Microsoft Quick C. The software simulates a three jointed finger segments. These are scaled to be approximately the same relative lengths as a human index finger. The angle between the simulated segments are determined by capturing the voltage signal from the TRA angle sensors. These signals are then converted into a number useful to the program. The software also simulates a square object on the screen. The object can be moved to various points on the screen. The object has been designed to simulate a harder force the deeper a finger segment penetrates. This demonstrates the ability to simulate different degrees of reaction forces.

The software uses calls that are specific to the PC-30D interface board. However, the code can be altered by changing the commented lines where a different set of board commands would need to be placed. This allows for different interface boards to be used. The only requirements is that the interface board contains three analog to digital input lines and three digital to analog output lines. Command controls are described in the manual under the software section.

Software

The software and a simple instruction manual are provided in an appendix. The software is only rudimentary. It is used as an engineering tool for study and is not intended as a user friendly commercial interface. Better software is not really indicated at this point in the development and should be developed in concert with a more refined Phase III implementation.

The software is designed to read in a signal from the angle sensor and display a three segment finger. The angles between the adjacent segments will mimic the angle read by the angle sensors. The angle sensor outputs a voltage which is a function of its angular position. These signals are read by an analog-to-digital interface board and inputted into the software.

The screen will also display a square, movable object on the screen. The software will register any collision between the finger segments and the square. If contact is detected the system will output a virtual force signal (via a digital-to-analog interface board) to the TRA's electronic control board. The level of the output signal will be determined by the depth at which the finger segment penetrates the square.

Control Keys:

Up Arrow: Moves the virtual object towards the top of the screen.
Down Arrow: Moves the virtual object towards the bottom of the screen.
Left Arrow: Moves the virtual object towards the left.
Right Arrow: Moves the virtual object towards the right.

0 (Zero): Activates/Deactivates the virtual object.

Esc or 'q': Quits the program.

Finger interface

To accommodate a large number of hand sizes and geometry's we developed system which is comprised of an adjustable ring and a sliding rails. The rings are configured as u-shaped rings which are slotted on the sides to allow tightening. We have provided three different u-ring sizes. This will fit most individuals. The slots on the sides of the u-rings interface with a plate which is on the top or dorsal side of the fingers. This plate is provided with two female dove tail slots. These slots interface with corresponding male dove tails on the virtual joint and inchworm motor assemblies. By moving the virtual joint assemble relative to the finger plate on is able to adjust the finger length and joint possition. This system is quite adaptable. But with adaptability comes complexity and adjusting the system to fit one hand is tedious but necessary to provide non binding motion of the joints. If the joint axis of the finger is not properly aligned a moment is produced on the virtual pivot and this increases friction.

Significant limitation is caused by using the large load cells. These require a larger than necessary u-ring geometry.

Wire routing

We have not addressed the issue of wiring of the exoskeleton to any significant extent. Each joint on the finger has 6 wires from the motor, 4 from the angle sensor and 4 from the strain gage load cells. This makes a total of 14 separate wires for one joint or 42 for the three joints on this prototype. Just combining grounds would reduce this count to 30.

Exoskeleton Joints

There are numerous concepts which have been proposed and or tested to measure finger joint position and or provide force feedback. During this project we have also investigated several possible configurations that would be compatible with the motor we were developing. They are namely: Fixed Axis Joint Concepts, Multi - Axis Joint Concepts, Congruent Axis Joint Concepts, Fixed Axis - Slider Joint Concepts and Virtual Axis Joints.

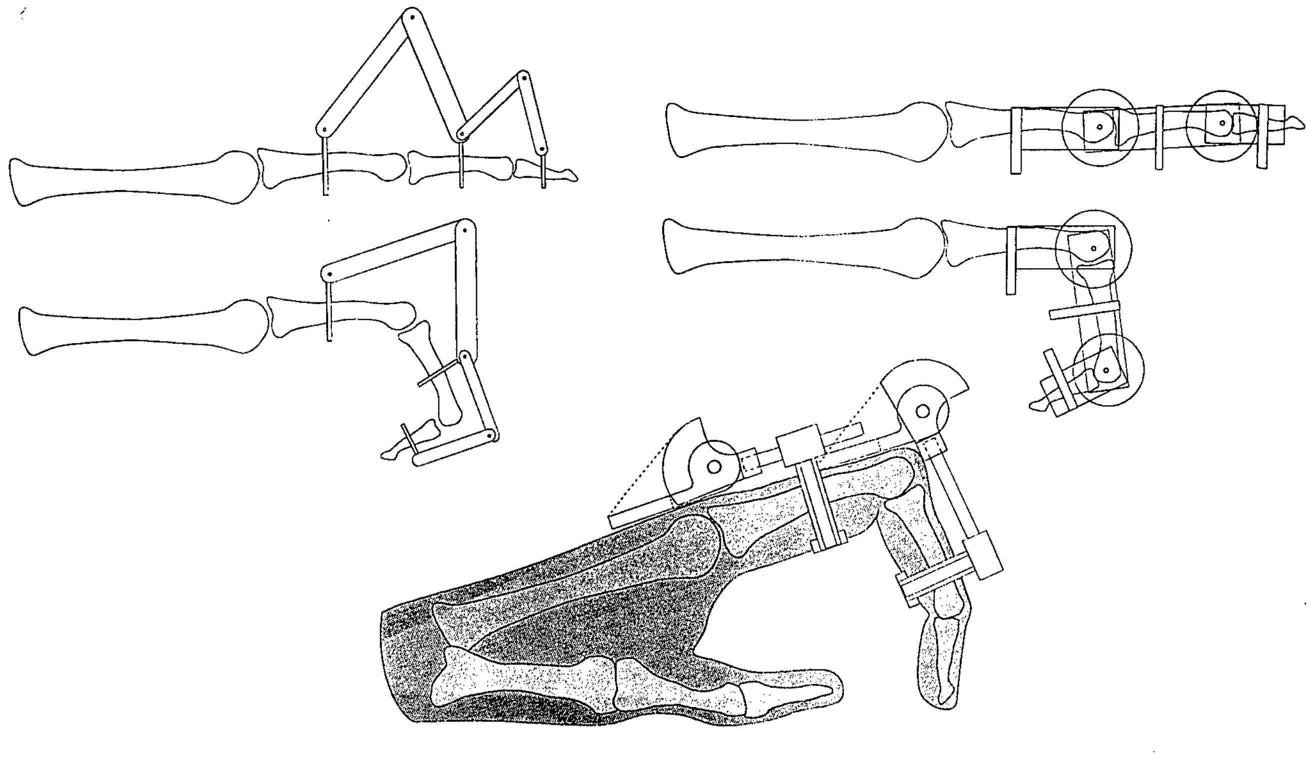

Figure 38. Exoskeleton joint concepts.

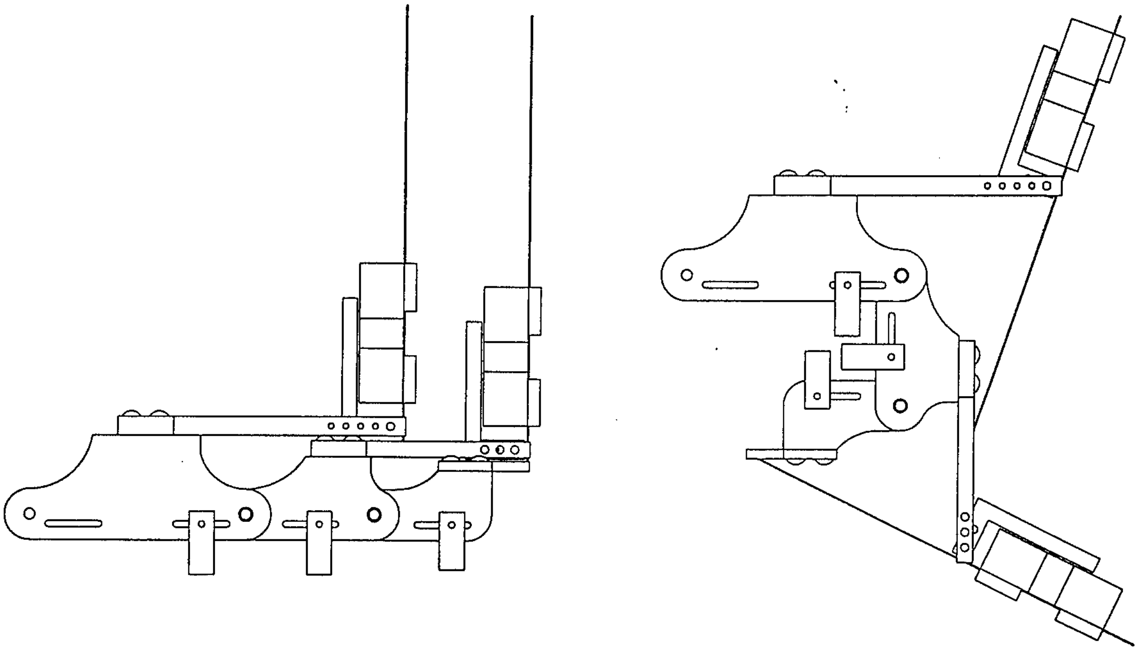

Figure 39. Pinned configuration with motor in marionette location.

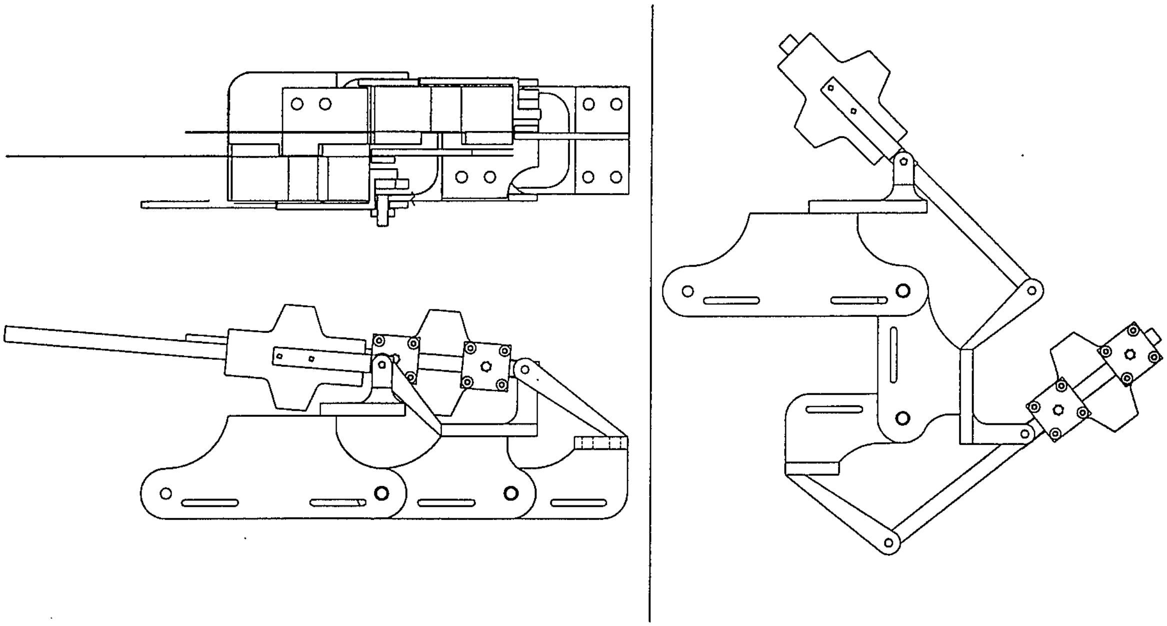

Figure 40. Pinned configuration with motor in parallel location.

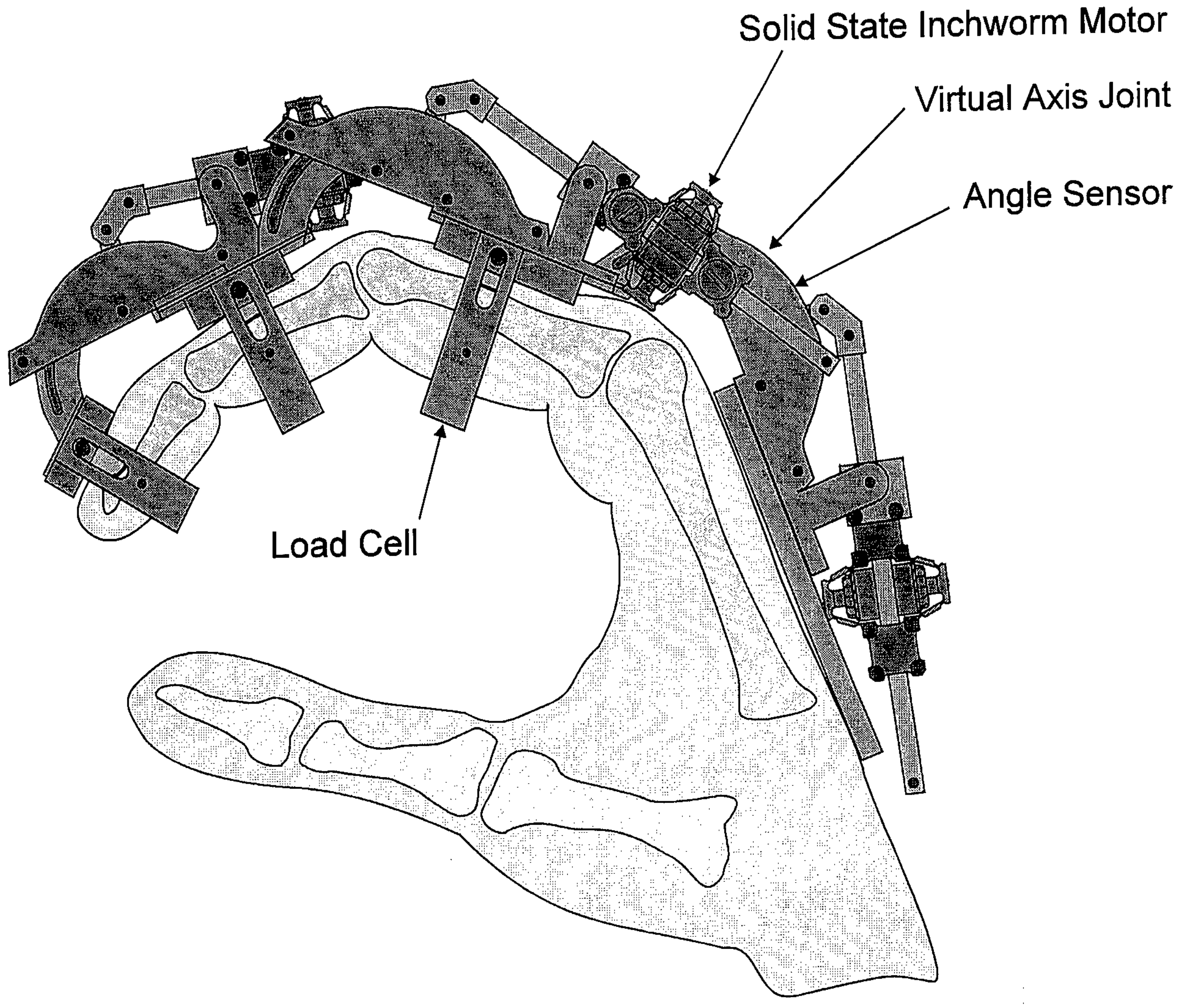
Solid State Inchworm Motor
Virtual Axis Joint
Angle Sensor
Load Cell
Terfenol-D Force Feedback Handmaster

Figure 41. Virtual Joint Configuration.

Final Integration

In our evaluation of the pro's and con's of the pinned and virtual joint configurations, noted in the figures above, it was decided that both would be prototyped and evaluated. The major advantage of the pinned configuration is its ability to accommodate a wide range of hand sizes with out a need for significant adjustment. It's main disadvantage has to do with the thickness of the finger attachments and associated angle sensing. This becomes a real problem if multifingered configurations are envisioned. In our final effort during this project we have decided to integrate the inchworm motor with the Virtual Axis Joint concepts. Figure 41 illustrates the final exoskeleton device concept. The figure in the user manual itemizes each component.

The virtual joint concept, while not yet fully refined has the has several important long range advantages.

- It minimizes the amount of structure on the sides and back of the fingers.

  By minimizing structure on the sides, and inside of the fingers we provide the capability of performing closed fisted grasping.

- It is adjustable to fit various finger lengths.

  The virtual joint concepts facilitates the placement of sliding rails for adjustment which are non obtrusive to grasping motions.

- It is a ridged structure.

  The ridged structure is important for precise measurement of joint angles and control of either virtual, or slave robotic applications.

- It facilitates integration of the angle sensing methods, polarizer, slotted encoder or others.

  A polarize angle sensor is embedded into the virtual joint configuration and does not add to the size of the device. The concept would also be directly compatible with a slotted encoder embedded in the same fashion.

- It is compatible with Phase III integration of the motor into the virtual pivot.

  With the virtual joint configuration it is proposed that Terfenol-D type inchworm motor could be directly embedded into the virtual joint. This could easily be accomplished by having the motor inchworm its way along the virtual arc rather than as independent motor. The arc of the virtual joint would replace the ribbon drive shaft and the motor would be embedded into the existing arc housing structure. This would be a very compact, light weight and capable configuration.

The final prototype was fabricated in-house using a combination of Delrin plastic and Aluminum. This makes for a very light weight finger. Photograph 34 shows an exploded assembly view of all the components needed to assemble one joint. Photograph 35 shows the virtual pivot finger near completion with the Terfenol-D inchworm motors attached. The finger has three actuated degrees of freedom and one nonactive degree.

Progress - **Task 5. Documentation**

During the course of the project the progress achieved was documented. Included in the Appendices are engineering drawings for the project. The project also produced this final report, 7 quarterly reports, and two technically detailed presentations for the Air Force technical monitors.

◆ Problems for Future Improvement ◆

At this point in the development of Terfenol-D inchworm motors we have identified and provided engineering solutions to a number of problems to get to the state of the art as it is. However some engineering problems and opportunities have not been resolved or implemented in the current device. These problems are implementation or engineering related. <u>At this point we have not hit up against any of the physically inherent limitations of the Terfenol-D material.</u> This means that significant strides in performance can be expected without heroic efforts or breakthroughs in material properties, though the Terfenol-D materials are improving. As an example when this project began the literature related to Terfenol-D had shown eddy current limitations around 8 kHz. This was subsequently shown to be a false assumption. Currently commercial Terfenol-D actuators are for sale with flat mechanical responses exceeding 40 kHz (ETREMA, Inc.). The US Navy also continues to push this envelop. Laminated structures will certainly raise this higher.

In this section of the report problems are identifige and presented in list form. Accompanying each known problem are some suggested solutions or directions. The list is in two sections though the topics are not exclusive. The first relating to the magnetostrictive motors and the second to the exoskeletal issues.

<u>Problem areas and concepts and methods for their solution.</u>

Inchworm motor.

- Noise at 5 kHz
  - Noise is indicative of both the resonant frequency of the structure and mechanical energy losses in the system.
    - Solved by:
    - Increasing frequency above audible.
    - Smaller size reduces acoustic air coupling
    - Higher frequenies couple less well to air
    - Eliminate mechanical slapping
    - Strategic use of shielding, damping
    - Harmonic dissipation

- Waste heat from coils.
  - Effects efficiency, undesirable thermal expansion, burn out.
    - Solved by:
    - Shaped Pulsed signals (non-square),
    - Reduced size,
    - Lower coil resistance,
    - Heat sinking,
    - Heat fins and surface area increases,
    - Black body radiation coating,

    - Thermally conductive coil potting,
    - Air convection -eddy cooling / integrated micro pumping structures,
    - Pulse-Width Modulation / Duty cycle,
    - Current control on pulsing.

Braking efficiency and friction can be to be improved.
- Solved by:
    - Improved materials selection
    - Non isotropic lubricants.
    - Surface finish enhancement.
    - New ceramic composites.
    - Higher precission

Brake wear.
- To be solved by:
    - non square wave signals,
    - improved materials selection,
    - better adjustment methods,

Fabrication costs.
- To be improved by:
    - refined design,
    - custom tooling,
    - volume production and methods,
    - reduced parts count

Size.
- To be improved by:
    - refined design,
    - refined fabrication fixtures and method,
    - improve tolerances on key elements,
    - possible inertial drive, single brake methods.

Terfenol-D rod breakage.
- To be solved by:
    - Calibrated preloading measurements,
    - Better machining of rod ends,
    - Better parallelism on tolerances,
    - Torsion de coupling.

Coil insulation wear
- Solved by combination of:
    - Terfenol friction isolation, Teflon,
    - Mechanical isolation gap,
    - Thermally conductive lubricants,
    - Potting coil to motive cell housing,

        - End cap centering.

- Motor control
    - Improves with:
        - Higher frequency motor,
        - Higher PWM bandwidth,
        - Possible Current control,

Exoskeleton issues.

- Enhanced by:
    - More elegant (superior) motor/joint integration,
    - Smaller motor,
    - Stiffer drive shaft,
    - Possible motor- virtual joint integration,
    - Better manufacturing tolerances,
    - More rigid materials;
        - Use of engineering plastics such as,
        - graphite filled and LC polymers.
    - More elegant implementation,
    - Reduced friction in Joints;
        - Bearings, lubricants, materials
    - Smaller load cells on finger pads,
    - Smaller angle sensor implementation,
    - Minimize cabling,
    - Reduce cable stiffness;
        - Higher grade cable materials for flexibility
    - Simpler adjustability methods.
    - Reduced parts count.

The list is not comprehensive but should give a good indication of future development and improvements that can be effected with continued engineering. It is reasonable to expect improve performance as the technology matures.

At this position in the report we include photographs which have been referenced above.

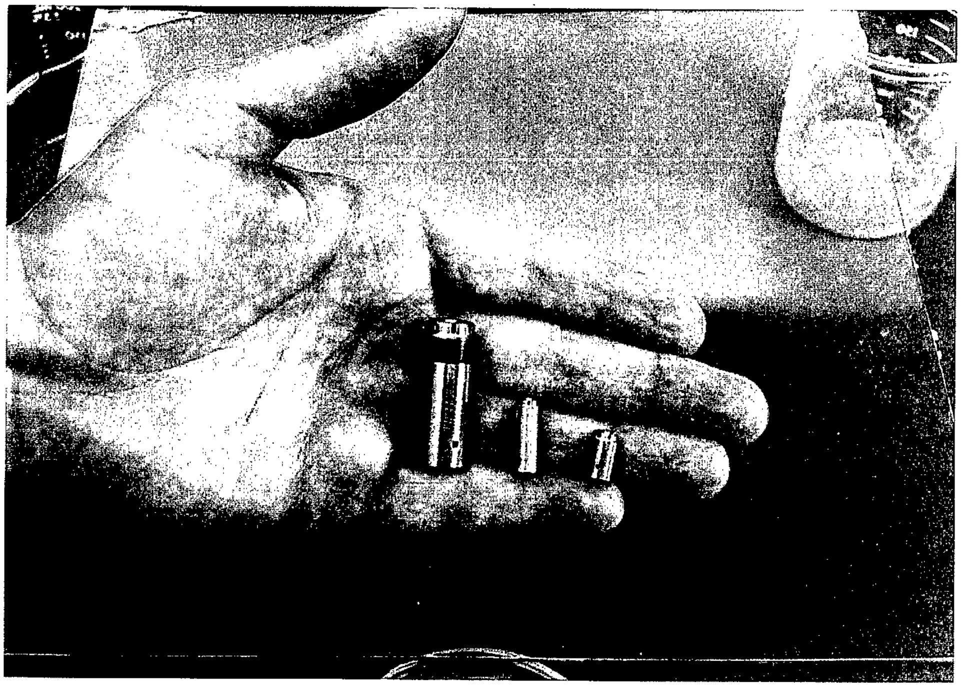

Photograph 1. Three early Motive Cell prototype configurations.

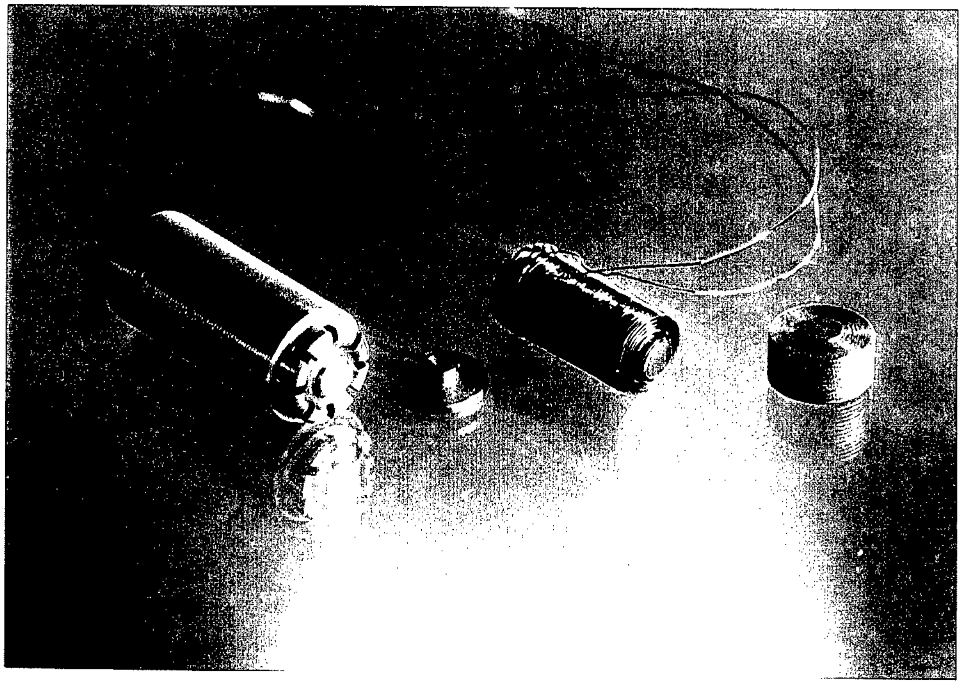

Photograph 2. Motive Cell before assembly

This page intentionally left blank.

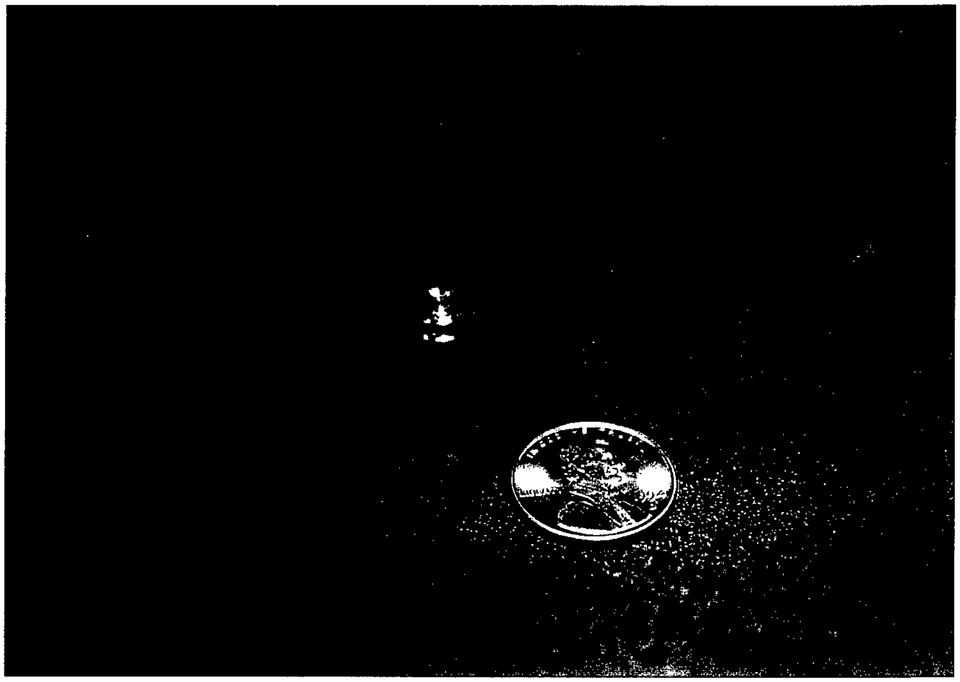

Photograph 3. Motive Cell for frequency response testing.

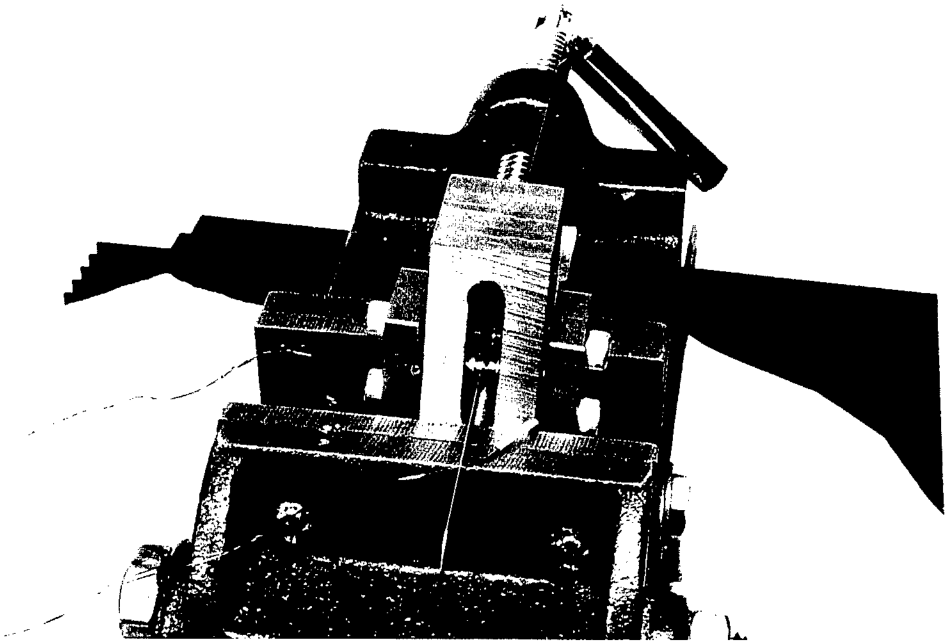

Photograph 4. Motive Cells as brakes, testing wear and forces on shaft materials.

This page intentionally left blank.

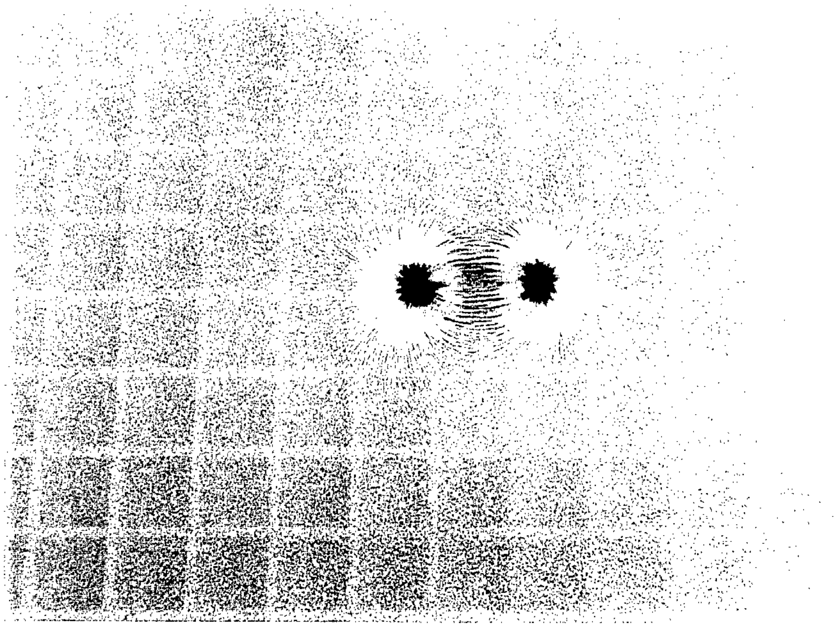

Photograph 5. Magnetic circuit testing, coil and Terfenol-D.

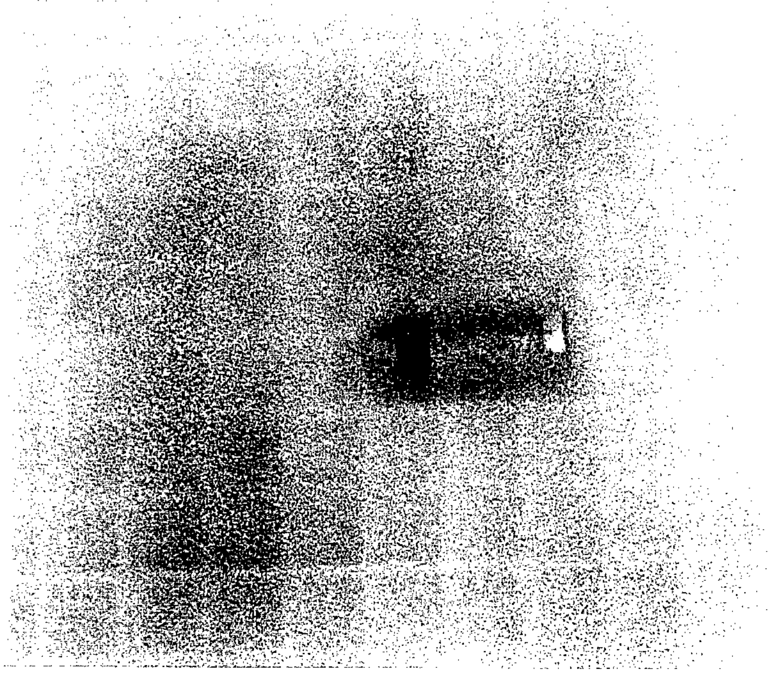

Photograph 6. Magnetic circuit testing, Motive Cell with flux return element.

This page intentionally left blank.

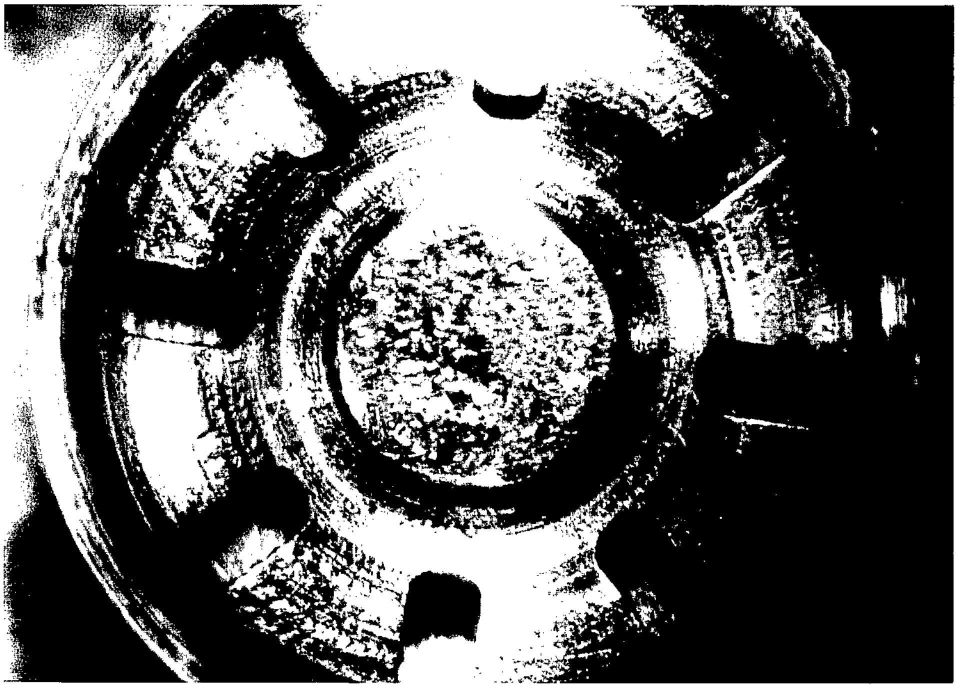

Photograph 7. Failure study, wear on Motive Cell brake pad.

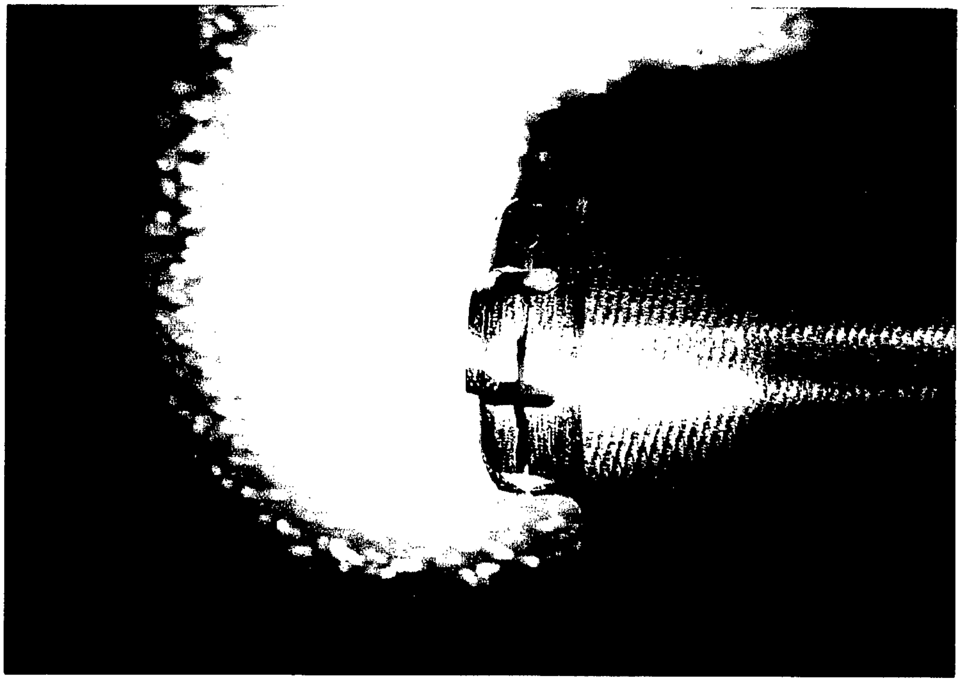

Photograph 8. Failure study on flexure failure. Failure due to poor machining tolerances.

This page intentionally left blank.

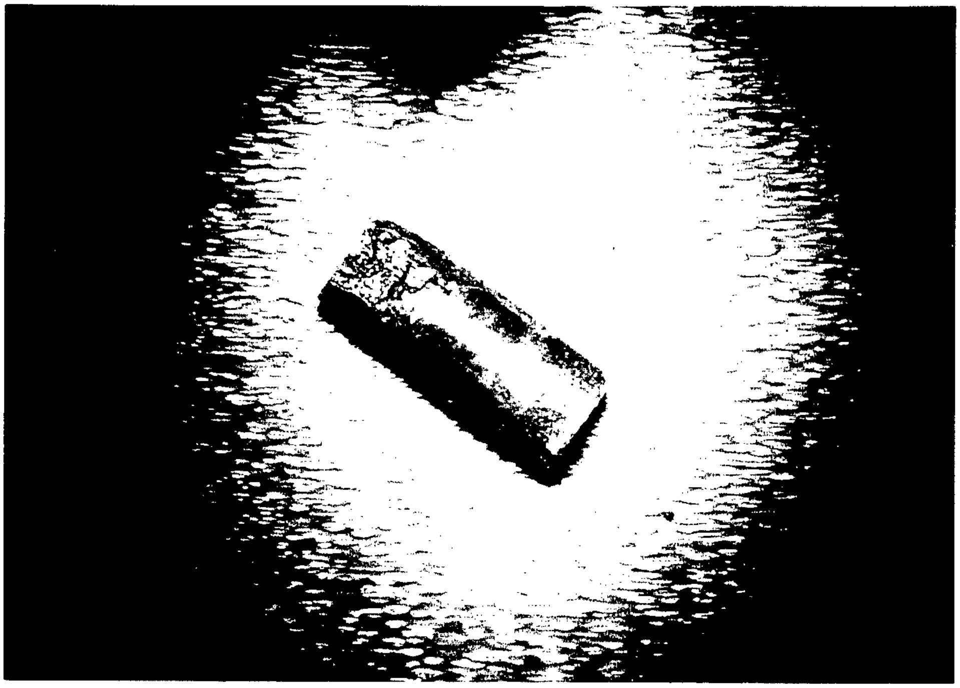

Photograph 9. Terfenol-D rod failure due to over tightening Motive Cell.

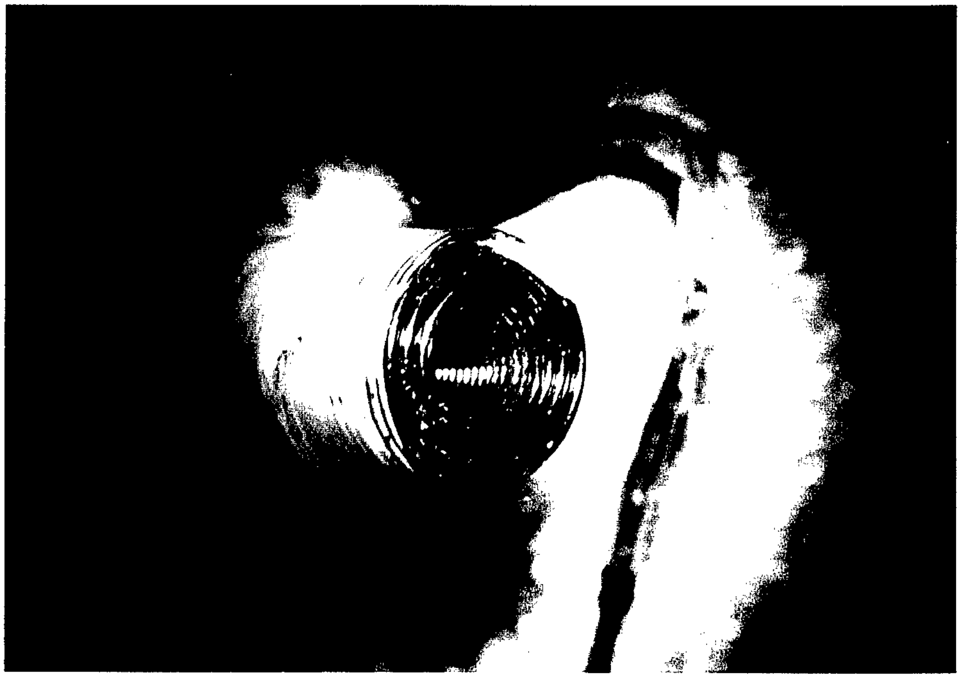

Photograph 10. Motive Cell failure due to insulation wear on driving coil.

This page intentionally left blank.

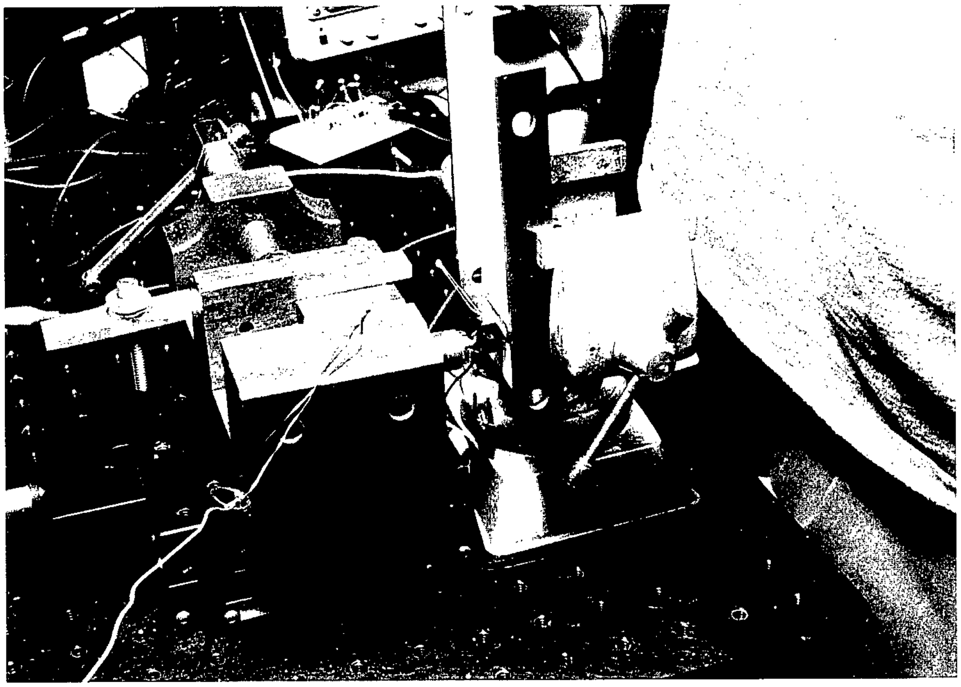

Photograph 11. Motive Cell frequency response testing setup.

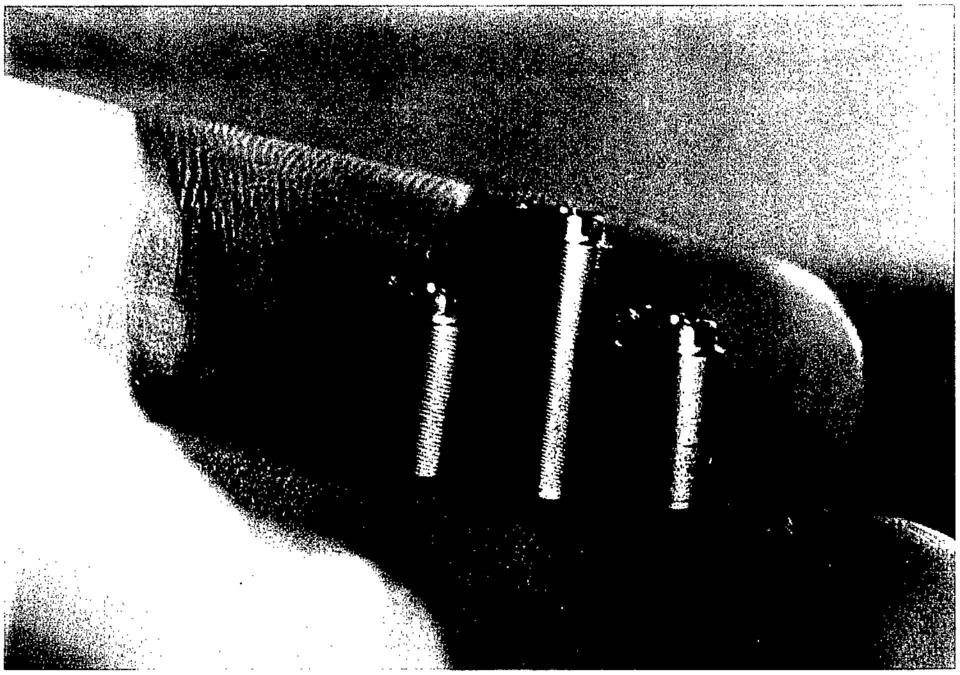

Photograph 12. Selected Motive Cell sizes to be integrated into final motor.

This page intentionally left blank.

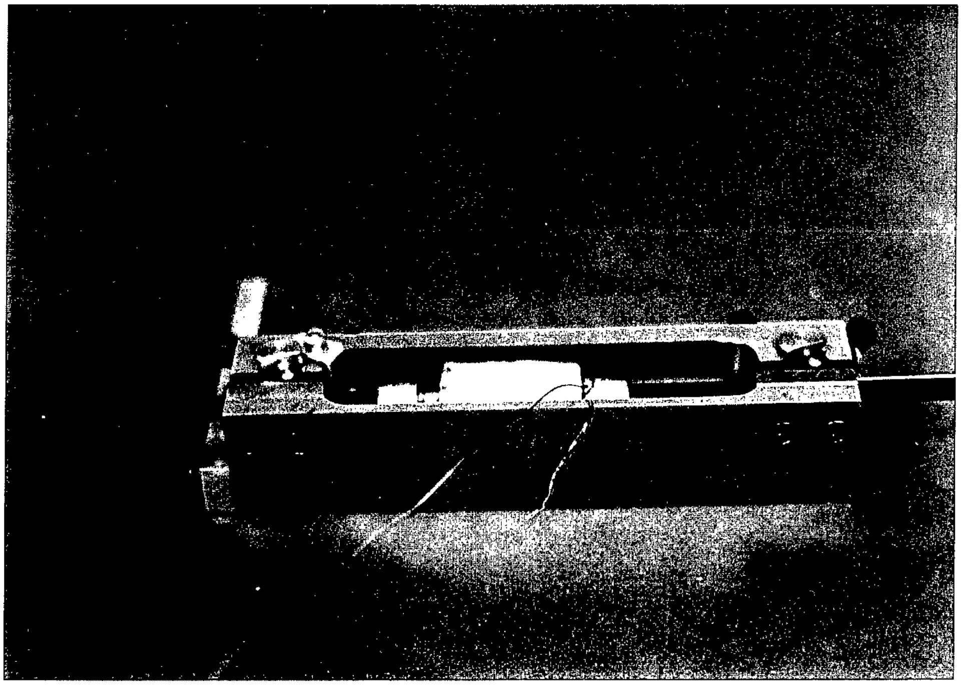

Photograph 13. Inchworm concept, brake test prototype.

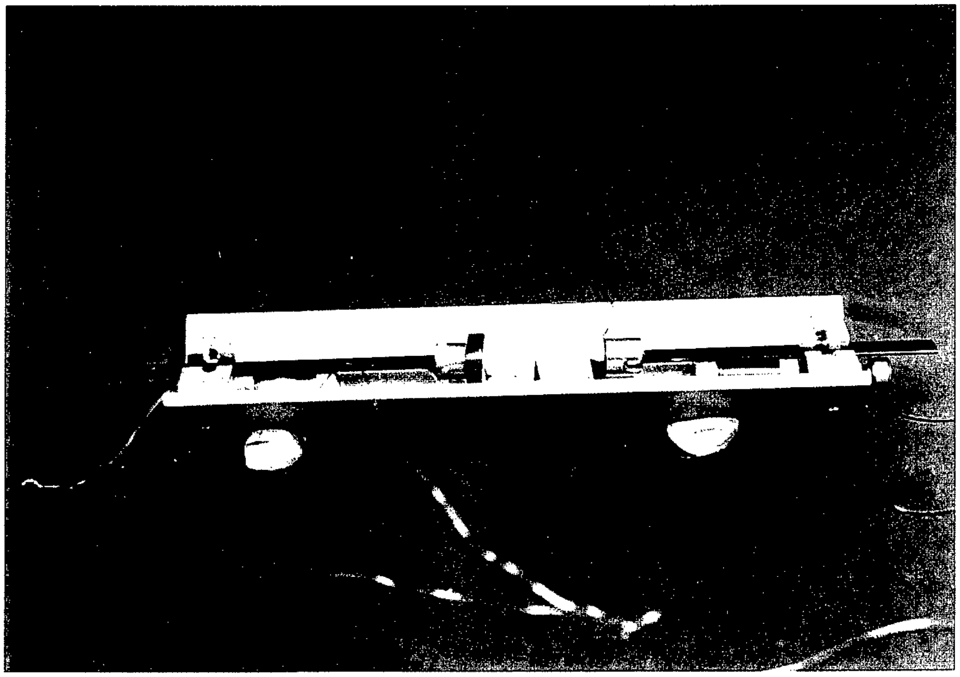

Photograph 14. Inchworm concept test prototype.

This page intentionally left blank.

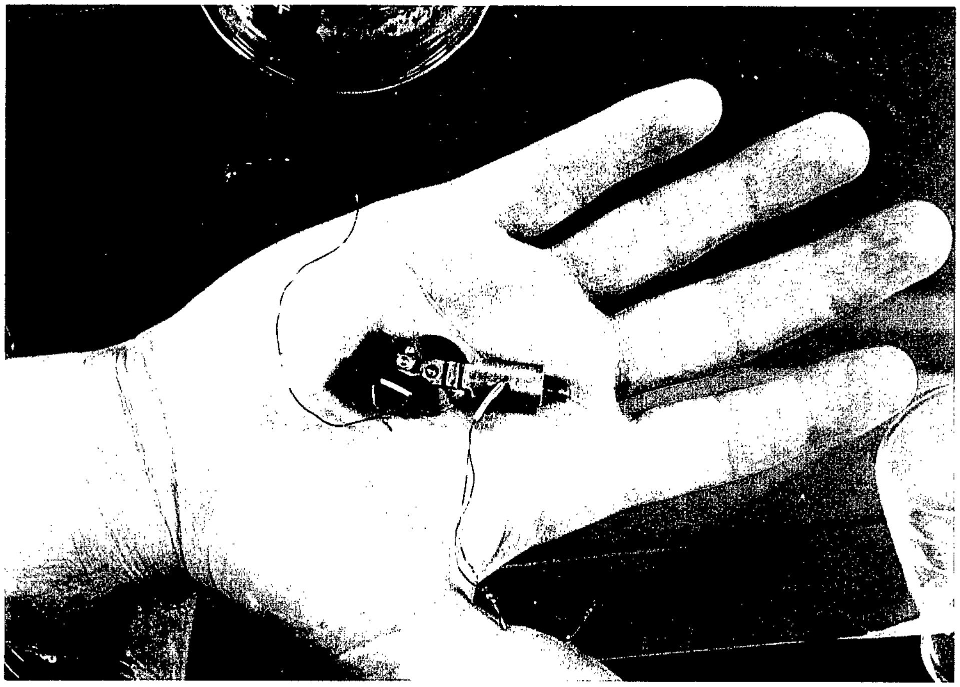

Photograph 15. Two element motor concept prototype.

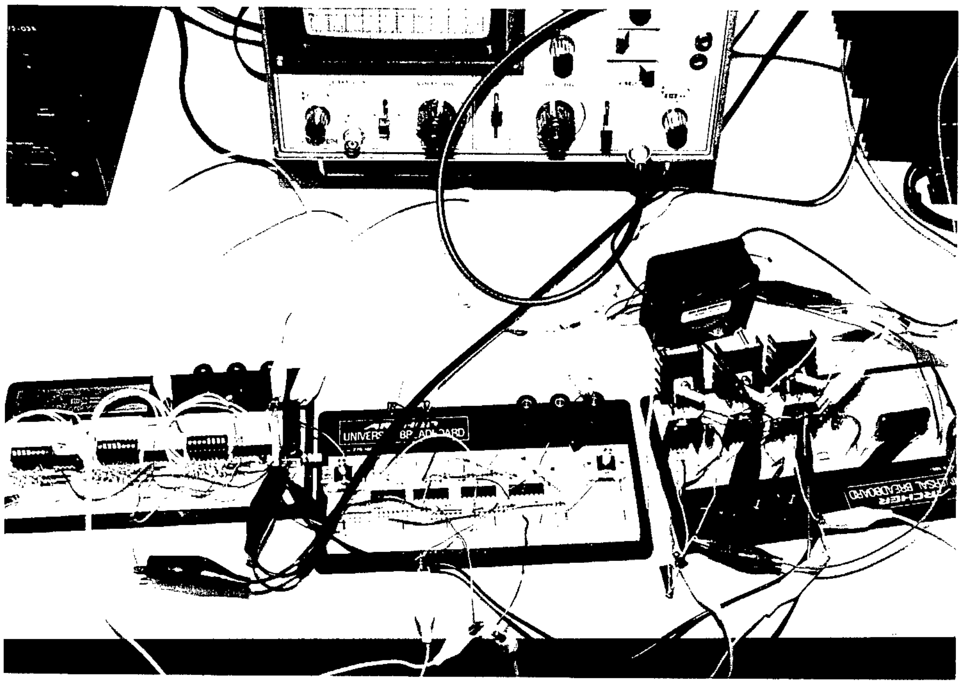

Photograph 16. First generation drive circuits.

This page intentionally left blank.

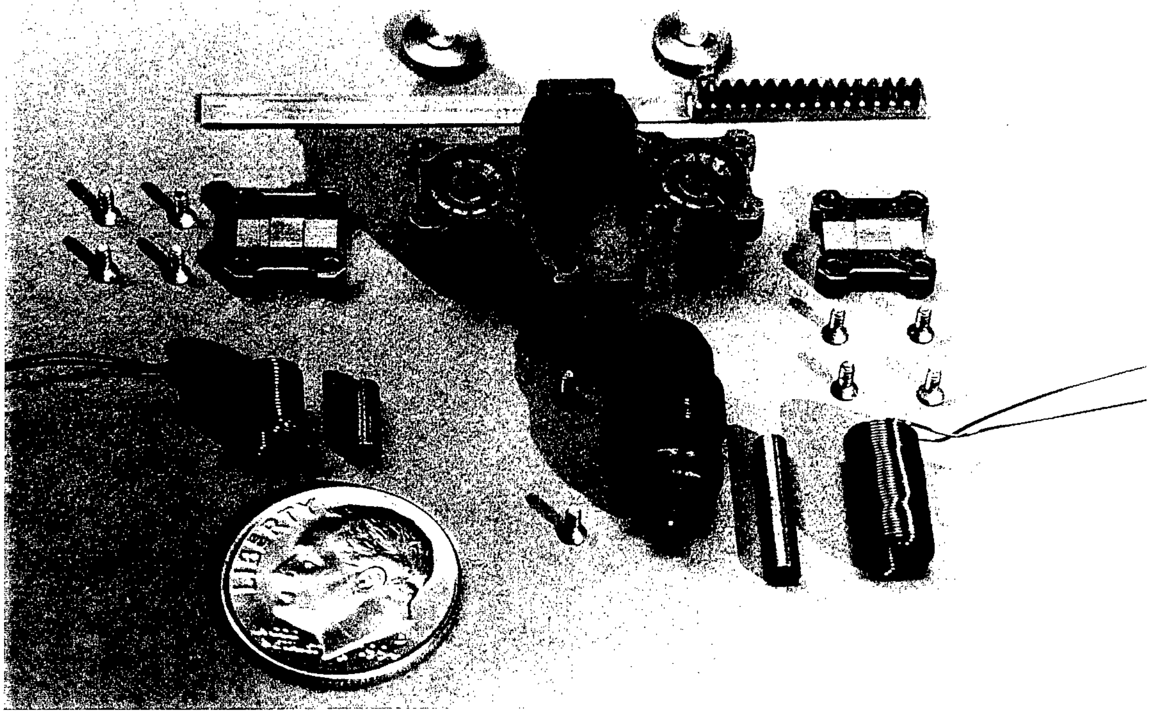

Photograph 17. Phase II inchworm motor before assembly.

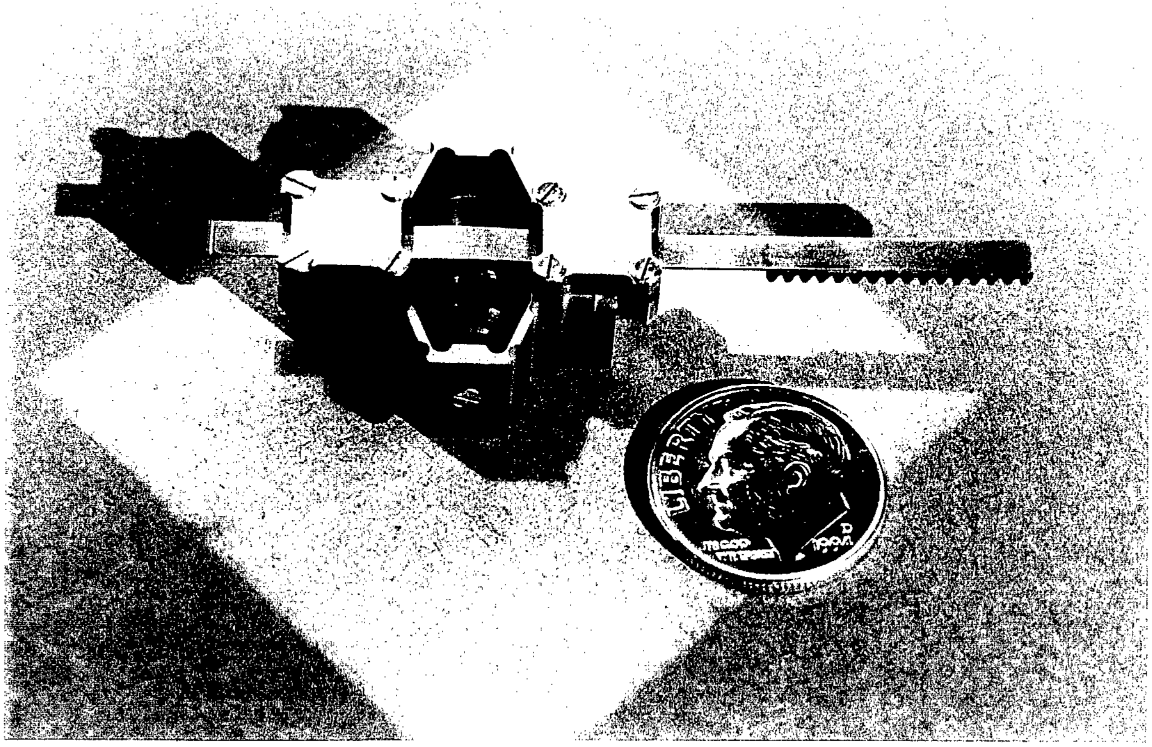

Photograph 18. Assembled Terfenol-D inchworm motor.

This page intentionally left blank.

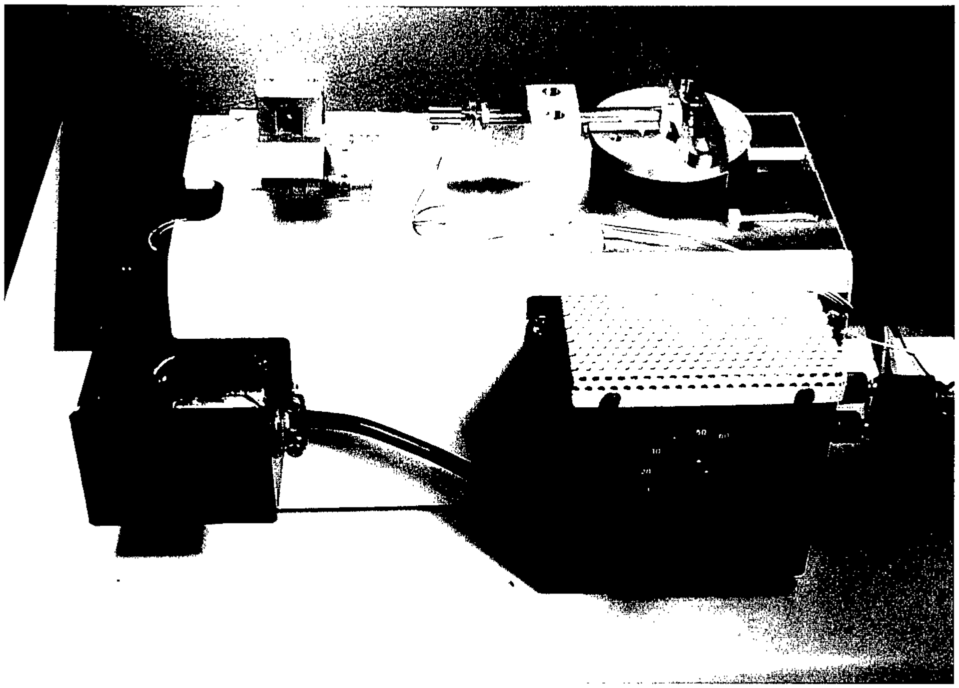

Photograph 19. Force testing apparatus.

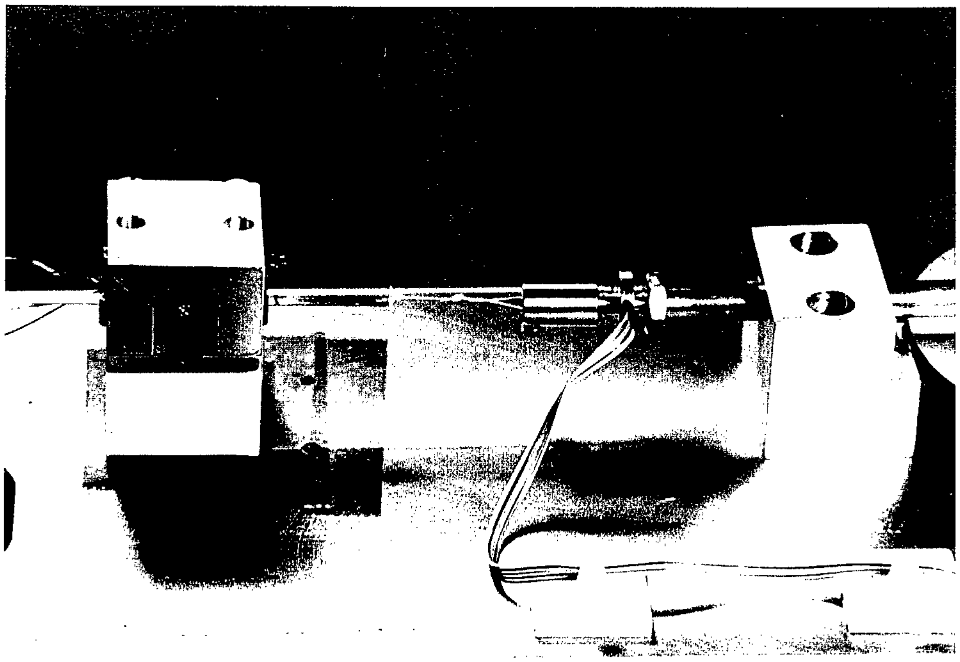

Photograph 20. Inchworm motor coupled to load cell on force, and position control.

This page intentionally left blank.

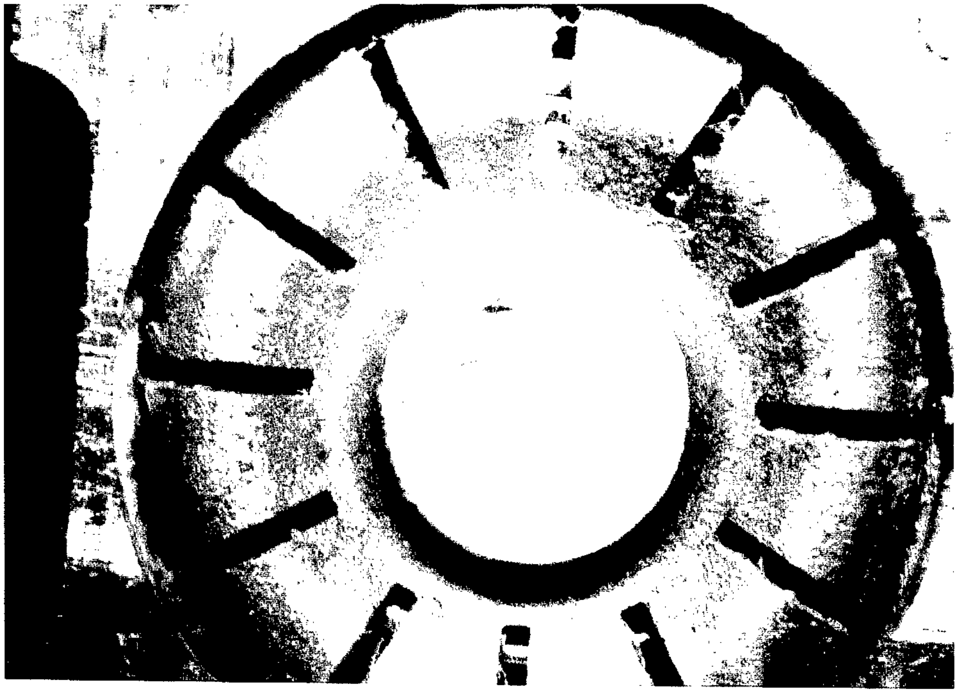

Photograph 21. Wear study on inchworm motor Motive Cell pad.

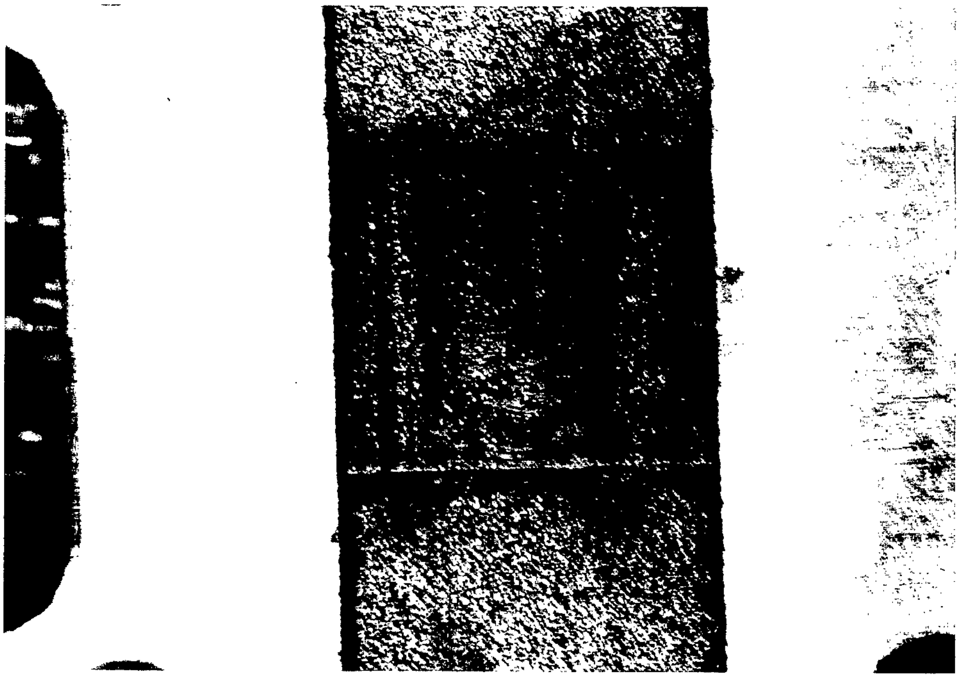

Photograph 22. Wear study on inchworm motor brake pad.

This page intentionally left blank.

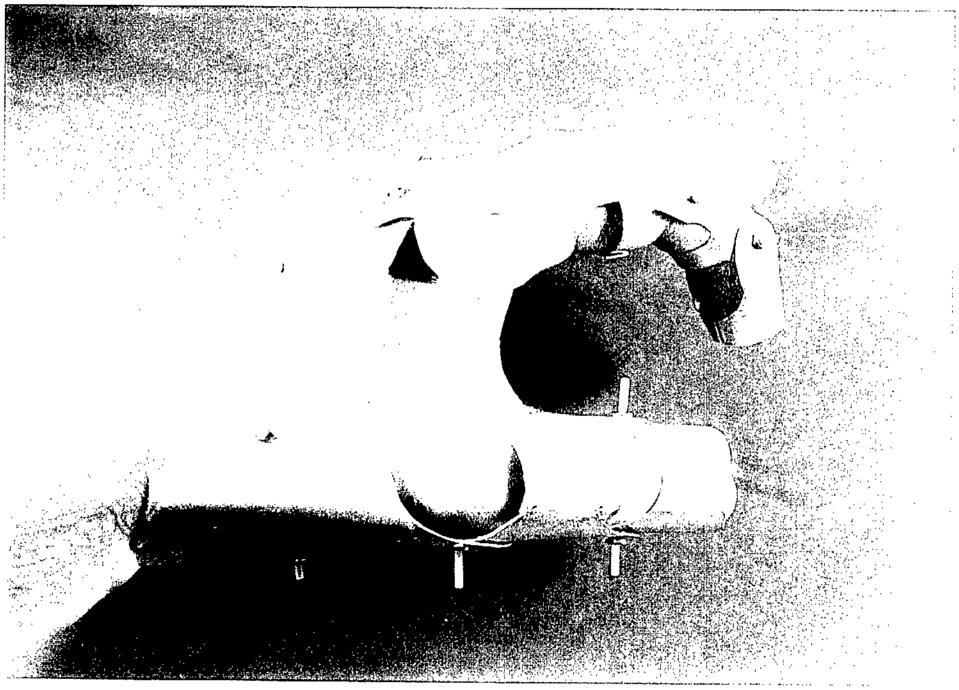

Photograph 23. Exoskeleton joint study prototype.

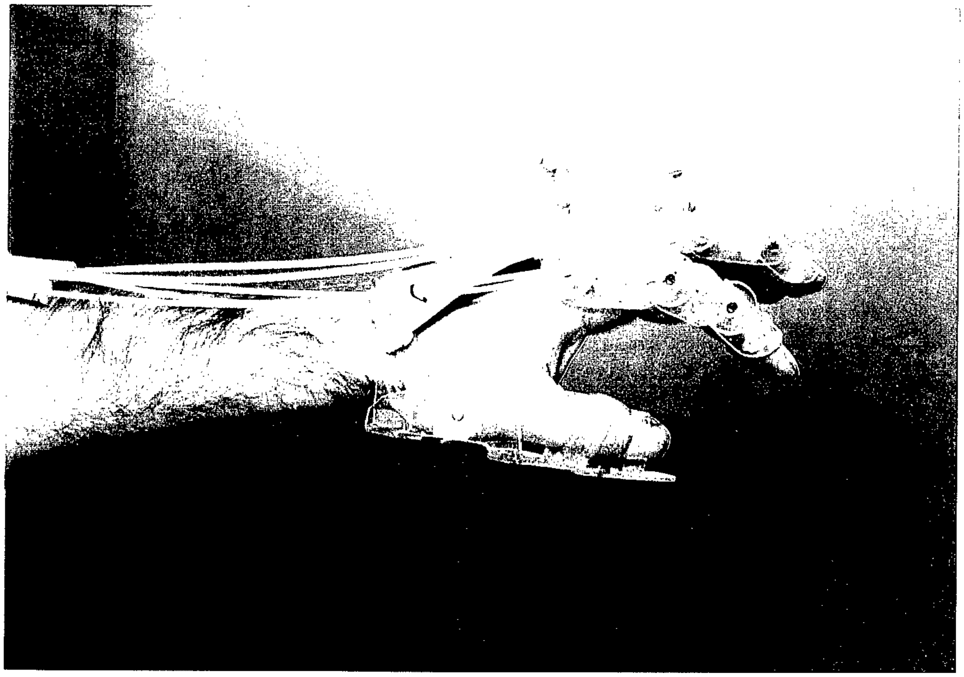

Photograph 24. Exoskeleton joint study prototype.

This page intentionally left blank.

Photograph 25. Joint coupled exoskeleton prototype.

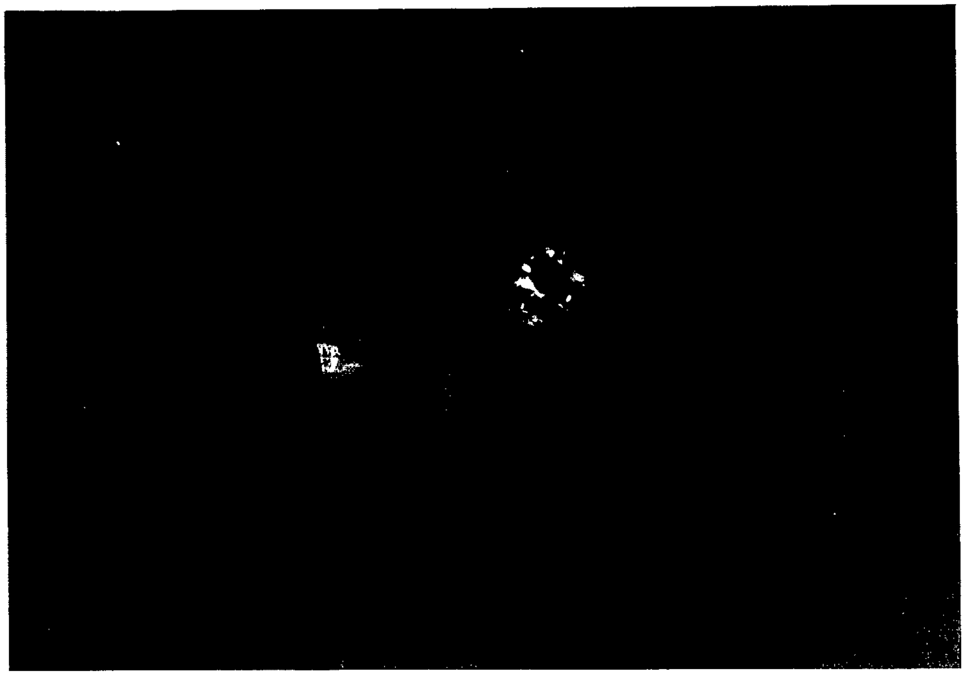

Photograph 26. Novel polarizer angle sensor.

This page intentionally left blank.

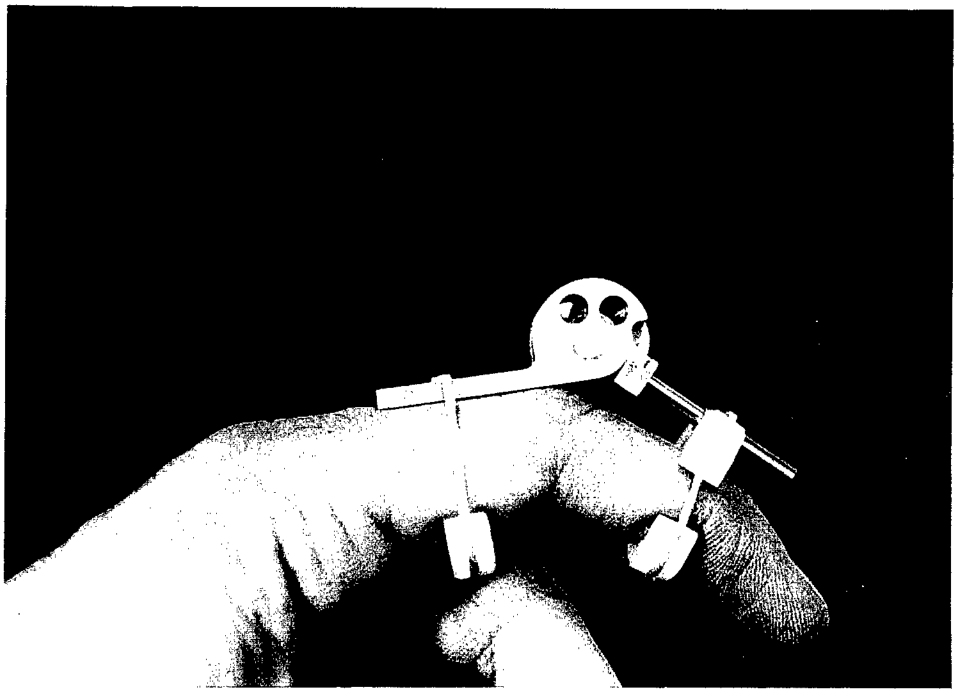

Photograph 27. Embedded angle sensor, joint study.

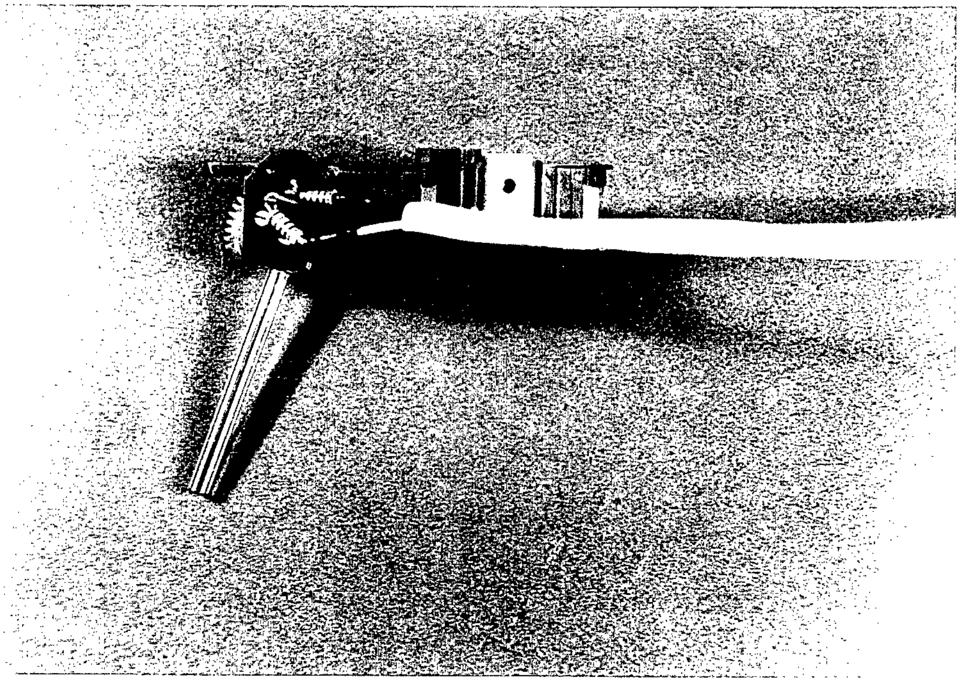

Photograph 28. Integrated rack and pinion joint, inchworm motor and angle sensor.

This page intentionally left blank.

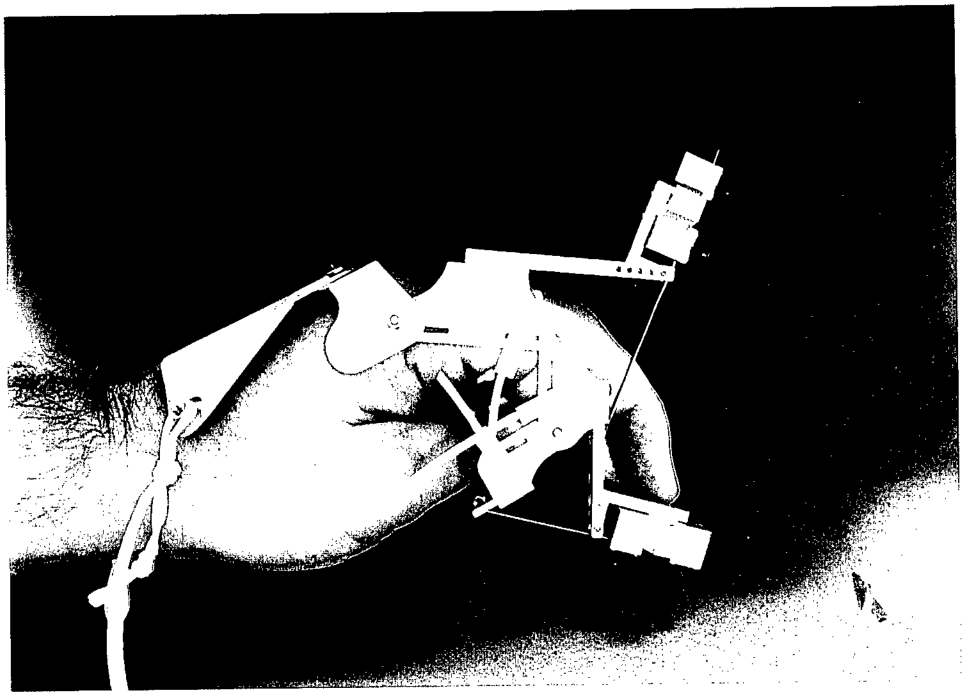

Photograph 29. Pinned joint exoskeleton study with inchworm motor integration.

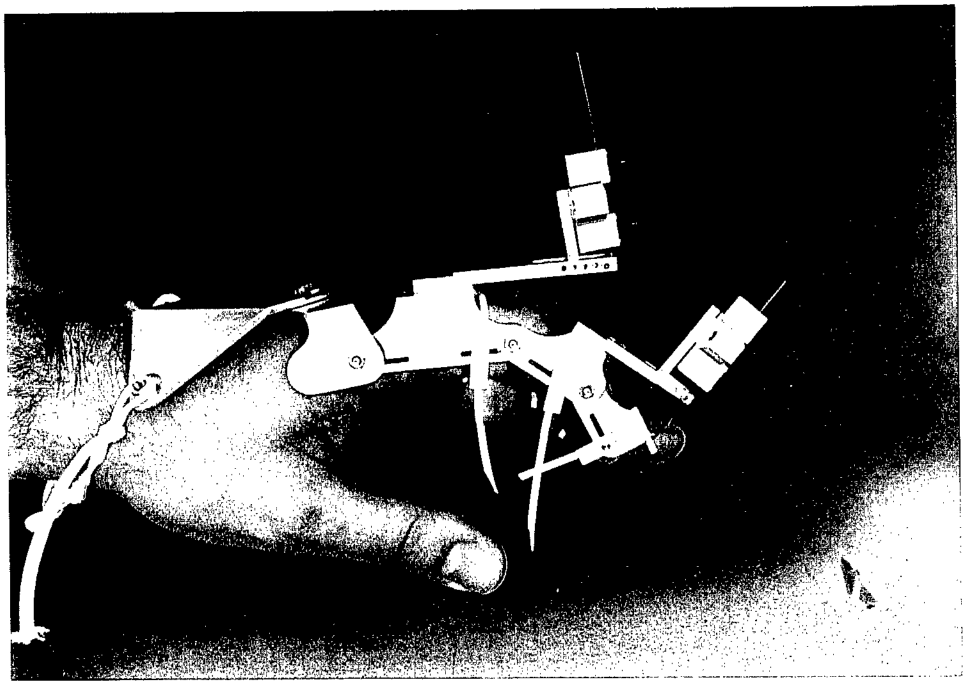

Photograph 30. Pinned joint exoskeleton study with inchworm motor integration.

This page intentionally left blank.

Photograph 31. Virtual Joint prototypes.

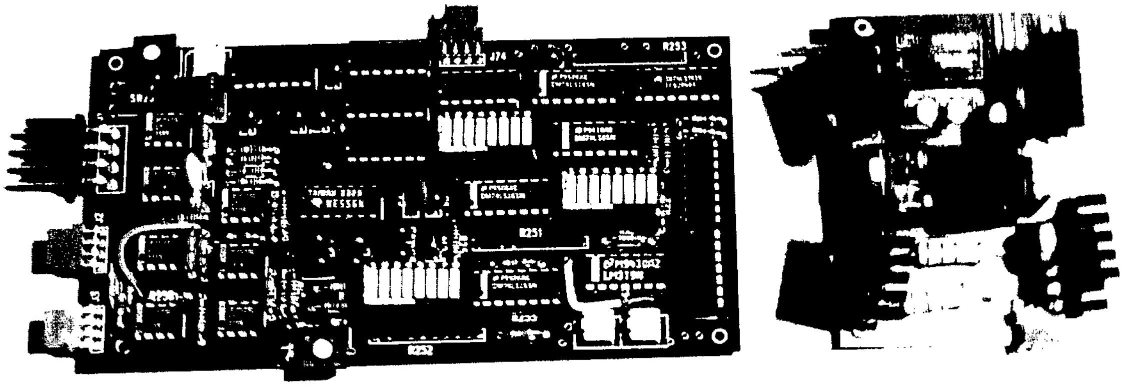

Photograph 32. Inchworm motor controller board, and motor switches.

This page intentionally left blank.

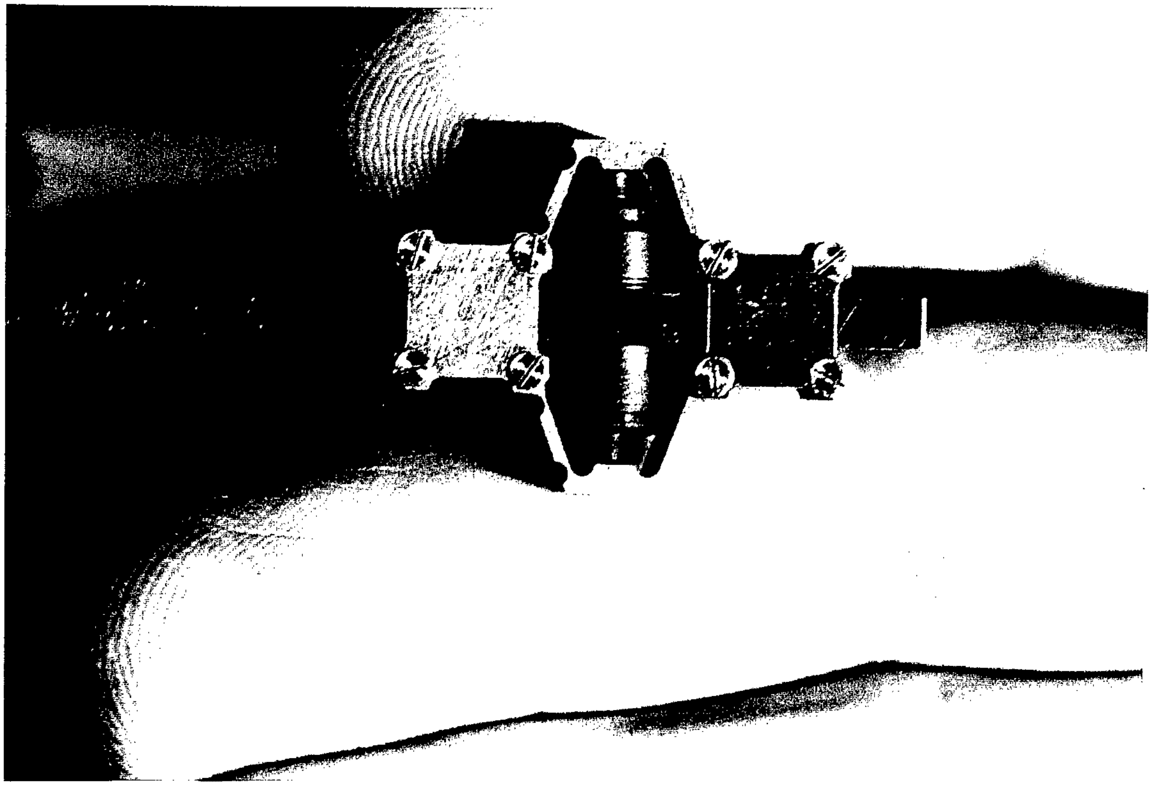

Photograph 33. Phase II final inchworm motor prototype.

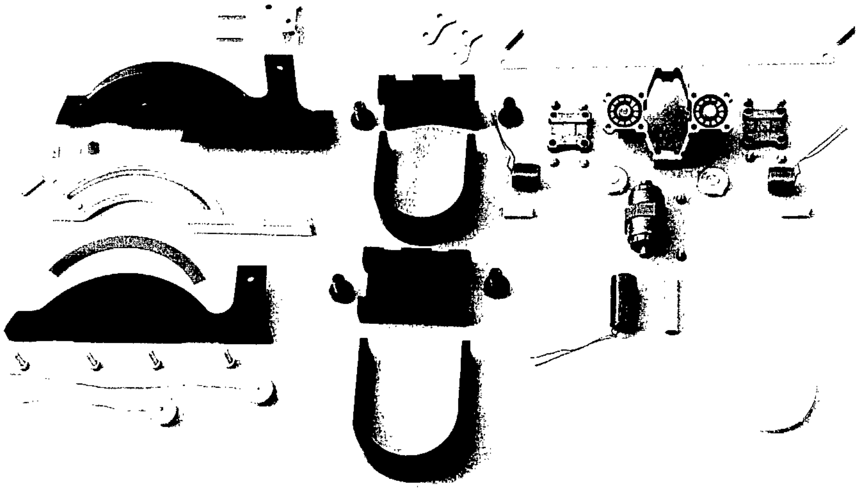

Photograph 34. Exploded assembly photograph showing virtual joint and motor.

This page intentionally left blank.

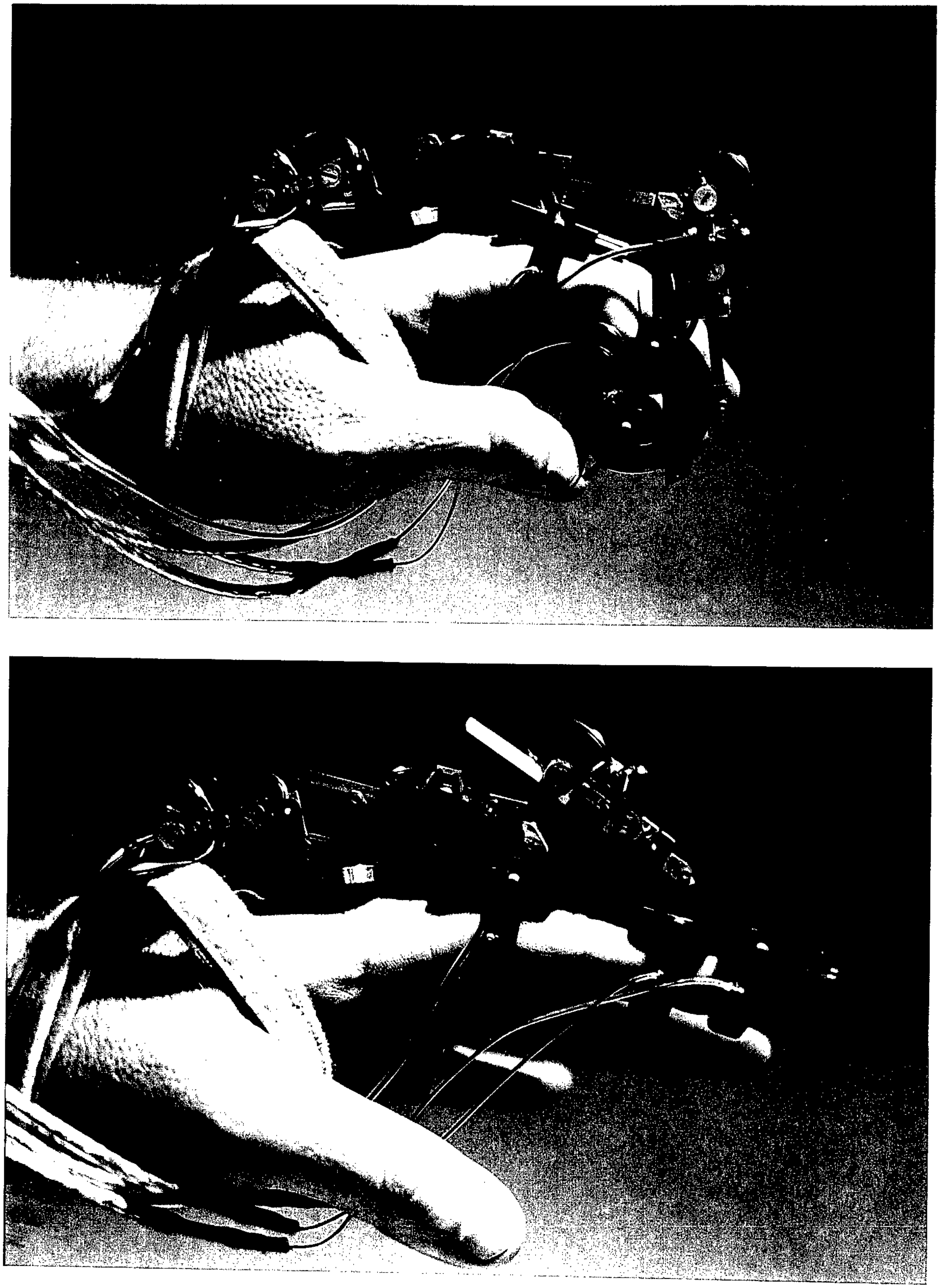

Photograph 35. Final Phase II prototype, virtual joint exoskeleton. Three joint finger with imbedded polarizer angle sensors, Terfenol-D inchworm motors, and strain gage load cells.

This page intentionally left blank.

◆ Conclusions & Recommendation ◆

During the course of this SBIR Phase II project we have developed a novel magnetostrictive inchworm motor driven by Terfenol-D. It is appropriately scaled for dexterous exoskeletal feedback systems. The motor has demonstrated several new concepts and features previously untested using Terfenol-D. They include the following:

Low voltage device.
Small Size ~ 3 cc.
Weight ~ 16 grams
Forces compatible with human finger joints forces. ~ 10 N (per brake, i.e. 20 N max.)
Velocity compatible with human finger joint velocities. 14.5 cm/sec =
Rapid response time. 0.2 msec compatible with human tactile senses.
High Frequency Driving (brakes to 10 kHz, motor to 5 kHz).
Digital pulse control.
Adjustability, i.e.. Locked or Freely backdrivable when power is off.
Pulse Width Modulation Speed control.
Pulse Width Modulation Force control.
Current control of Force.
Arbitrary force generation.
Arbitrary force tracking.
Constant force tracking on a moving object.
Modular, mass production compatible.

In addition to the development of the new Terfenol-D motor prototypes we also developed several viable exoskeletal methods to integrate with the new motor. A new small geometry angle sensor was developed using polarizing elements. In this project the system of study included the human hand, force actuators, position sensors, force sensors, exoskeletal structure, electrical controllers, computer, software and ergonomic issues. Each of these elements also has subsystems such as coils, Terfenol-D, etc., which had to be developed in order to complete the overall goal of a demonstration exoskeletal joint with force feedback. The nature or broad scope of the project and its funding limits sculpted the final efforts. A broad understanding of the problem has been achieved and solutions to the problem have been identified. Patentable, state of the art systems have been designed, fabricated and tested. But much room for improvement can be identified. While the device developed for this project demonstrates size, force and velocity characteristics appropriate to the task at hand it can be significantly improved with some fairly simple design changes. Also solutions to the exoskeletal issues have been developed. Implementation of exoskeleton also needs improvement. The rudimentary software control and interface needs improvement. We have identified a number of problems and developed viable solutions but implementation will wait for future funding.

One of the most limiting parameters is the operational frequency. The motor, as built, is not particularly efficient above 5 KHz and driving the motor at 5 KHz creates a noise problem for this application. We have not addressed the noise problem at this point of the project since the longer range goal was to develop a system that would operate above the audible range. Design for operation at higher frequencies has other advantages, such as increasing the energy density and improving heat transfer characteristics.

The exoskeletal virtual joints developed in this project also show significant promise. They provide a rigid, yet size adjustable platform. The system places the magnetostrictive actuators, virtual axes, and angle sensors out of the way of grasping motions, on the back of the fingers. The Terfenol-D motor/exoskeleton integration is in it's "Rube Goldberg" stage and needs future refinement and simplifying optimization. In continuing research the Terfenol-D motors could be imbedded into this virtual joint structure reducing bulk and streamlining the system. The motors have a high frequency response which could facilitate the development of an integrated tactile / force feedback system with a single digitally controled inchworm motor /actuator.

In summary, Terfenol-D based actuators show great promise as both a force actuators and a high fidelity integrated tactile/force actuators. The technology is still in its infancy when compared to DC motors, hydraulics, etc., but has inherent advantages such as energy density, and response time. The broader topic of anthropomorphic dexterous robotics and force feedback is also just getting a good start toward its desired long range objectives. The continued development of high energy density magnetostrictive devices could very well aid in overcoming exoskeletal related obstacles such as size, force, velocity, weight and fidelity.

Bibliography

Brimhall, O.D., Hasser, K.J., Magnetostrictive Linear Devices for Force Reflection in Dexterous Telemanipulation, Proceedings SPIE Smart Structures and Materials, Smart Structures and Intelligent Systems, Vol. 2190, 508-519, 1994.

Brimhall, O.D. "Advanced Development of New Actuators for Human Sensory Feedback", (TRA - Phase II SBIR Proposal, 1993).

Brimhall, O.D., et al, Magnetostrictive Actuators for human Sensory feedback, Feb 1993, Final Report, Armstrong Laboratory, U.S. Air Force, Cont. No. AL/CF-TR-1993-0074.

Brimhall, O.D., Linear Actuator Apparatus and Method, U.S. Patent # 5,389,845, 1995.

Brimhall, O.D., Kinesthetic Feedback Apparatus, U.S. Patent #, 5,396,266, 1995 Kinesthetic Feedback Apparatus.

Buchholz B, Armstrong TJ, "An Ellipsoidal Representation of Human Hand Anthropometry," Human Factors 33(4):429-441, 1991.

Buchholz B, Armstrong T, Goldstein T, "Antrhopometric data for describing the kinematics of the human hand", Ergonomics 35:261-273, 1992.

Buchholz B, Armstrong T, " A kinematic model of the human hand to evaluate its prehensile capabilities", J Biomechanics 25(2): 149-162m 1992.

Burdea G., et al., "Virtual Reality Graphics Simulation with Force Feedback", Core Bldg. CAIP Center, Rutgers University, NJ.)

Burdea G., and Zhuang J., "Dexterous telerobotics with force feedback - an overview. Part 1: Human factors," Robotica 9:171-178, 1991.

Burdea G., and Zhuang J., "Dexterous telerobotics with force feedback - an overview. Part 2: Control and implementation," Robotica 9:171-178, 1991.

Butler, John L. "Application of Manual for the Design of ETREMA Terfenol-D Magnetostrictive Transducers ", EDGE Technologies, Inc. 1988.

Chang, S., et al., "Sensing, Perception, and Feedback for Virtual Reality" *VR Systems Conference*, Manhattan, NY, Oct 1993.

Chappell, P.H., and Kyberd, P.J., "Prehensile control of a hand prosthesis by a microcontroller," J. Biomed. Eng. 134:363-369, 1991.

Chodack, J., P. Spampinato, "Spacesuit Glove Thermal Micrometeoroid Garment Protection Versus Human Factors Design Parameters" *Proc. SAE Conf on Space Station and Advanced EVA*, (Society of Automotive Engineers, Publication No. SP-872 ISBN 1-56091-152-2) pp. 67-83 (July 1991).

Clark, A.E., Verhoven, J.D., McMasters, O.D., Gibson, E.D, "Magnetostriction in Twinned [112] Crystal of $Tb_{.27}Dy_{.73}Fe_2$", (ETRAMA Products, Inc., Ames, Iowa) pp. 16.

Delaney, B., "Its Own Little Worlds", *The Star-Ledger* (Wed, Oct 14, 1992).

Fanson, J.L., Blackwood, G.H. and Chu, C.C., 1989, "Active-Member Control of Precision Structures, " Proceedings, 28th SDM Conf., Montery, CA, pp.588-598.

Flatt A.E., and Fischer G.W., "Restraints of the metcarpophalangeal joints: a force analysis," Surgical Forum 19:459-460, 1968.

Garrett, JW. "Anthropometry of the hands of female air force flight personnel", Report No. AMRL-TR-69-26, Aerospace Medical Research Laboratory, Aerospace Medical Division, Air Force Systems Command, Wright-Patterson AFB, Ohio, 1970.

Garrett, J.W. "Anthropometry of the hands of male air force flight personnel," Report No. AMRL-TR-69-42, Aerospace Medical Research Laboratory, Aerospace Medical Division, Air Force Systems Command, Wright-Patterson AFB, Ohio, 1970.

Goodfriend, Mel, Edge Technologies, "Materials Breakthrough Spurs Actuator Design", Machine Design, March 21, 1991, pp. 147-150.

Goodfriend, M.J., Shoop, K.M., McMasters, O.D. "Characteristics of the Magnetostrictive Alloy Terfenol-D Produced for the Manufacture of Devices". (ETREMA Products Inc., a subsidiary of Edge Technologies, Inc., Ames, Iowa).

Hasser, C.J., "Force-Reflecting Anthropomorphic Hand Masters", July 1995, AL/CF-TR-1995-0110, Armstrong Laboratory, Crew Systems Directorate, Biodynamics and Biocommunications Division, W-P. AFB.

Hertzberg H.T.E., Daniels G.S., Churchill E., "Anthropometry of Flying Personnel," WADC Technical Report 52-321, USAF Wright Air Development Center, Wright Patterson AFB, Ohio, 1954.

Hollister, A, et al, The Axes of Rotation of the Thumb Carpometacarpal Joint, J Orhopaedic Research, 10:454-460 1992

Hollister, Giuriantano, D., How Joints Move, Clinical Mechanics of the Hand, 2nd, Ed., 1993, Mosby.

Hume M.C., Gellman H., McKellop H., Brumfield R.H., "Functional range of motion of the joints of the hand," Journal of Hand Surgery 15A(2):240-243.

Jensen T.R., Radwin RG, Webster JG, "A conductive polymer sensor for measuring external finger forces," J. Biomechanics 24(9):851-858,1991.

Juvinall, Robert C. Fundamentals of Machine Component Design, John Wiley & Sons, New York. 1983, p.205.
Long, G.L., C.L. Collins, "A Pantograph Linkage Parallel Platform Master Hand Controller for Force Reflection", *Proceedings - IEEE International Conference On Robotics and Automation* 1, pp. 390-395 (1992).

Long, G.L., Collings, C.L., "A Pantograph Linkage Parallel Platform Master Hand Controller for Force Reflection", Proceedings - IEEE Interantional Conference On Tobotics and Automation 1, pp. 390-395 (1992).

"Material Breakthrough Spurs Actuator Design" *Machine Design* Vol. 63, No. 6, p. 147 (21 Mar 1991).

Micks J.E., Reswick J.B., Hager D.L., "The mechanisms of the instrinsic-minus finger: a biomechanical study," Journal of Hand Surgery 3:333-341, 1978.

Pagowski S. and Piekarski K., "Biomechanics of metacarpophalangeal joint," Journal of Biomechanics 10:205-209, 1977.

Poznanski A., The Hand in Radiologic Diagnosis, Second Edition. W.B. Saunders Company, Philadelphia, pp 35-40, 1984.

Shaw J, "Virtual Reality Resource Guide", Virtual Reality 93, Fall Sp. Report, Al Exper, San Fansico, 1993.

Schebor, F.S., J.L. Turney, "Realistic and Consistent Telerobotic Simulation" *Proc of the IEEE International Conf on Systems, Man, and Cybernetics* 2, pp. 889-894 (1991).

Shimoga, K.B., "Perceptual Feedback Issues in Dexterous Telemanipulation: Part I. Finger Force Feedback"

Takahara, K. et al, "Piezo Linear Actuaotrs for Adaptive Truss Structures:, ASME, AD-Vol.15, 1989, pp 83-88.

Tamai K., Ryu J., An K.N., Lincheid R.L., Cooney W.P., Chao E.Y.S., "Three-dimensional geometric analysis of the metacarpophalangeal joint," Journal of Hand Surgery 13A: 521-529, 1988.

Wada, B.K., Fanson, J.L., Crawley, E.F., "Adaptive Structures", ASME, AD-Vol.15, 1989, pp. 1-8.

Walker P.S., Erkman M.J., "Laboratory evaluation of a metal-plastic type of metacarpophalangeal joint prosthesis," Clinical Orthopedics and Related Research 112:349-356.

Wang, W., Busch-Vishniac, "A High Precision Micropositioner Based on Magnetostriction Principal" *Rev. Sci. Instum.* Vol. 63, No. 1, 249 (Jan 1992).

Weightman B., Amis A.A., "Finger joint force predictions related to design of joint replacements," J Biomed Eng 4, 1982.

Wise S. Gardner W., Sabelman E., Valainis E., Wong Y., Glass K., Drace J., Rosen J., "Evaluation of a fiber optic glove for semi-automated goniometric measurements," Journal of Rehabilitation Research and Development 27(4):411-424, 1990.

Youm Y., Gillespie T.E., Flatt A.E., Sprague B.L., "Kinematic investigation of normal MCP joint," Journal of Biomechanics 11:109-118, 1978.

◆ Appendix A ◆

Mechanical Engineering Drawings

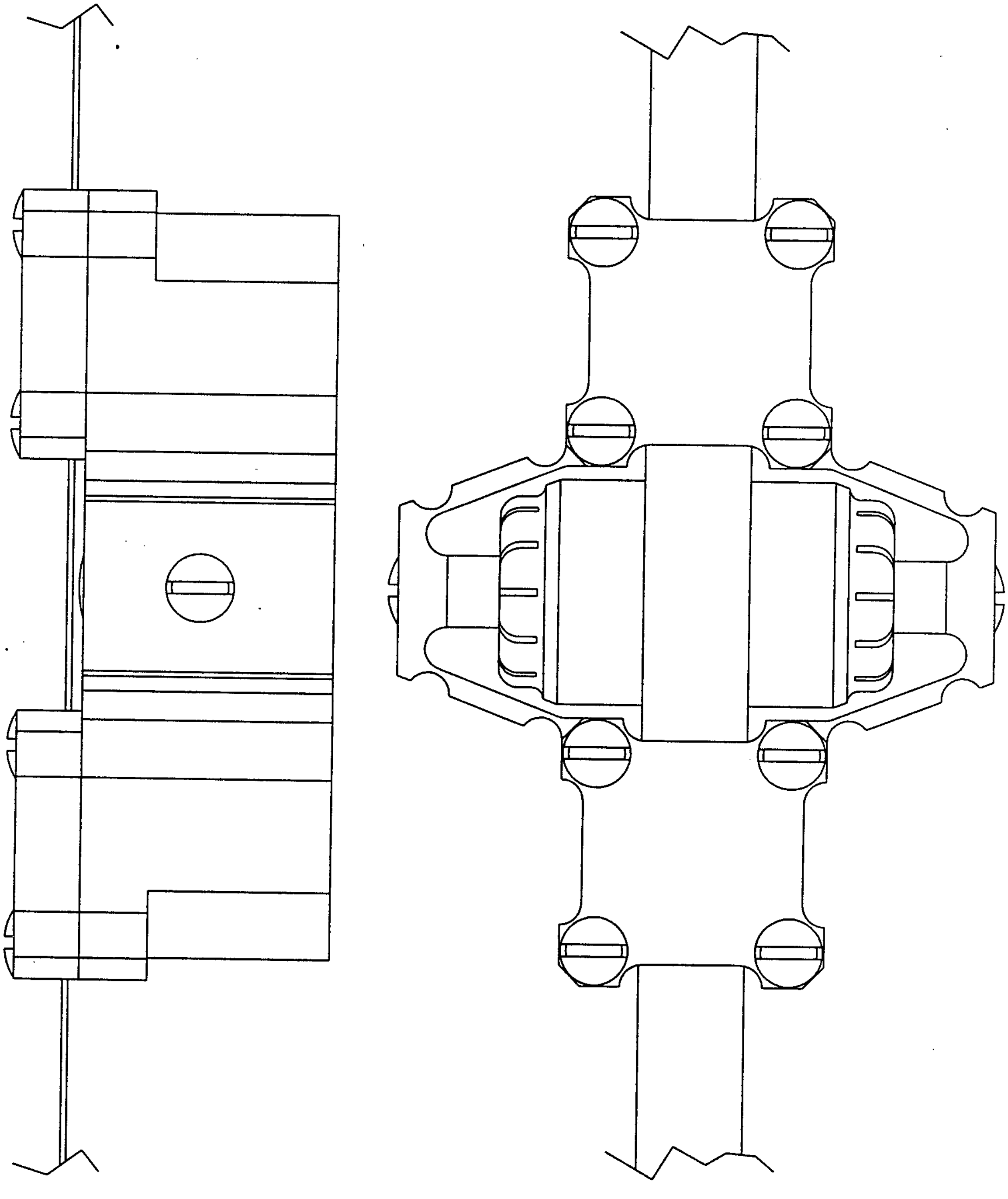

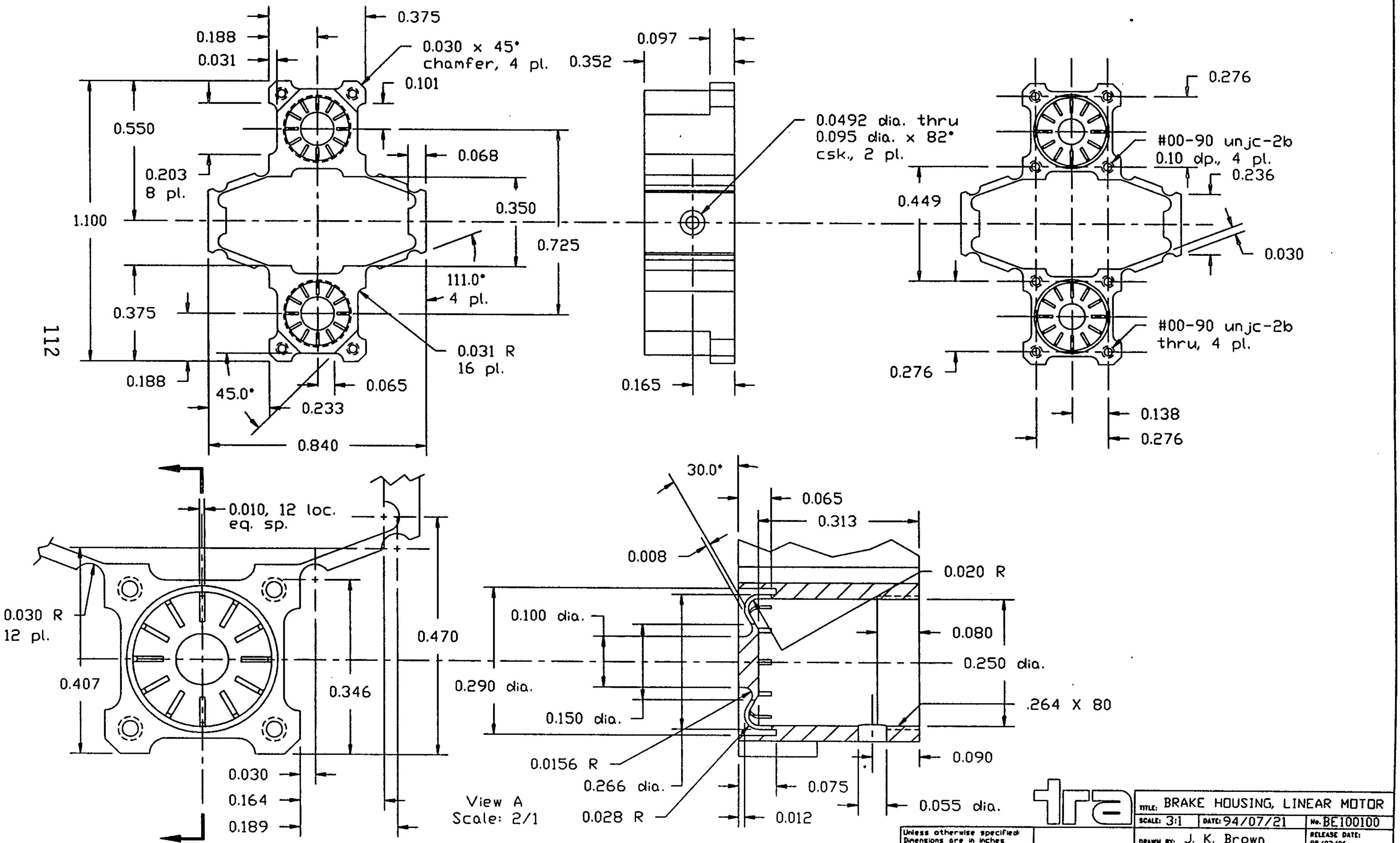

		TITLE: BRAKE HOUSING, LINEAR MOTOR	
		SCALE: 3:1 DATE: 94/07/21	No. BE100100
Unless otherwise specified: Dimensions are in inches		DRAWN BY: J. K. Brown	RELEASE DATE: 95/03/06
Tolerances on angles ± 0° 30' Decimals .XX ± .01, .XXX ± .002	Mat'l: 4130 STEEL Heat Treat : N/A	PROJECT: Actuators II FILE NAME: lmotor1.dep	APPROVAL:

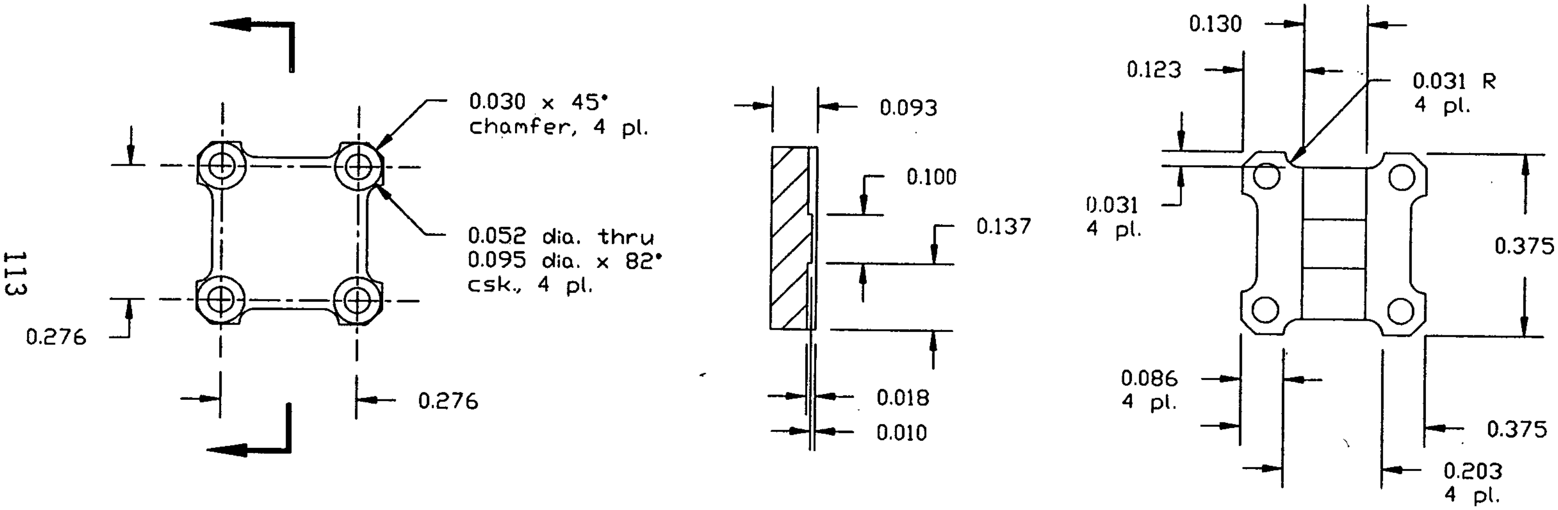

tra

TITLE: BRAKE CAP, LINEAR MOTOR
SCALE: 4:1
DATE: 94/07/27
No. BE100101
DRAWN BY: J. K. Brown
RELEASE DATE: 94/07/27
PROJECT: Actuators II
FILE NAME: lmotor2.dwg
APPROVAL:

Unless otherwise specified:
Dimensions are in inches
Tolerances on angles ± 0° 30'
Decimals .XX ± .01, .XXX ± .002

Matl: 4130 STEEL
Heat Treat : N/A

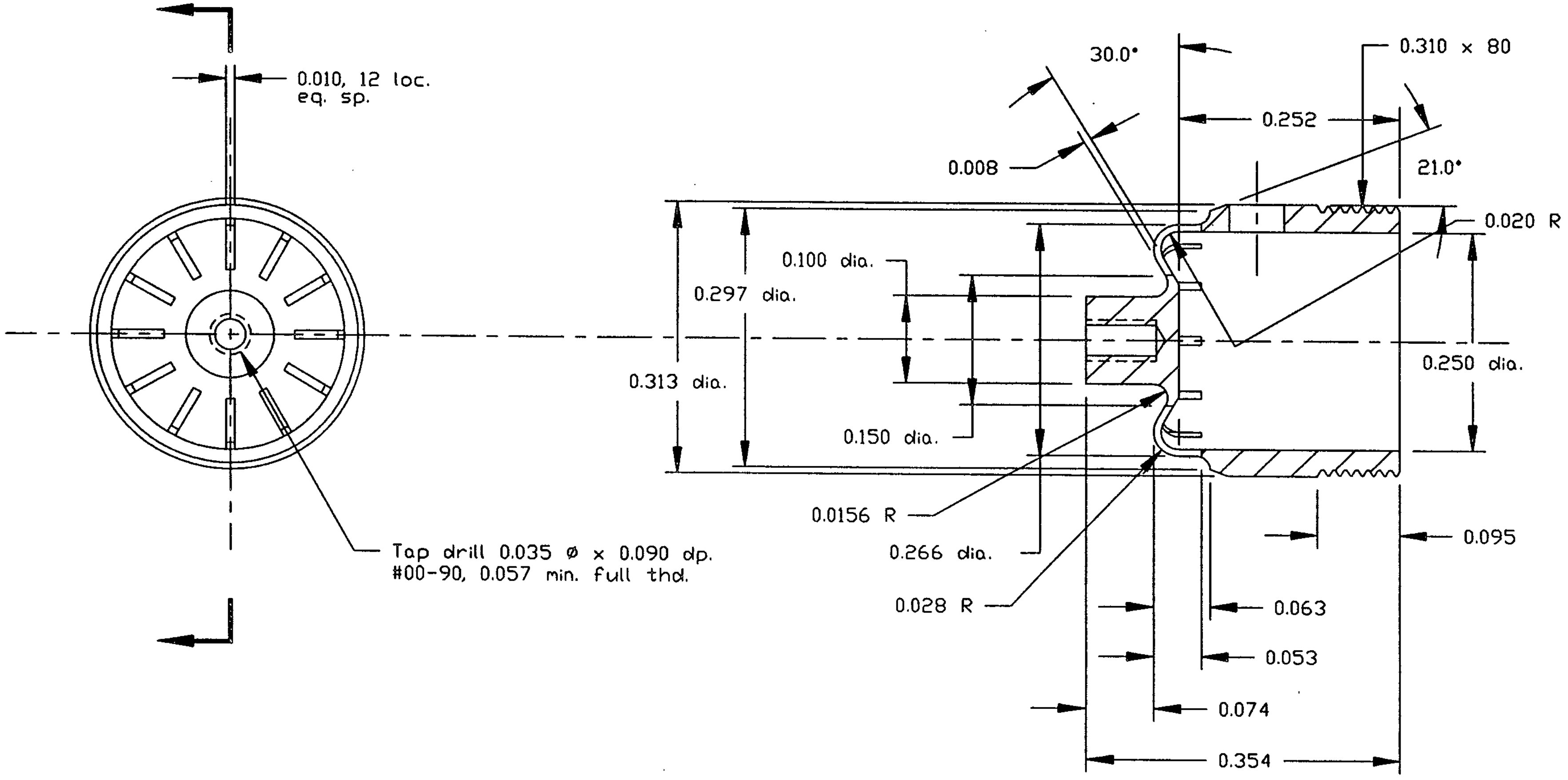

TITLE: MALE END CAP, MOTIVE CELL
SCALE: 8:1
DATE: 94/07/28
No. BE100102
DRAWN BY: J. K. Brown
RELEASE DATE: 94/07/28
PROJECT: Actuators II
APPROVAL:
FILE NAME: lnotor3.dwg
Mat'l: 4130 STEEL
Heat Treat : N/A
Unless otherwise specified:
Dimensions are in inches
Tolerances on angles ± 0° 30'
Decimals .XX ± .01, .XXX ± .002

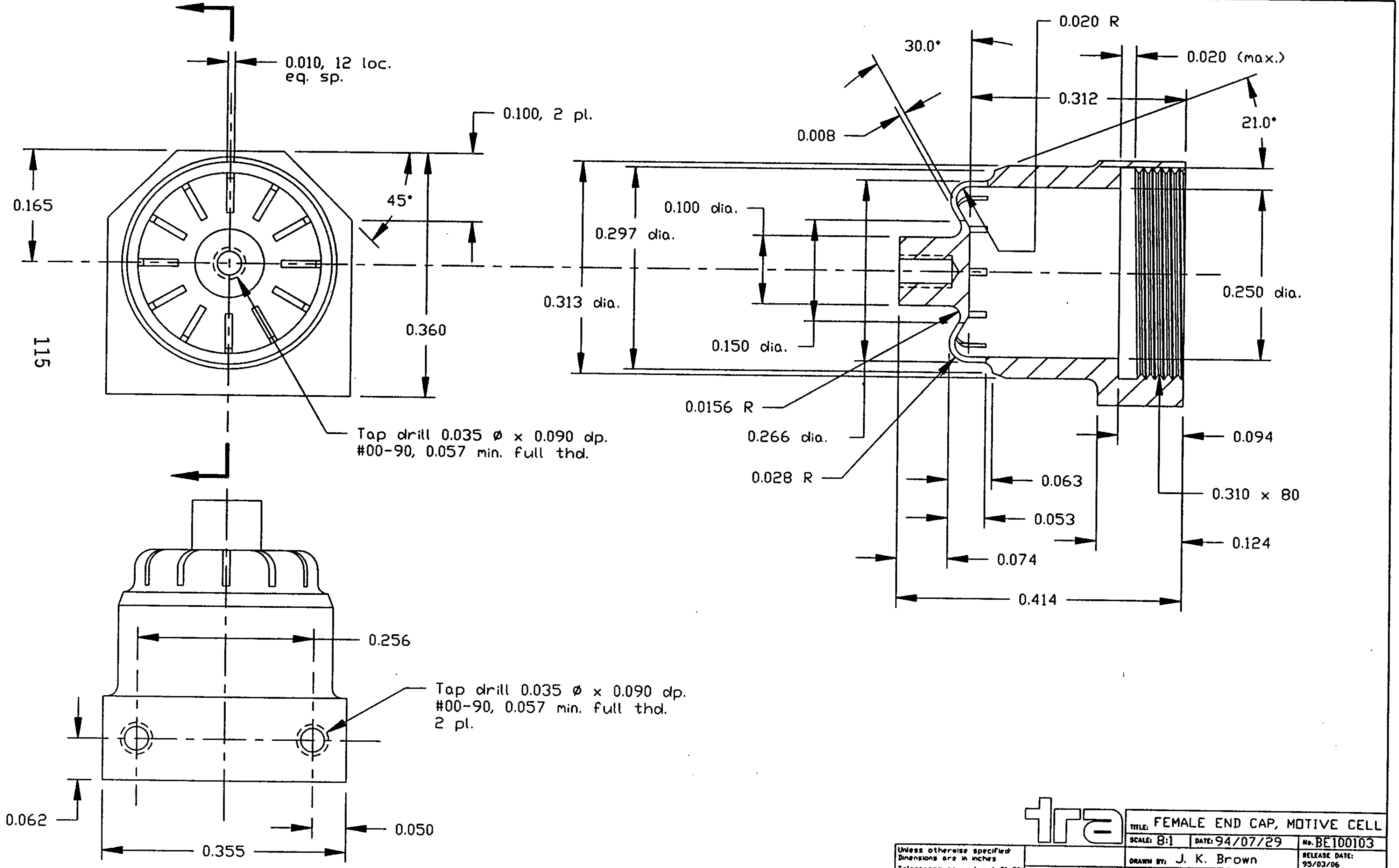

TITLE: FEMALE END CAP, MOTIVE CELL

SCALE: 8:1	DATE: 94/07/29	No. BE100103
DRAWN BY: J. K. Brown		RELEASE DATE: 95/03/06
PROJECT: Actuators II		APPROVAL:
FILE NAME: lnotor4.dwg		

Unless otherwise specified
Dimensions are in inches
Tolerances on angles ± 0° 30'
Decimals .XX ± .01 .XXX ± .002

Matl: 4130 STEEL
Heat Treat : N/A

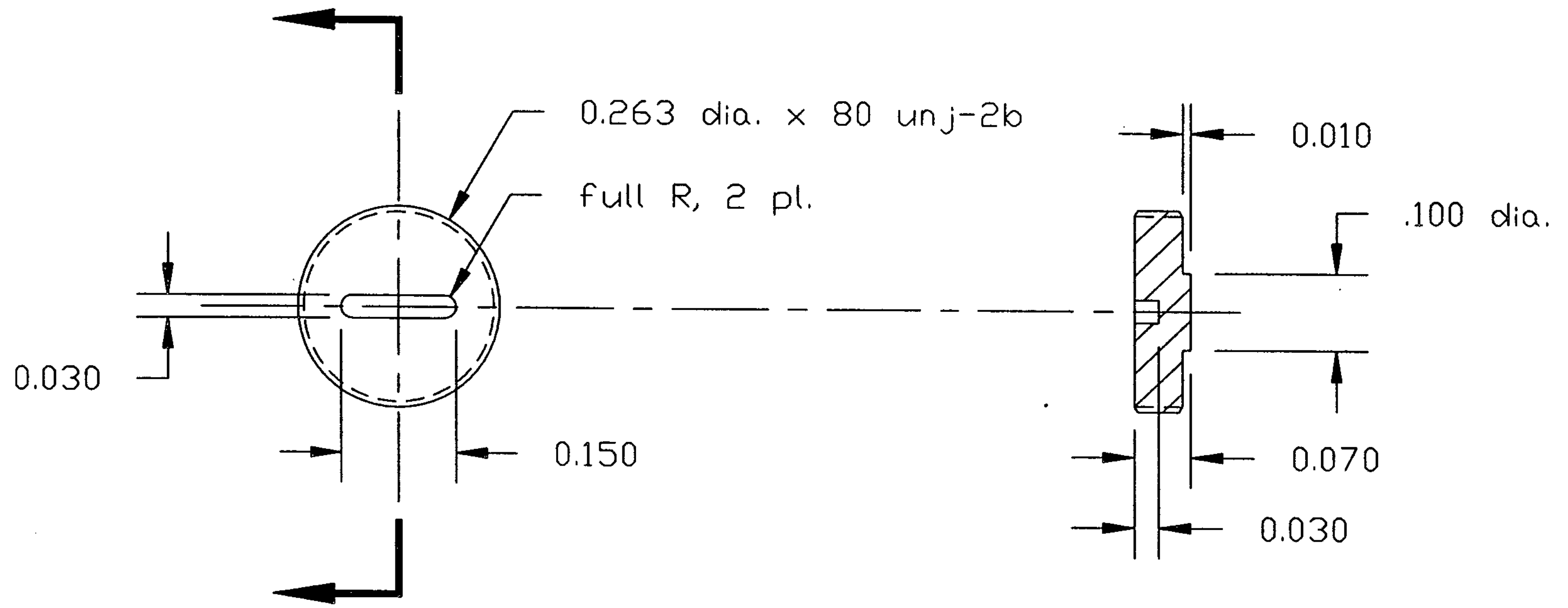

		TITLE: END CAP, LINEAR MOTOR	
		SCALE: 4:1 DATE: 94/09/30	No. BE100109
Unless otherwise specified: Dimensions are in inches		DRAWN BY: J. K. Brown	RELEASE DATE: 94/09/30
Tolerances on angles ± 0° 30' Decimals .XX ± .01, .XXX ± .002	Matl: 12L14 STEEL	PROJECT: Actuators II	APPROVAL:
	Heat Treat : N/A	FILE NAME: lmotor5.dwg	

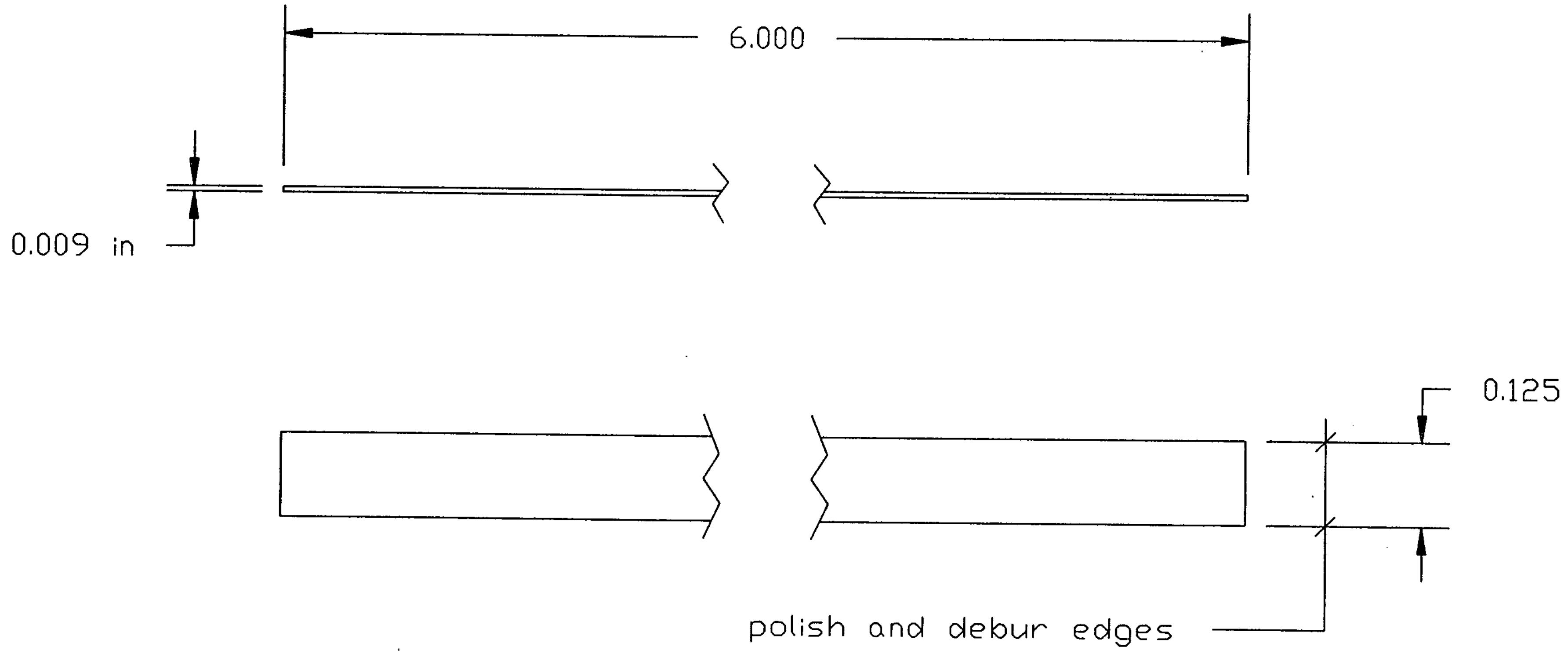

1. Make from Starrett No. 667-9 feeler stock
lapped to indicated thickness +/- 50e-6 in.

Unless otherwise specified:
Dimensions are in inches
Tolerances on angles ± 0° 30'
Decimals .XX ± .01, .XXX ± .002
Matl: NOTED
Heat Treat : N/A

TITLE: RIBBON, LINEAR MOTOR
SCALE: 4:1
DATE: 94/09/30
No. BE100117
DRAWN BY: J. K. Brown
RELEASE DATE: 95/01/04
PROJECT: Actuators II
APPROVAL:
FILE NAME: lnotor6.dwg

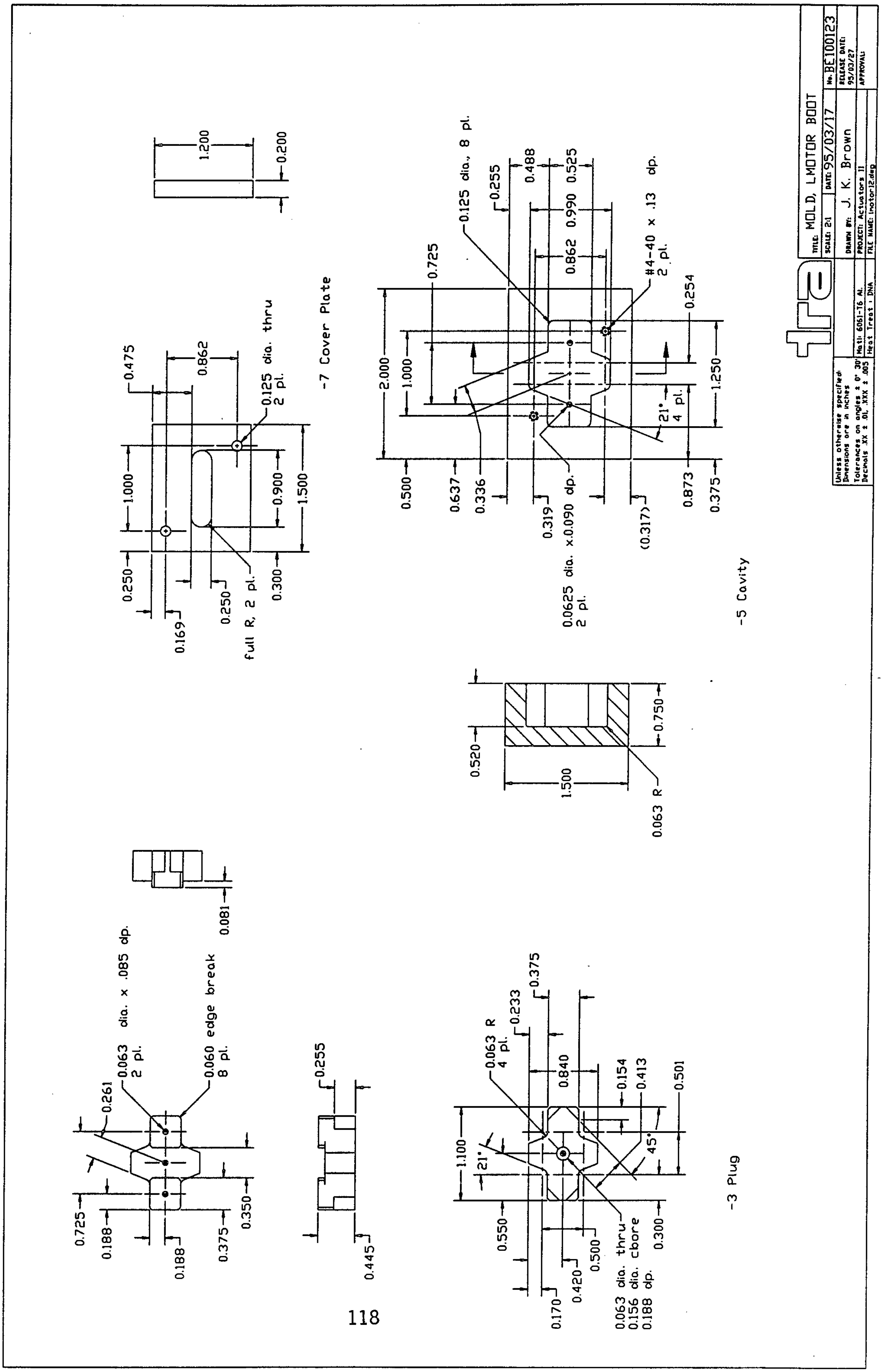
TITLE: MOLD, LMOTOR BOOT
No. BE100123
SCALE: 2:1
DATE: 95/03/17
RELEASE DATE: 95/03/27
DRAWN BY: J. K. Brown
APPROVAL:
PROJECT: Actuators II
FILE NAME: lmotor12.dwg
Mat'l: 6061-T6 Al.
Heat Treat : DNA
Unless otherwise specified: Dimensions are in inches
Tolerances on angles ± 0° 30'
Decimals .XX ± .01, .XXX ± .005
-7 Cover Plate
1.200
0.200
0.475
0.862
0.125 dia. thru
2 pl.
1.000
0.900
1.500
0.250
0.169
0.250
full R, 2 pl.
0.300
-5 Cavity
0.125 dia., 8 pl.
0.255
0.488
0.525
0.990
0.862
0.725
#4-40 x .13 dp.
2 pl.
0.254
2.000
1.000
1.250
21°
4 pl.
0.500
0.637
0.336
0.319
0.0625 dia. x.0.090 dp.
2 pl.
(0.317)
0.873
0.375
0.520
0.750
1.500
0.063 R
-3 Plug
0.063 dia. x .085 dp.
2 pl.
0.060 edge break
8 pl.
0.261
0.725
0.188
0.188
0.375
0.350
0.081
0.255
0.445
0.063 R
4 pl.
0.233
0.375
0.840
0.154
0.413
0.501
1.100
21°
45°
0.550
0.170
0.420
0.500
0.300
0.063 dia. thru
0.156 dia. cbore
0.188 dp.

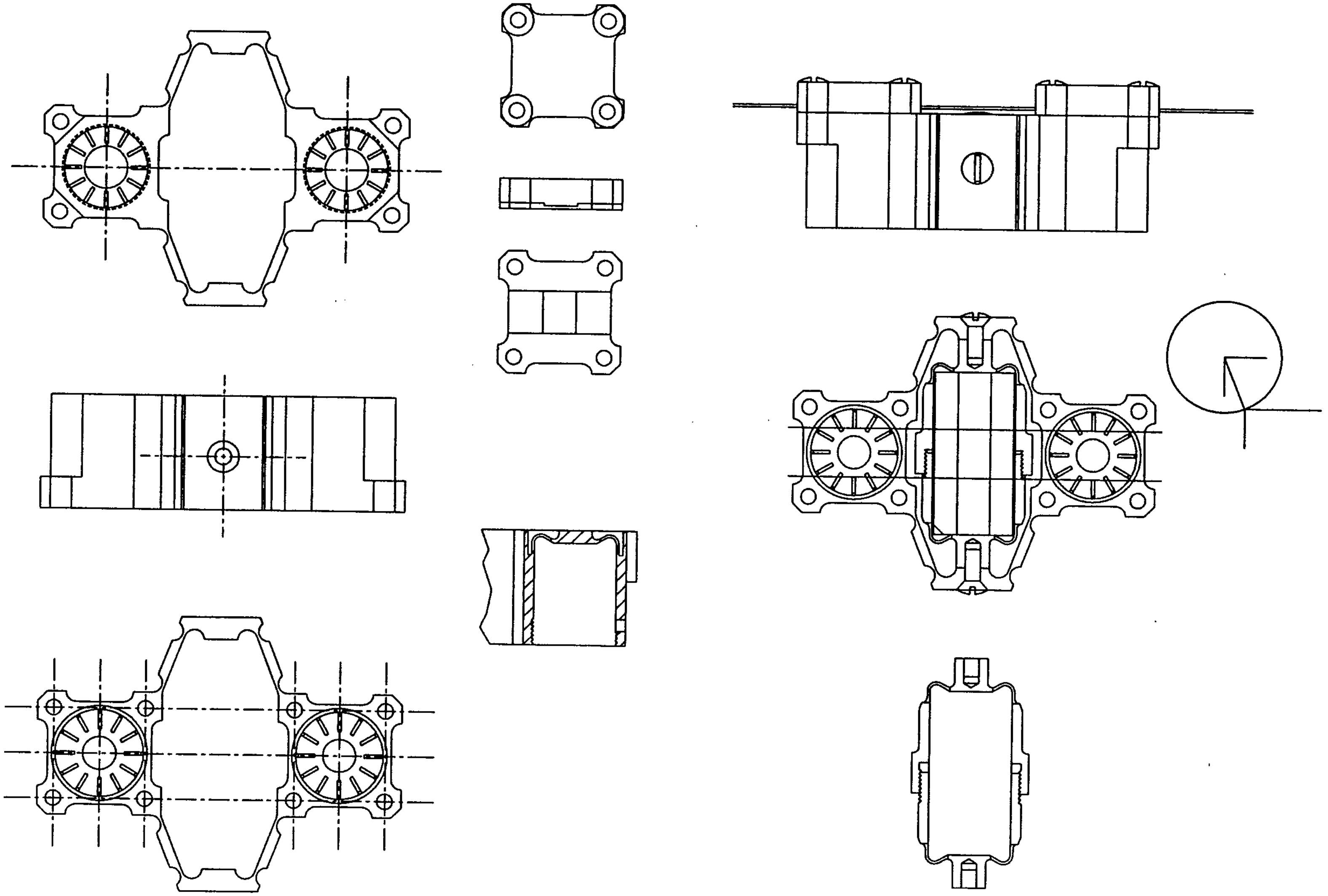

tra

TITLE: XXX

SCALE: 4:1

DATE: XXX

No. BE00xxx

Unless otherwise specified:
Dimensions are in inches
Tolerances on angles ± 0° 30'
Decimals .XX ± .03, .XXX ± .010

REV A

Mat'l: XXX

Heat Treat : XXX

DRAWN BY: XXX

PROJECT: ACTUATOR II

FILE NAME: MOTCELB.DWG

RELEASE DATE:
3 MAR 94

APPROVAL:

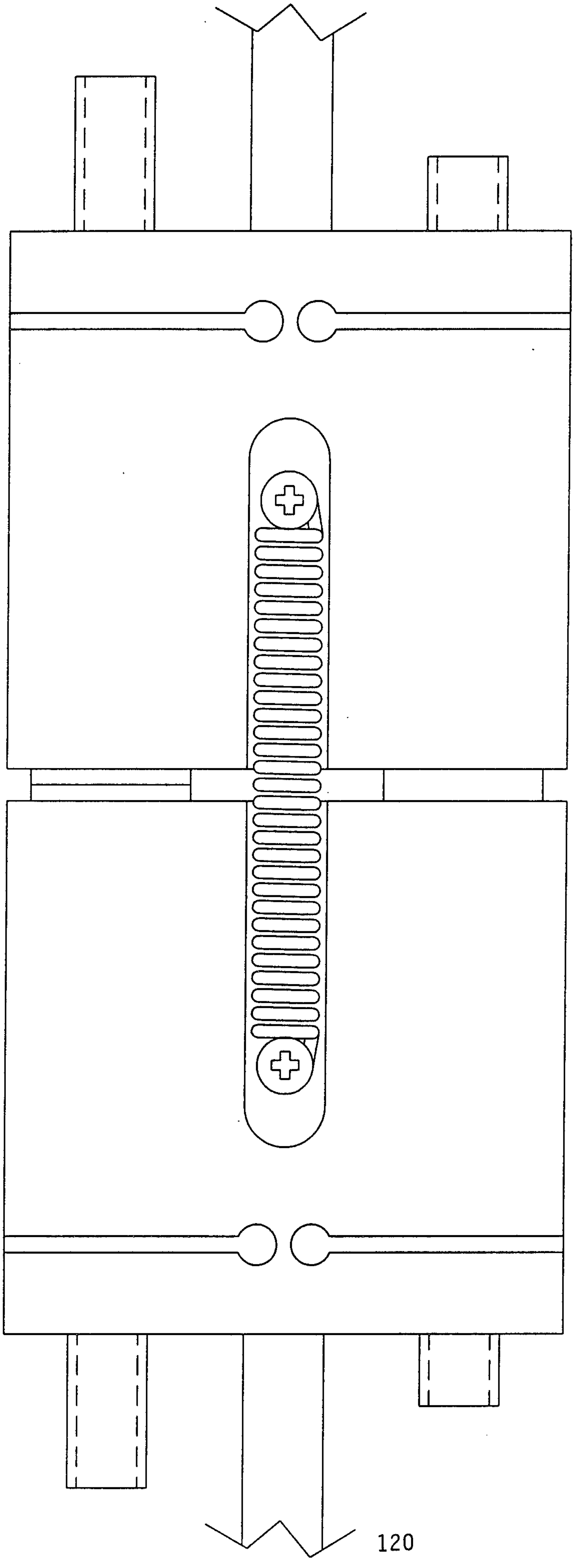

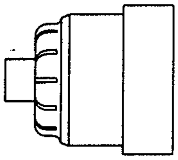

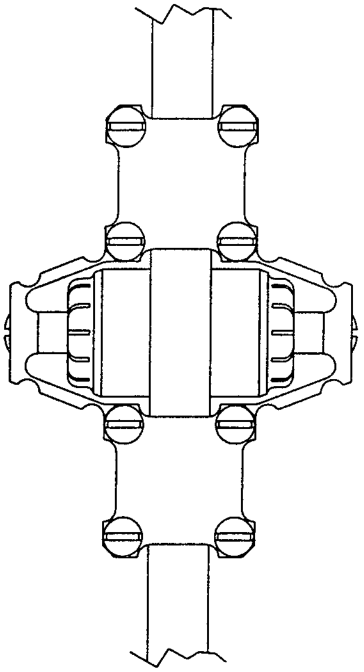

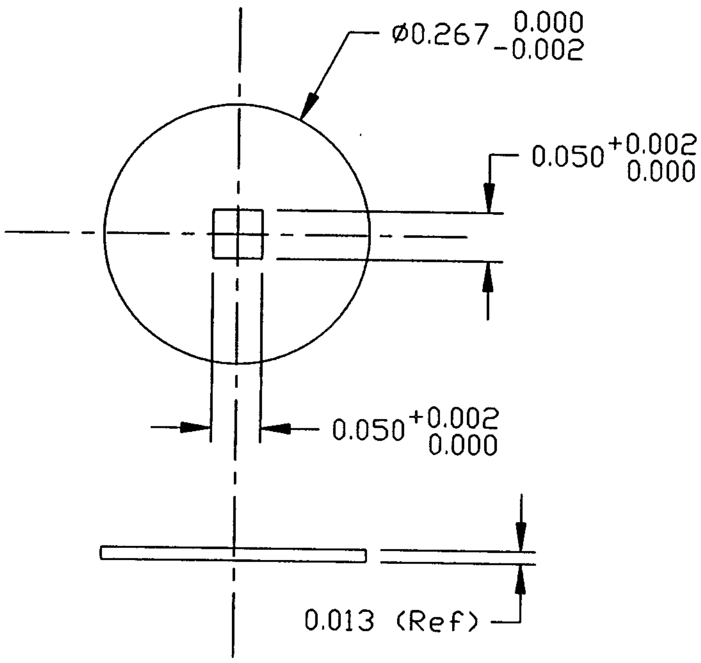

-3 Detail

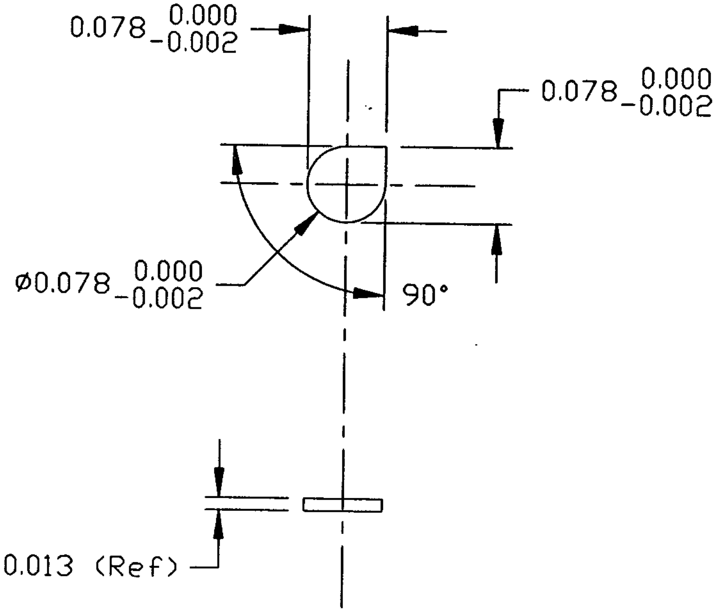

-5 Detail

1. Make from Glare Stop polarizing filter matl.
Visual Pursuits, Inc.

tra

		TITLE: POLARIZER ELEMENTS, R SENSOR	
		SCALE: 8:1 DATE: 94/08/30	No. BE100104
Unless otherwise specified: Dimensions are in inches		DRAWN BY: J. K. Brown	RELEASE DATE: 94/09/01
Tolerances on angles ± 0° 30' Decimals .XX ± .01, .XXX ± .002	Matl: Noted	PROJECT: Actuators II	APPROVAL:
	Heat Treat : N/A	FILE NAME: rsensor1	

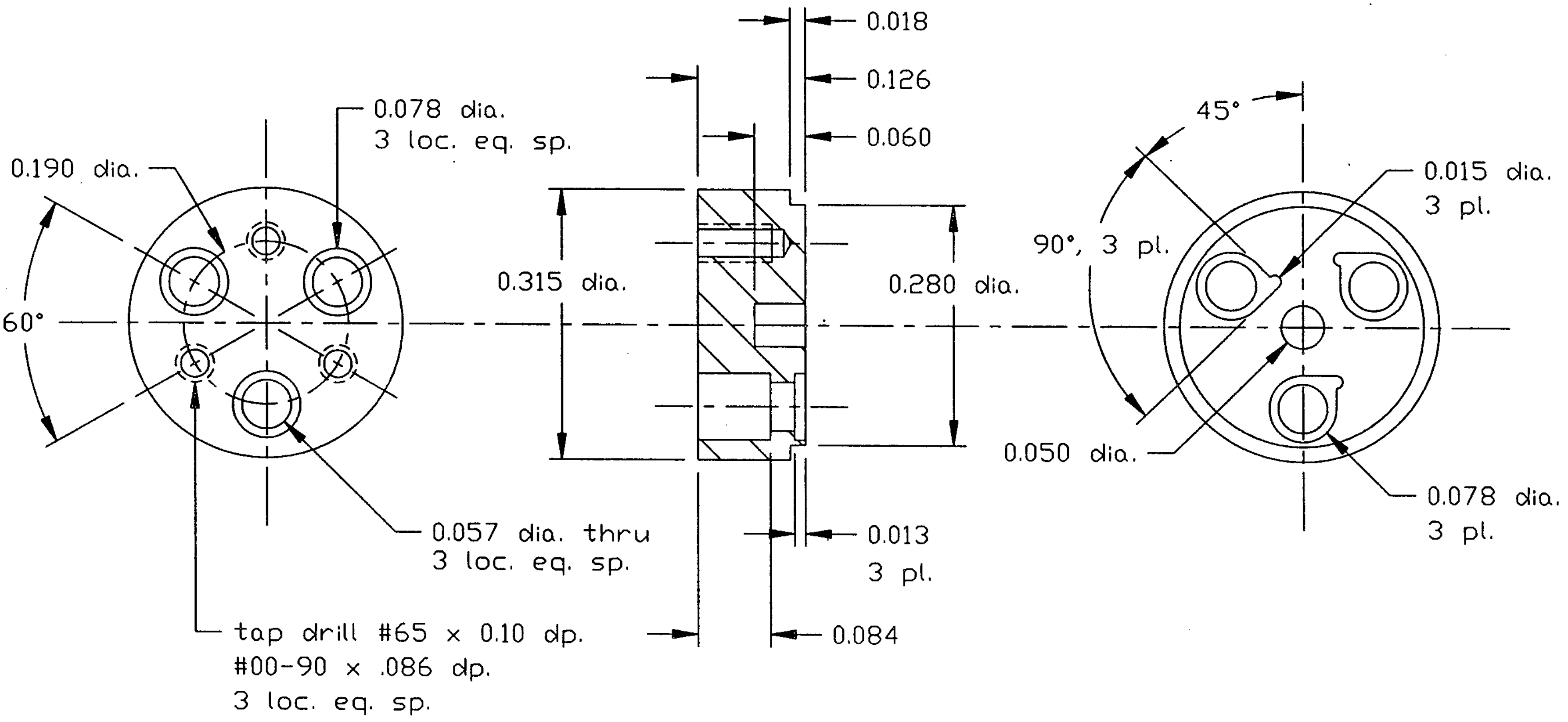

Unless otherwise specified: Dimensions are in inches Tolerances on angles ± 0° 30' Decimals .XX ± .01, .XXX ± .002	Matl: Brass Heat Treat : N/A	TITLE: DIODE HOUSING, R SENSOR	
		SCALE: 8:1 DATE: 94/09/01	No. BE100105
		DRAWN BY: J. K. Brown	RELEASE DATE: 94/09/01
		PROJECT: Actuators II FILE NAME: rsensor2	APPROVAL:

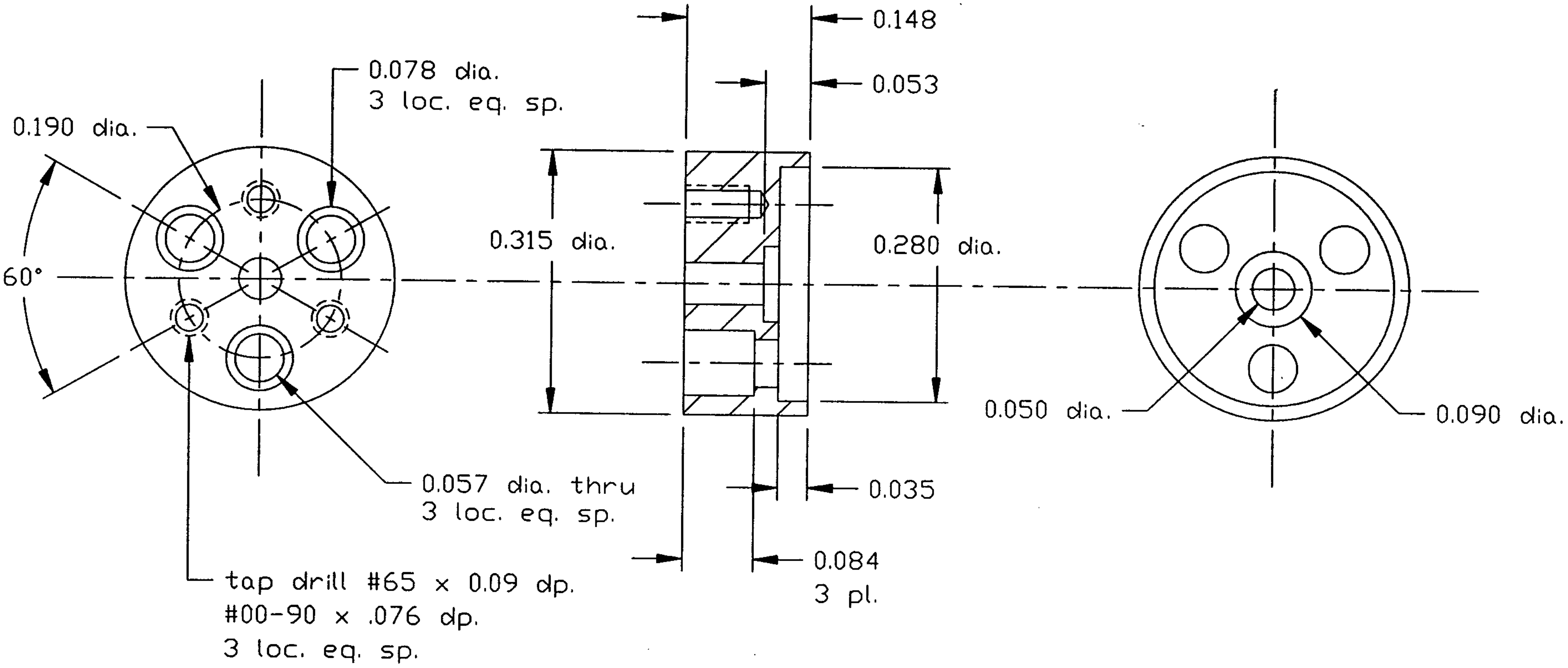

tra

TITLE: DETECTOR HOUSING, R SENSOR
SCALE: 8:1 DATE: 94/09/02 No. BE100106
DRAWN BY: J. K. Brown
RELEASE DATE: 94/09/02
PROJECT: Actuators II
FILE NAME: rsensor3
APPROVAL:

Unless otherwise specified:
Dimensions are in inches
Tolerances on angles ± 0° 30'
Decimals .XX ± .01, .XXX ± .002
Mat'l: Brass
Heat Treat : N/A

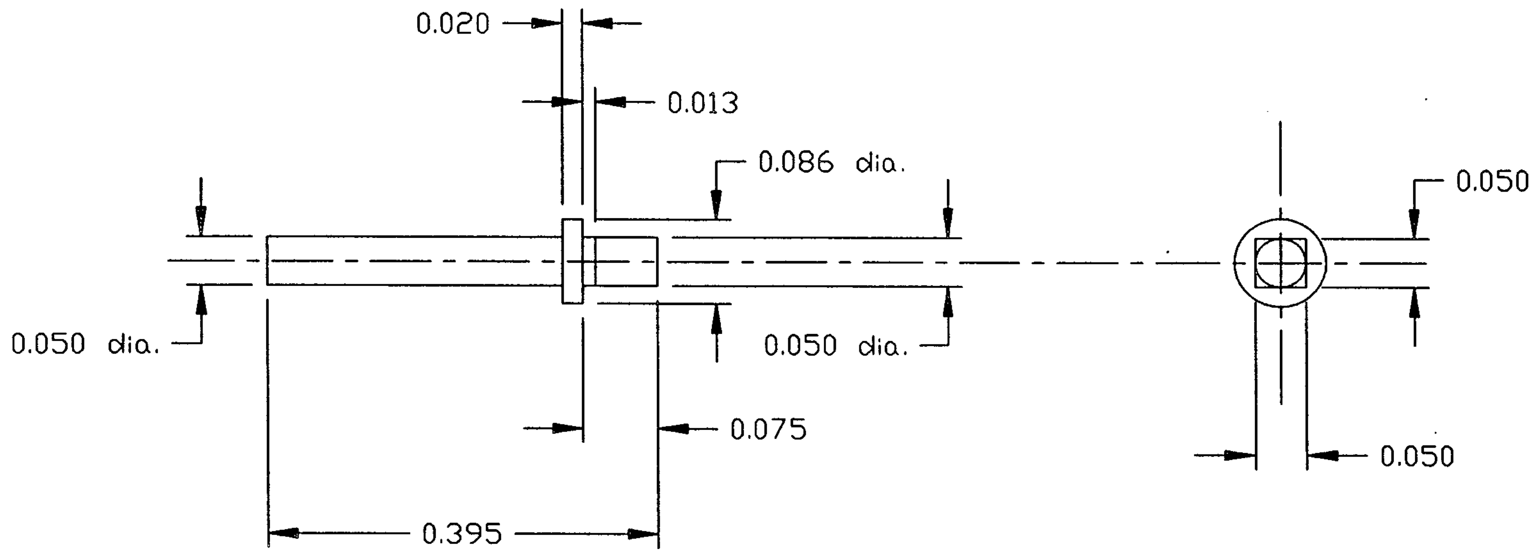

Unless otherwise specified:
Dimensions are in inches
Tolerances on angles ± 0° 30'
Decimals .XX ± .01 .XXX ± .002

Mat'l: 303 Cres
Heat Treat : N/A

tra

TITLE: SHAFT, R SENSOR
SCALE: 8:1
DATE: 94/09/08
No. BE100107
DRAWN BY: J. K. Brown
RELEASE DATE: 94/09/08
PROJECT: Actuators II
FILE NAME: rsensor4
APPROVAL:

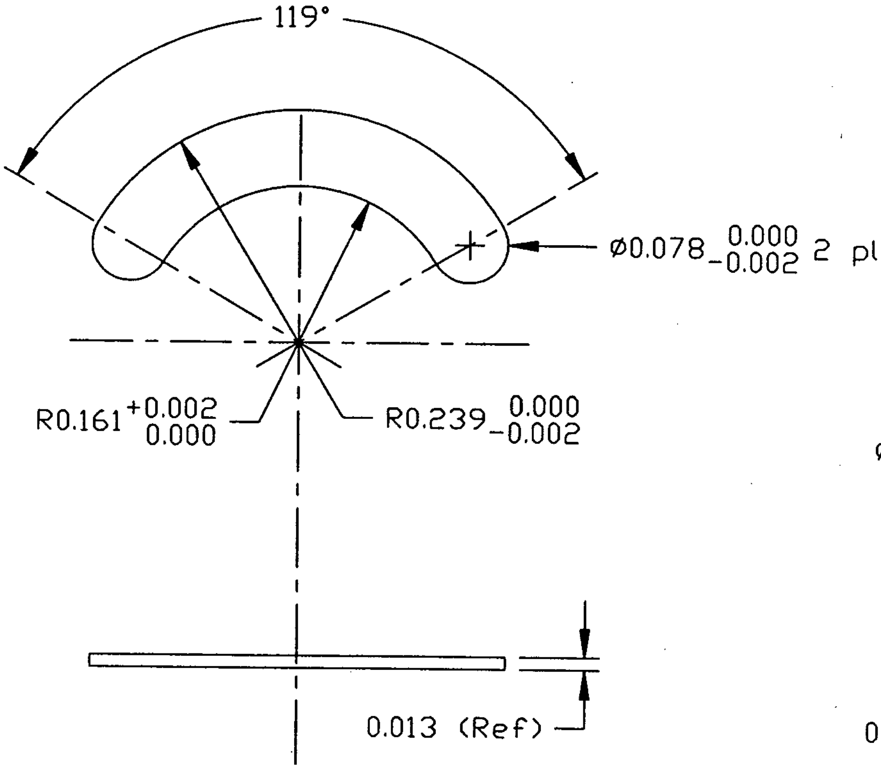

-3 Detail

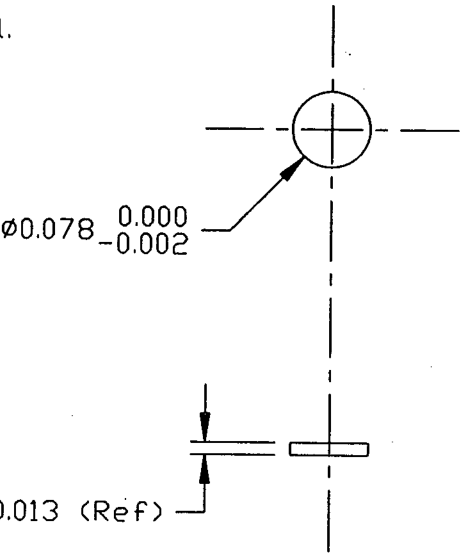

-5 Detail

1. Make from Glare Stop polarizing filter matl.
   Visual Pursuits, Inc.

		TITLE: POLARIZER ELEMENTS, HAND ACT		
		SCALE: 8:1	DATE: 94/09/23	No. BE100108
Unless otherwise specified: Dimensions are in inches		DRAWN BY: J. K. Brown		RELEASE DATE: 94/09/01
Tolerances on angles ± 0° 30' Decimals .XX ± .01 .XXX ± .002	Matl: Noted	PROJECT: Actuators II		APPROVAL:
	Heat Treat : N/A	FILE NAME: handact1		

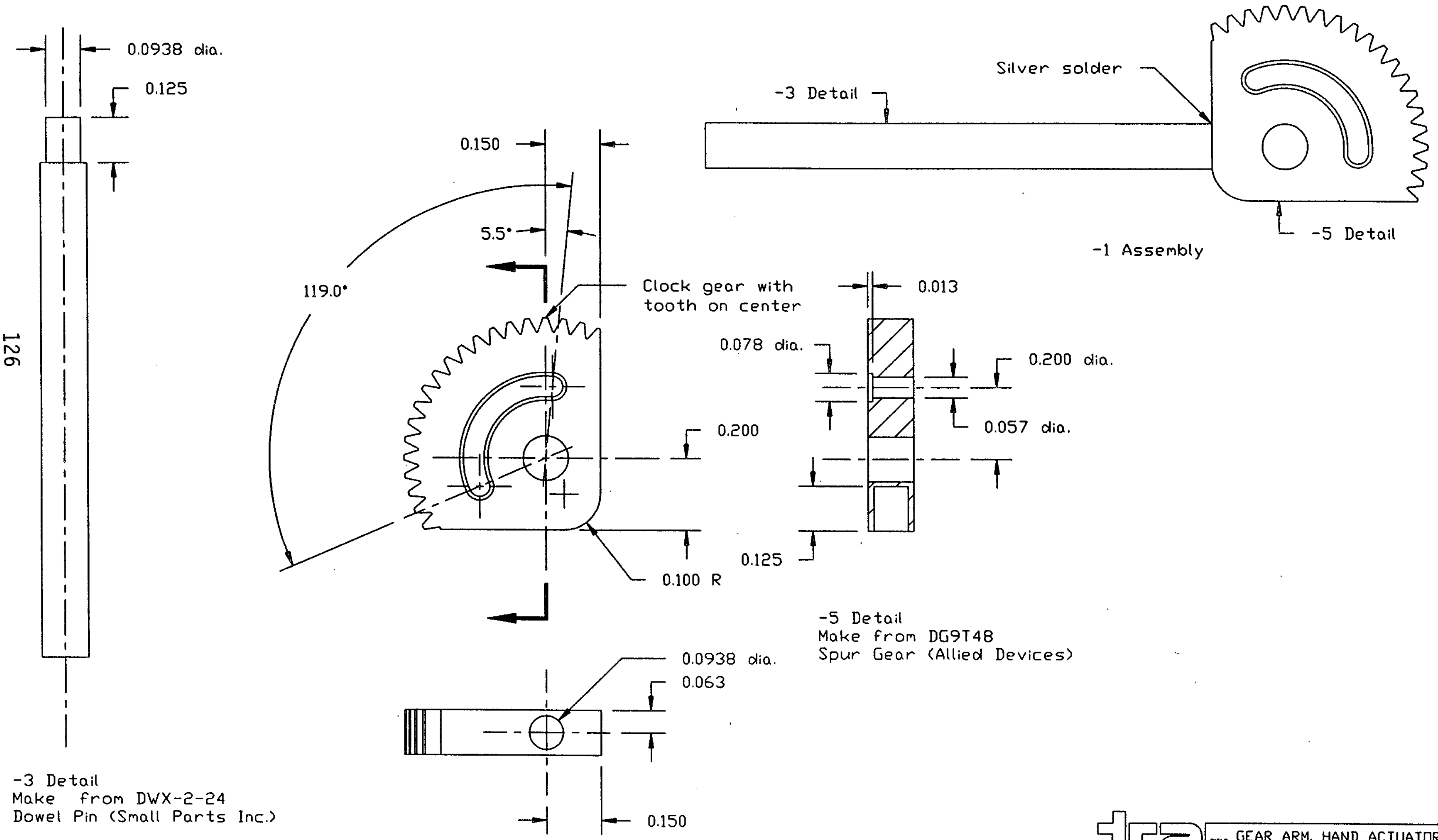

-3 Detail
Make from DWX-2-24
Dowel Pin (Small Parts Inc.)

-5 Detail
Make from DG9T48
Spur Gear (Allied Devices)

Unless otherwise specified:
Dimensions are in inches
Tolerances on angles ± 0° 30'
Decimals .XX ± .01, .XXX ± .002

Matl: NOTED
Heat Treat : N/A

TITLE: GEAR ARM, HAND ACTUATOR
SCALE: 4:1
DATE: 94/10/03
No. BE100110
DRAWN BY: J. K. Brown
RELEASE DATE: 94/10/03
PROJECT: Actuators II
APPROVAL:
FILE NAME: handact2.dwg

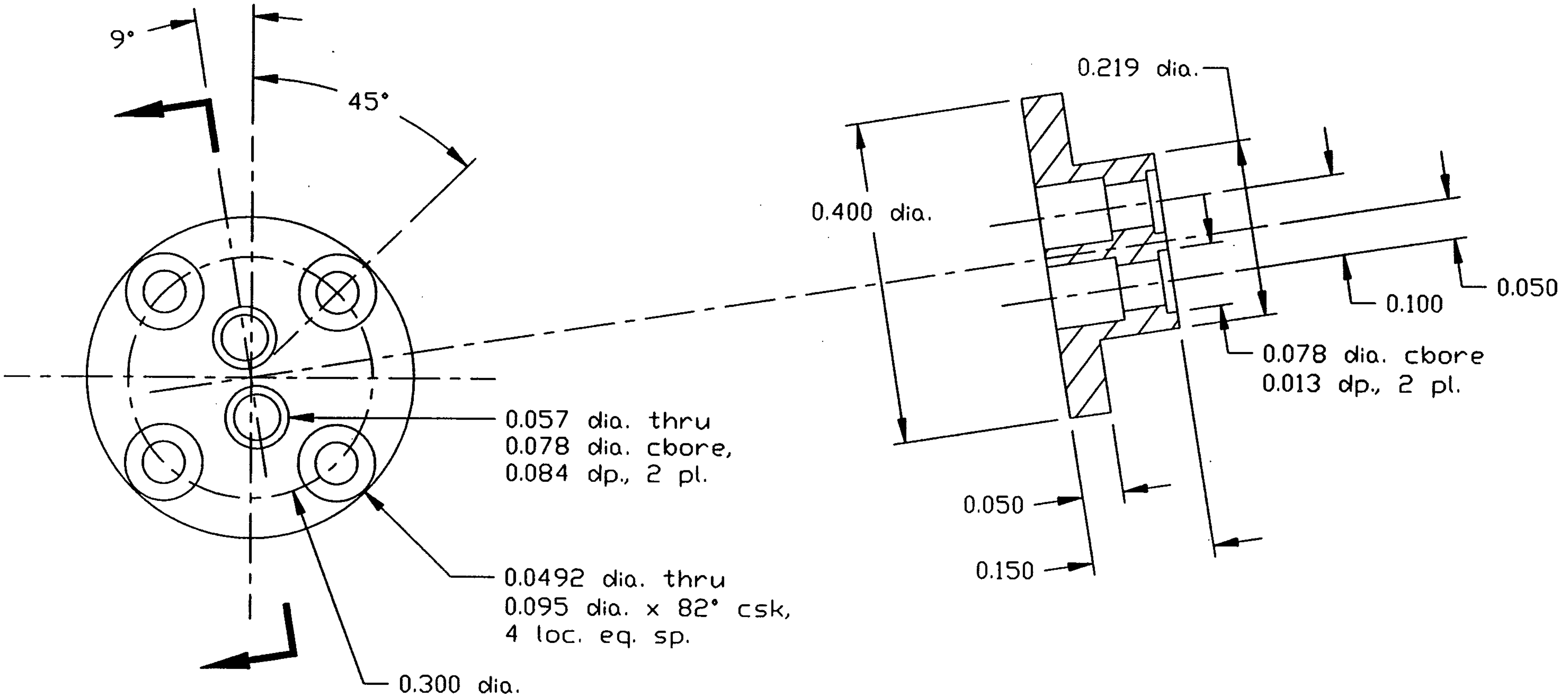

-3 Detail

		TITLE: DIODE ADAPTER, HAND ACTUATOR	
		SCALE: 8:1 DATE: 94/10/06	No. BE100111
Unless otherwise specified Dimensions are in inches		DRAWN BY: J. K. Brown	RELEASE DATE: 94/10/06
Tolerances on angles ± 0° 30' Decimals .XX ± .01, .XXX ± .002	Mat'l: Black Delrin Heat Treat : N/A	PROJECT: Actuators II FILE NAME: handact4	APPROVAL:

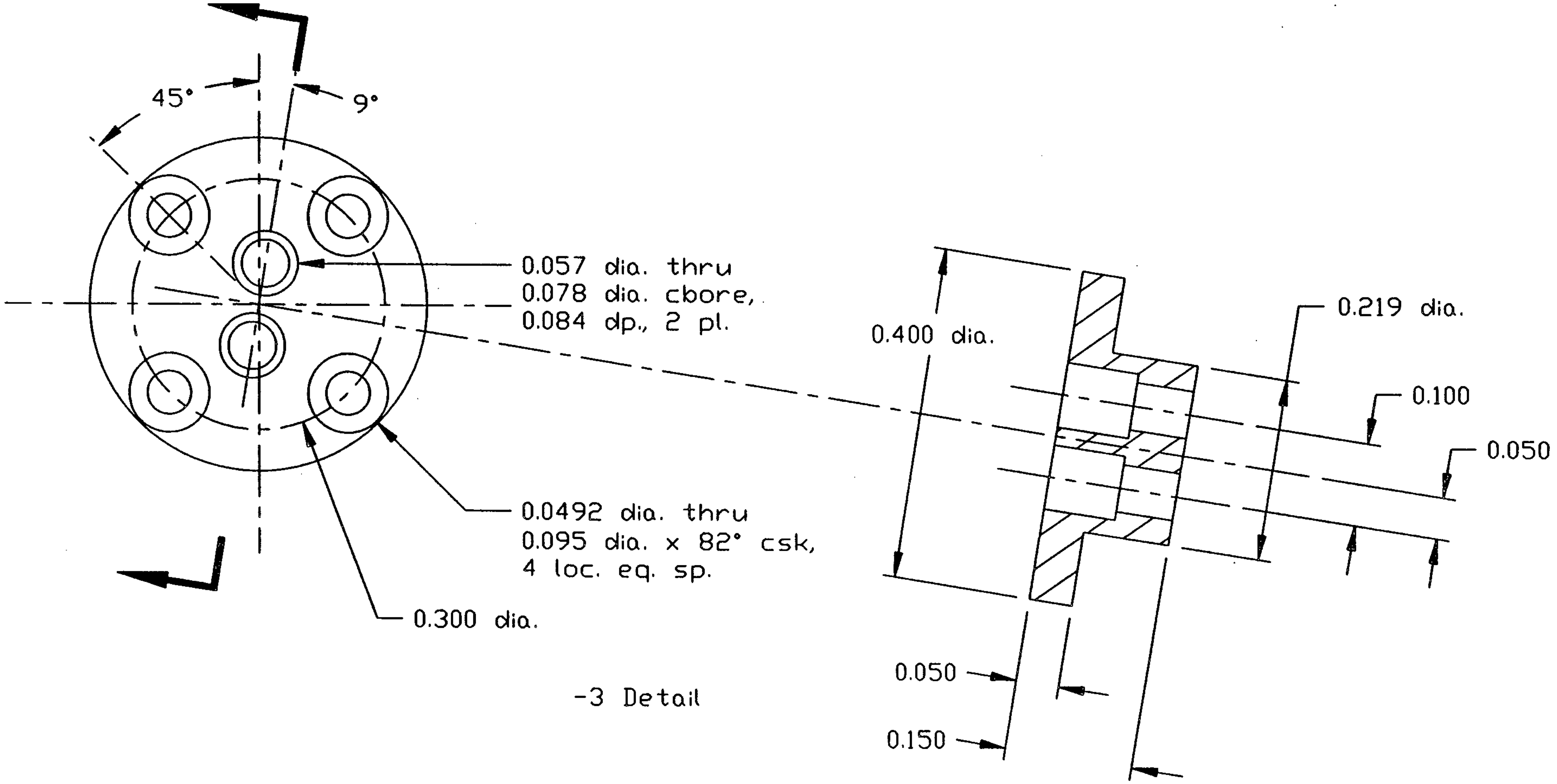

TITLE: DETECTOR ADAPTER, HAND ACT.
SCALE: 8:1 DATE: 94/10/06 No. BE100112
DRAWN BY: J. K. Brown
RELEASE DATE: 94/10/06
APPROVAL:
PROJECT: Actuators II
FILE NAME: handact5
Mat'l: Black Delrin
Heat Treat - N/A
Unless otherwise specified
Dimensions are in inches
Tolerances on angles ± 0° 30'
Decimals .XX ± .01, .XXX ± .002

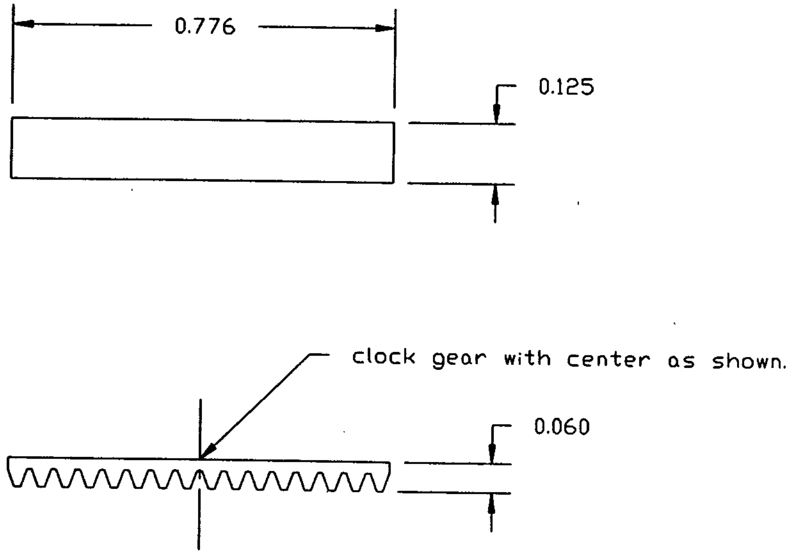

-3 Detail
Make from DAG13
Rack Gear (Allied Devices)

Unless otherwise specified: Dimensions are in inches Tolerances on angles ± 0° 30' Decimals .XX ± .01, .XXX ± .002	Mat'l: NOTED Heat Treat : N/A	TITLE: RACK GEAR, HAND ACTUATOR	
		SCALE: 4:1 DATE: 94/10/10	No. BE100113
		DRAWN BY: J. K. Brown	RELEASE DATE: 94/10/10
		PROJECT: Actuators II	APPROVAL:
		FILE NAME: handact6.dwg	

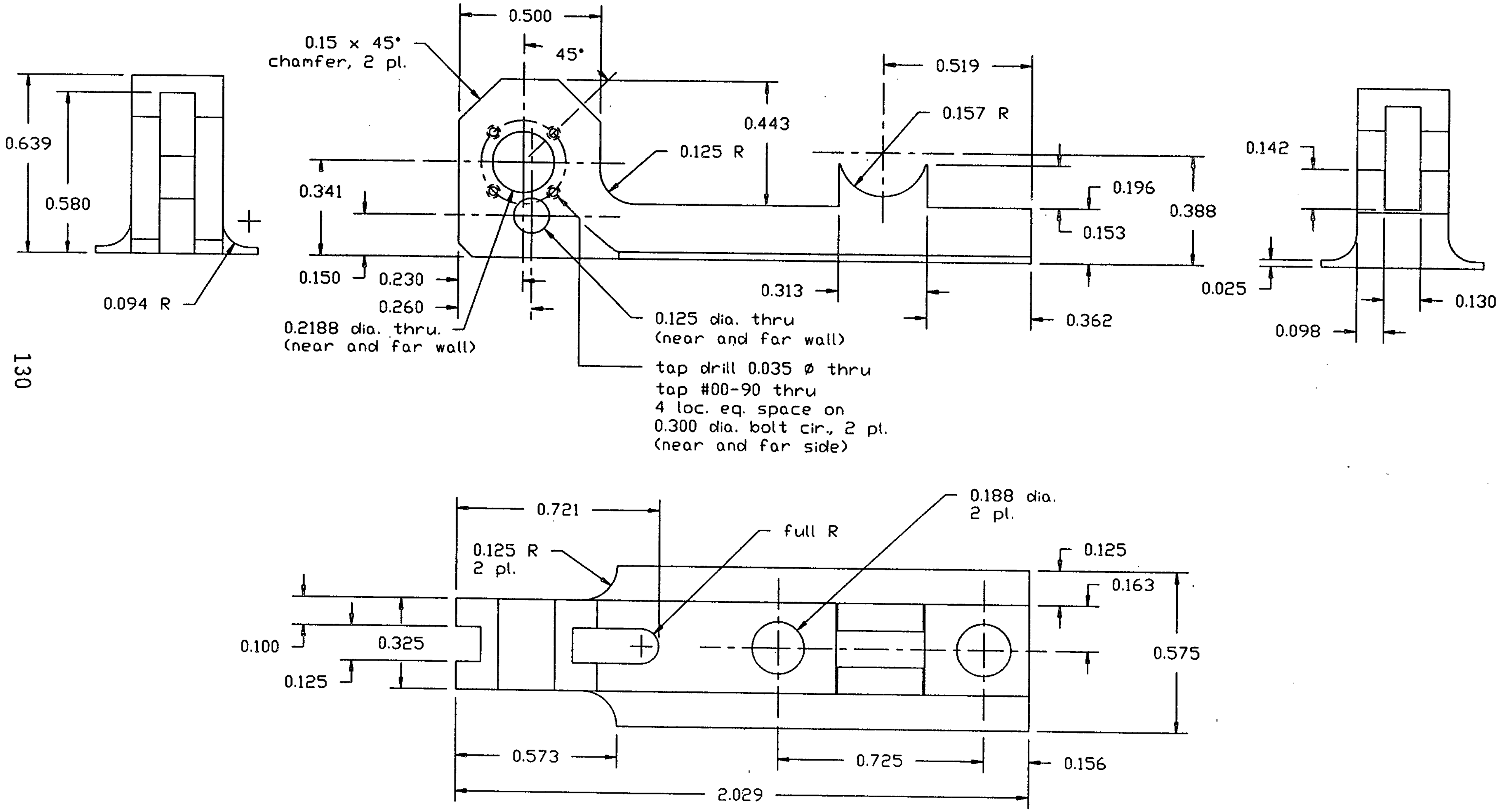

0.15 x 45° chamfer, 2 pl.

0.2188 dia. thru. (near and far wall)

0.125 dia. thru (near and far wall)

tap drill 0.035 ø thru
tap #00-90 thru
4 loc. eq. space on
0.300 dia. bolt cir., 2 pl.
(near and far side)

-3 Detail

Unless otherwise specified:
Dimensions are in inches
Tolerances on angles ± 0° 30'
Decimals .XX ± .01, .XXX ± .002

tra

Mat'l: 6061-T6 Al
Heat Treat : N/A

TITLE: HOUSING, HAND ACTUATOR
SCALE: 3:1
DATE: 94/10/10
No. BE100114
DRAWN BY: J. K. Brown
RELEASE DATE: 94/10/10
PROJECT: Actuators II
APPROVAL:
FILE NAME: handact7.dwg

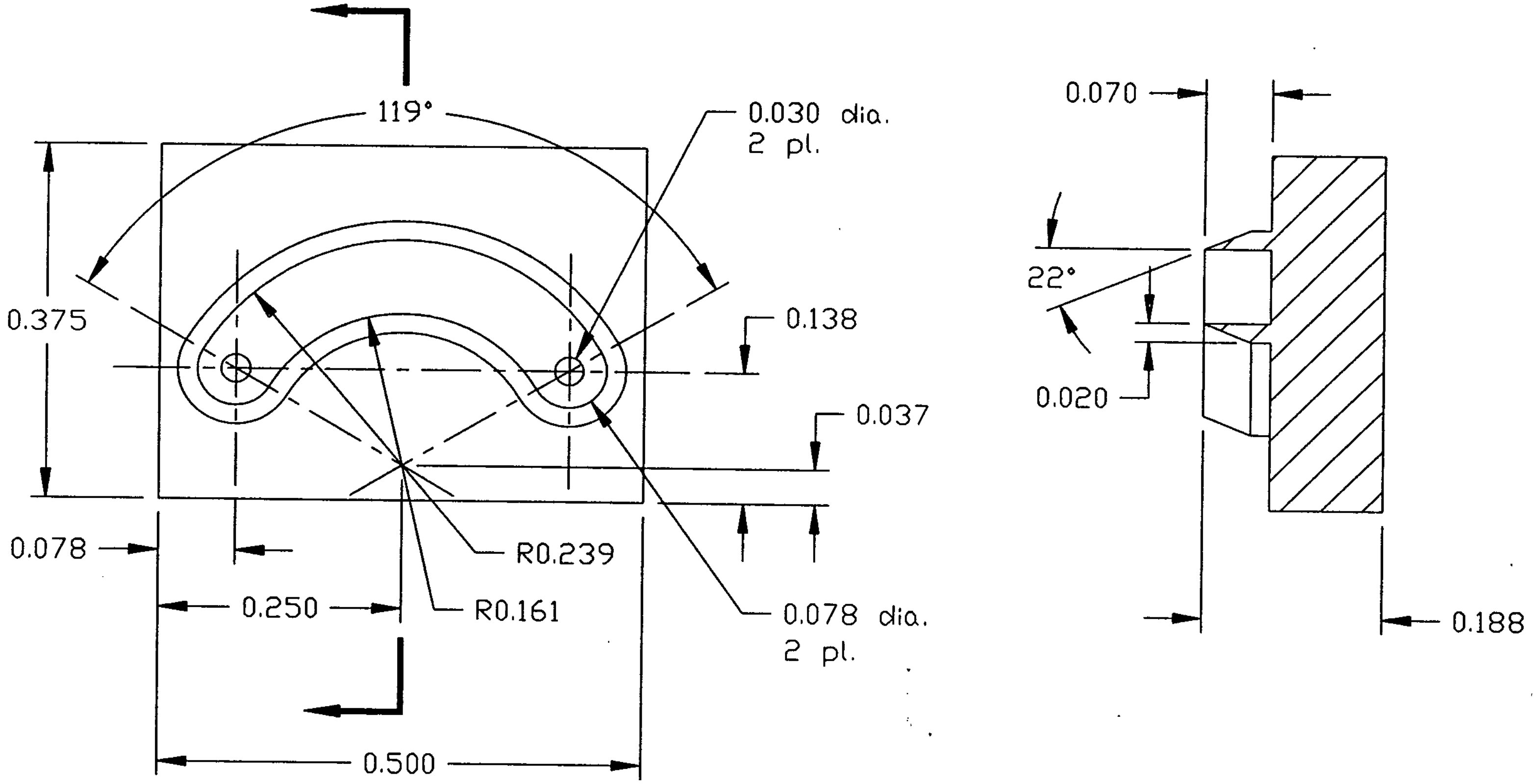

TITLE: DIE, POLARIZER ELEMENT
SCALE: 8:1
DATE: 94/10/26
No. BE100116
DRAWN BY: J. K. Brown
RELEASE DATE: 94/10/26
PROJECT: Actuators II
APPROVAL:
FILE NAME: handact8
Unless otherwise specified:
Dimensions are in inches
Tolerances on angles ± 0° 30'
Decimals .XX ± .01, .XXX ± .002
Mat'l: Steel
Heat Treat : N/A

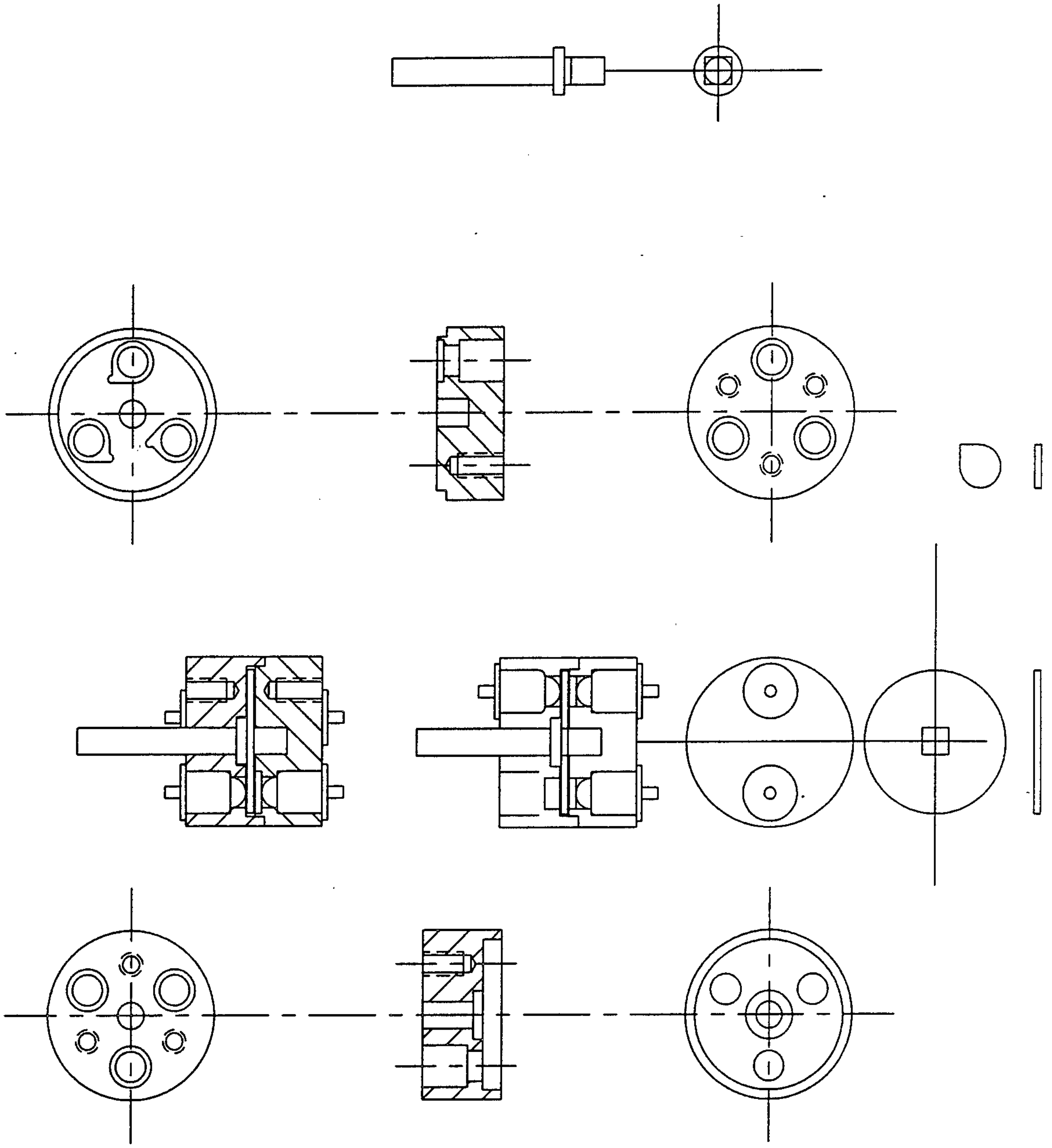

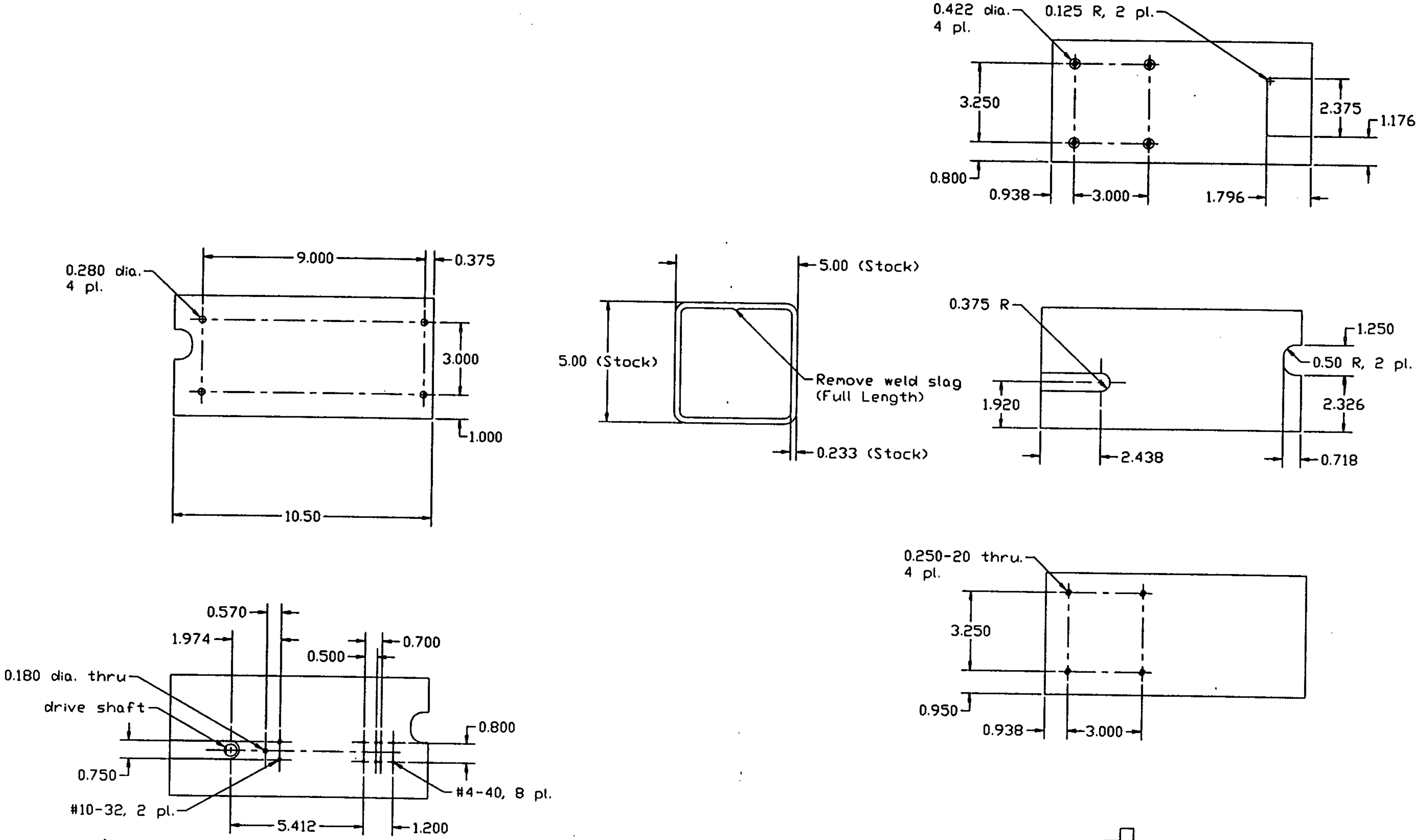

Component Mounting Locations

TITLE: FRAME, LMOTOR TEST BED
SCALE: 1:2
DATE: 94/12/20
No. BE100118
DRAWN BY: J. K. Brown
RELEASE DATE: 94/12/20
PROJECT: Actuators II
APPROVAL:
FILE NAME: lmotor7
Mat'l: Steel
Heat Treat : N/A
Unless otherwise specified:
Dimensions are in inches
Tolerances on angles ± 0° 30'
Decimals .XX ± .03, .XXX ± .010

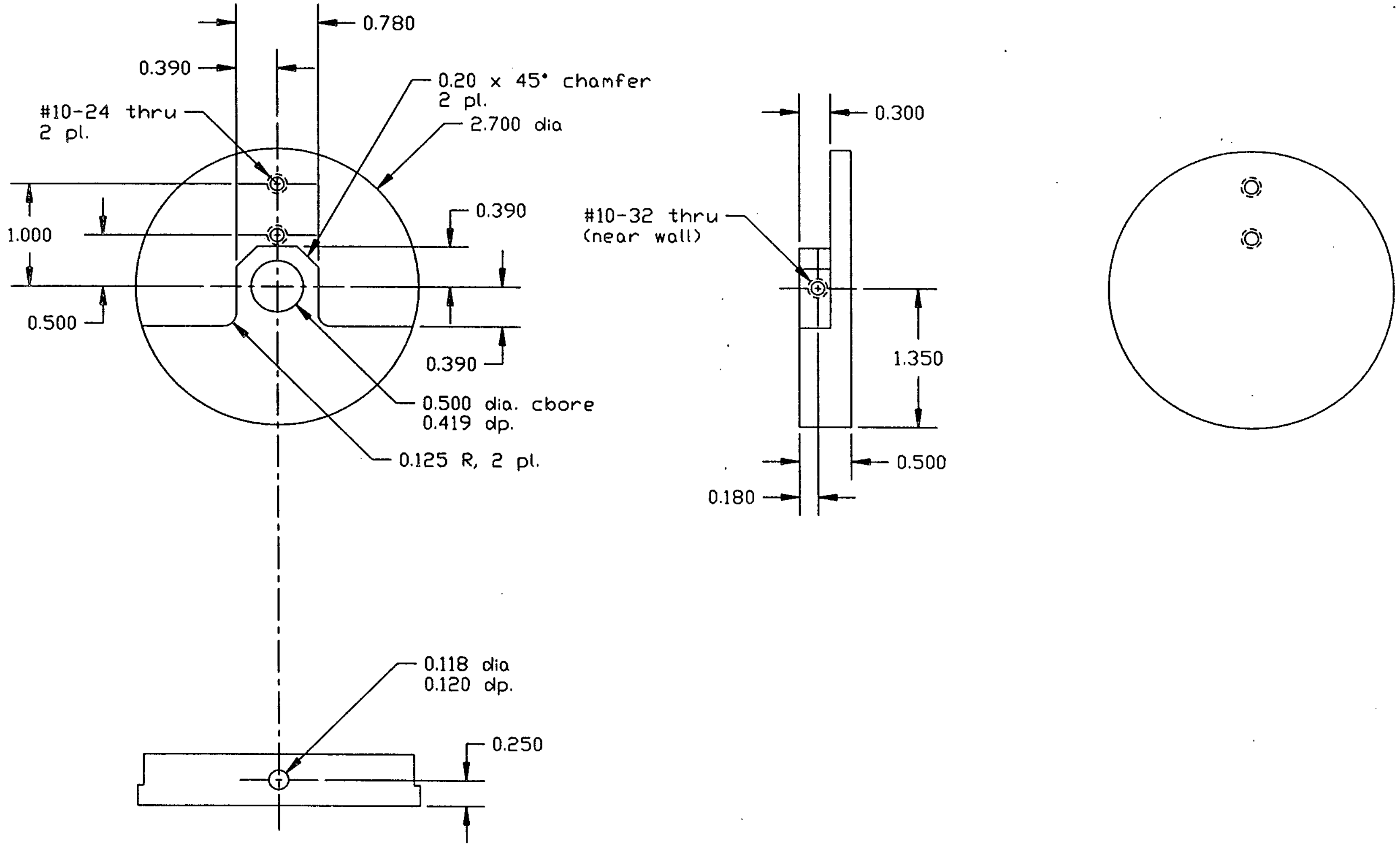

TITLE: CRANK, LMOTOR TEST BED
SCALE: 1:1
DATE: 94/12/22
No. BE100119
DRAWN BY: J. K. Brown
RELEASE DATE: 94/12/22
PROJECT: Actuators II
APPROVAL:
FILE NAME: lmotorB.dwg
Mat'l: 6061-T6 Al
Heat Treat : N/A
Unless otherwise specified:
Dimensions are in inches
Tolerances on angles ± 0° 30'
Decimals .XX ± .03, .XXX ± .010

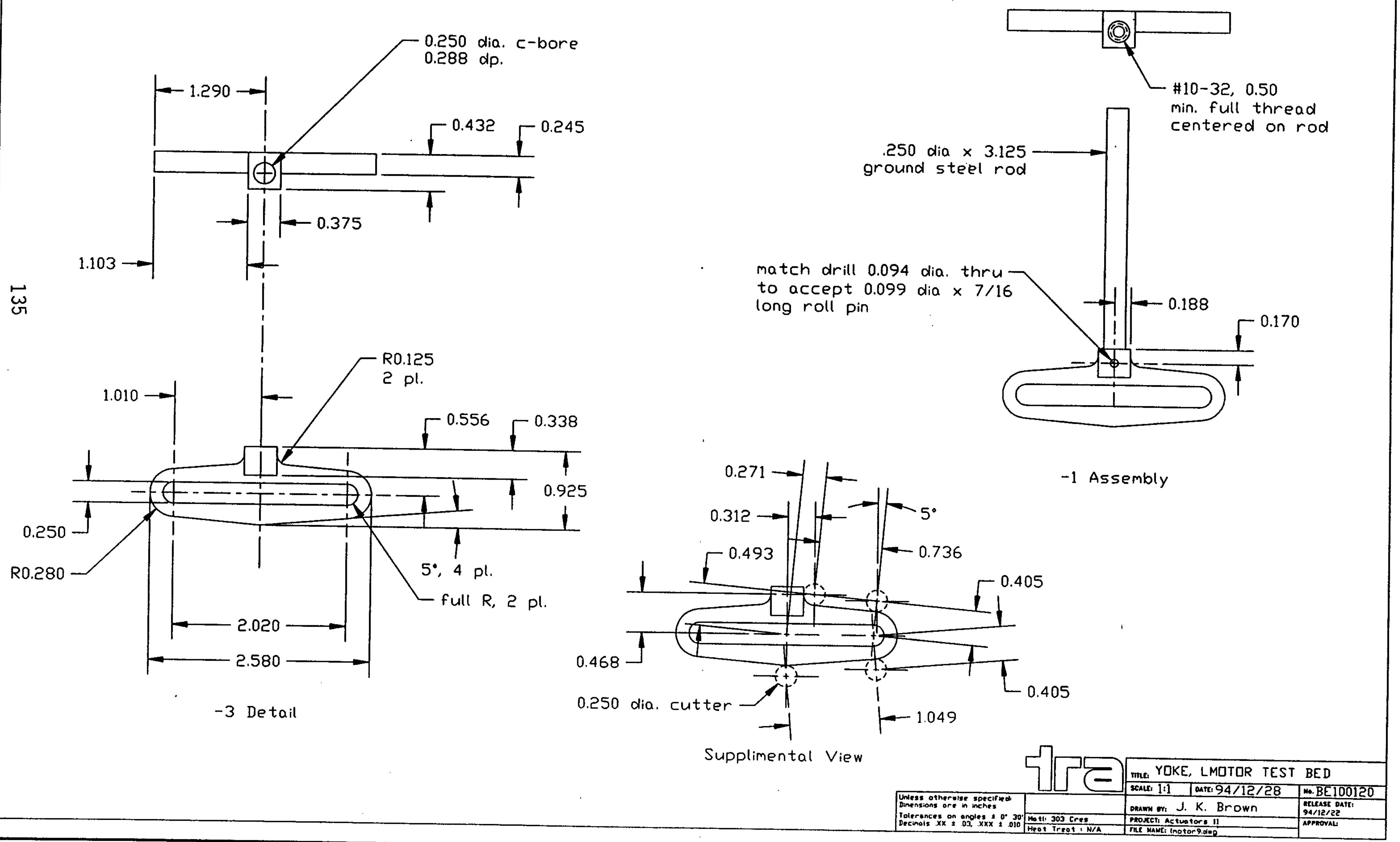
0.250 dia. c-bore
0.288 dp.
1.290
0.432
0.245
0.375
1.103
R0.125
2 pl.
1.010
0.556
0.338
0.925
0.250
R0.280
5°, 4 pl.
full R, 2 pl.
2.020
2.580
-3 Detail
#10-32, 0.50
min. full thread
centered on rod
.250 dia x 3.125
ground steel rod
match drill 0.094 dia. thru
to accept 0.099 dia x 7/16
long roll pin
0.188
0.170
-1 Assembly
0.271
0.312
0.493
5°
0.736
0.405
0.468
0.250 dia. cutter
0.405
1.049
Supplimental View
Unless otherwise specified:
Dimensions are in inches
Tolerances on angles ± 0° 30'
Decimals .XX ± .03, .XXX ± .010
Matl: 303 Cres
Heat Treat : N/A
TITLE: YOKE, LMOTOR TEST BED
SCALE: 1:1
DATE: 94/12/28
No. BE100120
DRAWN BY: J. K. Brown
RELEASE DATE: 94/12/22
PROJECT: Actuators II
FILE NAME: lnotor9.dwg
APPROVAL:

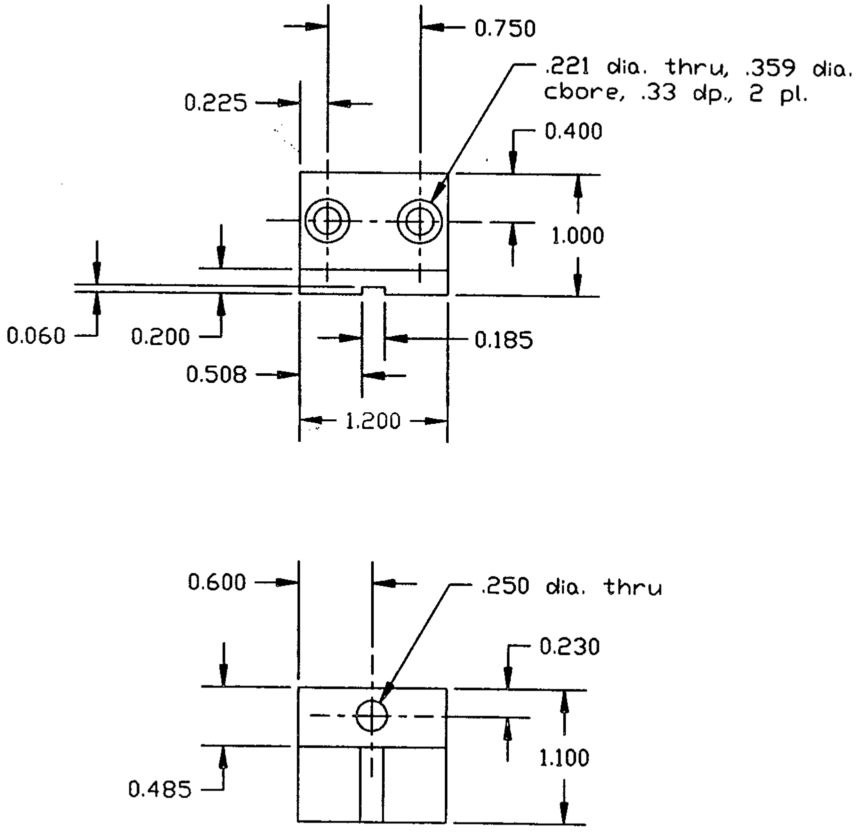

-3 detail
Matl: 6061-T6 Al

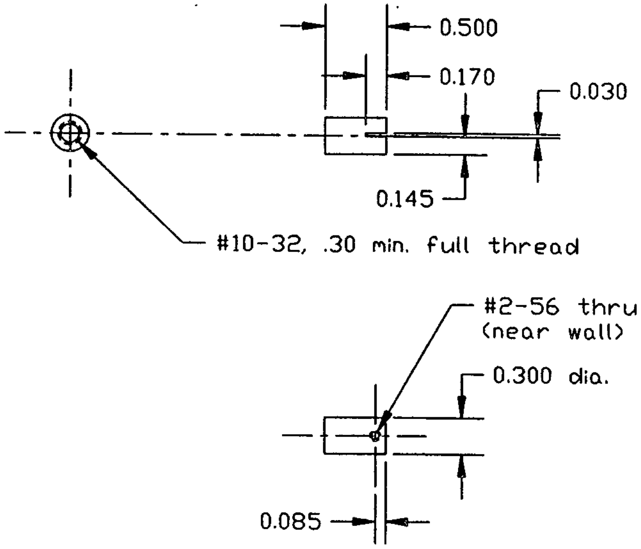

-5 detail
Matl: 304 Cres

Unless otherwise specified:
Dimensions are in inches
Tolerances on angles ± 0° 30'
Decimals .XX ± .03, .XXX ± .010

Matl: Noted
Heat Treat : N/A

tra

TITLE: DETAILS, LMOTOR TEST BED
SCALE: 1:1
DATE: 94/12/28
No. BE100121
DRAWN BY: J. K. Brown
RELEASE DATE: 95/01/09
PROJECT: Actuators II
FILE NAME: lmotor10.dwg
APPROVAL:

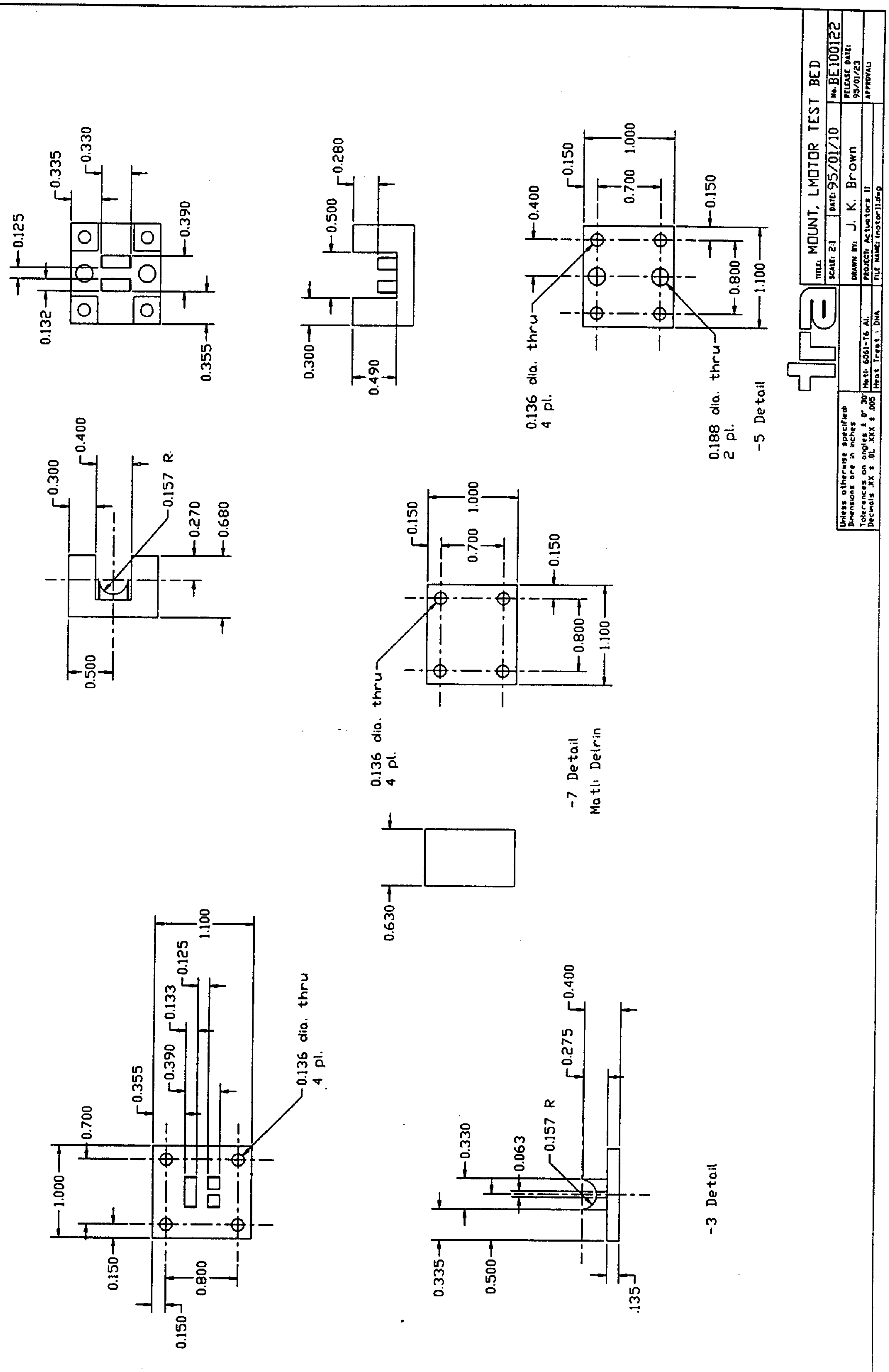
TITLE: MOUNT, LMOTOR TEST BED
No. BE100122
SCALE: 2:1
DATE: 95/01/10
RELEASE DATE: 95/01/23
DRAWN BY: J. K. Brown
APPROVAL:
PROJECT: Actuators II
FILE NAME: lmotor1l.dwg
Mat'l: 6061-T6 AL.
Heat Treat : DNA
Unless otherwise specified
Dimensions are in inches
Tolerances on angles ± 0° 30'
Decimals .XX ± .01 .XXX ± .005
-5 Detail
0.136 dia. thru
4 pl.
0.188 dia. thru
2 pl.
0.400
0.150
0.700
1.000
0.150
0.800
1.100
0.500
0.280
0.300
0.490
0.125
0.335
0.330
0.390
0.132
0.355
-7 Detail
Mat'l: Delrin
0.136 dia. thru
4 pl.
0.150
0.700
1.000
0.150
0.800
1.100
0.300
0.400
0.157 R
0.270
0.680
0.500
0.630
-3 Detail
0.400
0.275
0.157 R
0.330
0.063
0.335
0.500
.135
0.136 dia. thru
4 pl.
1.100
0.125
0.133
0.390
0.355
0.700
1.000
0.150
0.800
0.150

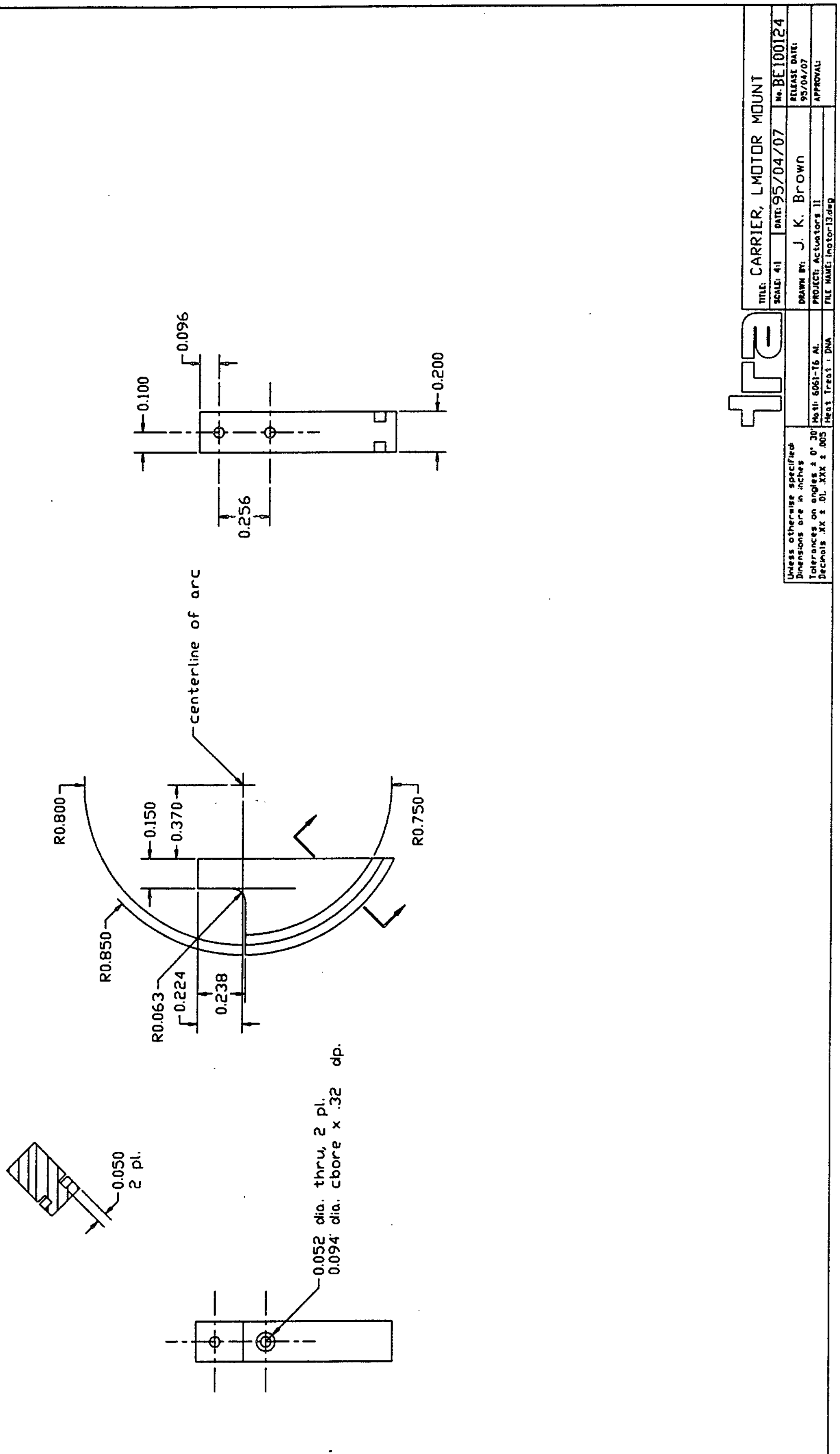
0.096
0.100
0.200
0.256
centerline of arc
R0.800
0.150
0.370
R0.750
R0.850
R0.063
0.224
0.238
0.050
2 pl.
0.052 dia. thru, 2 pl.
0.094 dia. cbore x .32 dp.
TITLE: CARRIER, LMOTOR MOUNT
SCALE: 4:1
DATE: 95/04/07
No. BE100124
RELEASE DATE: 95/04/07
APPROVAL:
DRAWN BY: J. K. Brown
PROJECT: Actuators II
FILE NAME: lmotor13.dwg
Unless otherwise specified: Dimensions are in inches
Tolerances on angles ± 0° 30'
Decimals .XX ± .01 .XXX ± .005
Mat'l: 6061-T6 Al.
Heat Treat : DNA

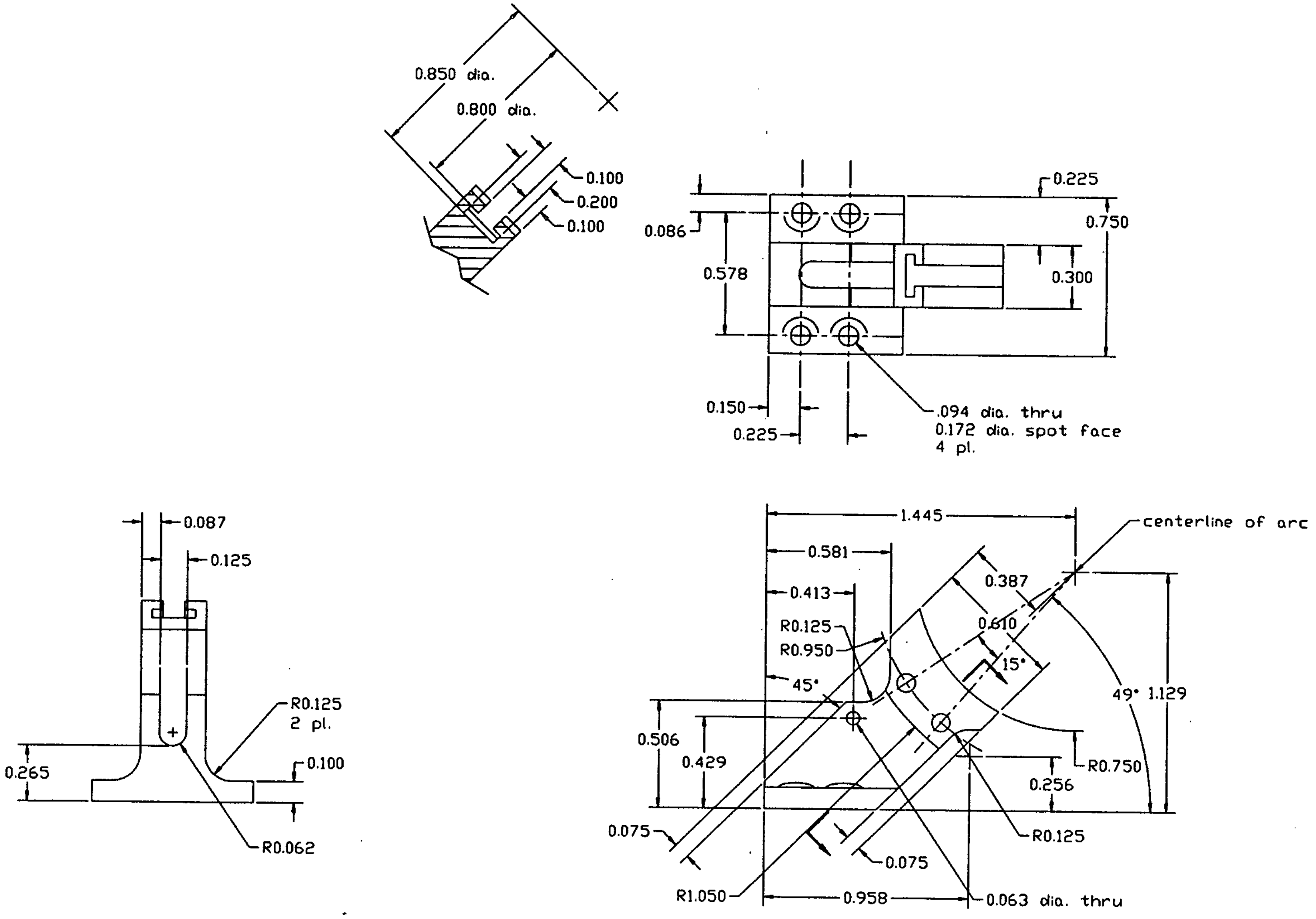

Unless otherwise specified:
Dimensions are in inches
Tolerances on angles ± 0° 30'
Decimals .XX ± .01, .XXX ± .005

Matl: Black Delren
Heat Treat : DNA

tra

TITLE: MOUNT, MIDDLE JOINT
SCALE: 4:1
DATE: 95/04/07
No. BE100125
DRAWN BY: J. K. Brown
RELEASE DATE: 95/04/07
PROJECT: Actuators II
APPROVAL:
FILE NAME: lnotor14.dwg

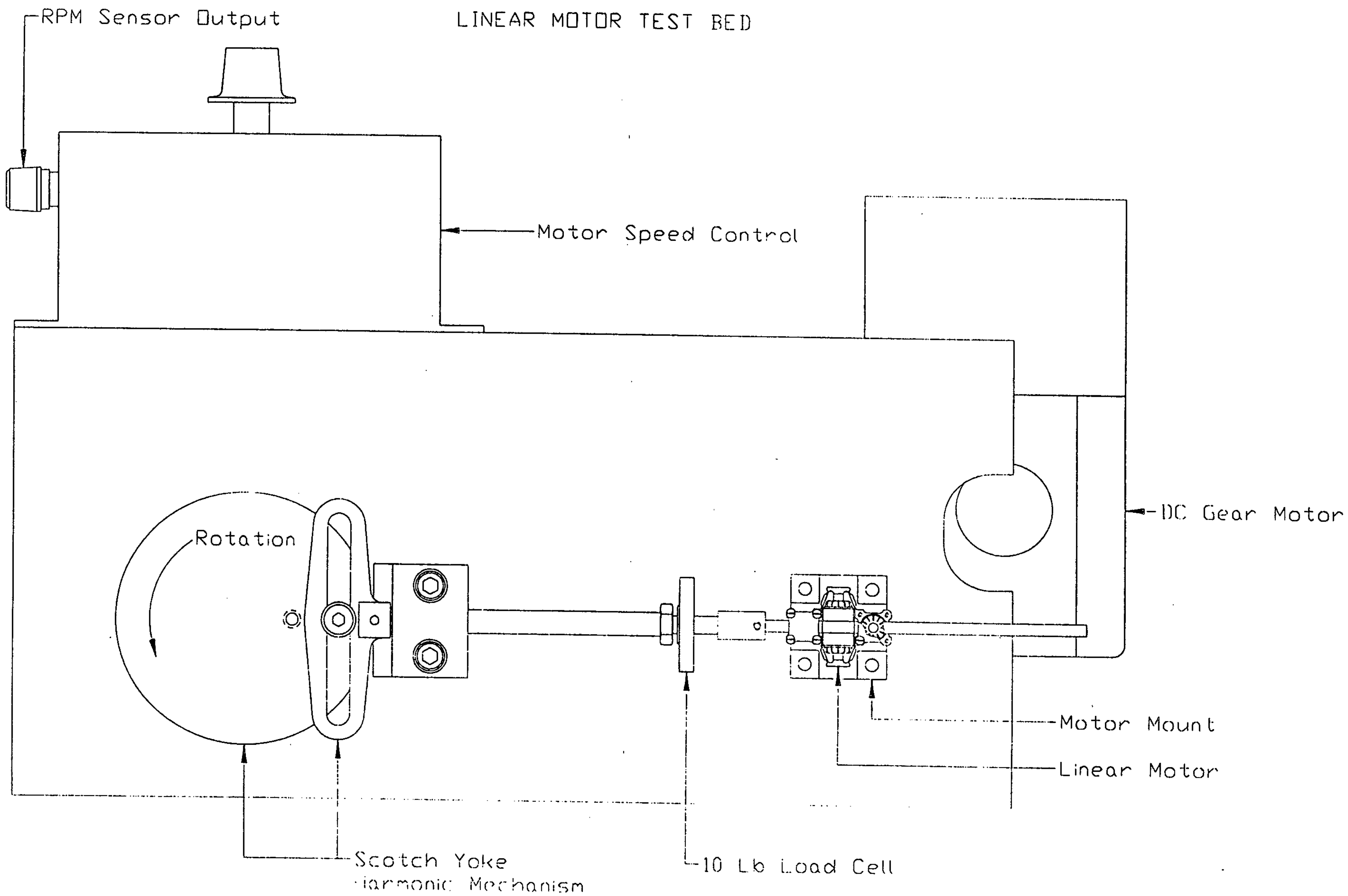

LINEAR MOTOR TEST BED

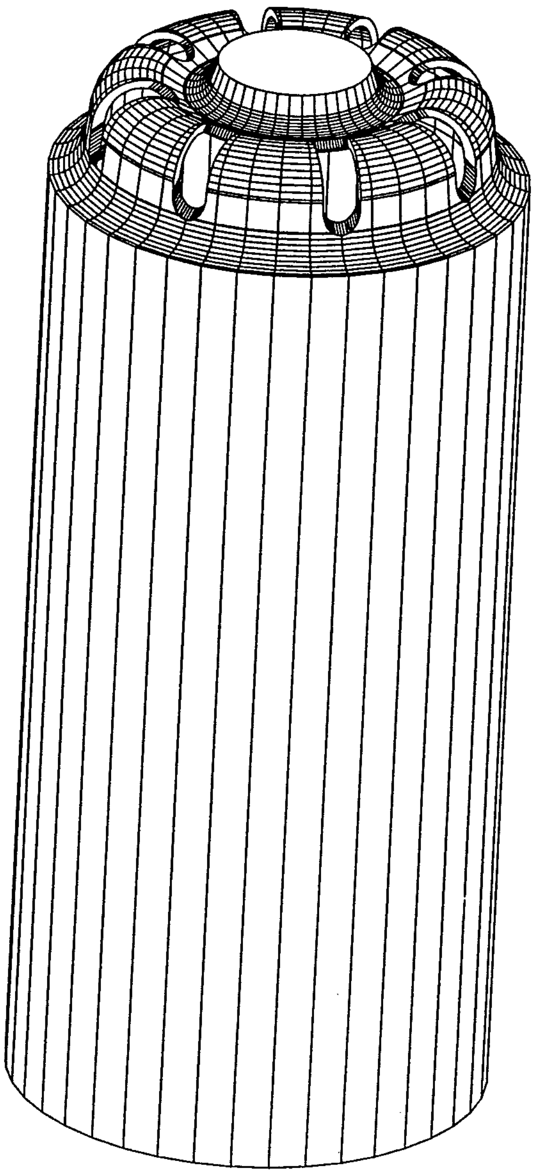

tra

TITLE: MOTIVE CELL 3-D
SCALE: 8:1
DATE: 3 MAR 94
No. BE00117

Unless otherwise specified
Dimensions are in inches
Tolerances on angles ± 0° 30'
Decimals .XX ± .03, .XXX ± .010

REV A
Mat'l: XXX
Heat Treat : XXX

DRAWN BY: AP Hilton
PROJECT: ACTUATOR II
FILE NAME: be00117.DWG

RELEASE DATE:
3 MAR 94
APPROVAL:

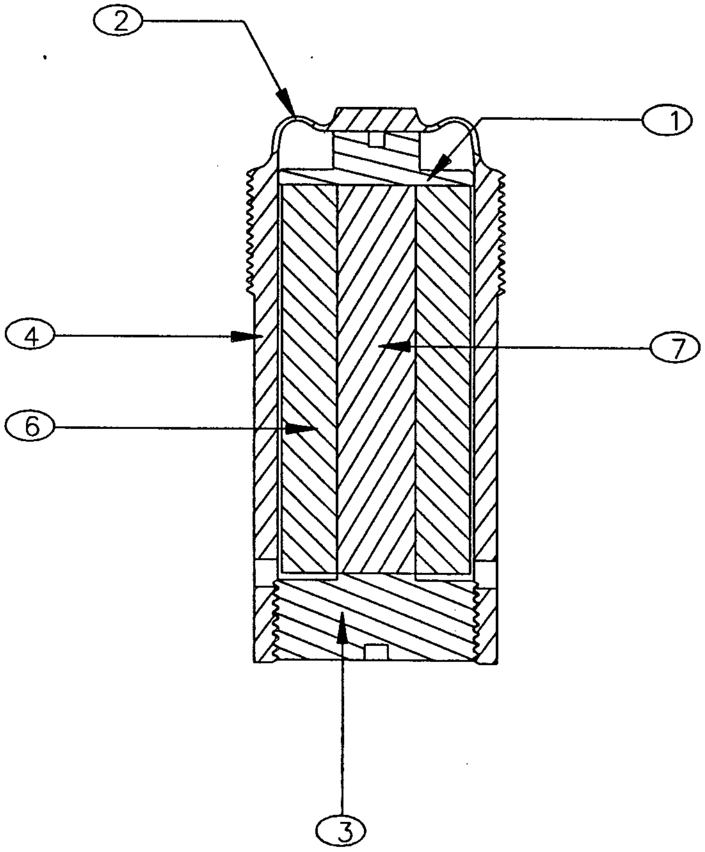

③ ETREMA, Ames,Iowa 1-800-327-7291
② MWS WIRE, Westlake Village, CA 818-991-8553
① Use BE000119 to wind coils

	QTY REQD	ITEM NO.	PART NO.	DESCRIPTION	MAT'L/SPEC
③	1	7	TRA P.O.- 7140-1	TERFENOL-D ROD	TERFENOL-D
① ②	1	6	TRA P.O.- 7169-2	COIL	MAG WRE, 30
		5			
	1	4	BE000112-3	HOUSING	---
	1	3	BE000114-3	END CAP	---
	1	2	BE000118-3	FLEXURE	---
	1	1	BE000115-3	MAGNETIC RETURN PATH	---
	---		BE000113	MOTIVE CELL ASSEMBLY	---

PARTS LIST

tra

TITLE: MOTIVE CELL - ASSEMBLY
SCALE: 4:1
DATE: 2 Mar 94
No. BE000113
Unless otherwise specified:
Dimensions are in inches
Tolerances on angles ± 0° 30'
Decimals .XX ± .03, .XXX ± .005
REV C
Mat'l: XXX
Heat Treat : XXX
DRAWN BY: A.P. Hilton
PROJECT: ACTUATOR II
FILE NAME: be00113c.DWG
RELEASE DATE: 10 Feb 95
APPROVAL:

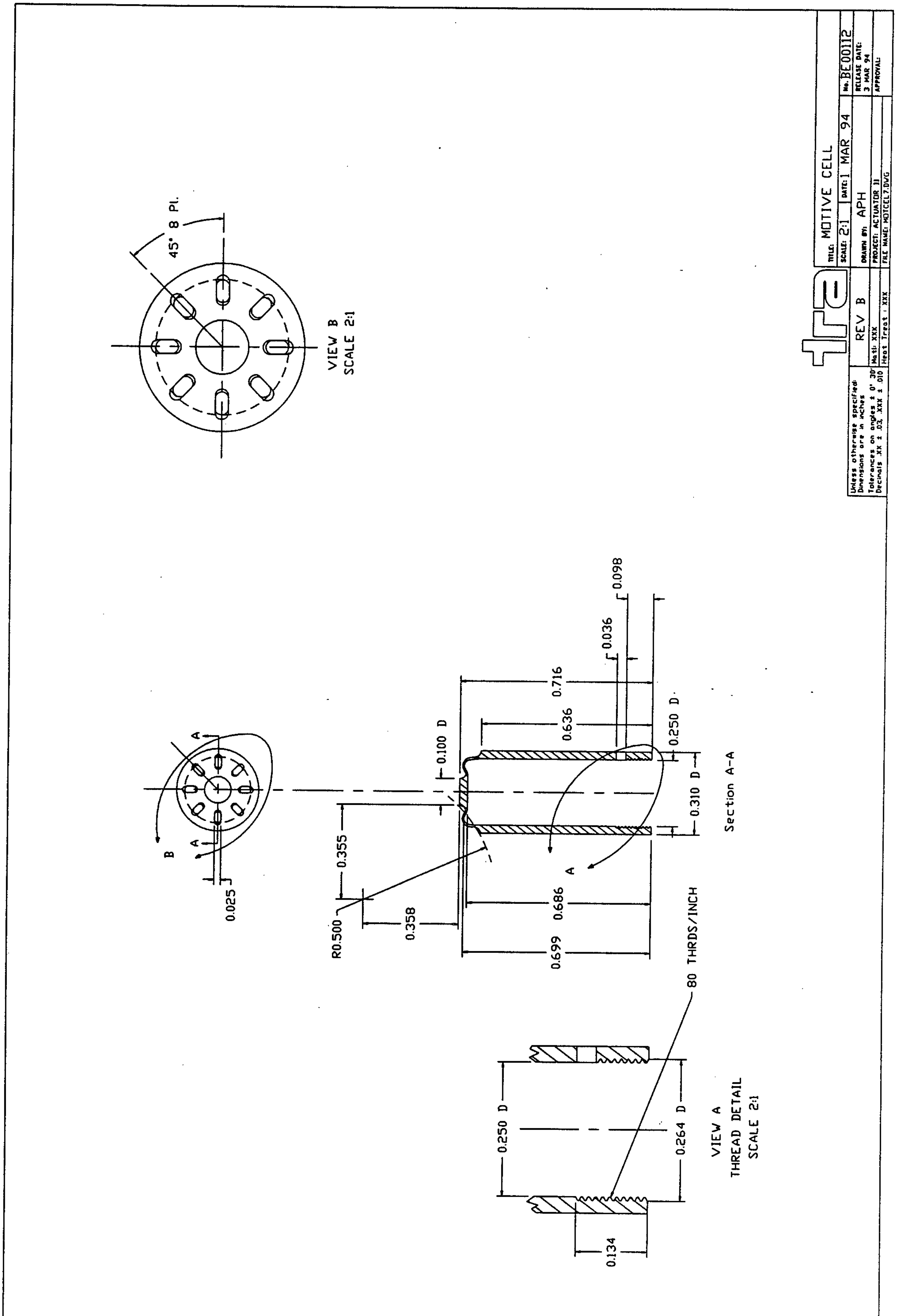
45° 8 PL.
VIEW B
SCALE 2:1
A
A
B
0.025
0.100 D
0.355
R0.500
0.358
0.716
0.636
0.036
0.098
0.250 D
0.310 D
0.686
0.699
A
Section A-A
80 THRDS/INCH
0.250 D
0.264 D
0.134
VIEW A
THREAD DETAIL
SCALE 2:1
Unless otherwise specified:
Dimensions are in inches
Tolerances on angles ± 0° 30'
Decimals .XX ± .03, .XXX ± .010
REV B
Mat'l: XXX
Heat Treat : XXX
TITLE: MOTIVE CELL
SCALE: 2:1
DATE: 1 MAR 94
DRAWN BY: APH
PROJECT: ACTUATOR II
FILE NAME: MOTCEL7.DWG
No. BE00112
RELEASE DATE:
3 MAR 94
APPROVAL:

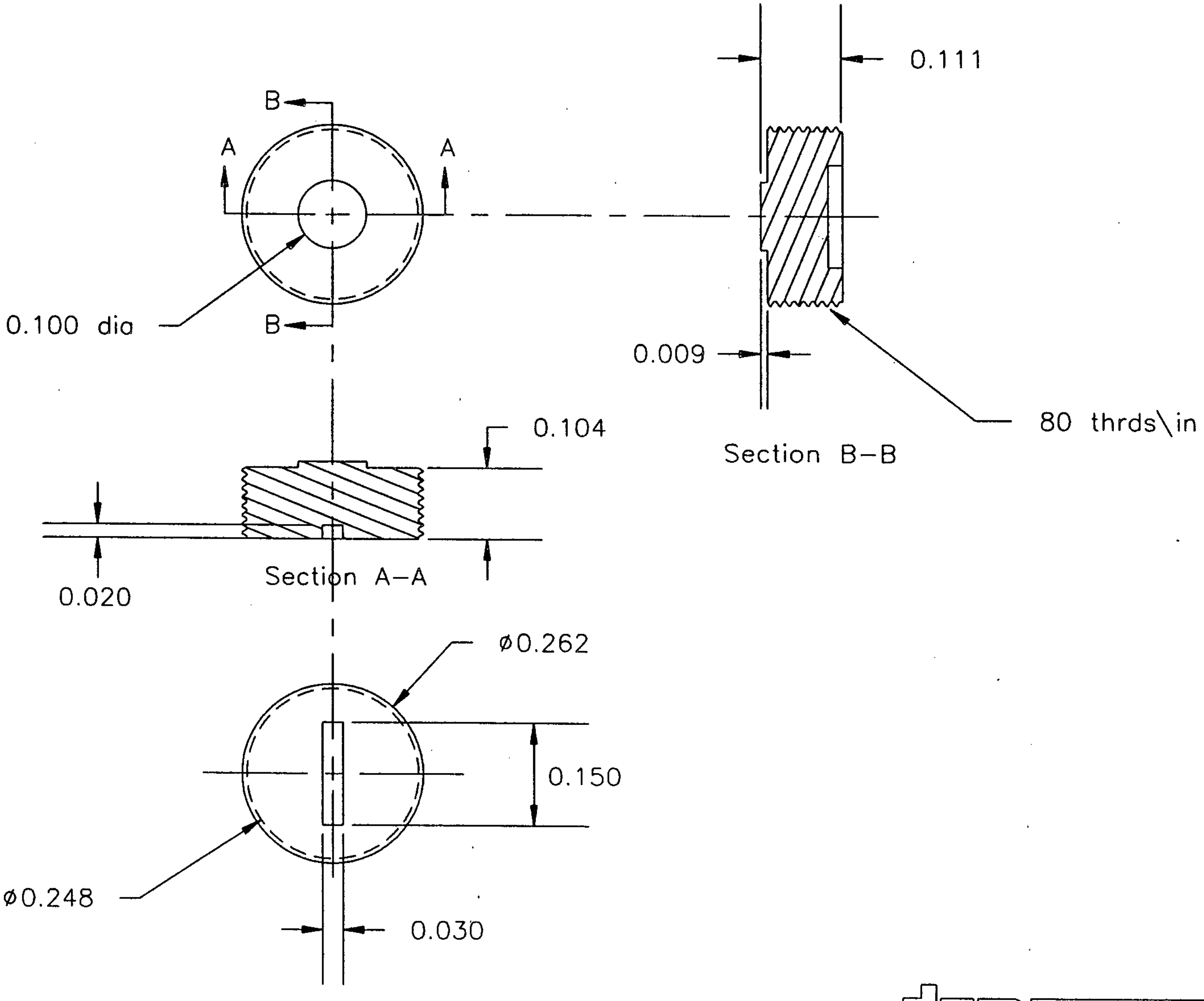

–3 Detail

Unless otherwise specified:
Dimensions are in inches
Tolerances on angles ± 0° 30'
Decimals .XX ± .03, .XXX ± .005

REV D
Matl: 4340 steel
Heat Treat : XXX

TITLE: END CAP
SCALE: 4:1
DATE: 2 Mar 94
DRAWN BY: AP Hilton
PROJECT: ACTUATOR II
FILE NAME: be00114d.DWG

No. BE000114
RELEASE DATE:
16 Dec 94
APPROVAL:

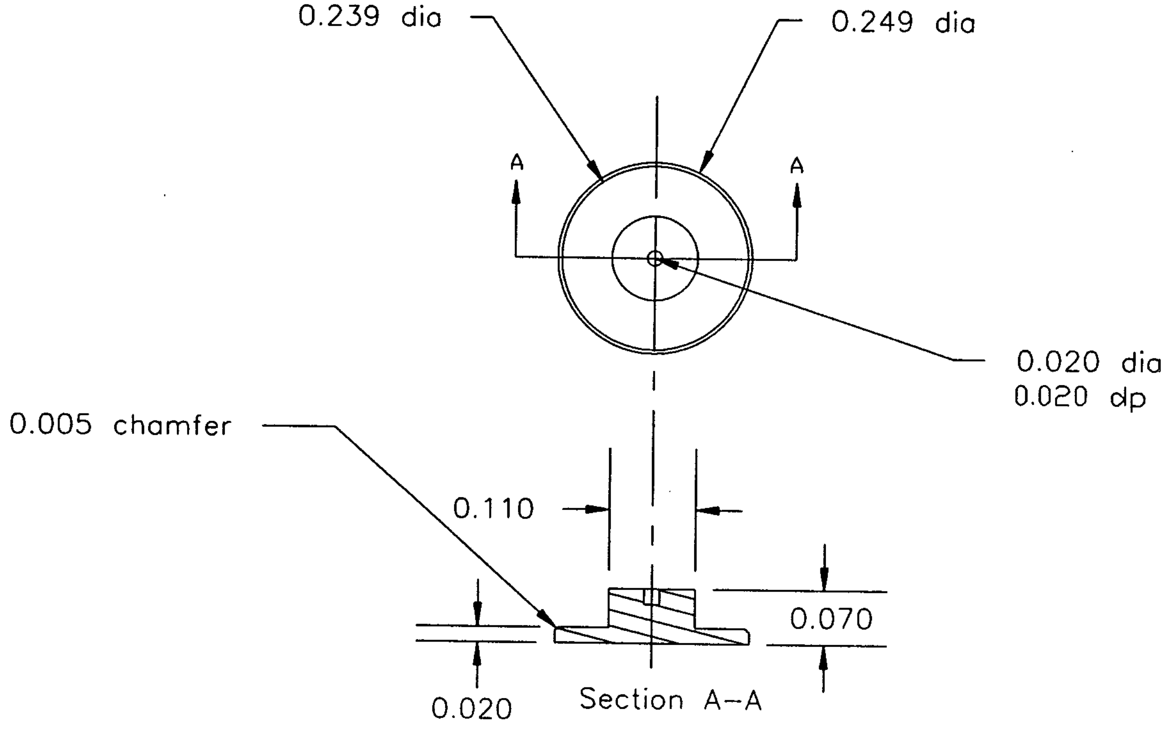

–3 Detail

Unless otherwise specified:
Dimensions are in inches
Tolerances on angles ± 0° 30'
Decimals .XX ± .03, .XXX ± .010

REV A
Mat'l: 4340 steel
Heat Treat : XXX

TITLE: MAGNETIC RETURN PATH
SCALE: 4:1
DATE: 2 MAR 94
No. BE000115
DRAWN BY: APH
PROJECT: ACTUATOR II
FILE NAME: be00115.dwg
RELEASE DATE: Mar 94
APPROVAL:

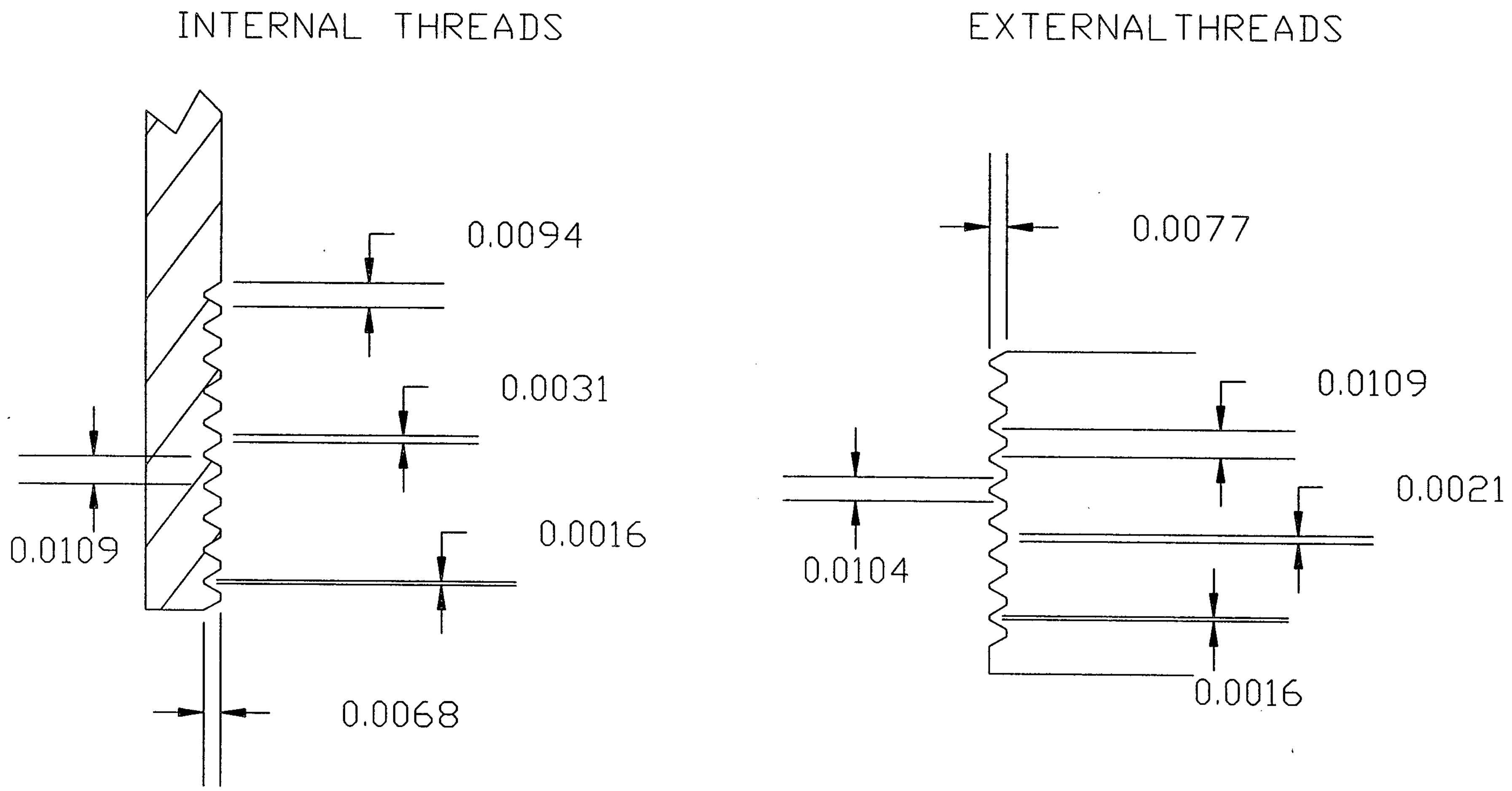

80 THREADS/INCH

Unless otherwise specified:
Dimensions are in inches
Tolerances on angles ± 0° 30'
Decimals .XX ± .03, .XXX ± .010

REV A
Matl: XXX
Heat Treat : XXX

TITLE: THREAD DETAIL - MOTIVE CELL
SCALE: 15:1
DATE: 3 MAR 94
No. BE00116
DRAWN BY: AP Hilton
RELEASE DATE: 3 MAR 94
PROJECT: ACTUATOR II
APPROVAL:
FILE NAME: be00116.DWG

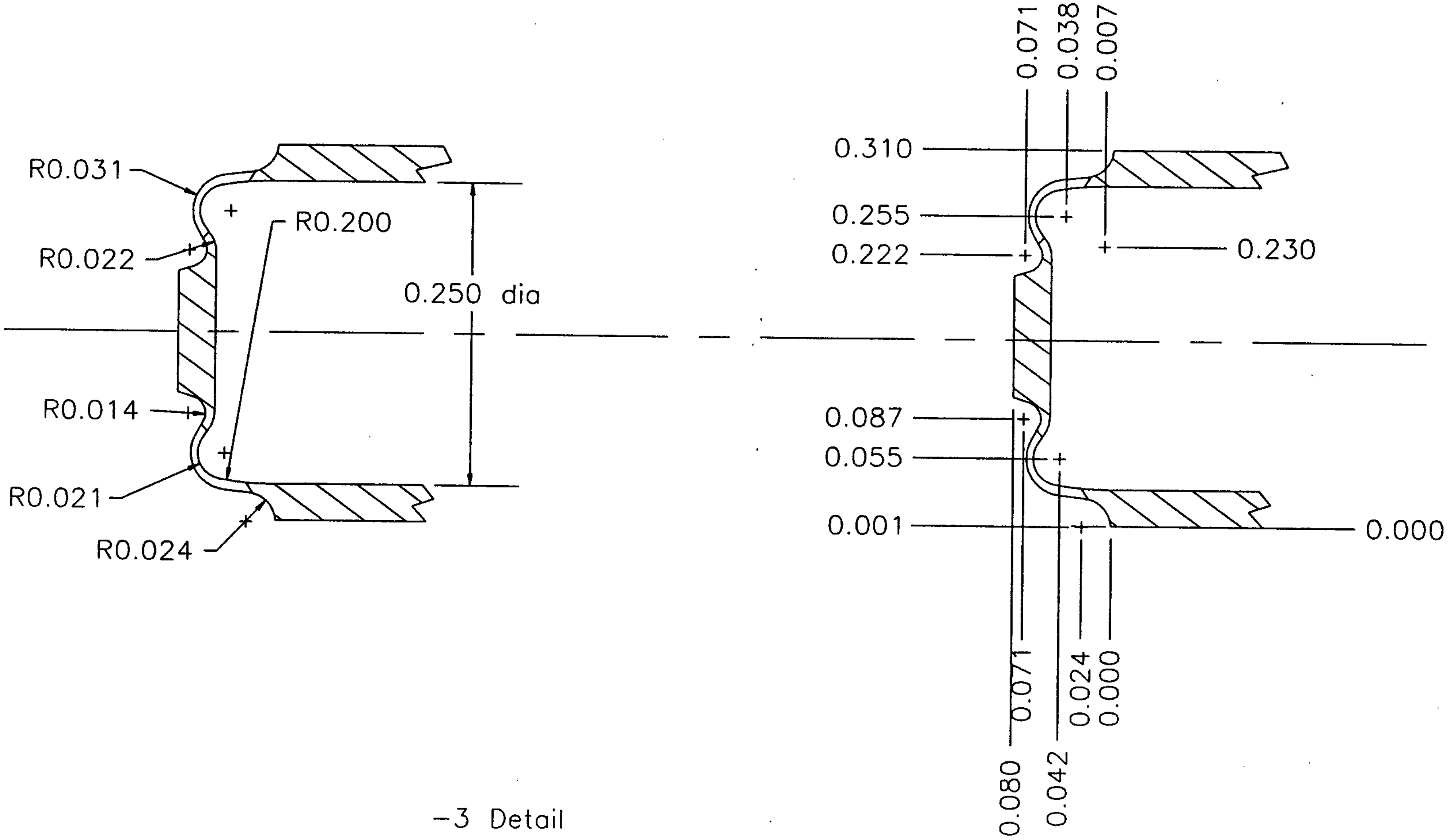

−3 Detail

Unless otherwise specified:
Dimensions are in inches
Tolerances on angles ± 0° 30'
Decimals .XX ± .03, .XXX ± .010

REV A
Matl: 4340 steel
Heat Treat : XXX

TITLE: FLEXURE DETAIL
SCALE: 7:1
DATE: 14 MAR 94
No. BE000118
DRAWN BY: AP Hilton
PROJECT: ACTUATOR II
FILE NAME: be00118.dwg
RELEASE DATE: 14 MAR 94
APPROVAL:

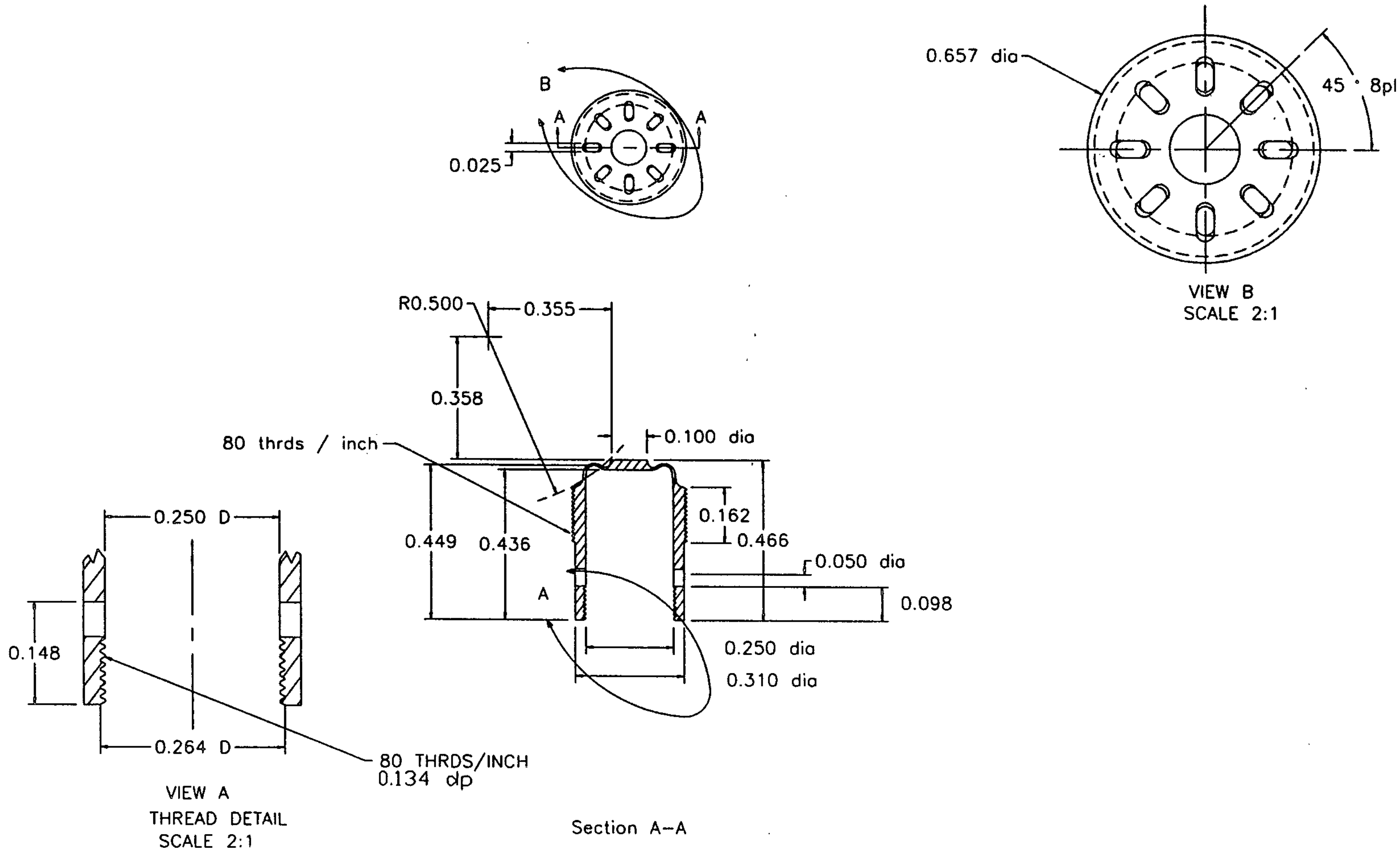

Unless otherwise specified:
Dimensions are in inches
Tolerances on angles ± 0° 30'
Decimals .XX ± .03, .XXX ± .005

REV B
Mat'l: XXX
Heat Treat : XXX

TITLE: MOTIVE CELL - 1/4" LONG
SCALE: 2:1
DATE: 16 Dec 94
No. BE00124
DRAWN BY: AP Hilton
RELEASE DATE: Dec 94
PROJECT: ACTUATOR II
FILE NAME: be00124b.dwg
APPROVAL:

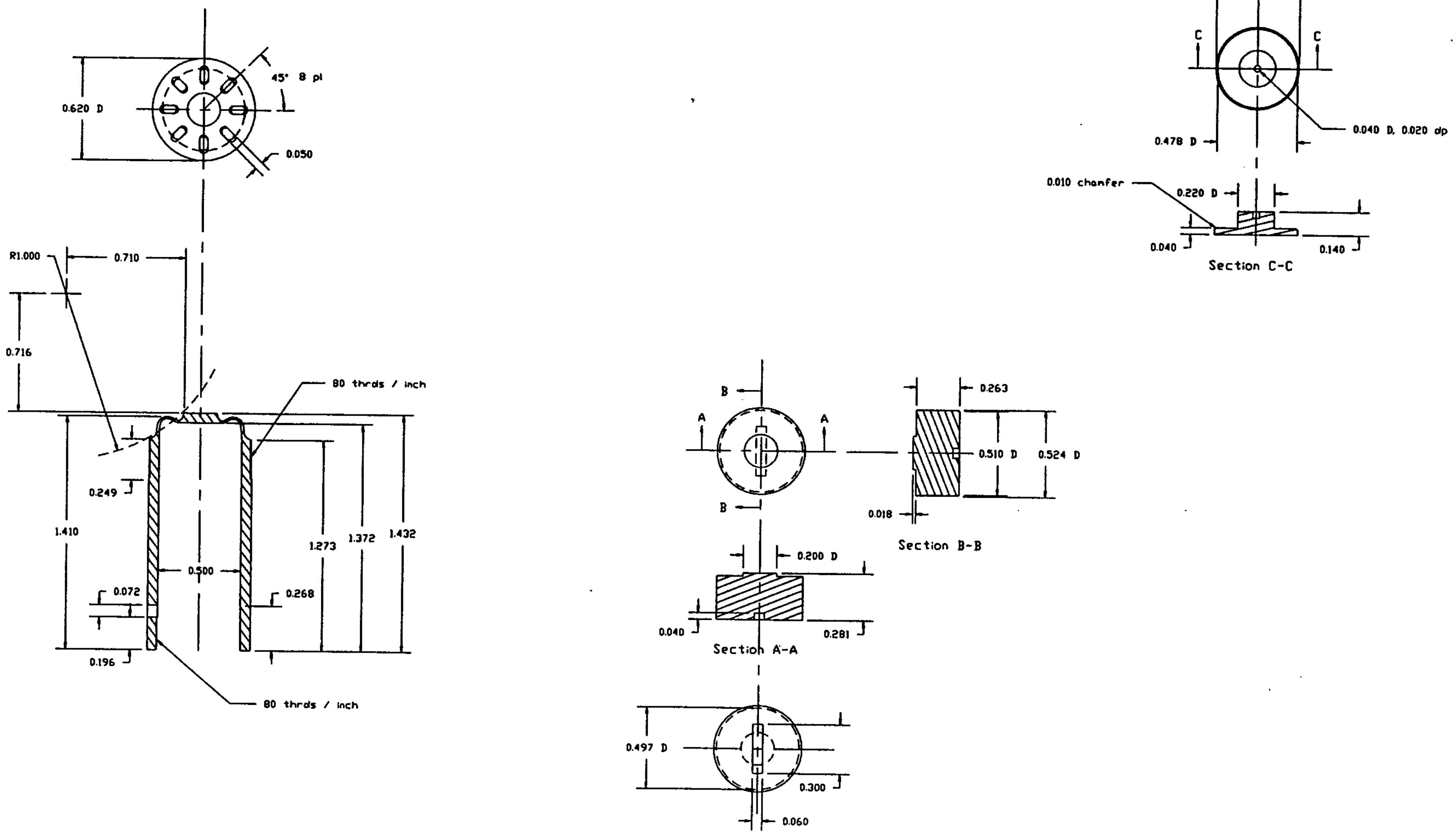

tra

TITLE: Motive Cell; 1 inch

Unless otherwise specified: Dimensions are in inches	REV A	SCALE: 1:1	DATE: 7 Jul 94
Tolerances on angles ± 0° 30' Decimals .XX ± .03, .XXX ± .005	Mat'l: XXX Heat Treat : XXX	DRAWN BY: A. Hilton PROJECT: Actuator II FILE NAME: be00139.dwg	No. BE00139 RELEASE DATE: XXX APPROVAL:

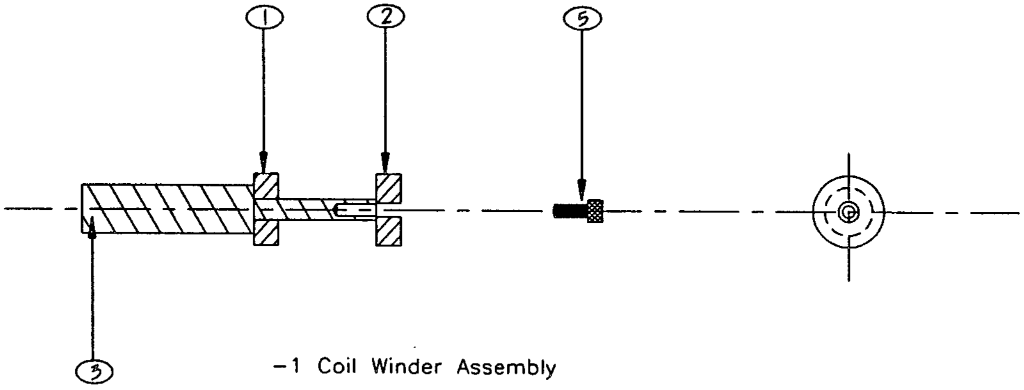

-1 Coil Winder Assembly

① Small Parts Inc., Miami Lakes, FL 305-557-8222

QTY REQD	ITEM NO.	PART NO.	DESCRIPTION	MAT'L/SPEC
1	6	XXX	XXX	---
① 1	5	Q-SHCX-172-4	#1-72 x 1/4" HEX HD SCREW	SS
1	4	XXX	XXX	---
1	3	BE000119-3	WINDER CORE	---
1	2	BE000119-7	TEFLON WASHER	TEFLON
1	1	BE000119-5	TEFLON WASHER	TEFLON
---		BE000195	COIL WINDER ASSEMBLY	---

PARTS LIST

tra

Unless otherwise specified: Dimensions are in inches Tolerances on angles ± 0° 30' Decimals .XX ± .03, .XXX ± .005	REV A Matl: (Noted) Heat Treat : NO	TITLE: COIL WINDER ASSEMBLY SCALE: 1:1 DATE: 24 Feb 95 DRAWN BY: AP Hilton PROJECT: ACTUATOR II FILE NAME: be00195.dwg	No. BE000195 RELEASE DATE: XXX APPROVAL:

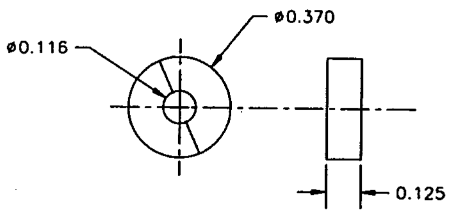

-5 Back Washer #1
Mat'l: teflon

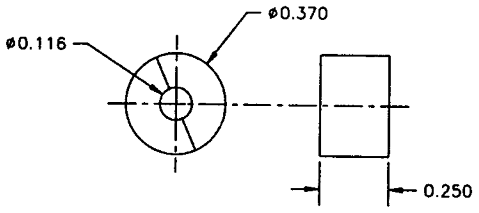

-7 Back Washer #2
Mat'l: teflon

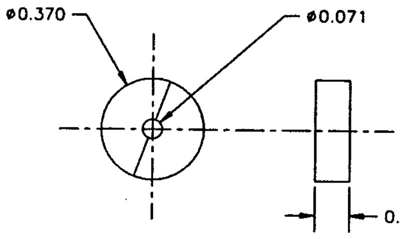

-9 Front Washer
Mat'l: teflon

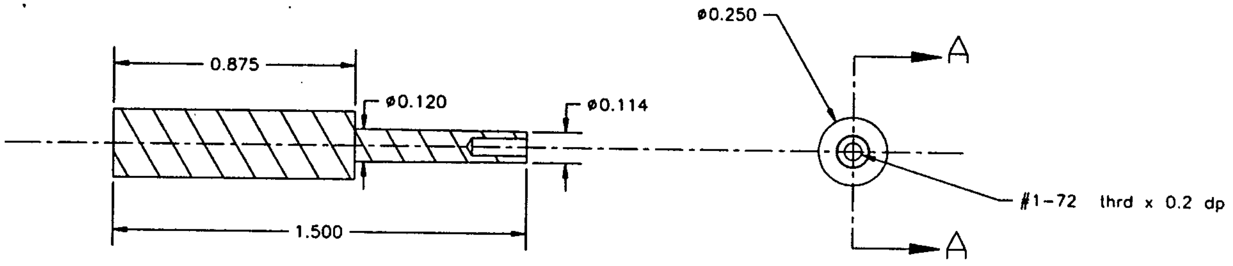

-3 Mandrel

		TITLE: Detail; Coil Winder		
		SCALE: 3:1	DATE: 17 Mar 94	No. BE000119
Unless otherwise specified: Dimensions are in inches	Rev C	DRAWN BY: A. P. Hilton		RELEASE DATE: 3 Oct 95
Tolerances on angles ± 0° 30' Decimals .XX ± .03, .XXX ± .005	Matl: Steel	PROJECT: Actuator II		APPROVAL:
	Heat Treat:	FILE NAME: BE00119c.dwg		C

See BE00127 for details

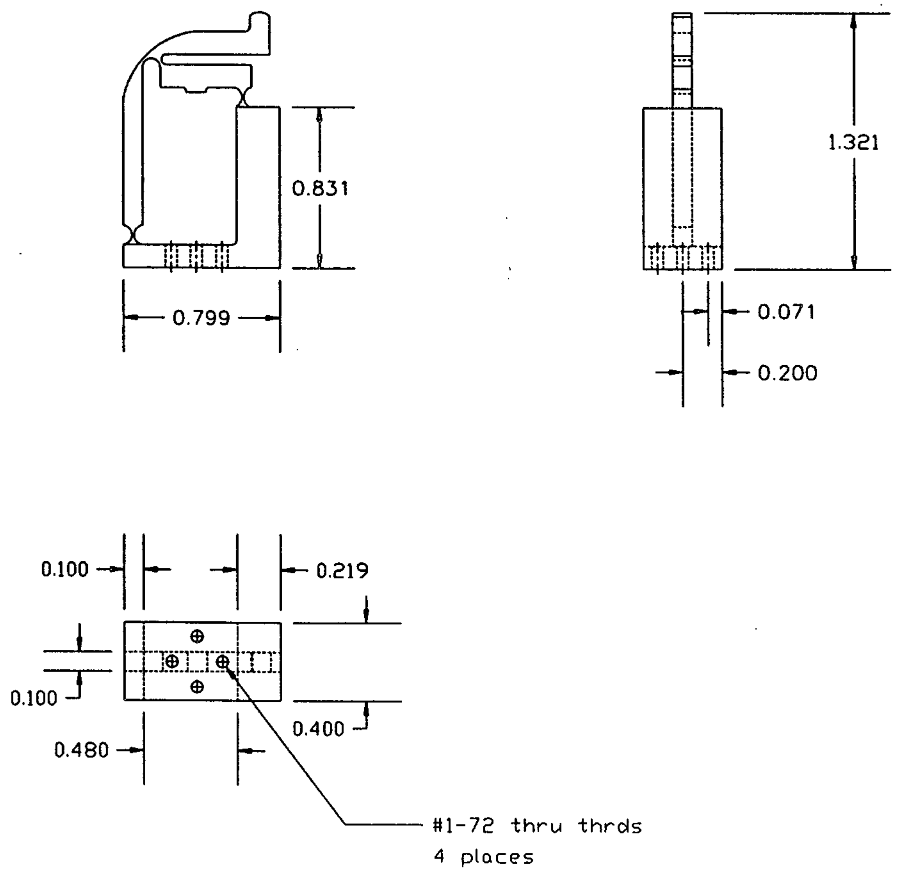

Unless otherwise specified:
Dimensions are in inches
Tolerances on angles ± 0° 30'
Decimals .XX ± .03, .XXX ± .010

REV A
Matl: Steel
Heat Treat : XXX

TITLE: Deflection Magnifier
SCALE: 1:1
DATE: 9 May 94
No. BE00126
DRAWN BY: AP Hilton
PROJECT: Actuator II
FILE NAME: BE00126.dwg
RELEASE DATE: XXX
APPROVAL:

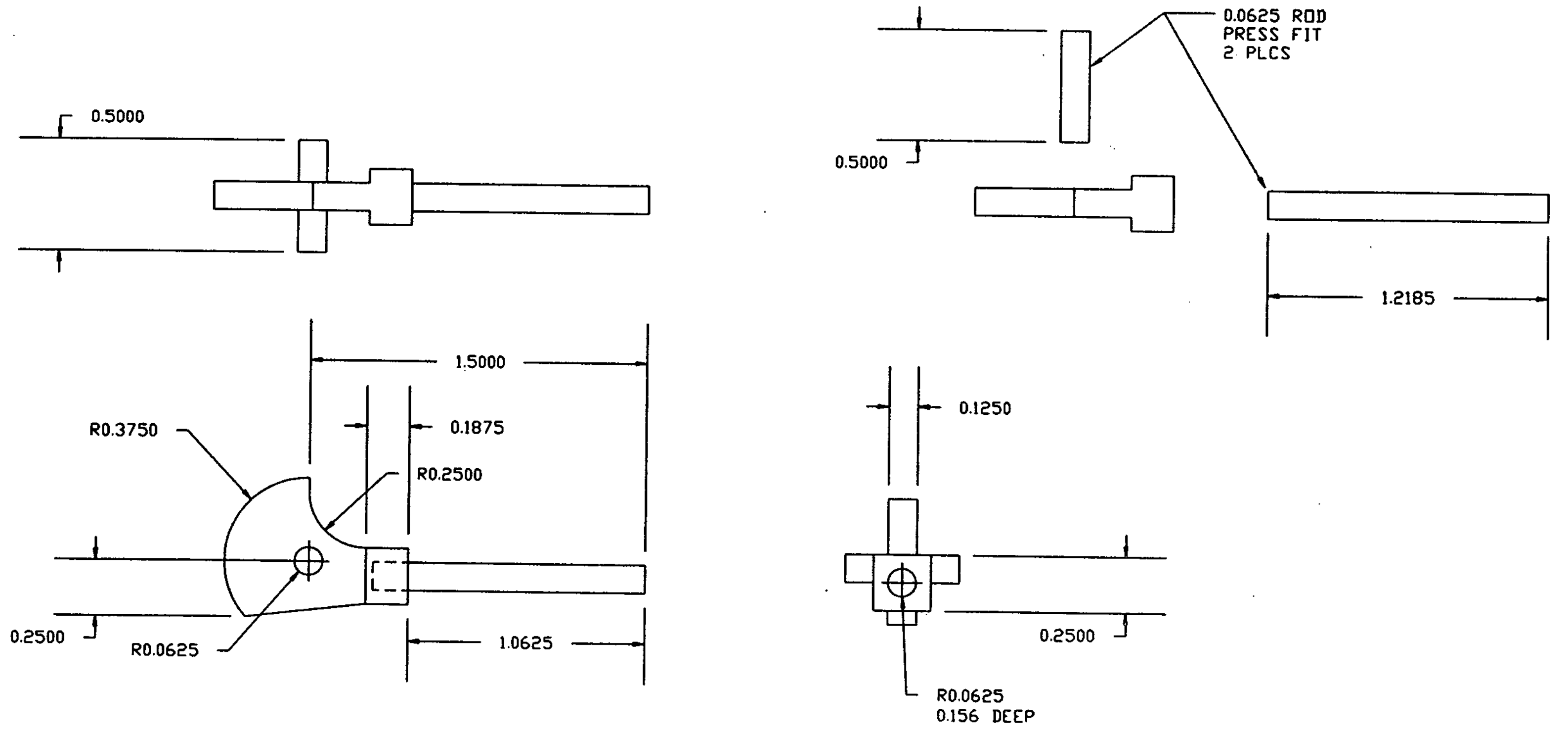

TITLE: CAM
SCALE: NTS
DATE: 11/12/93
No. 100300
DRAWN BY: R.R.GOODWIN
REV C
PROJECT: Actuator II
FILE NAME: 100300.DWG

TITLE: TRUNION
SCALE:
DATE: 11/12/93
No. 100301
DRAWN BY: R.R.GOODWIN
REV C
PROJECT: Actuator II
FILE NAME: 100301.DWG

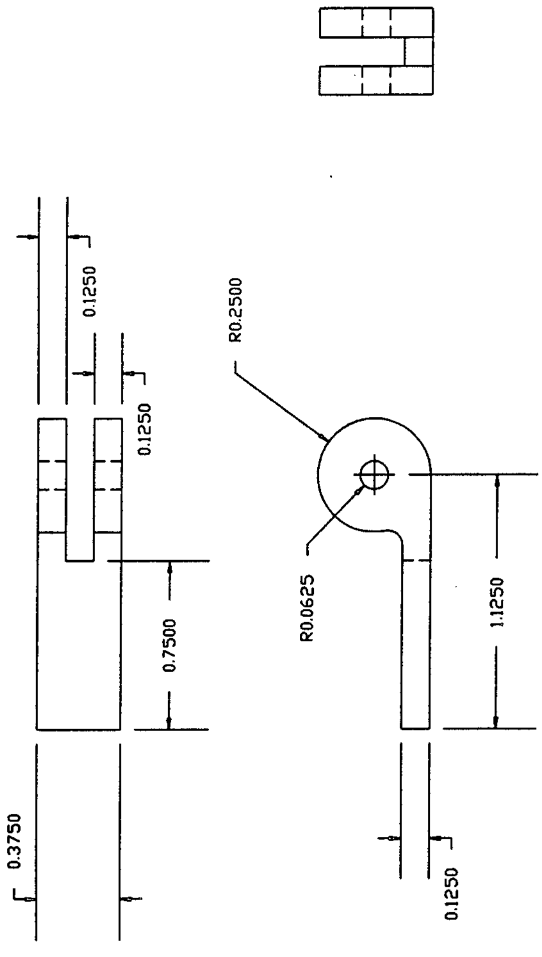

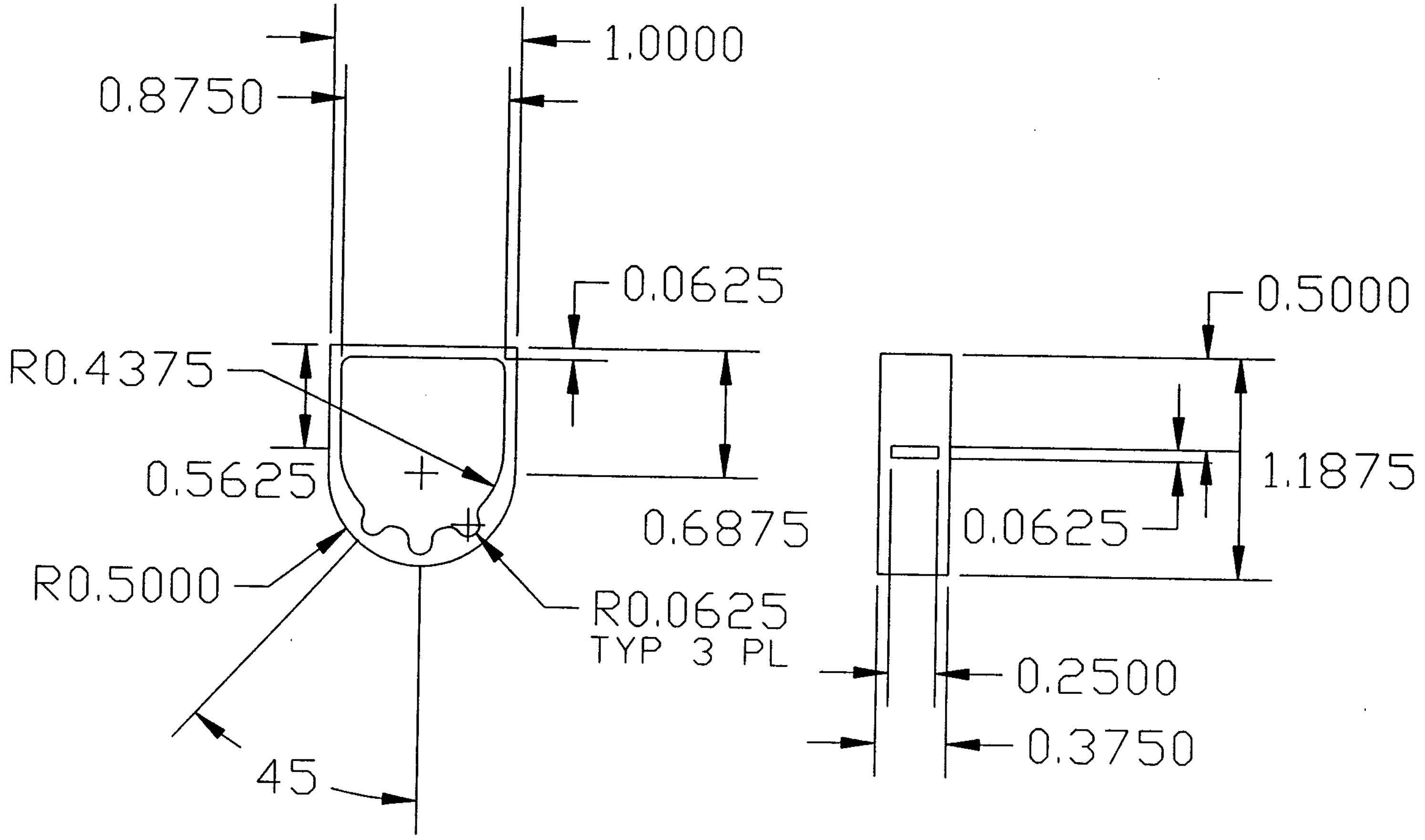

tra

TITLE: FINGER ATTACHMENT
SCALE: 1:1
DATE: 1/7/94
No. 100302
DRAWN BY: R.R.GOODWIN
REV A
PROJECT: Actuator II
FILE NAME: 100302.DWG

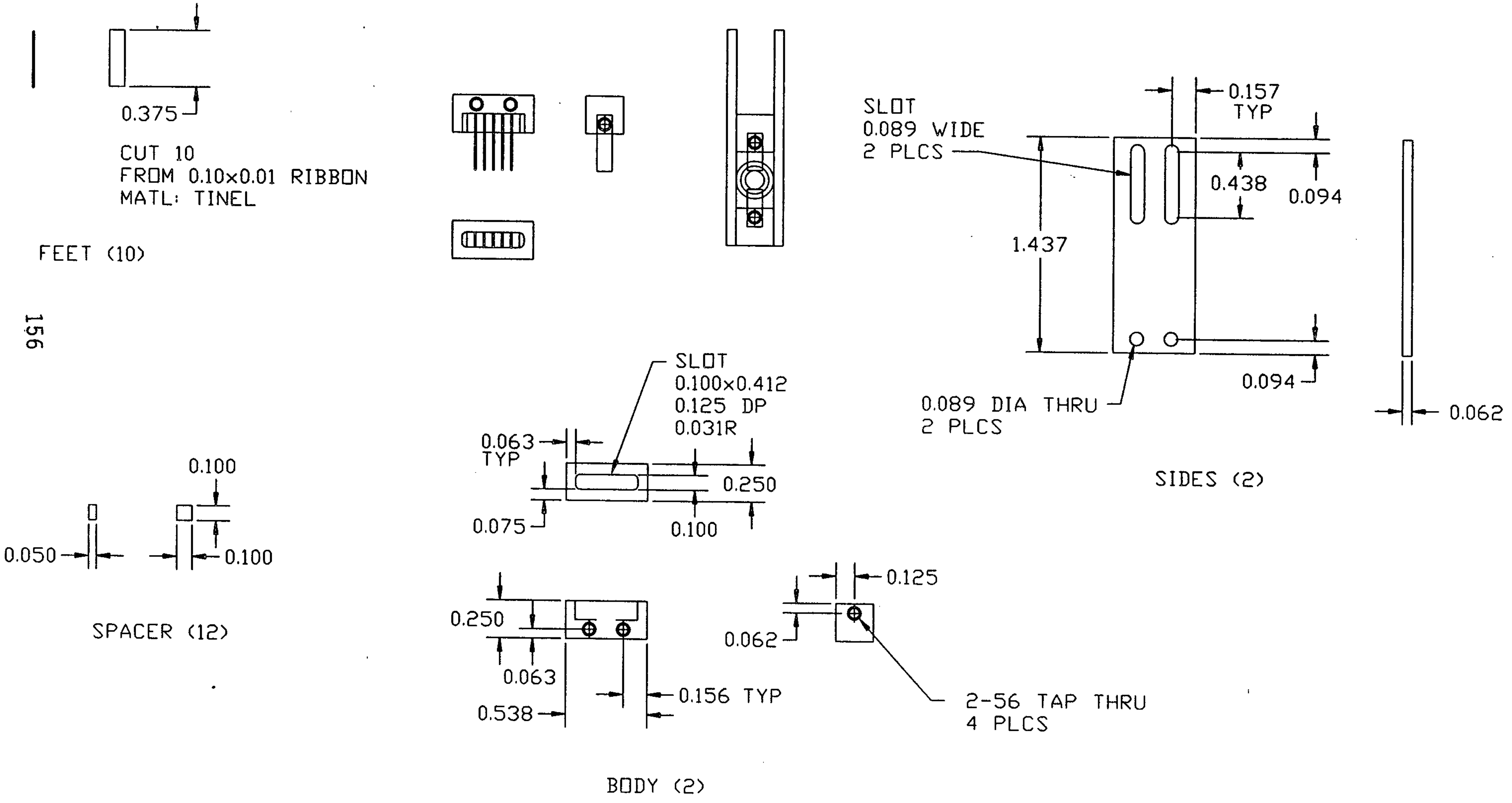

tra

TITLE: CRAWLER ASSY
SCALE: 1:1 DATE: 2/23/94 No. 100303
DRAWN BY: GOODWIN RELEASE DATE:
PROJECT: ACTUATOR II APPROVAL:
FILE NAME: 100303.DWG

Unless otherwise specified:
Dimensions are in inches
Tolerances on angles ± 0° 30'
Decimals .XX ± .03, .XXX ± .010
Matl: XXX
Heat Treat : XXX

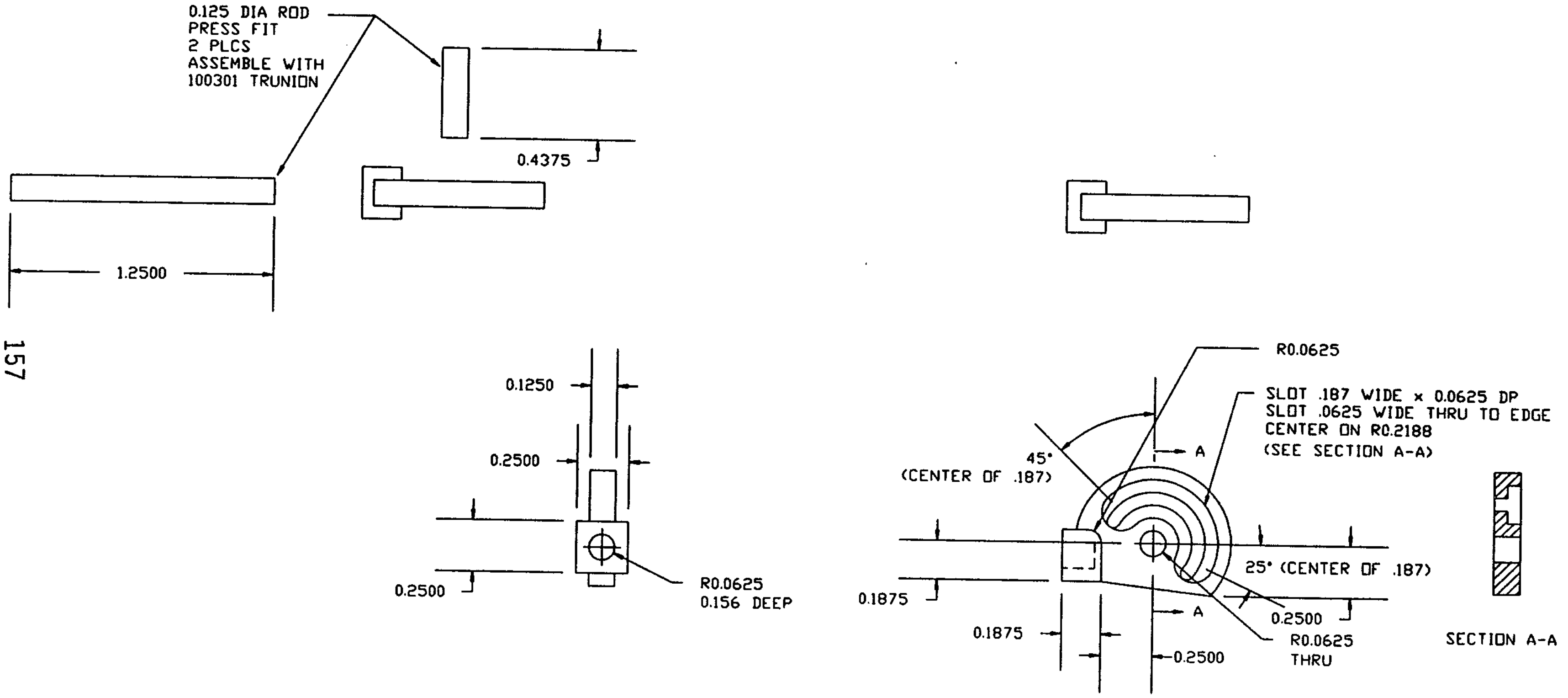

tra

TITLE: OPTICAL XDUCER CAM
SCALE: NTS
DATE: 1/7/94
No. 100304
DRAWN BY: R.R.GOODWIN
PROJECT: Actuator II
FILE NAME: 100304.DWG

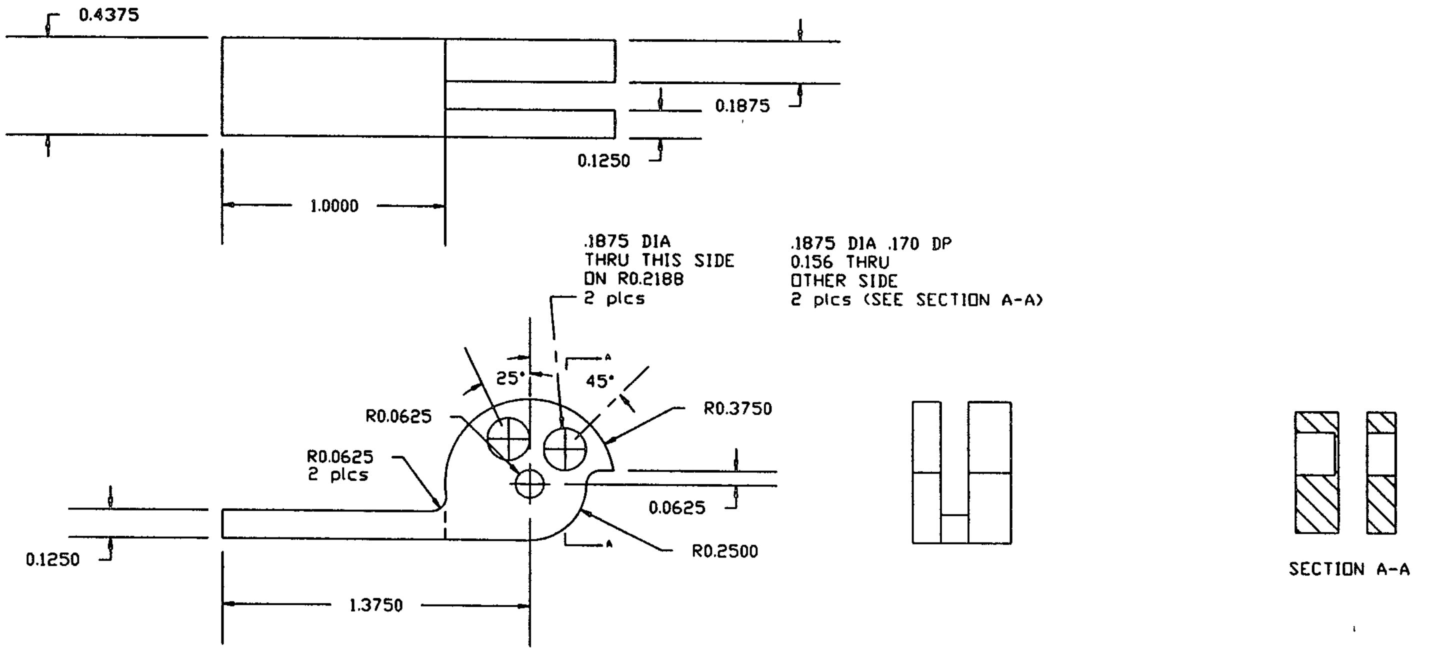

TITLE: OPTICAL XDUCER TRUNION
SCALE: DATE: 1/7/94 No. 100305
DRAWN BY: R.R.GOODWIN
PROJECT: Actuator II
FILE NAME: 100305.DWG

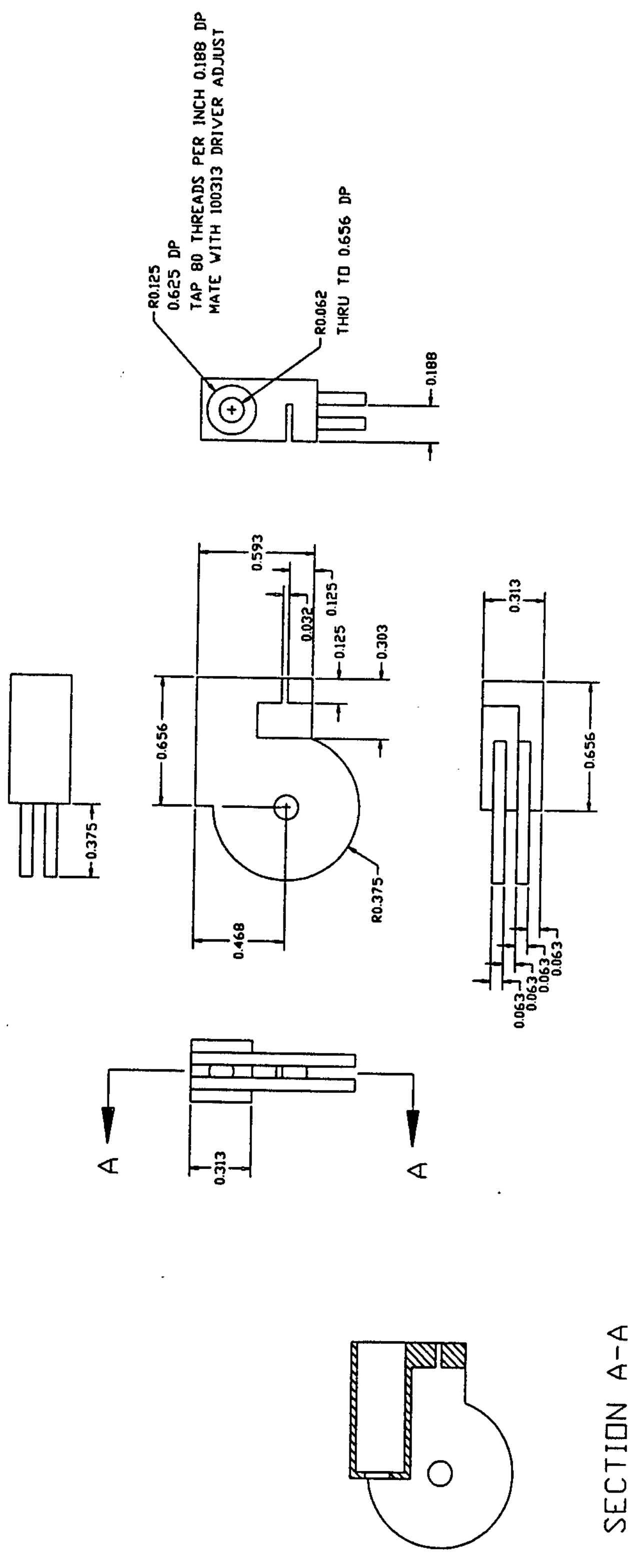

TITLE: DRIVER HOUSING
SCALE: 1:1 DATE: 3/30/94 No. 100307
DRAWN BY: GOODWIN RELEASE DATE:
PROJECT: ACTUATOR II
FILE NAME: 100307.DWG APPROVAL:

Unless otherwise specified:
Dimensions are in inches
Tolerances on angles ± 0° 30'
Decimals .XX ± .03, .XXX ± .010

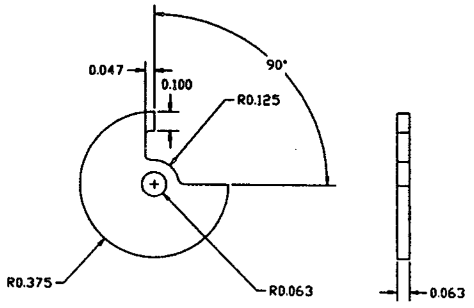

Unless otherwise specified:
Dimensions are in inches
Tolerances on angles ± 0° 30'
Decimals .XX ± .03, .XXX ± .010

tra

TITLE: STEPPER
SCALE: 1:1
DATE: 3/30/94
No. 100308
DRAWN BY: GOODWIN
RELEASE DATE: XXX
PROJECT: ACTUATOR II
APPROVAL:
FILE NAME: 100308.DWG

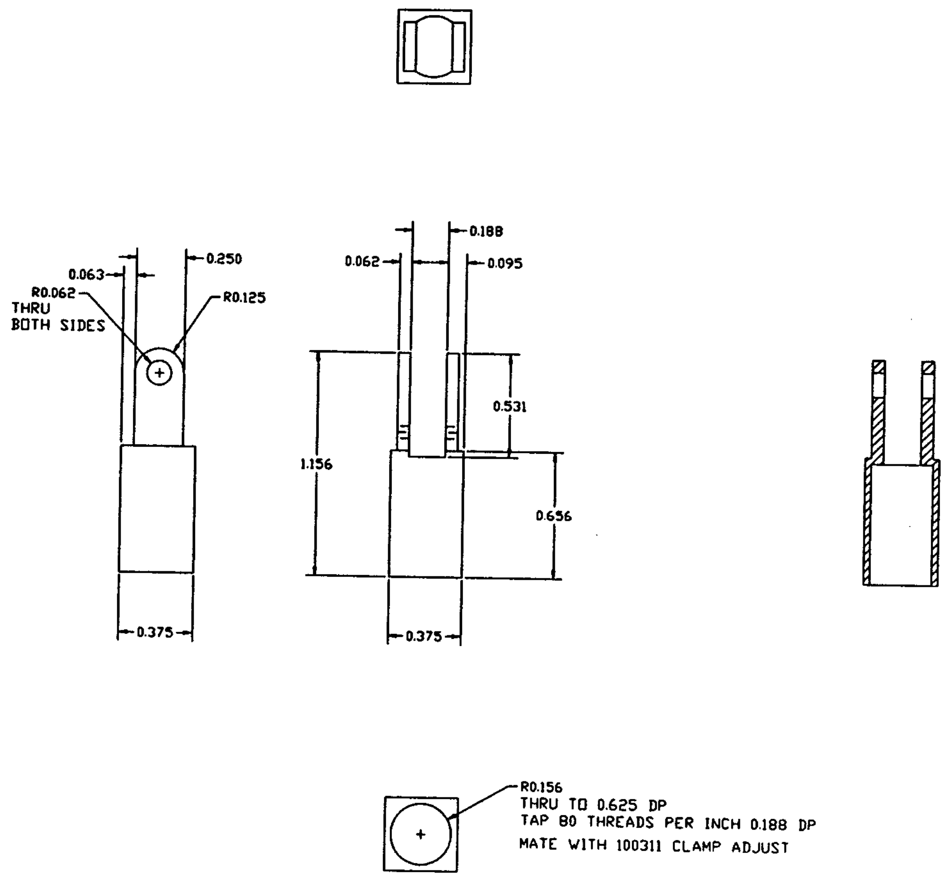

Unless otherwise specified:
Dimensions are in inches
Tolerances on angles ± 0° 30'
Decimals .XX ± .03, .XXX ± .010

tra

TITLE: CLAMP HOUSING
SCALE: 1:1
DATE: 3/30/94
No. 100309
DRAWN BY: GOODWIN
RELEASE DATE: XXX
PROJECT: ACTUATOR II
FILE NAME: 100309.DWG
APPROVAL:

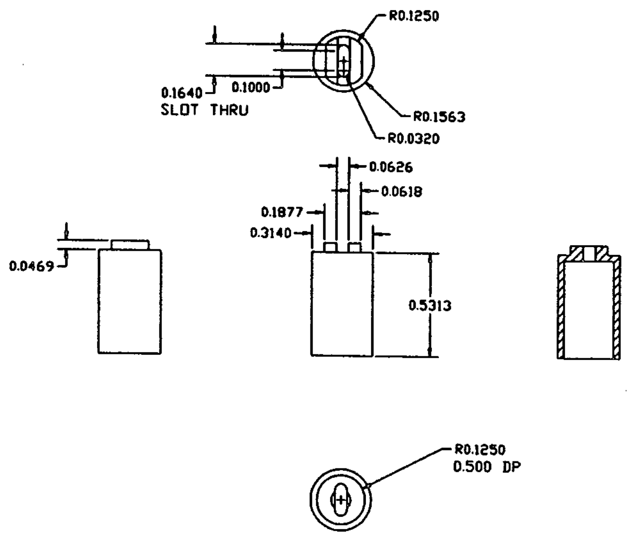

Unless otherwise specified:
Dimensions are in inches
Tolerances on angles ± 0° 30'
Decimals .XX ± .03, .XXX ± .010

tra

TITLE: PASSIVE CLAMP
SCALE: 1:1
DATE: 3/30/94
No. 100310
DRAWN BY: GOODWIN
RELEASE DATE: XXX
PROJECT: ACTUATOR II
APPROVAL:
FILE NAME: PSVCLMP

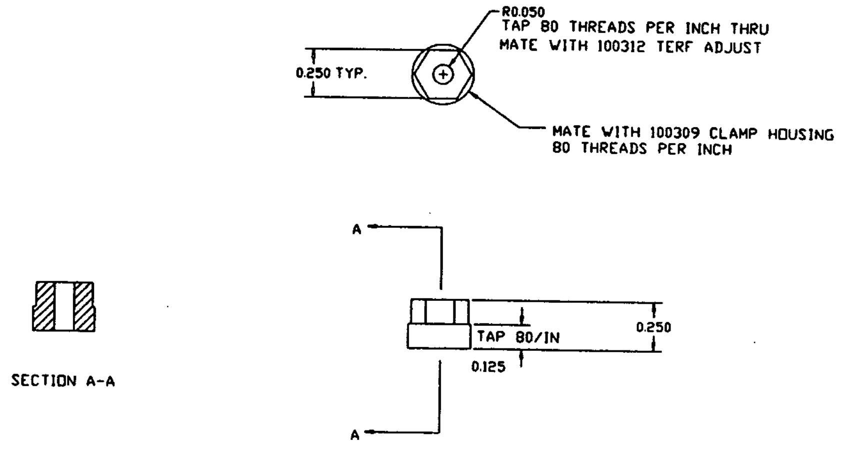
R0.050
TAP 80 THREADS PER INCH THRU
MATE WITH 100312 TERF ADJUST
0.250 TYP.
MATE WITH 100309 CLAMP HOUSING
80 THREADS PER INCH
A
A
TAP 80/IN
0.250
0.125
SECTION A-A

Unless otherwise specified Dimensions are in inches Tolerances on angles ± 0° 30' Decimals .XX ± .03, .XXX ± .010	TITLE: CLAMP ADJUST		
	SCALE: 1:1	DATE: 3/31/94	No. 100311
	DRAWN BY: GOODWIN		RELEASE DATE: XXX
	PROJECT: ACTUATOR II		APPROVAL:
	FILE NAME: CLMPAJST		

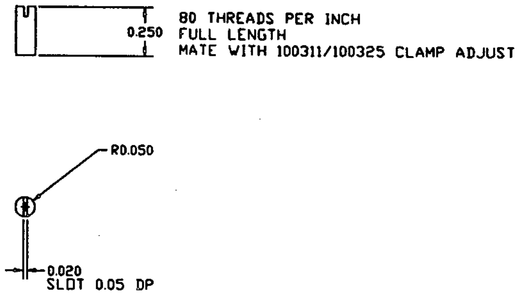

Unless otherwise specified:
Dimensions are in inches
Tolerances on angles ± 0° 30'
Decimals .XX ± .03, .XXX ± .010

TITLE: TERF ADJUST
SCALE: 1:1
DATE: 3/31/94
No. 100312
DRAWN BY: GOODWIN
RELEASE DATE:
PROJECT: ACTUATOR II
APPROVAL:
FILE NAME: TERFAJST

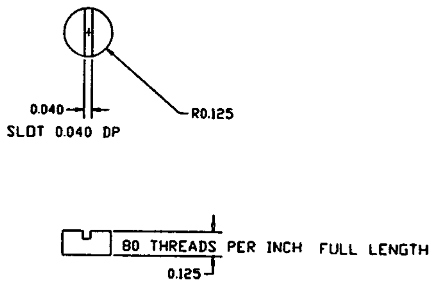

MATE WITH 100307/100316 DRIVER HOUSING

Unless otherwise specified:
Dimensions are in inches
Tolerances on angles ± 0° 30'
Decimals .XX ± .03, .XXX ± .010

tra

TITLE: DRIVER ADJUST		
SCALE: 1:1	DATE: 3/31/94	No. 100313
DRAWN BY: GOODWIN		RELEASE DATE: XXX
PROJECT: ACTUATOR II		APPROVAL:
FILE NAME: 100313.DWG		

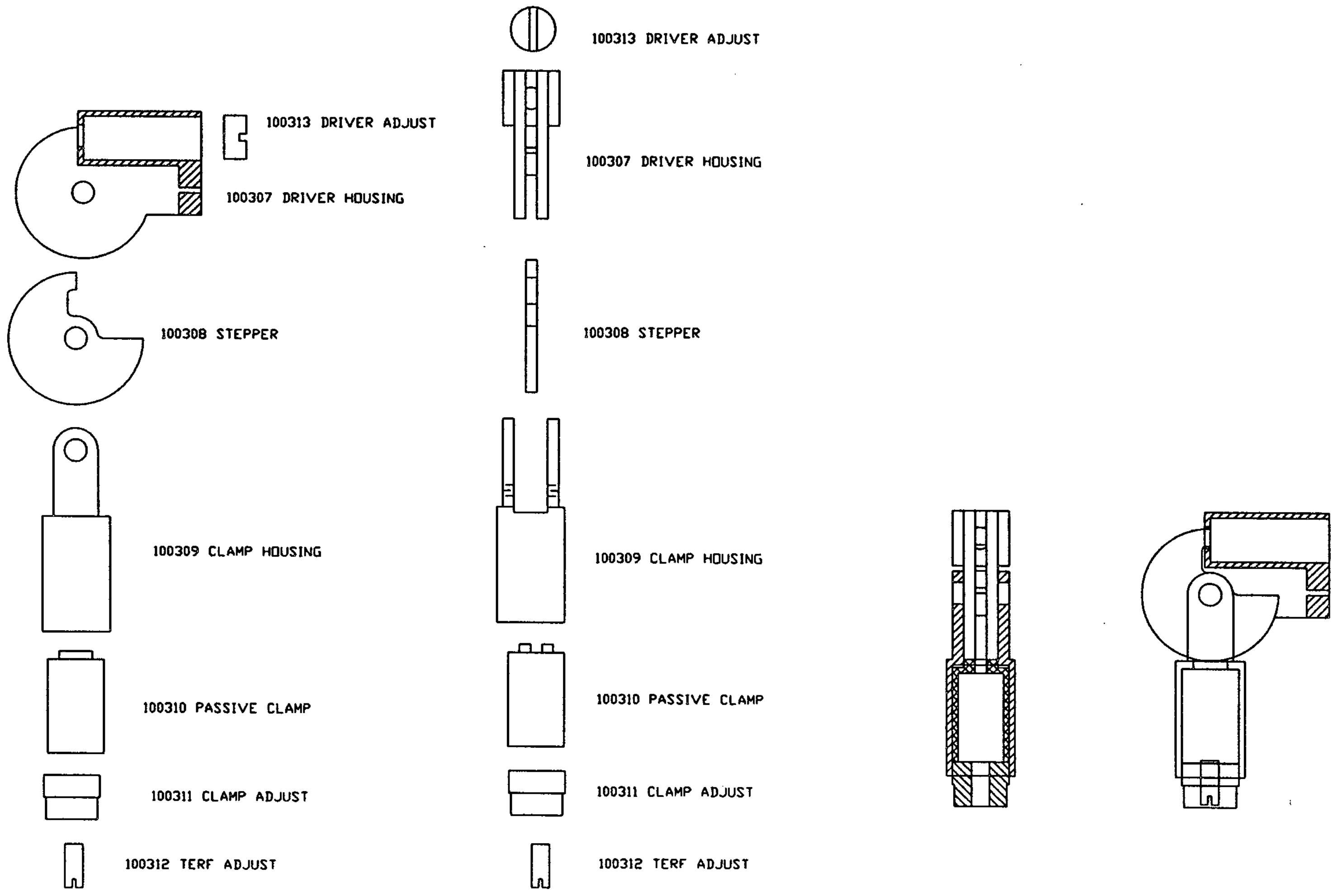

Unless otherwise specified:
Dimensions are in inches
Tolerances on angles ± 0° 30'
Decimals .XX ± .03, .XXX ± .010

tra

TITLE: ACTUATOR ASSEMBLY
SCALE: 1:1
DATE: 3/30/94
No. 100314
DRAWN BY: GOODWIN
RELEASE DATE:
PROJECT: ACTUATOR II
FILE NAME: MTRASSY
APPROVAL:

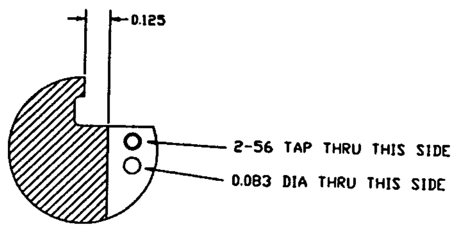

SECTION A-A

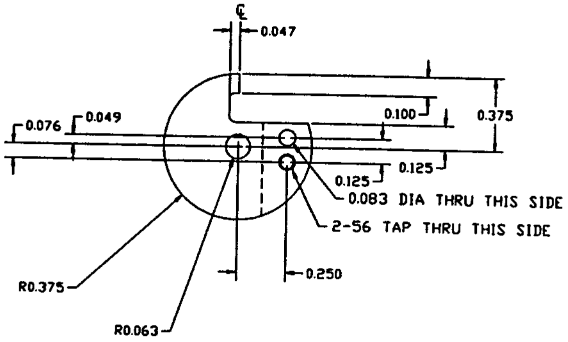

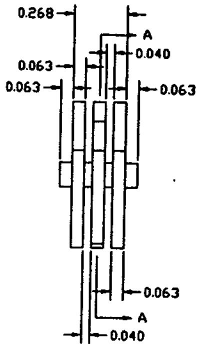

Unless otherwise specified:
Dimensions are in inches
Tolerances on angles ± 0° 30'
Decimals .XX ± .03, .XXX ± .010

tra

TITLE: DRIVER FLEXURE
SCALE: 1:1
DATE: 4/4/94
No. 100315
DRAWN BY: GOODWIN
RELEASE DATE:
PROJECT: ACTUATOR II
FILE NAME: 100315.DWG
APPROVAL:

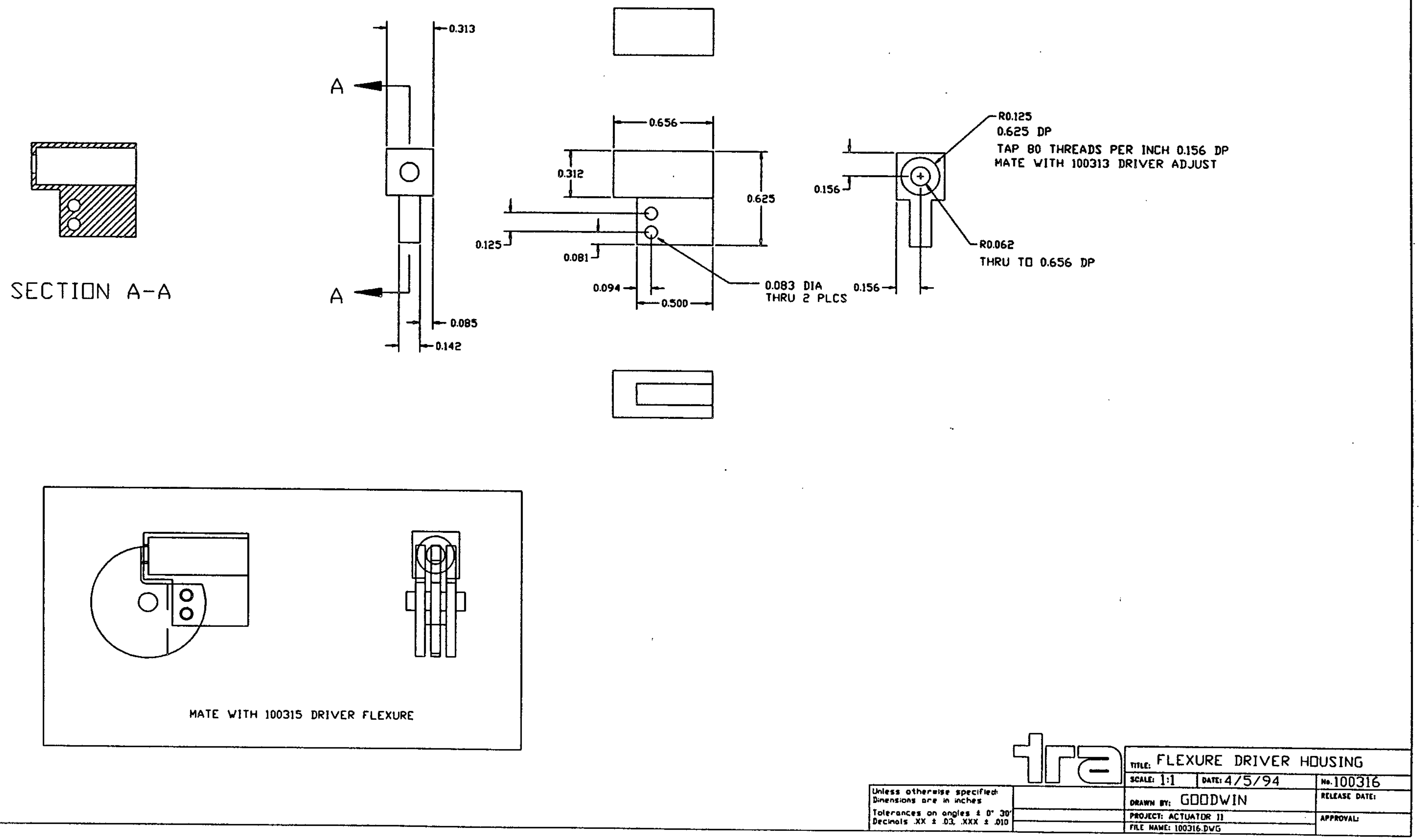
SECTION A-A
A
A
0.313
0.085
0.142
0.656
0.312
0.625
0.125
0.081
0.094
0.500
0.083 DIA
THRU 2 PLCS
R0.125
0.625 DP
TAP 80 THREADS PER INCH 0.156 DP
MATE WITH 100313 DRIVER ADJUST
0.156
R0.062
THRU TO 0.656 DP
0.156
MATE WITH 100315 DRIVER FLEXURE
Unless otherwise specified:
Dimensions are in inches
Tolerances on angles ± 0° 30'
Decimals .XX ± .03, .XXX ± .010
tra
TITLE: FLEXURE DRIVER HOUSING
SCALE: 1:1
DATE: 4/5/94
No. 100316
DRAWN BY: GOODWIN
RELEASE DATE:
PROJECT: ACTUATOR II
FILE NAME: 100316.DWG
APPROVAL:

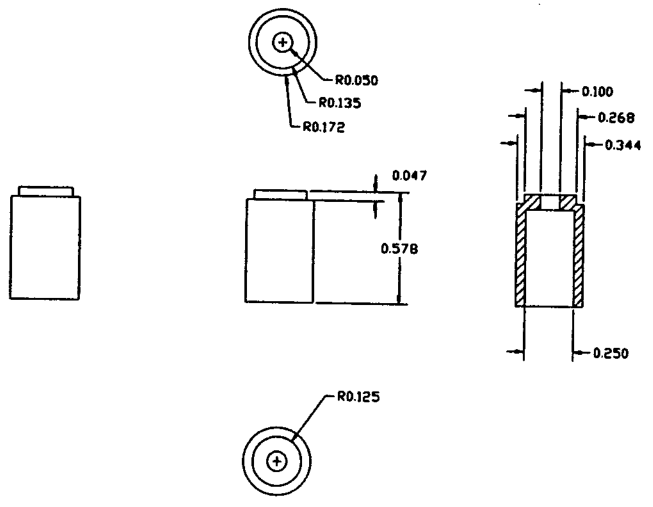

Unless otherwise specified:
Dimensions are in inches
Tolerances on angles ± 0° 30'
Decimals .XX ± .03, .XXX ± .010

tra

TITLE: PASSIVE CLAMP
SCALE: 1:1
DATE: 4/7/94
No. 100317
DRAWN BY: GOODWIN
RELEASE DATE: XXX
PROJECT: ACTUATOR II
FILE NAME: 100317.DWG
APPROVAL:

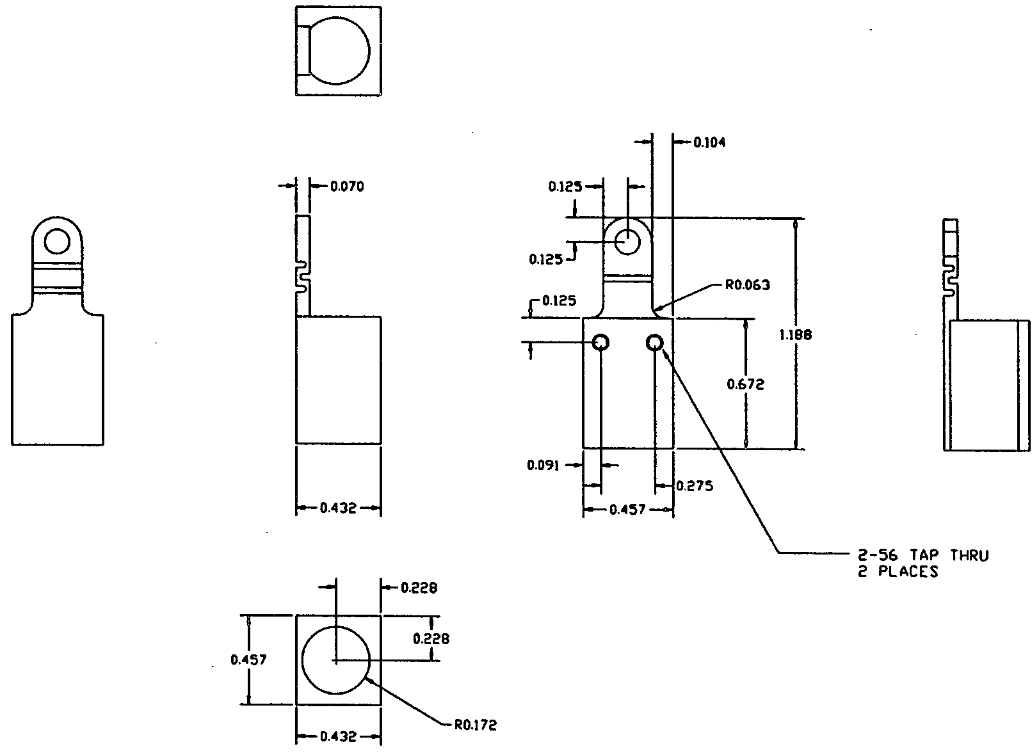

Unless otherwise specified:
Dimensions are in inches
Tolerances on angles ± 0° 30'
Decimals .XX ± .03, .XXX ± .010

TITLE: CLAMP FLEX HOUSING RIGHT
SCALE: 1:1
DATE: 3/30/94
No. 100318
DRAWN BY: GOODWIN
RELEASE DATE: XXX
PROJECT: ACTUATOR II
APPROVAL:
FILE NAME: 100318.DWG

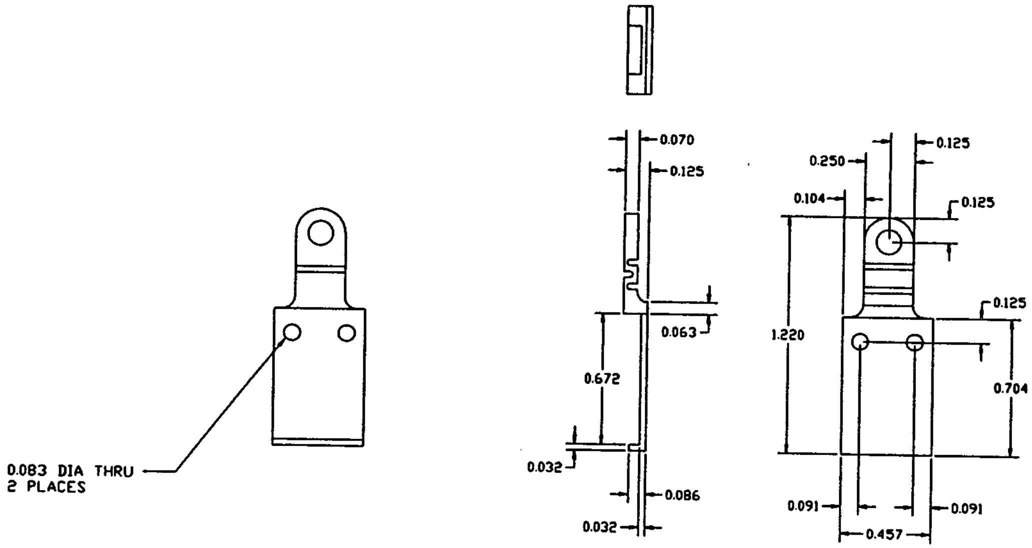

Unless otherwise specified:
Dimensions are in inches
Tolerances on angles ± 0° 30'
Decimals .XX ± .03, .XXX ± .010

TITLE: CLAMP FLEX HOUSING LEFT
SCALE: 1:1
DATE: 3/30/94
No. 100319
DRAWN BY: GOODWIN
RELEASE DATE: XXX
PROJECT: ACTUATOR II
APPROVAL:
FILE NAME: 100319.DWG

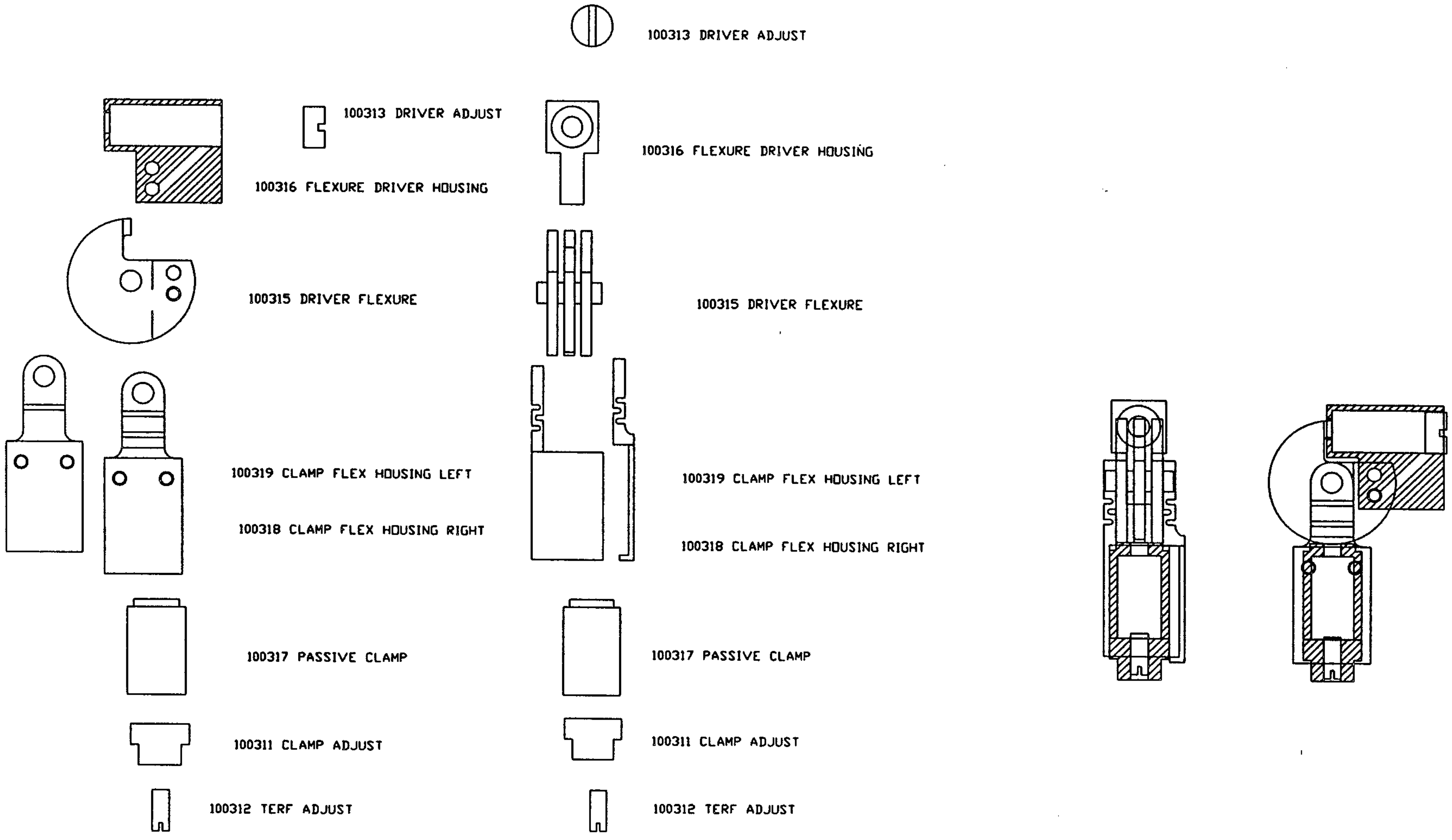

Unless otherwise specified:
Dimensions are in inches
Tolerances on angles ± 0° 30'
Decimals .XX ± .03, .XXX ± .010

TITLE: FLEXURE ACTUATOR ASSEMBLY
SCALE: 1:1
DATE: 4/8/94
No. 100320
DRAWN BY: GOODWIN
RELEASE DATE:
PROJECT: ACTUATOR II
FILE NAME: 100320.DWG
APPROVAL:

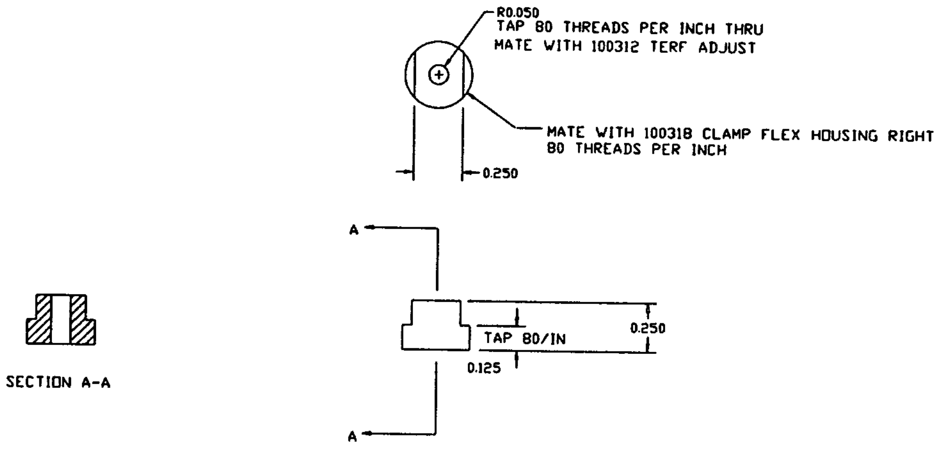
R0.050
TAP 80 THREADS PER INCH THRU
MATE WITH 100312 TERF ADJUST
MATE WITH 100318 CLAMP FLEX HOUSING RIGHT
80 THREADS PER INCH
0.250
A
A
TAP 80/IN
0.250
0.125
SECTION A-A

Unless otherwise specified
Dimensions are in inches
Tolerances on angles ± 0° 30'
Decimals .XX ± .03, .XXX ± .010

TITLE: FLEXURE CLAMP ADJUST
SCALE: 1:1
DATE: 3/31/94
No. 100321
DRAWN BY: GOODWIN
RELEASE DATE: XXX
PROJECT: ACTUATOR II
APPROVAL:
FILE NAME: 100321.DWG

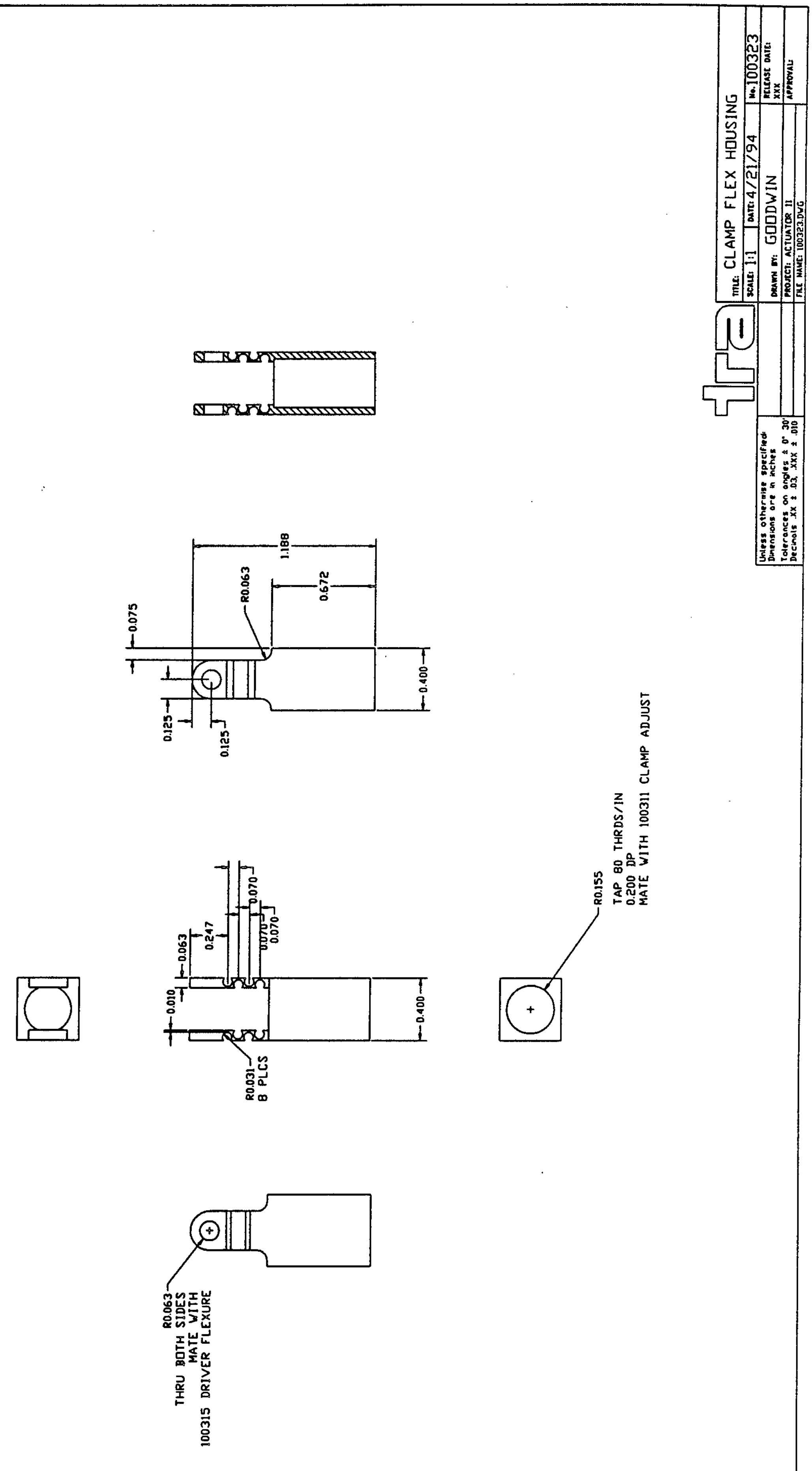TITLE: CLAMP FLEX HOUSING
SCALE: 1:1
DATE: 4/21/94
No. 100323
DRAWN BY: GOODWIN
RELEASE DATE: XXX
PROJECT: ACTUATOR II
FILE NAME: 100323.DWG
APPROVAL:
Unless otherwise specified:
Dimensions are in inches
Tolerances on angles ± 0° 30'
Decimals .XX ± .03, .XXX ± .010
1.188
0.672
R0.063
0.075
0.400
0.125
0.125
0.070
0.070
0.070
0.247
0.063
0.010
0.400
R0.031
8 PLCS
R0.155
TAP 80 THRDS/IN
0.200 DP
MATE WITH 100311 CLAMP ADJUST
R0.063
THRU BOTH SIDES
MATE WITH
100315 DRIVER FLEXURE

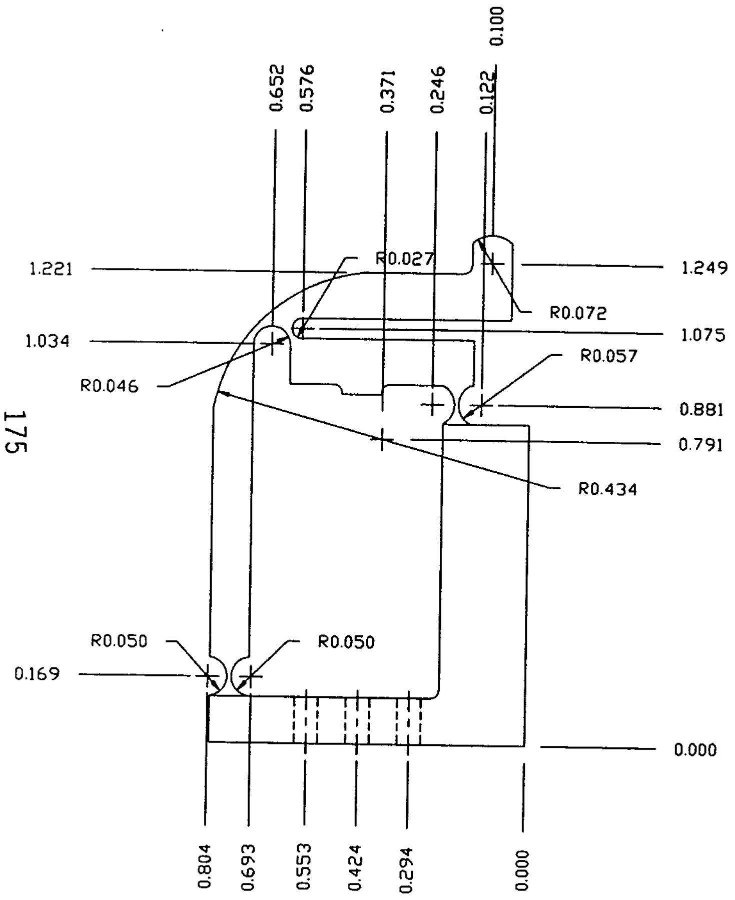

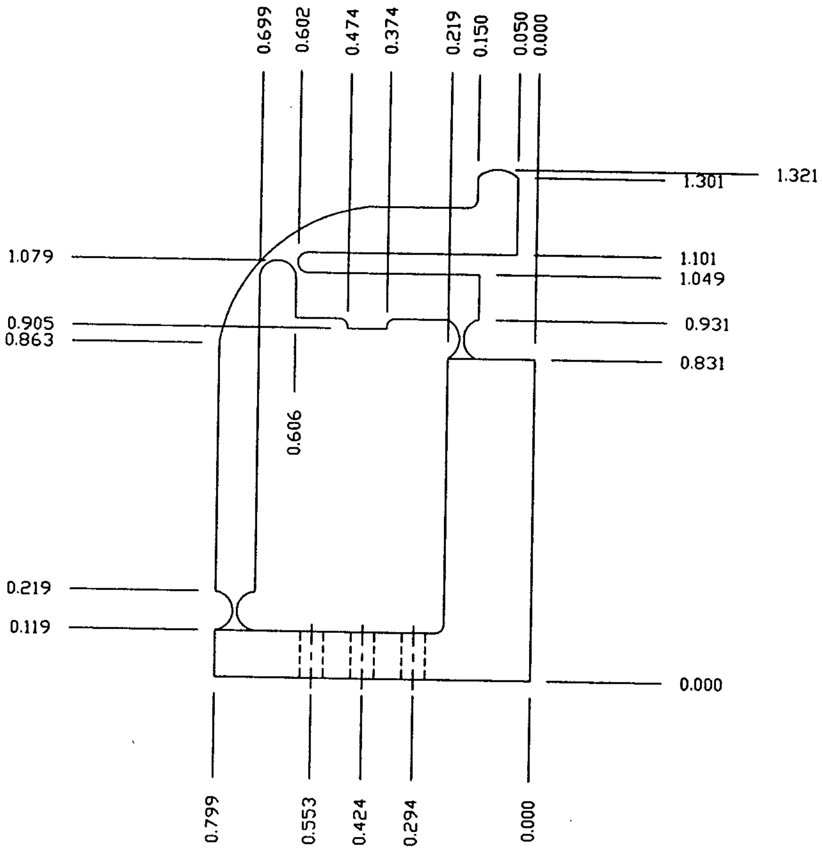

Unless otherwise specified:
Dimensions are in inches
Tolerances on angles ± 0° 30'
Decimals .XX ± .03, .XXX ± .010

tra

REV A

Mat'l: Steel

Heat Treat : XXX

TITLE: Detail - Deflection Magnifier

SCALE: 2:1

DATE: 9 May 94

No. BE00127

DRAWN BY: AP Hilton

RELEASE DATE: XXX

PROJECT: Actuator II

FILE NAME: BE00127.dwg

APPROVAL:

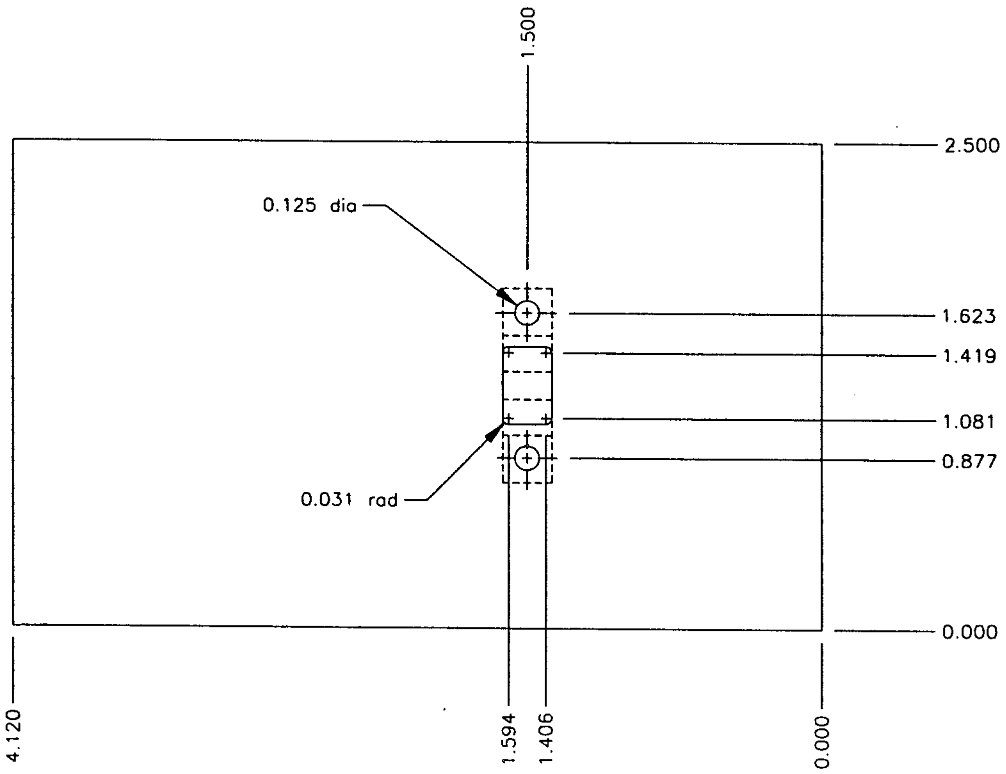

Unless otherwise specified:
Dimensions are in inches
Tolerances on angles ± 0° 30'
Decimals .XX ± .03, .XXX ± .005

REV A
Mat'l: Alum
Heat Treat : No

TITLE: Motion Detector Box Lid
SCALE: 1:1
DATE: 7 Nov 94
No. BE00163
DRAWN BY: A. P. Hilton
RELEASE DATE: XXX
PROJECT: Actuator II
APPROVAL:
FILE NAME: be00163.dwg

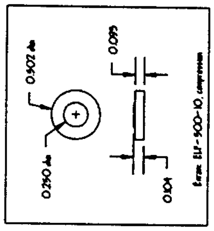

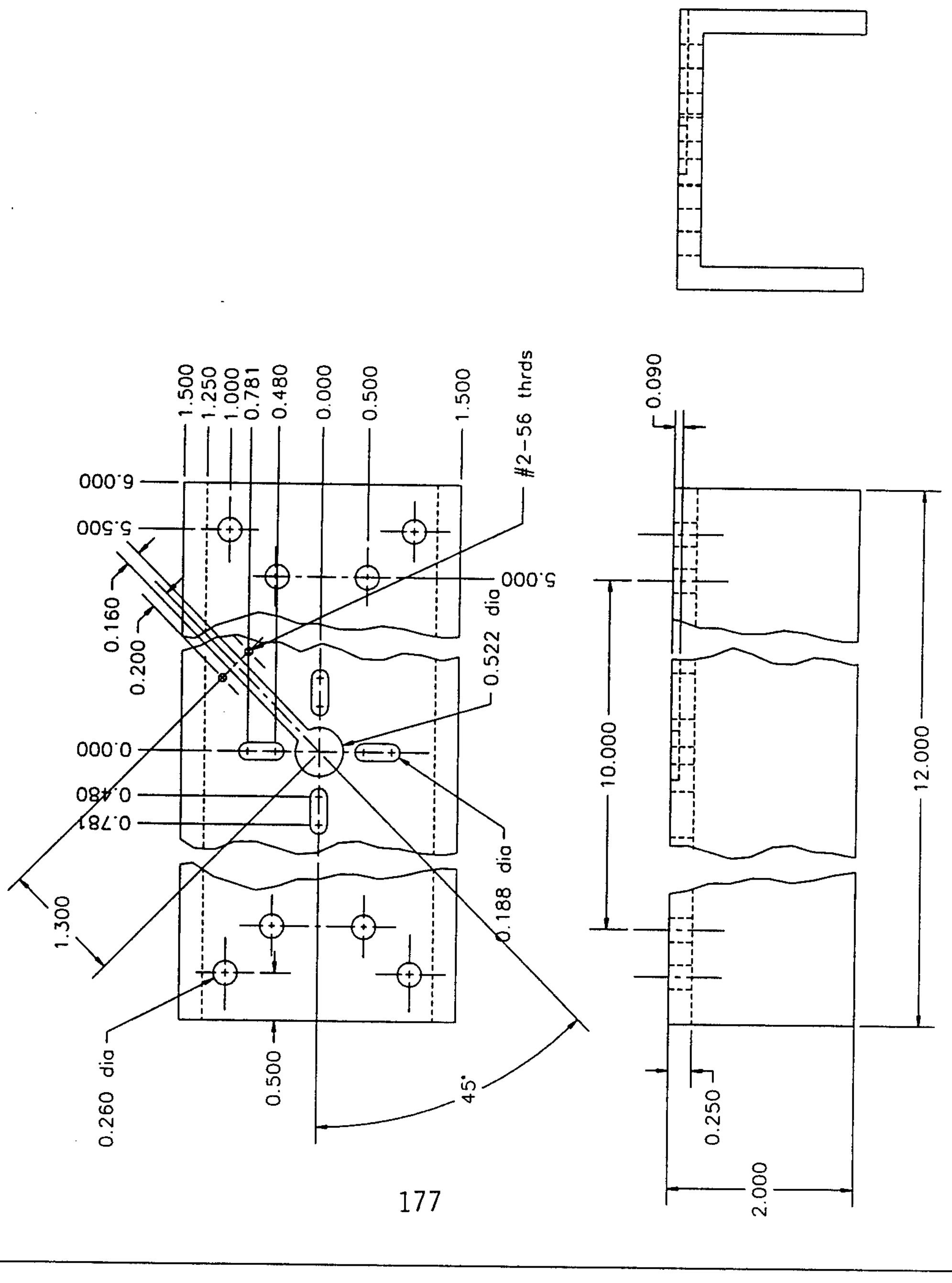

Unless otherwise specified:
Dimensions are in inches
Tolerances on angles ± 0° 30'
Decimals .XX ± .03, .XXX ± .005

tra

REV B

Mat'l: Aluminum
Heat Treat : No

TITLE: Load Cell Calibration Bed
SCALE: 1:2
DATE: 29 Dec 94
No. BE00177
DRAWN BY: A. P. Hilton
RELEASE DATE: XXX
PROJECT: Actuator II
APPROVAL:
FILE NAME: be00177.dwg

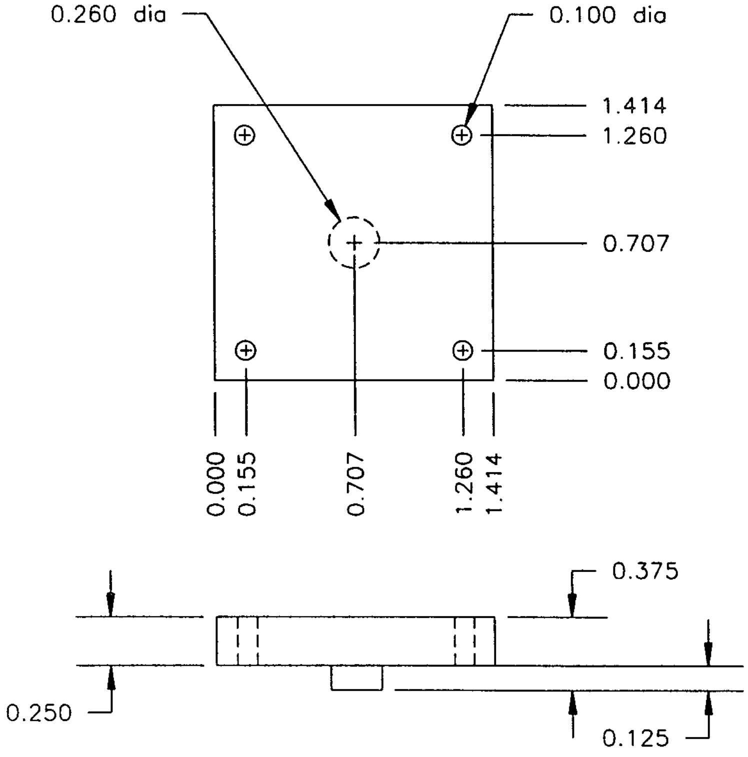

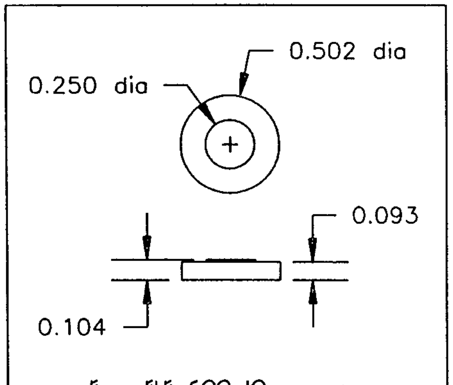

Enran: ELF-500-10, compression

Unless otherwise specified:
Dimensions are in inches
Tolerances on angles ± 0° 30'
Decimals .XX ± .03, .XXX ± .005

REV A
Matl: Plastic
Heat Treat : No

TITLE: Calibration Bed Load Positioner
SCALE: 1:1
DATE: 28 Dec 94
No. BE00178
DRAWN BY: A. P. Hilton
RELEASE DATE: XXX
PROJECT: Actuator II
APPROVAL:
FILE NAME: be00178.dwg

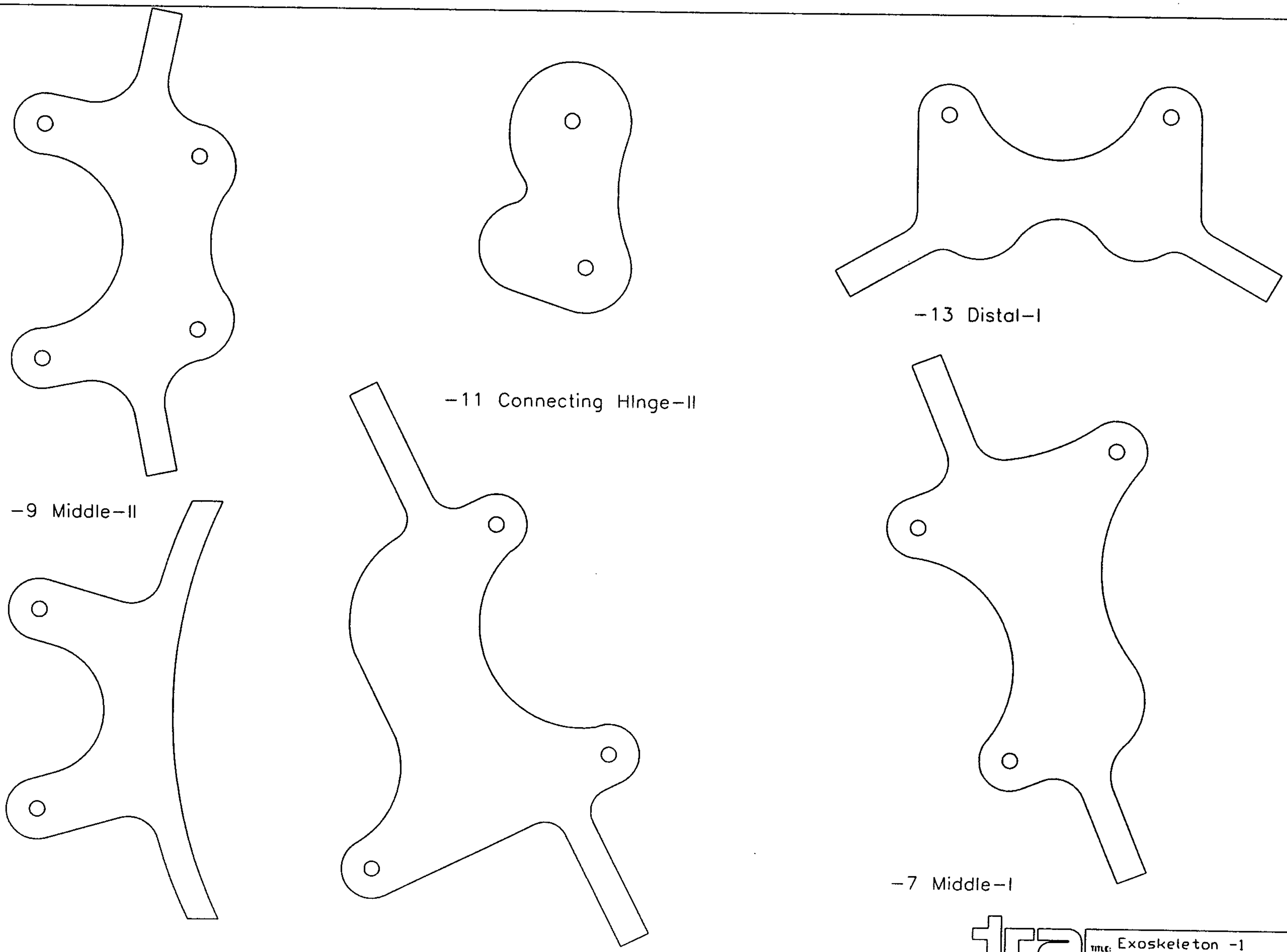

Unless otherwise specified: Dimensions are in inches	REV A	TITLE: Exoskeleton -1	
		SCALE: 1:1 DATE: 22 Feb 95	No. BE000193
		DRAWN BY: A. P. Hilton	RELEASE DATE: XXX
Tolerances on angles ± 0° 30' Decimals .XX ± .03, .XXX ± .005	Matl: Alum (soft)	PROJECT: Actuator II	APPROVAL:
	Heat Treat : No	FILE NAME: be00193.dwg	

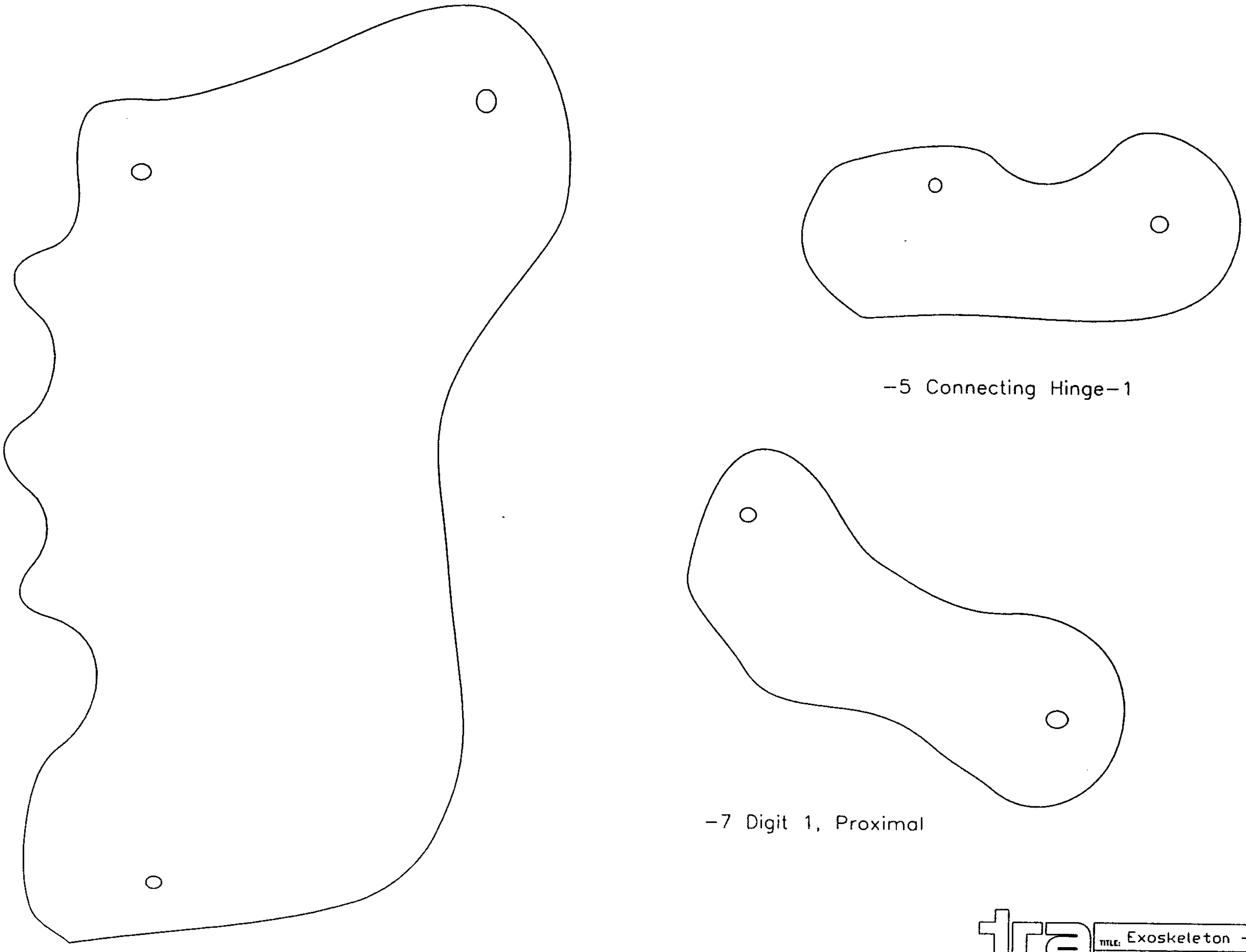

Unless otherwise specified:
Dimensions are in inches
Tolerances on angles ± 0° 30'
Decimals .XX ± .03, .XXX ± .005

REV B
Mat'l: Alum
Heat Treat : No

TITLE: Exoskeleton -2
SCALE: 1:1
DATE: 1 Mar 95
DRAWN BY: A. P. Hilton
PROJECT: Actuator II
FILE NAME: be00194.dwg

No. BE000194
RELEASE DATE: 1 Mar 95
APPROVAL:

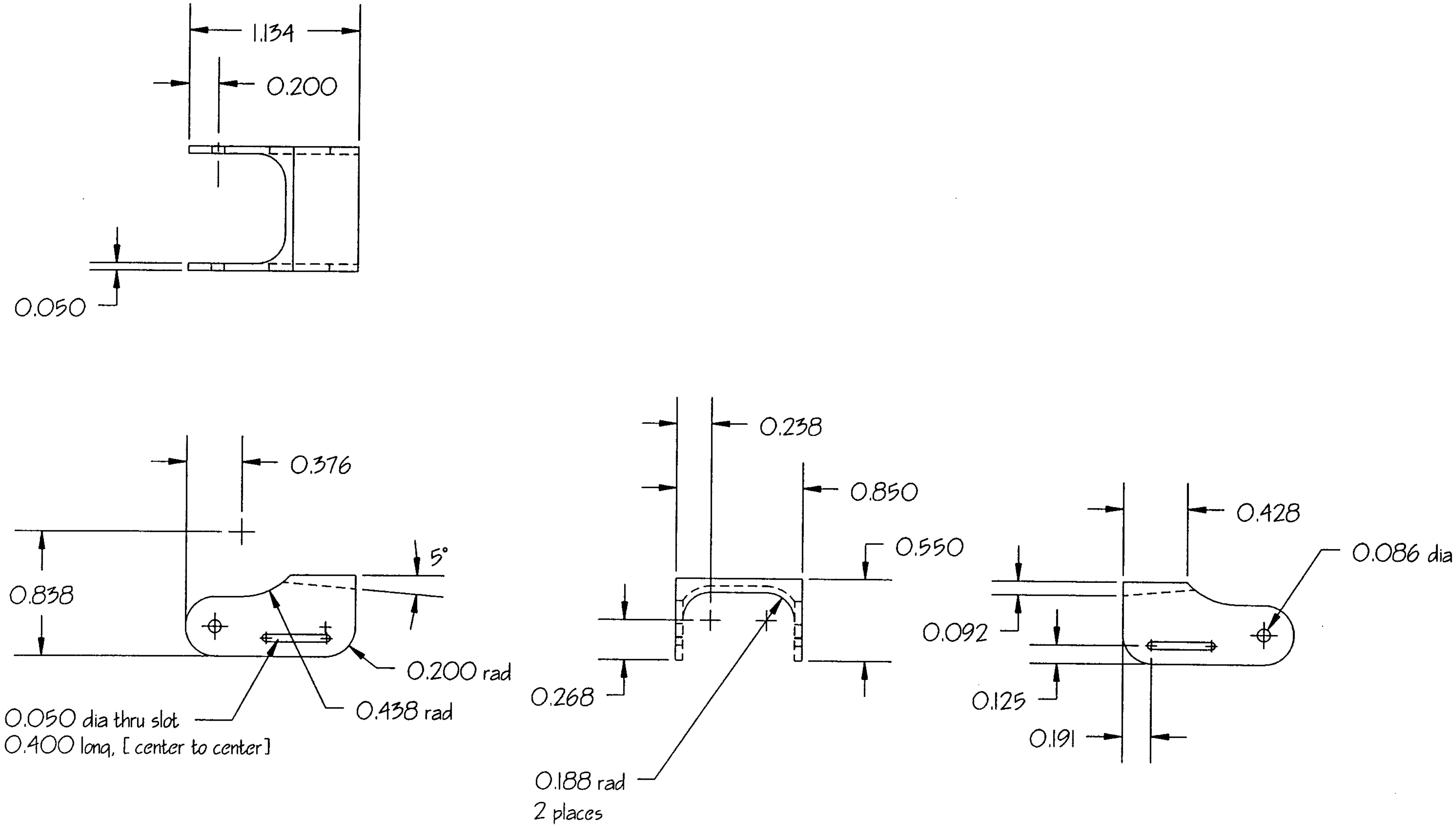

tra

		TITLE: Digit 2, Distal	
		SCALE: 1:1 DATE: 27 Feb 95	No. BE000196
Unless otherwise specified: Dimensions are in inches	REV B	DRAWN BY: A. P. Hilton	RELEASE DATE: 10 Mar 95
Tolerances on angles ± 0° 30' Decimals .XX ± .03, .XXX ± .005	Mat'l: Alum	PROJECT: Actuator II	APPROVAL:
	Heat Treat : No	FILE NAME: be00196.dwg	

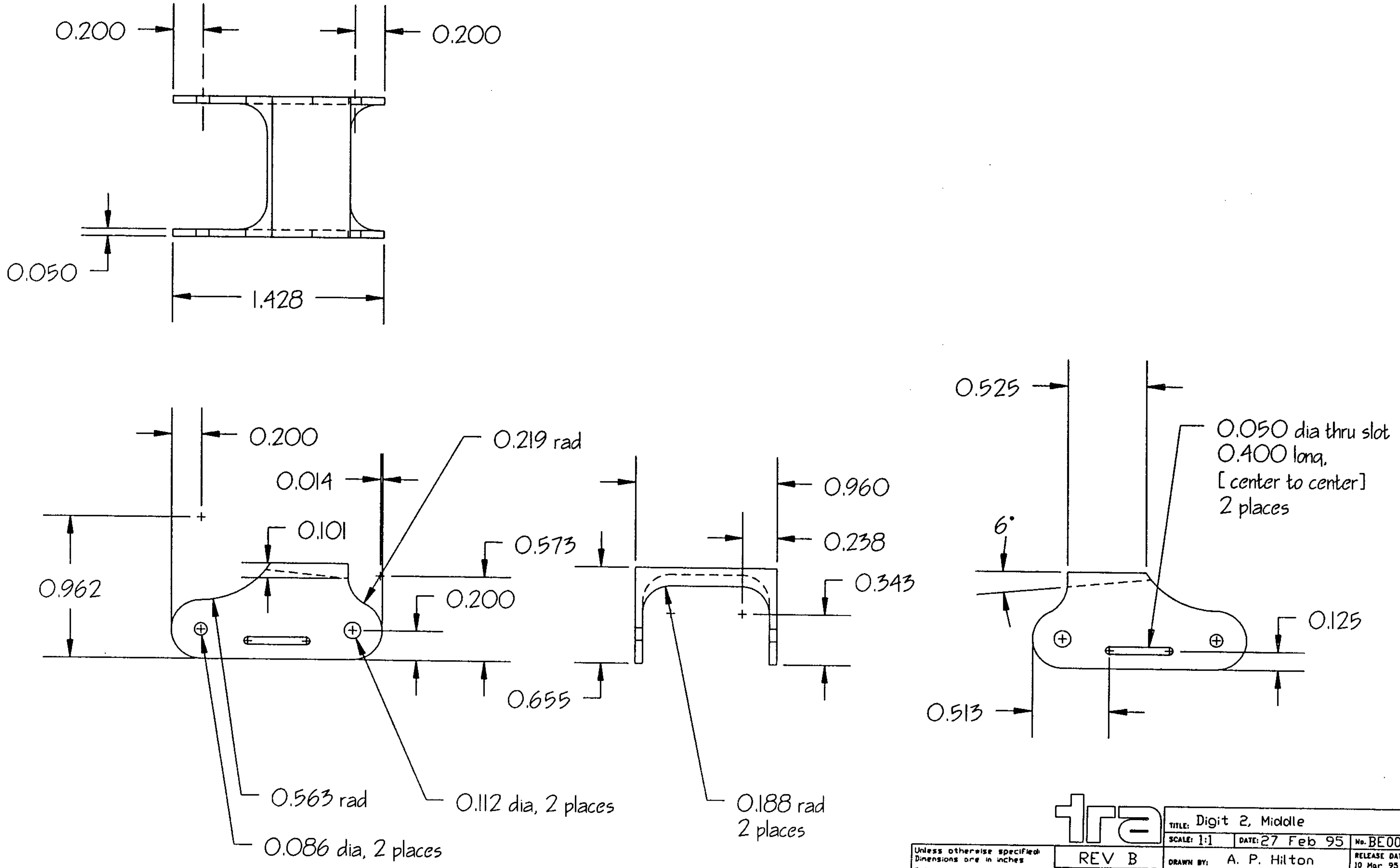

tra

TITLE: Digit 2, Middle

SCALE: 1:1 DATE: 27 Feb 95 No. BE000197

Unless otherwise specified:
Dimensions are in inches
Tolerances on angles ± 0° 30'
Decimals .XX ± .03, .XXX ± .005

REV B

DRAWN BY: A. P. Hilton

RELEASE DATE:
10 Mar 95

Mat'l: Alum

PROJECT: Actuator II

APPROVAL:

Heat Treat : No

FILE NAME: be00197.dwg

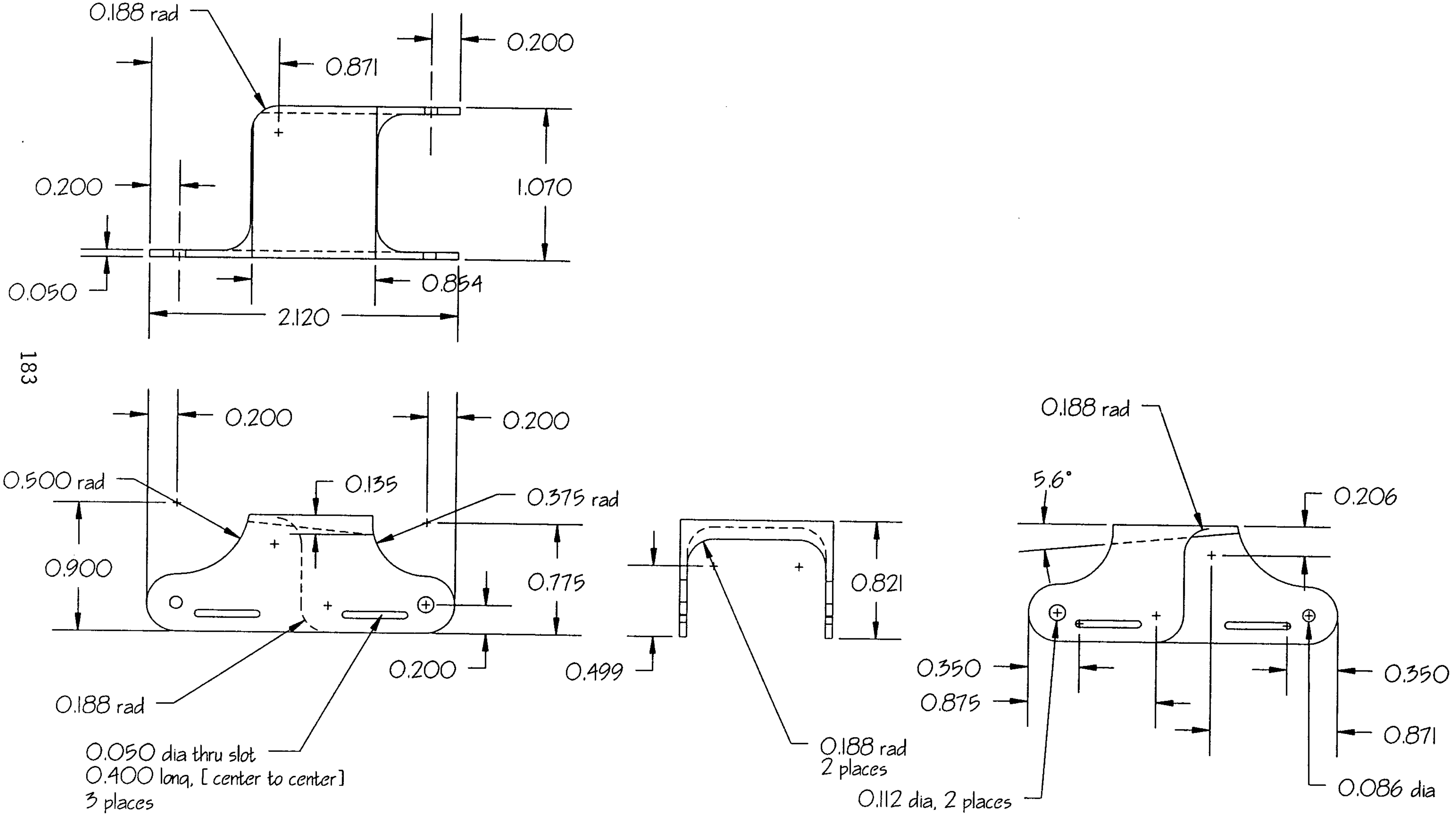

Unless otherwise specified: Dimensions are in inches Tolerances on angles ± 0° 30' Decimals .XX ± .03, .XXX ± .005	REV B	TITLE: Digit 2, Proximal	
		SCALE: 1:1 DATE: 27 Feb 95	No. BE000198
		DRAWN BY: A. P. Hilton	RELEASE DATE: 10 Mar 95
	Matl: Alum	PROJECT: Actuator II	APPROVAL:
	Heat Treat : No	FILE NAME: be00198.dwg	

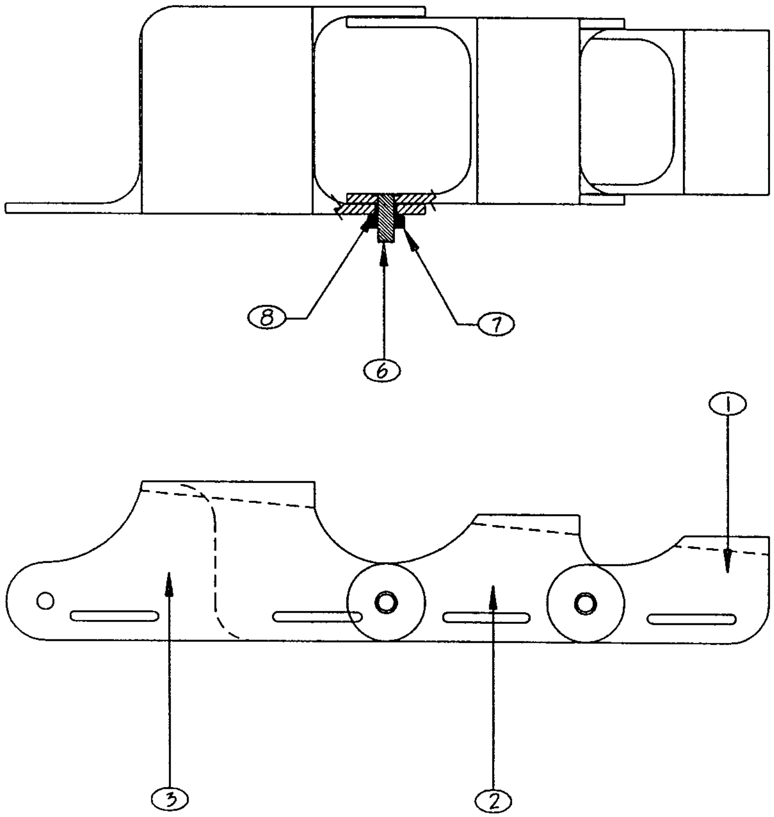

③ Small Parts, Miami Lakes, FL 305-557-8222
② Fasteners of Comparable Spec's Acceptable
① Hypodermic Tubing Cut to 0.065" Length

	QTY REQD	ITEM NO.	PART NO.	DESCRIPTION	MAT'L / SPEC
①③	5	8	Q-HTX-12	12 Gauge - Hypodermic Tubing	304W SS
②③	5	7	Q-HNX-256	#2-56 Hex Nut	SS
③	5	6	Q-SCSX-256-4	#2-56 x 1/4" Self Clinching Stud	-- SS
	1	5	XXX	XXX	---
	1	4	XXX	XXX	---
	1	3	BE000198	Digit 2, Proximal	---
	1	2	BE000197	Digit 2, Middle	---
	1	1	BE000196	Digit 2, Distal	---
	---		BE000199	Digit 2 - ASSEMBLY	---

PARTS LIST

TITLE: Assembly - Digit 2
SCALE: 1:1
DATE: 28 Feb 95
No. BE000199
Unless otherwise specified:
Dimensions are in inches
Tolerances on angles ± 0° 30'
Decimals .XX ± .03, .XXX ± .005
REV B
Matl: XXX
Heat Treat : No
DRAWN BY: A. P. Hilton
PROJECT: Actuator II
FILE NAME: be00199.dwg
RELEASE DATE: 10 Mar 95
APPROVAL:

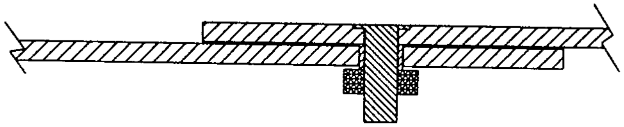

Unless otherwise specified:
Dimensions are in inches
Tolerances on angles ± 0° 30'
Decimals .XX ± .03, .XXX ± .005

REV A
Mat'l: XXX
Heat Treat : No

TITLE: Connector Detail
SCALE: 2:1
DATE: 28 Feb 95
No. BE000200
DRAWN BY: A. P. Hilton
RELEASE DATE: XXX
PROJECT: Actuator II
APPROVAL:
FILE NAME: be00299.dwg

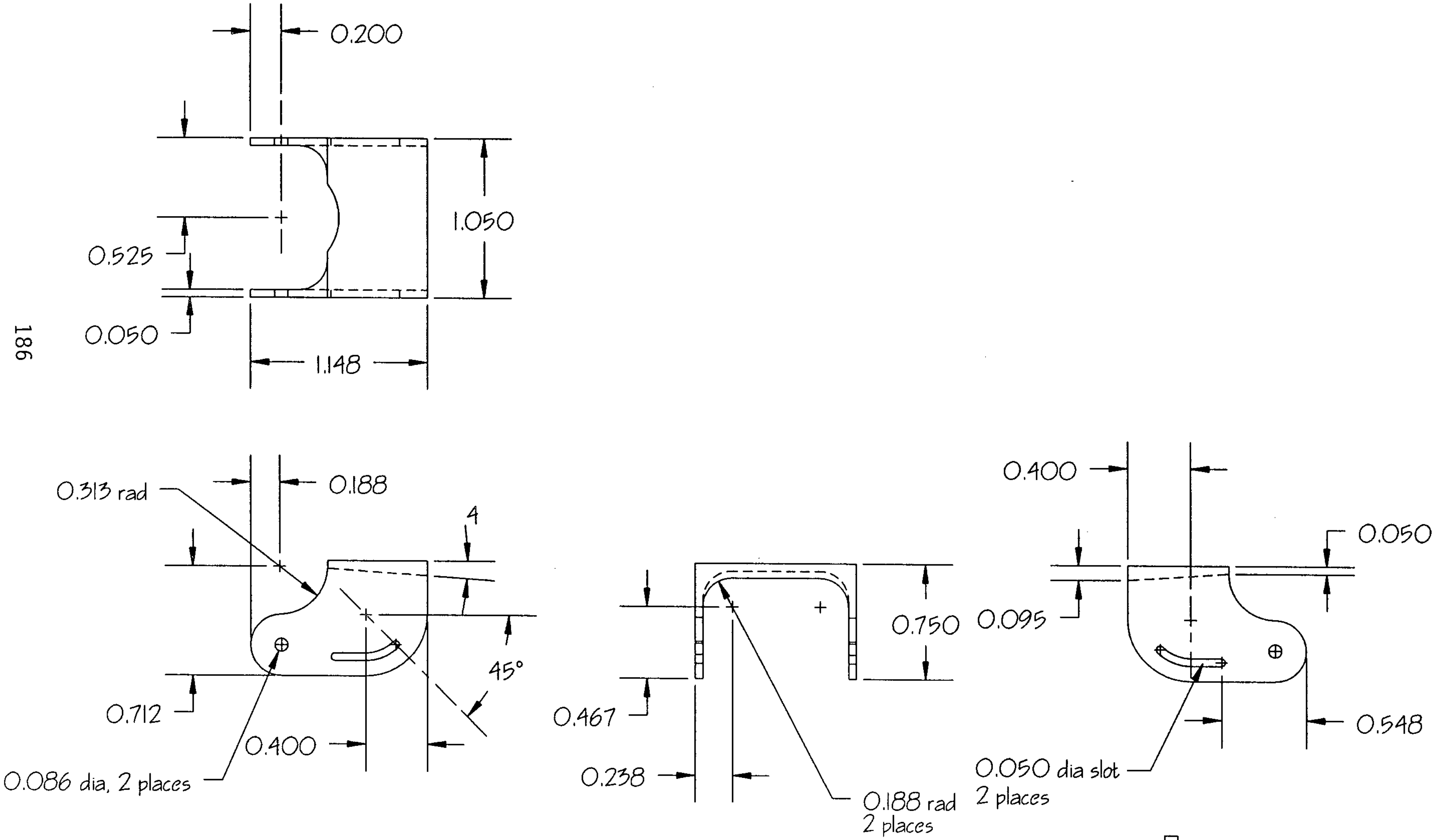

Unless otherwise specified:
Dimensions are in inches
Tolerances on angles ± 0° 30'
Decimals .XX ± .03, .XXX ± .005

REV B
Mat'l: Alum
Heat Treat : No

TITLE: Digit 1 - Distal
SCALE: 1:1
DATE: 1 Mar 95
No. BE000201
DRAWN BY: A. P. Hilton
RELEASE DATE: 10 Mar 95
PROJECT: Actuator II
APPROVAL:
FILE NAME: be00201.dwg

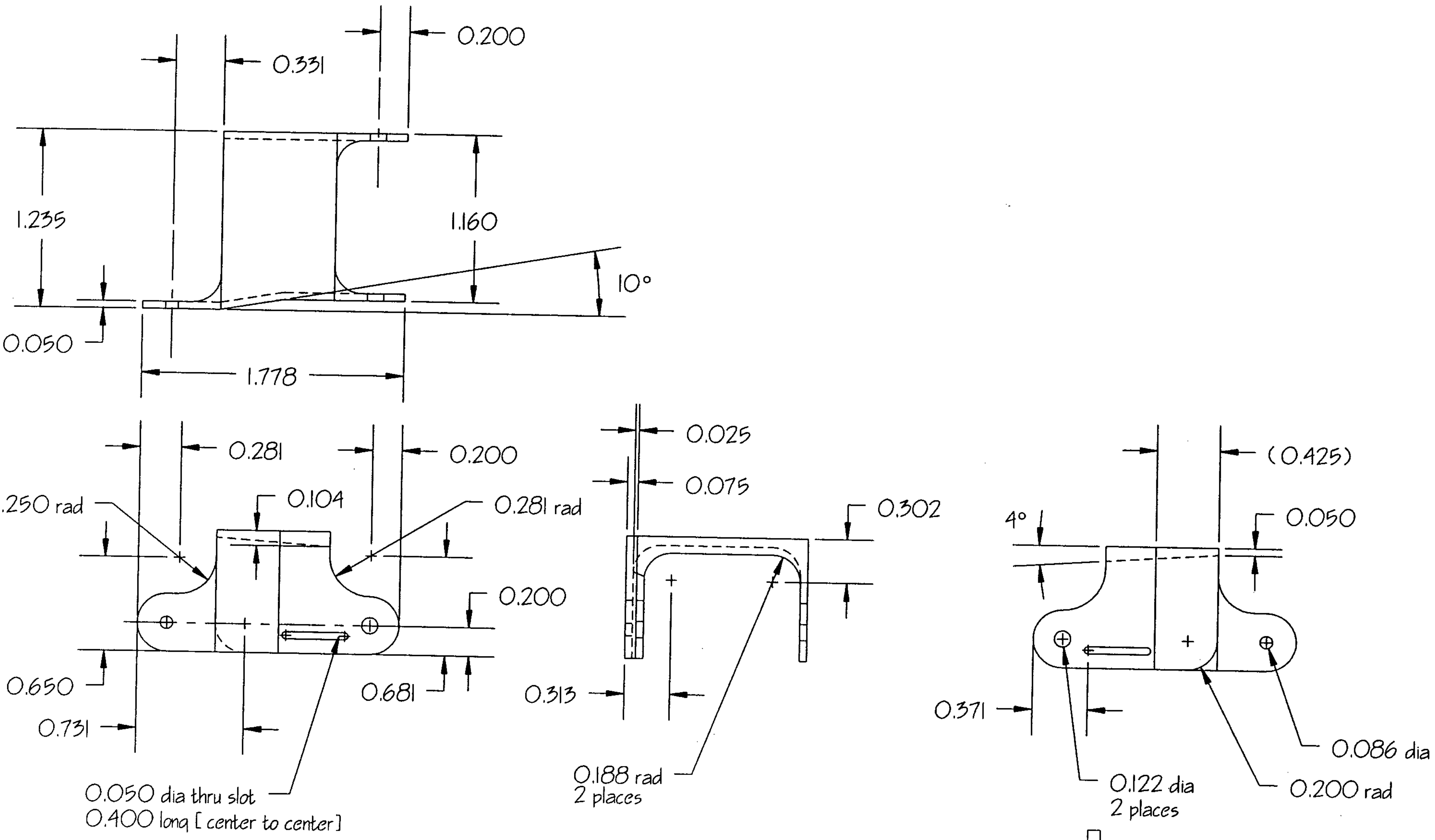

Unless otherwise specified:
Dimensions are in inches
Tolerances on angles ± 0° 30'
Decimals .XX ± .03, .XXX ± .005

REV B
Matl: Alum
Heat Treat : No

TITLE: Digit 1 - Middle
SCALE: 1:1
DATE: 1 Mar 95
DRAWN BY: A. P. Hilton
PROJECT: Actuator II
FILE NAME: be00202.dwg

No. BE000202
RELEASE DATE: 10 Mar 95
APPROVAL:

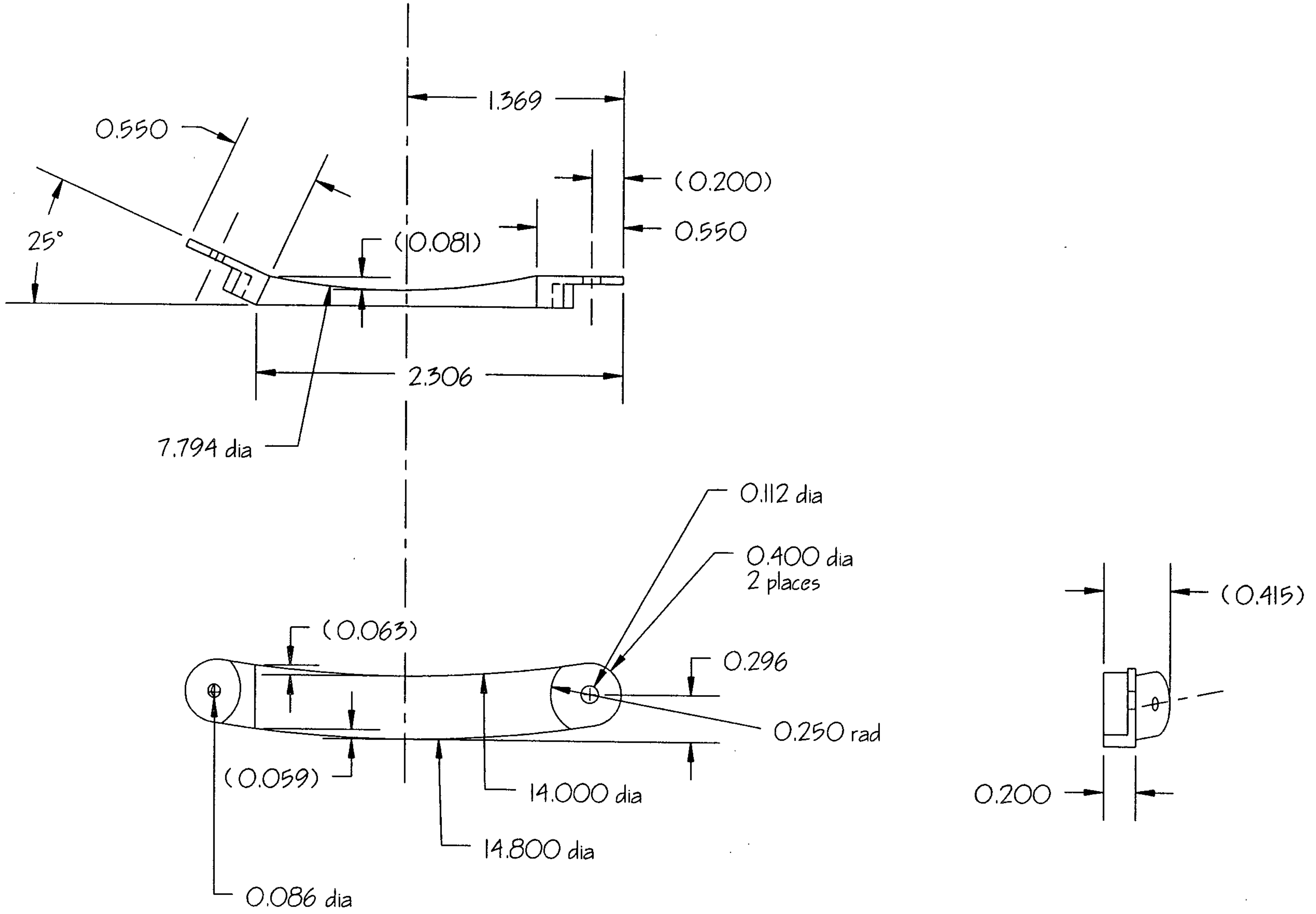

Unless otherwise specified: Dimensions are in inches Tolerances on angles ± 0° 30' Decimals .XX ± .03, .XXX ± .005	REV B	TITLE: Digit 1 - Proximal	
		SCALE: 1:1 DATE: 3 Mar 95	No. BE000203
		DRAWN BY: A. P. Hilton	RELEASE DATE: 10 Mar 95
	Matl: Alum	PROJECT: Actuator II	APPROVAL:
	Heat Treat : No	FILE NAME: be00203.dwg	

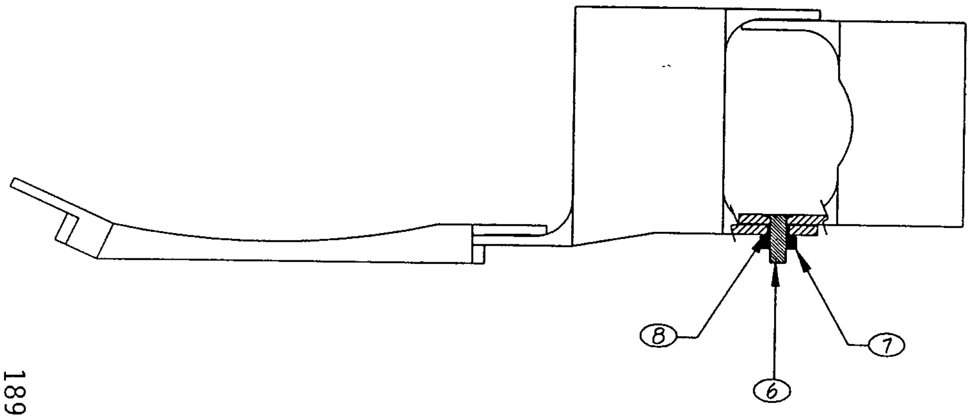

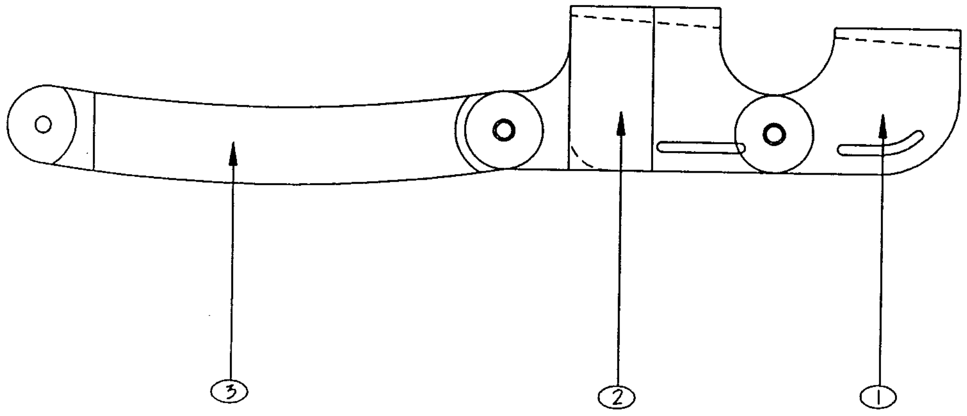

③ Small Parts, Miami Lakes, FL 305-557-8222
② Fasteners of Comparable Spec's Acceptable
① Hypodermic Tubing Cut to 0.065" Length

	QTY REQD	ITEM NO.	PART NO.	DESCRIPTION	MAT'L / SPEC
①③	5	8	Q-HTX-12	12 Gauge - Hypodermic Tubing	304W SS
②③	5	7	Q-HNX-256	#2-56 Hex Nut	SS
③	5	6	Q-SCSX-256-4	#2-56 x 1/4" Self Clinching Stud	-SS
	1	5	XXX	XXX	---
	1	4	XXX	XXX	---
	1	3	BE000203	Digit 1, Proximal	---
	1	2	BE000202	Digit 1, Middle	---
	1	1	BE000201	Digit 1, Distal	---
	---		BE000204	Digit 1 - ASSEMBLY	---

PARTS LIST

tra

TITLE: Assembly - Digit 2
SCALE: 1:1
DATE: 6 Mar 95
No. BE000204
Unless otherwise specified:
Dimensions are in inches
Tolerances on angles ± 0° 30'
Decimals .XX ± .03, .XXX ± .005
REV A
DRAWN BY: A. P. Hilton
RELEASE DATE: 6 Mar 95
Mat'l: XXX
PROJECT: Actuator II
APPROVAL:
Heat Treat : No
FILE NAME: be00204.dwg

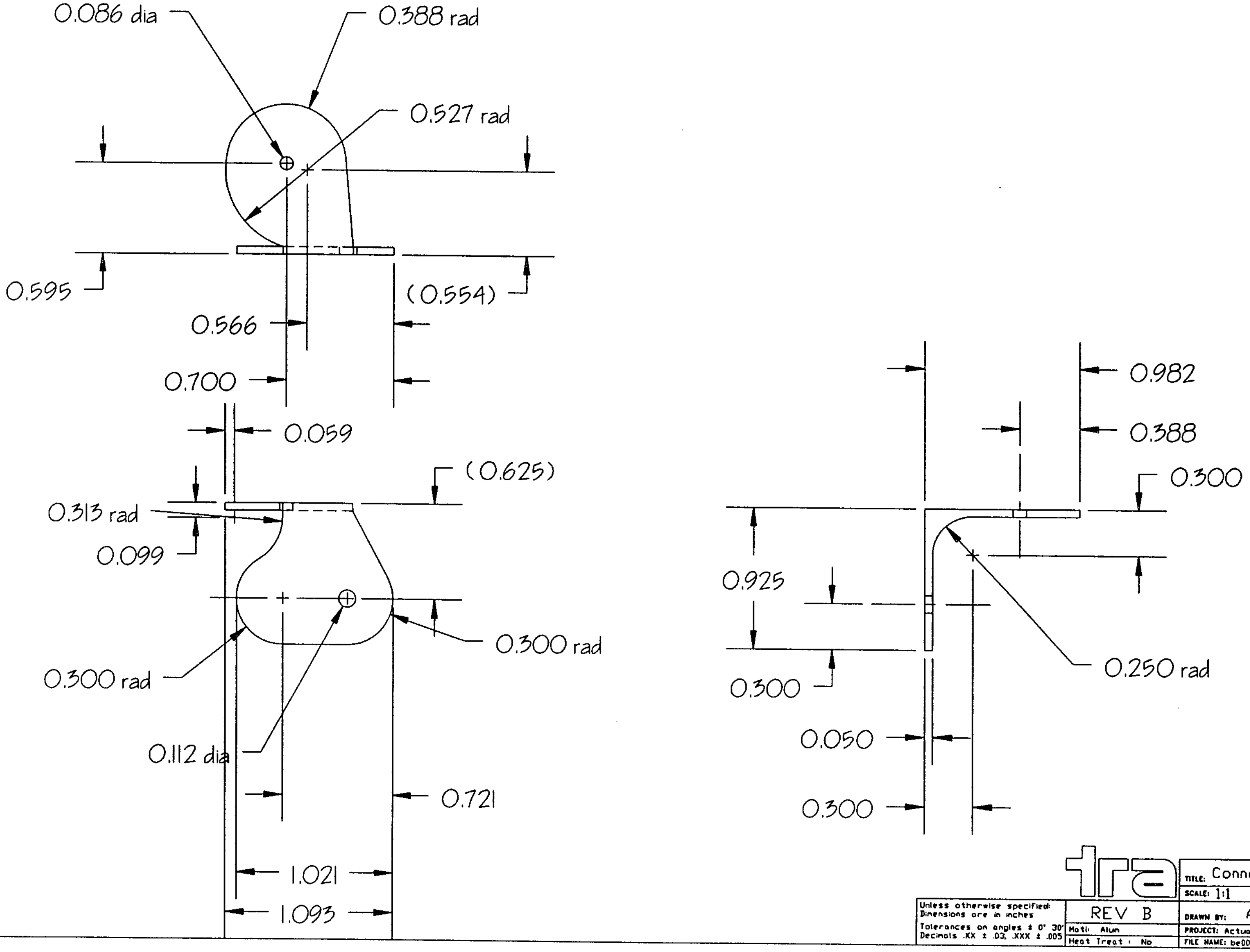

Unless otherwise specified:
Dimensions are in inches
Tolerances on angles ± 0° 30'
Decimals .XX ± .03, .XXX ± .005

REV B
Matl: Alum
Heat Treat : No

TITLE: Connecting Hinge - Digit 2
SCALE: 1:1
DATE: 6 Mar 95
No. BE000205
DRAWN BY: A. P. Hilton
RELEASE DATE: 10 Mar 95
PROJECT: Actuator II
FILE NAME: be00205.dwg
APPROVAL:

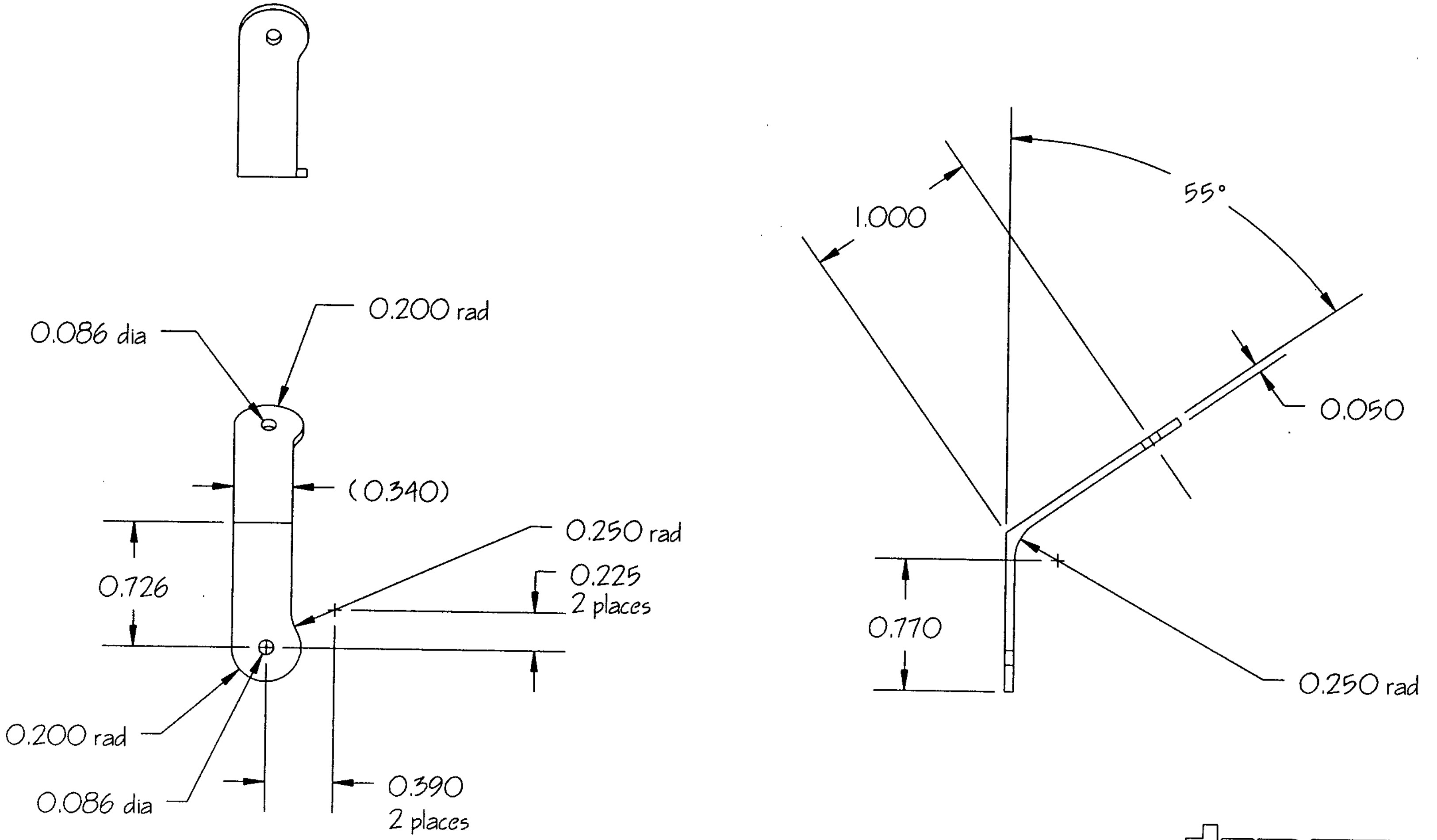

Unless otherwise specified:
Dimensions are in inches
Tolerances on angles ± 0° 30'
Decimals .XX ± .03, .XXX ± .005

tra

TITLE: Connecting Hinge - Digit 1		
SCALE: 1:1	DATE: 6 Mar 95	No. BE000206
REV B	DRAWN BY: A. P. Hilton	RELEASE DATE: 10 Mar 95
Matl: Alum	PROJECT: Actuator II	APPROVAL:
Heat Treat : No	FILE NAME: be00206.dwg	

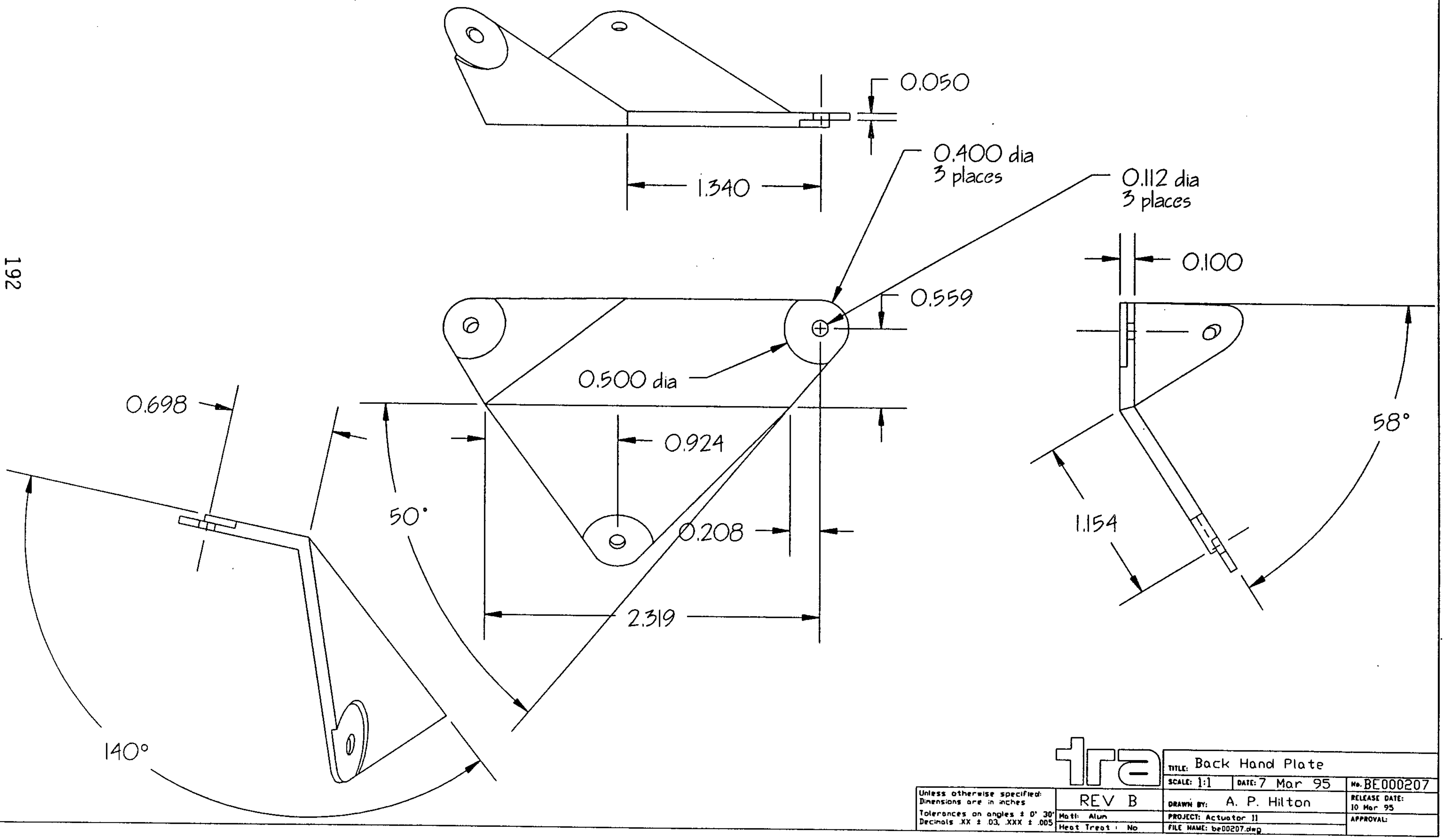

Unless otherwise specified:
Dimensions are in inches
Tolerances on angles ± 0° 30'
Decimals .XX ± .03, .XXX ± .005

tra

REV B

Mat'l: Alum

Heat Treat : No

TITLE: Back Hand Plate

SCALE: 1:1

DATE: 7 Mar 95

No. BE000207

DRAWN BY: A. P. Hilton

RELEASE DATE: 10 Mar 95

PROJECT: Actuator II

APPROVAL:

FILE NAME: be00207.dwg

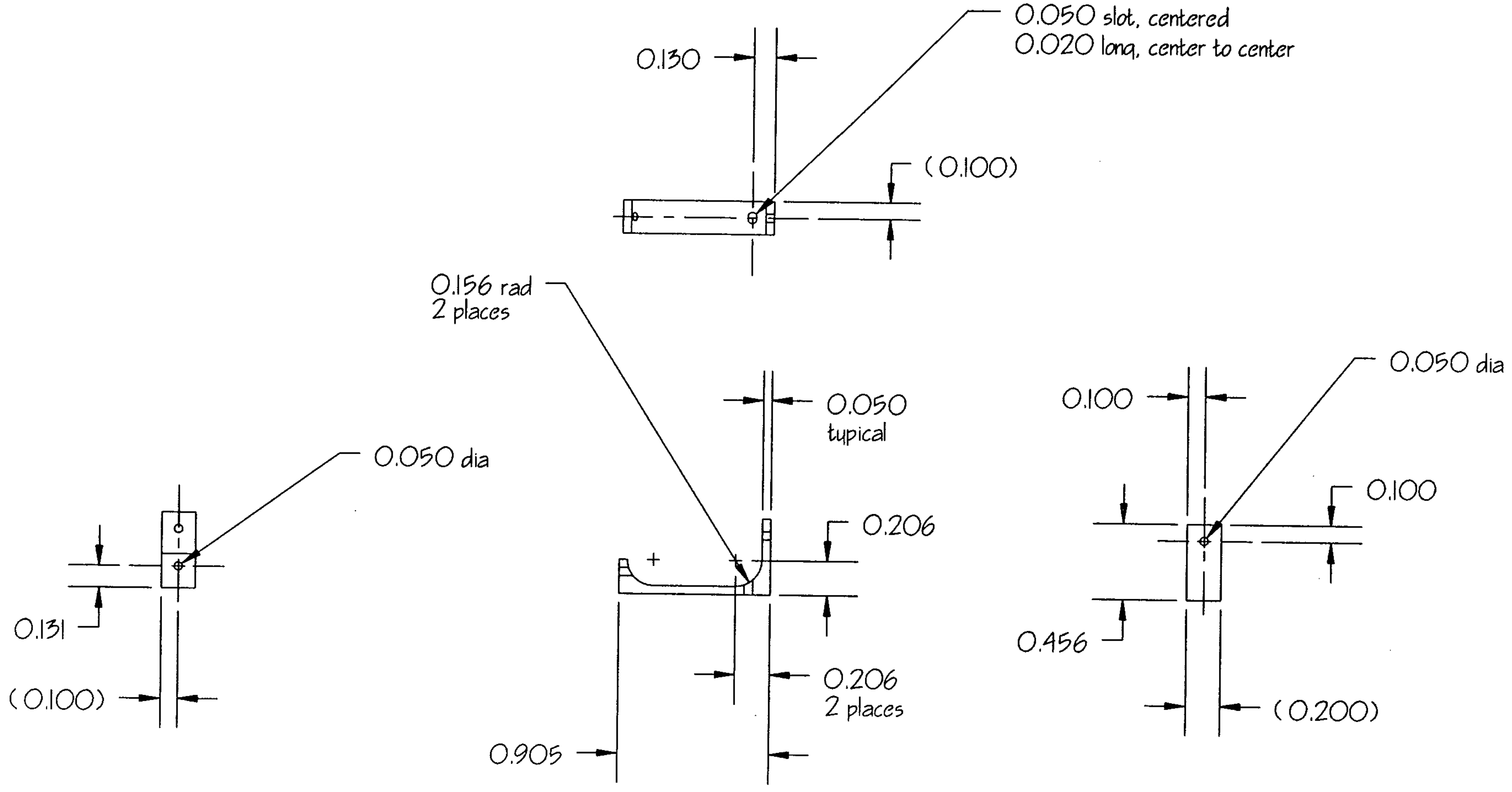

Note: Use 00-90 x 3/16 flat head screws

Unless otherwise specified:
Dimensions are in inches
Tolerances on angles ± 0° 30'
Decimals .XX ± .03, .XXX ± .005

REV A
Matl: Alum
Heat Treat : No

TITLE: J-Clip: Digit #2 - Distal
SCALE: 1:1
DATE: 23 Mar 95
No. BE000208
DRAWN BY: A. P. Hilton
RELEASE DATE: 23 Mar 95
PROJECT: Actuator II
APPROVAL:
FILE NAME: be00208.dwg

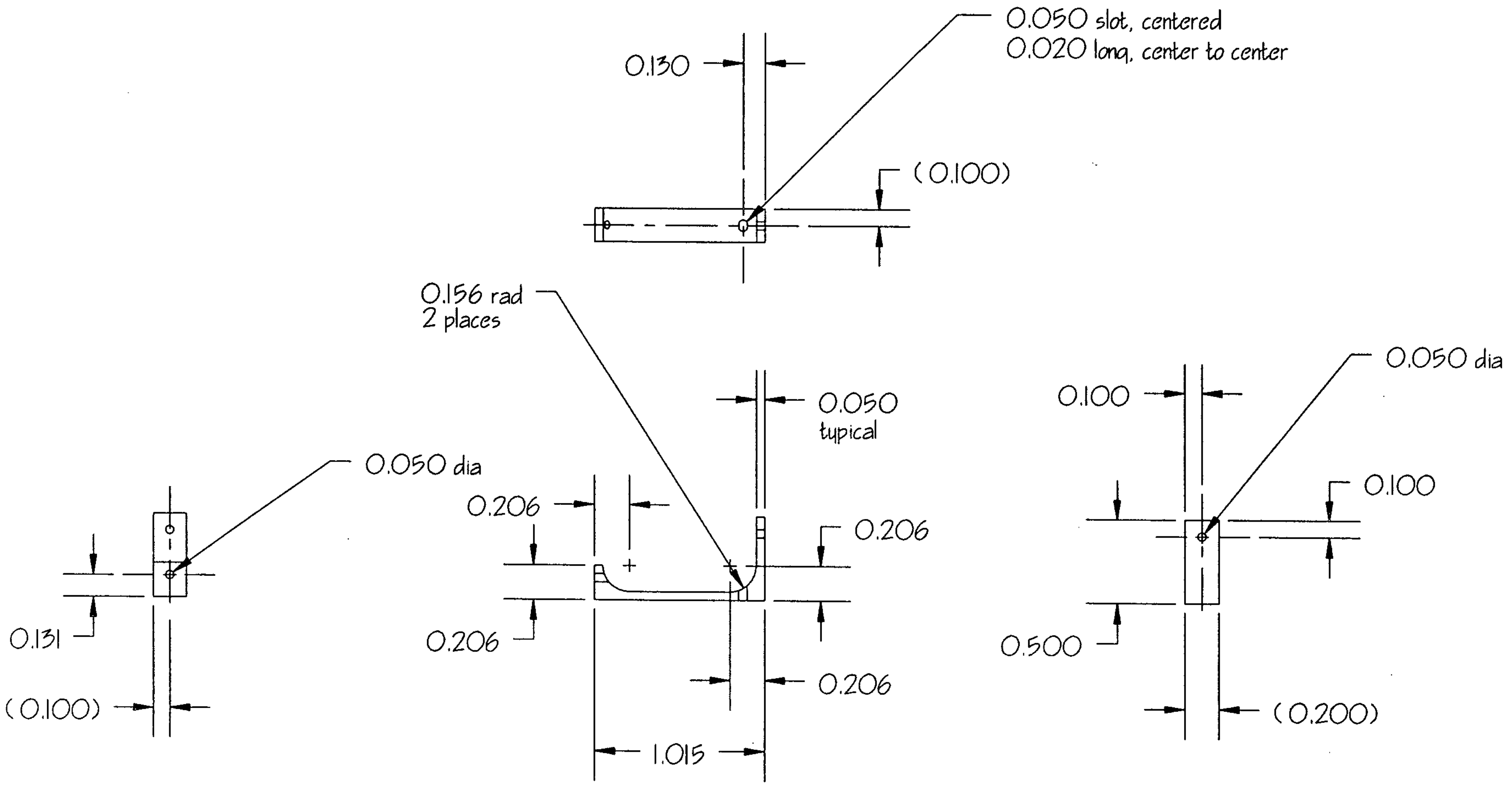

Note: Use 00-90 x 3/16 flat head screws

Unless otherwise specified:
Dimensions are in inches
Tolerances on angles ± 0° 30'
Decimals .XX ± .03, .XXX ± .005

REV A
Mat'l: Alum
Heat Treat : No

TITLE: J-Clip: Digit #2 - Middle
SCALE: 1:1
DATE: 24 Mar 95
No. BE000209
DRAWN BY: A. P. Hilton
RELEASE DATE: 24 Mar 95
PROJECT: Actuator II
FILE NAME: be00209.dwg
APPROVAL:

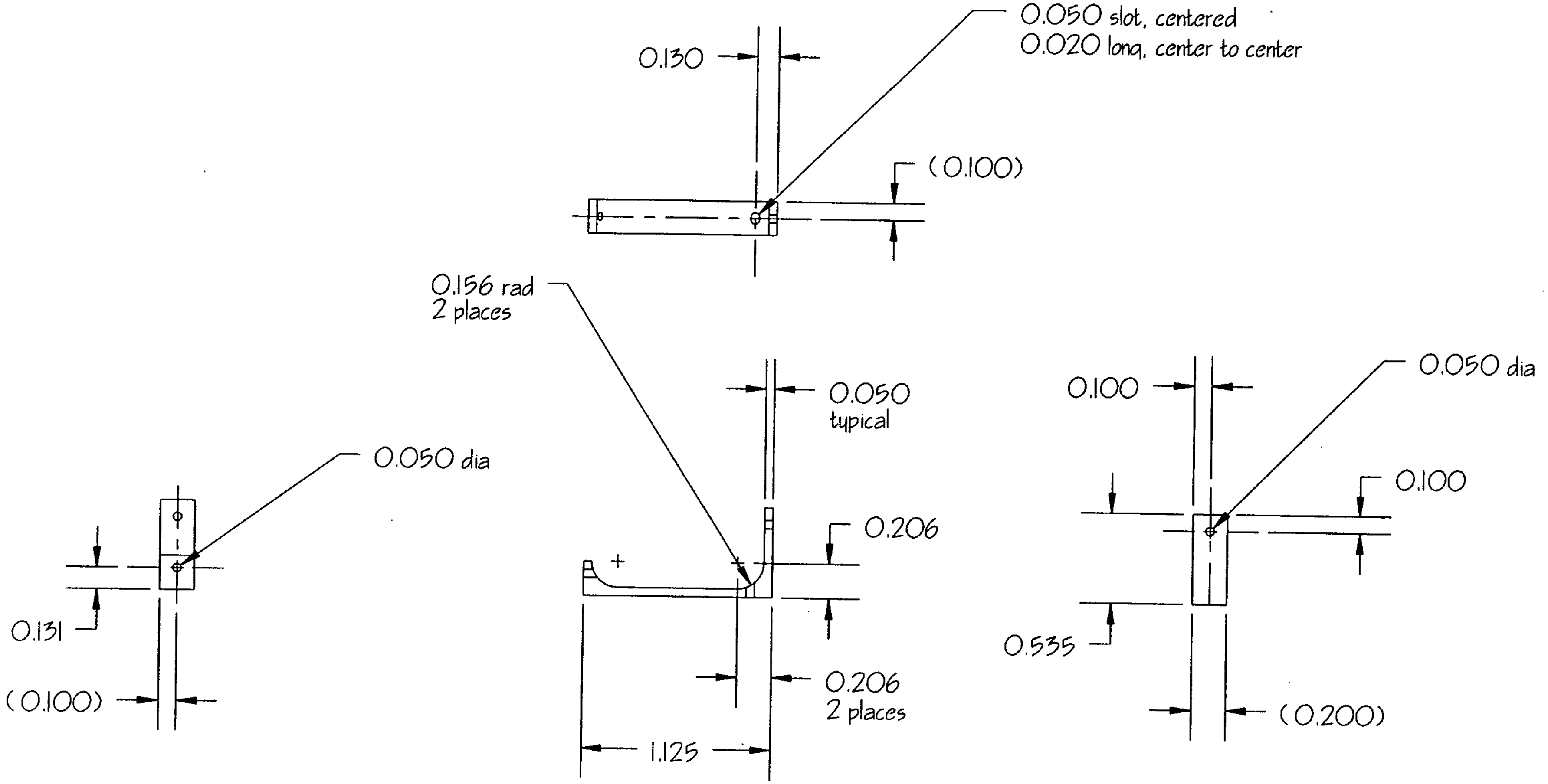

Note: Use 00-90 x 3/16 flat head screws

Unless otherwise specified:
Dimensions are in inches
Tolerances on angles ± 0° 30'
Decimals .XX ± .03, .XXX ± .005

REV A
Matl: Alum
Heat Treat : No

TITLE: J-Clip: Digit #2 - Proximal
SCALE: 1:1
DATE: 24 Mar 95
No. BE000210
DRAWN BY: A. P. Hilton
RELEASE DATE: 24 Mar 95
PROJECT: Actuator II
FILE NAME: be00210.dwg
APPROVAL:

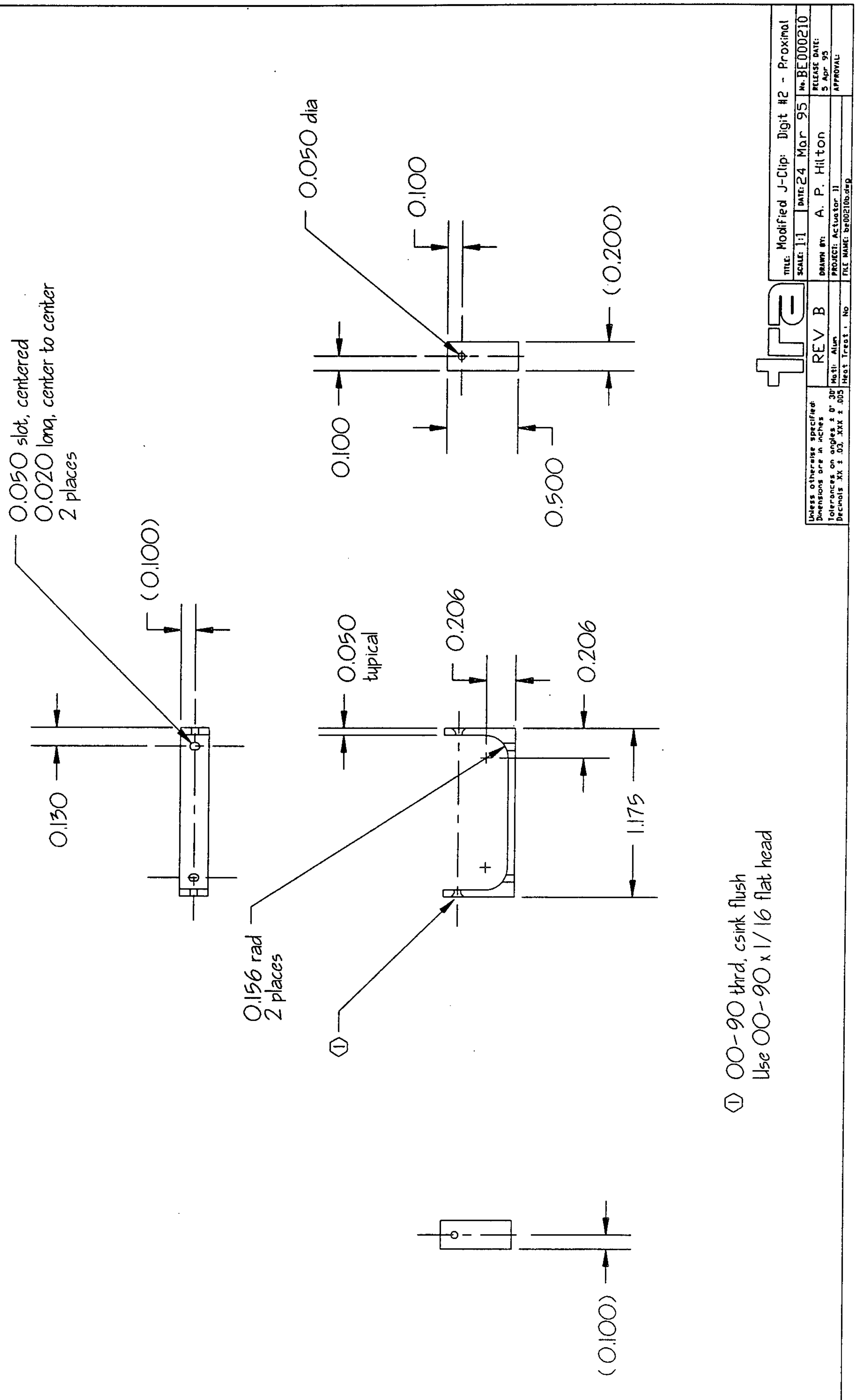
0.050 slot, centered
0.020 long, center to center
2 places
(0.100)
0.130
0.050 dia
0.100
(0.200)
0.100
0.500
0.050
typical
0.206
0.206
1.175
0.156 rad
2 places
①
(0.100)
① 00-90 thrd, csink flush
Use 00-90 x 1/16 flat head
TITLE: Modified J-Clip: Digit #2 - Proximal
SCALE: 1:1
DATE: 24 Mar 95
No. BE000210
DRAWN BY: A. P. Hilton
RELEASE DATE: 5 Apr 95
PROJECT: Actuator II
APPROVAL:
FILE NAME: be00210b.dwg
REV B
Mat'l: Alum
Heat Treat : No
Unless otherwise specified:
Dimensions are in inches
Tolerances on angles ± 0° 30'
Decimals .XX ± .03, .XXX ± .005

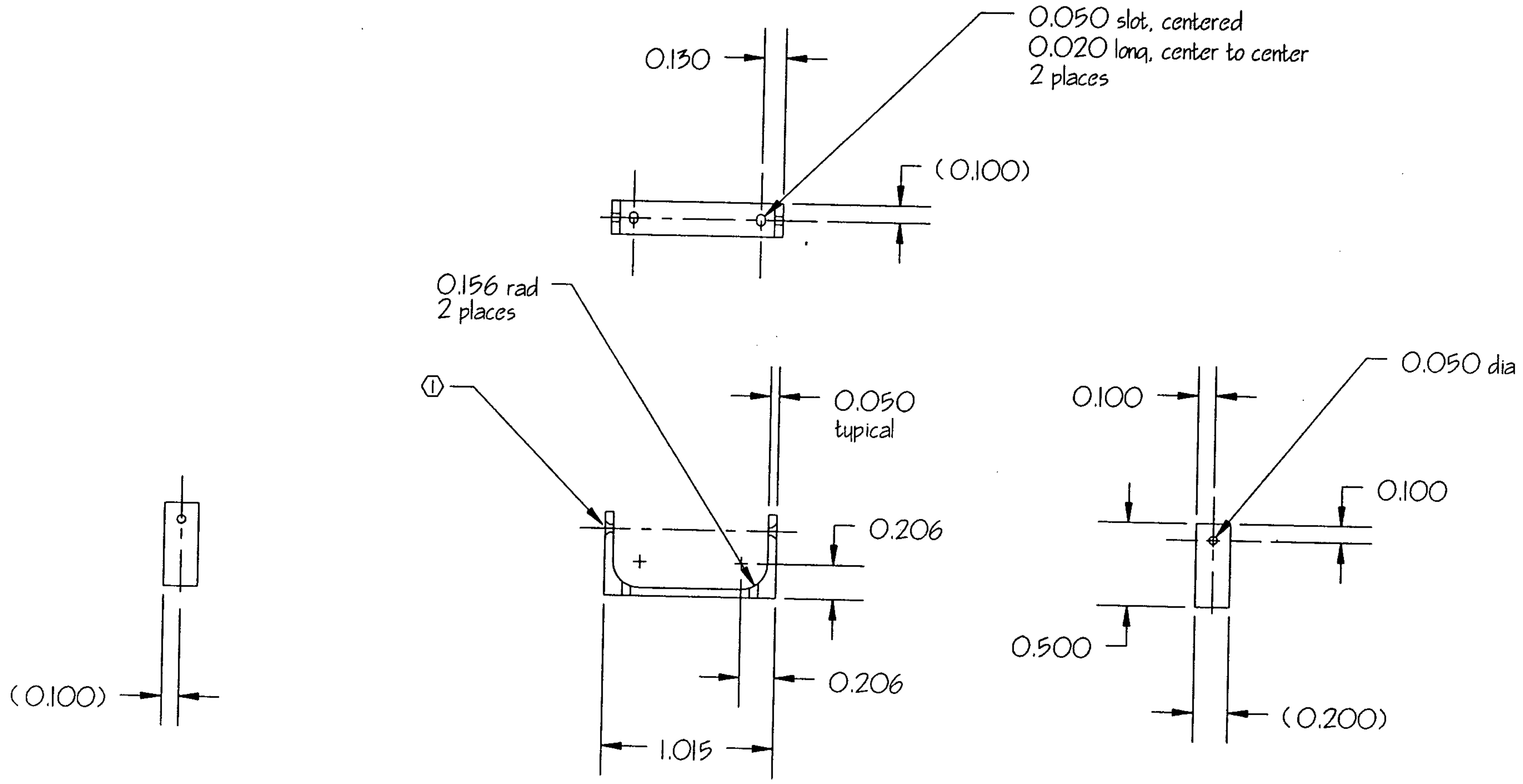

① 00-90 thrd, csink flush
Use 00-90 x 1/16 flat head

tra

TITLE: Modified J-Clip: Digit #2 - Middle
SCALE: 1:1
DATE: 24 Mar 95
No. BE000211
DRAWN BY: A. P. Hilton
RELEASE DATE: 24 Mar 95
PROJECT: Actuator II
APPROVAL:
FILE NAME: be00211.dwg
REV A
Matl: Alum
Heat Treat : No

Unless otherwise specified:
Dimensions are in inches
Tolerances on angles ± 0° 30'
Decimals .XX ± .03, .XXX ± .005

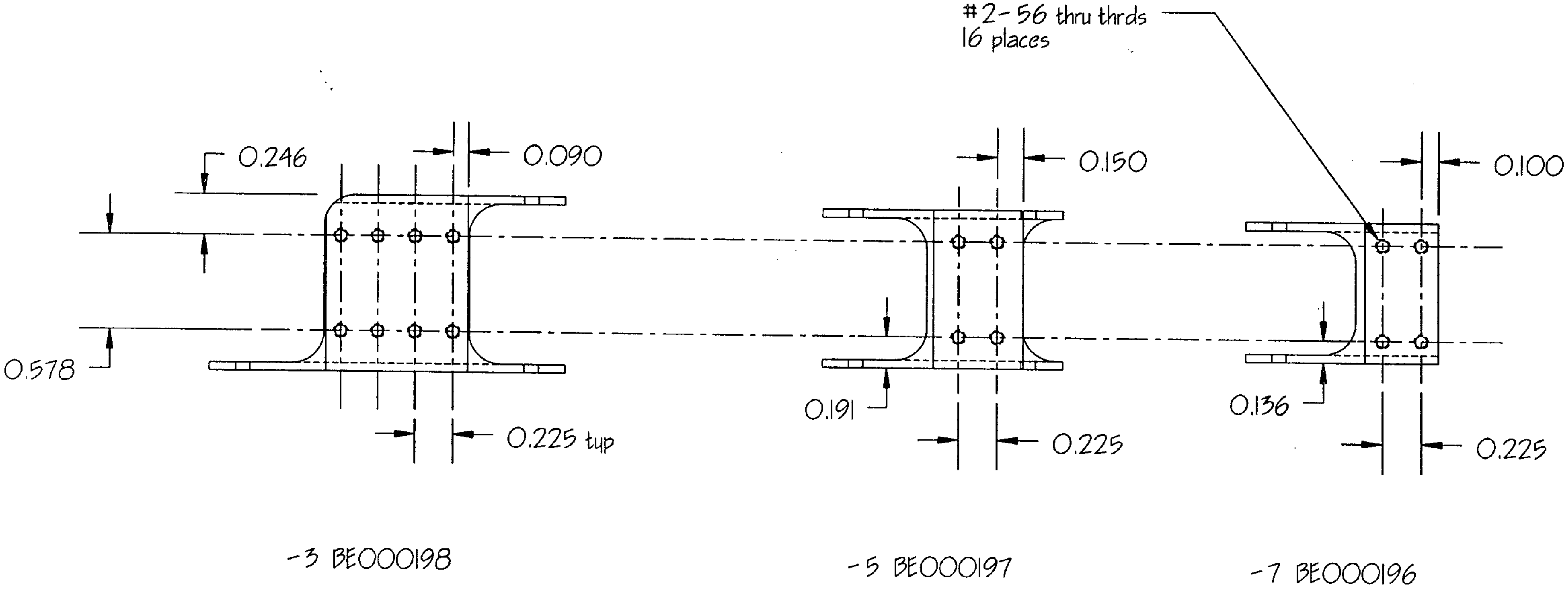

Unless otherwise specified:
Dimensions are in inches
Tolerances on angles ± 0° 30'
Decimals .XX ± .03, .XXX ± .005

tra

REV A
Mat'l: N/A
Heat Treat : No

TITLE: Mounting Holes Layout - Digit #2
SCALE: 1:1
DATE: 28 Mar 95
No. BE000212
DRAWN BY: A. P. Hilton
RELEASE DATE: 28 Mar 95
PROJECT: Actuator II
APPROVAL:
FILE NAME: be00212.dwg

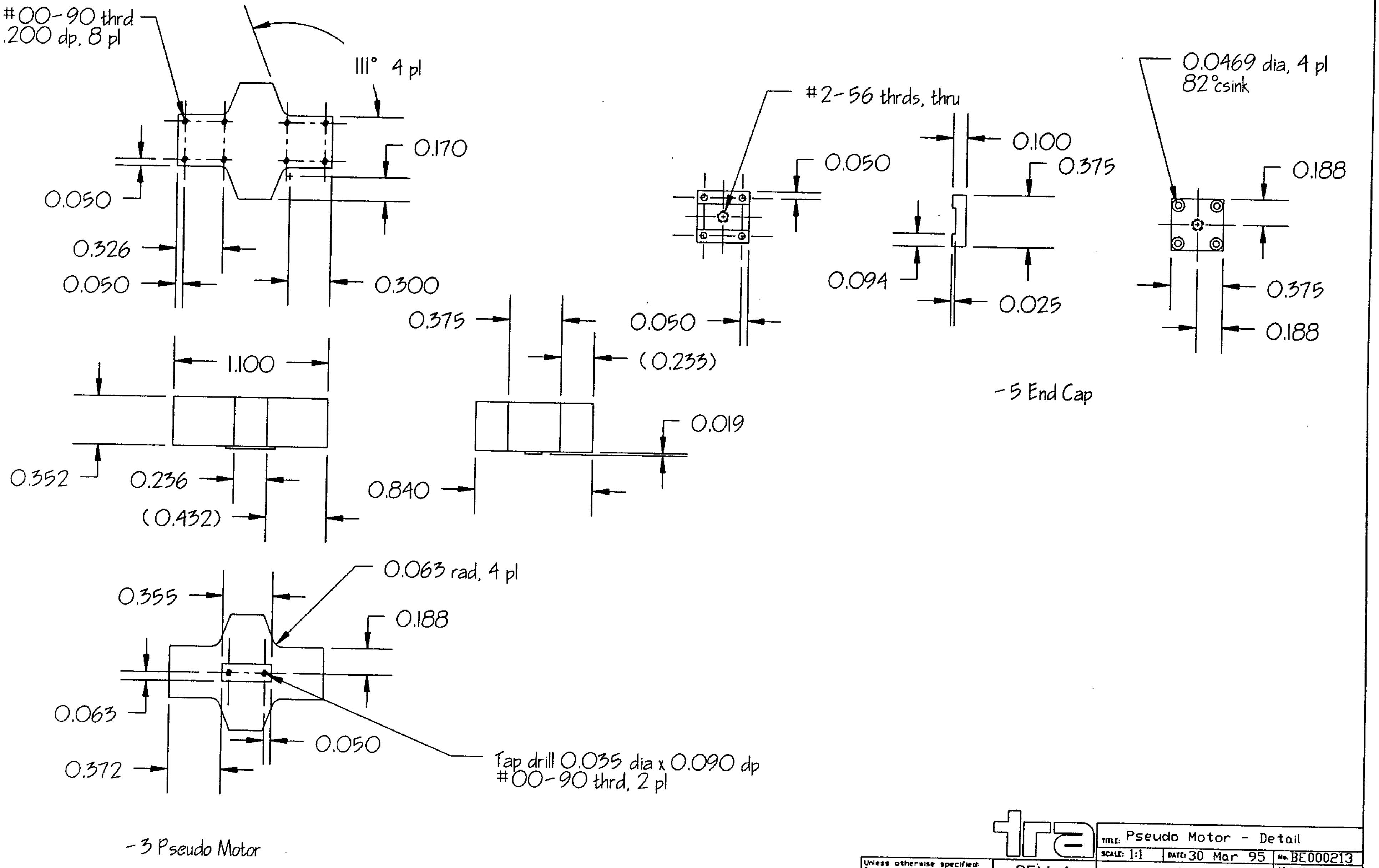

tra

TITLE: Pseudo Motor - Detail
SCALE: 1:1
DATE: 30 Mar 95
No. BE000213
Unless otherwise specified:
Dimensions are in inches
Tolerances on angles ± 0° 30'
Decimals .XX ± .03, .XXX ± .005
REV A
DRAWN BY: A. P. Hilton
RELEASE DATE: 30 Mar 95
Mat'l: Alum
PROJECT: Actuator II
APPROVAL:
Heat Treat : No
FILE NAME: be00213.dwg

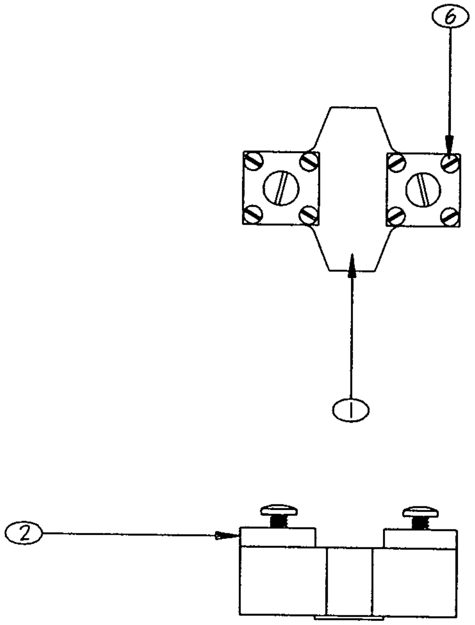

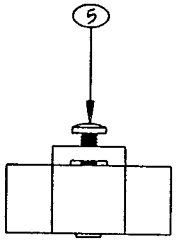

(2) Small Parts, Miami Lakes, FL 305-557-8222
(1) Fasteners of Comparable Spec's Acceptable

	QTY REQD	ITEM NO.	PART NO.	DESCRIPTION	MAT'L / SPEC
(2)(1)	2	6	MX-256-3B	#2-56 x 3/16 BH Scrw	18-8 SS
(2)(1)	8	5	MX-0090-3F	#00-90 x 3/16 FH Scrw	18-8 SS
	1	4	XXX	XXX	---
	1	3	XXX	XXX	---
	2	2	BE000213-5	End Cap	---
	1	1	BE000213-3	Pseudo Motor Housing	---
	---		BE000214	Pseudo Motor ASSEMBLY	---

PARTS LIST

tra

Unless otherwise specified: Dimensions are in inches Tolerances on angles ± 0° 30' Decimals .XX ± .03, .XXX ± .005	REV A Matl: XXX Heat Treat : No	TITLE: Pseudo Motor - Assembly SCALE: 1:1 DATE: 30 Mar 95 DRAWN BY: A. P. Hilton PROJECT: Actuator II FILE NAME: be00214.dwg	No. BE000214 RELEASE DATE: 30 Mar 95 APPROVAL:

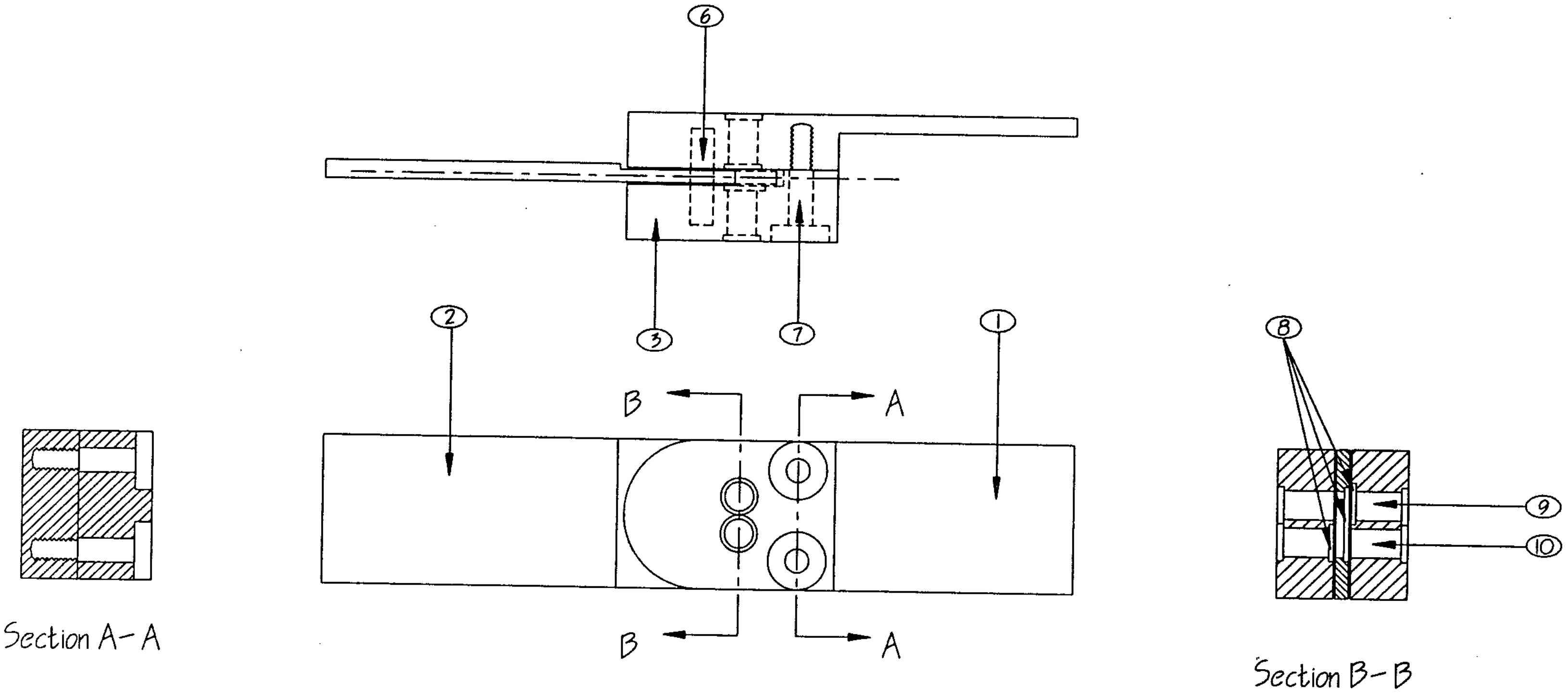

Section A- A

Section B- B

④ Small Parts, Miami Lakes, FL 305-557-8222
③ Fasteners of Comparable Spec's Acceptable
② Marshall
① Visual Pursuits, Inc.

	QTY REQD	ITEM NO.	PART NO.	DESCRIPTION	MAT'L / SPEC
②	2	10	SD1440-002	Photo Detector	---
②	2	9	SE1450-003	LED	---
①	3	8	XXX	Polarizing Filter	---
③④	2	7	MX-080-4B	#0-80 x 1/ 4 Bnd. Hd Scrws	18-8 SS
④	1	6	DWX-1-4	1/ 16 D x 1/ 4 Dowel Pin	303 SS
	1	5	XXX	XXX	---
	1	4	XXX	XXX	---
	1	3	BE000217	Clip	---
	1	2	BE000218	Proximal Section	---
	1	1	BE000216	Distal Section	---
	---		BE000215	ANGLE SENSOR ASSEMBLY	---

PARTS LIST

tra

TITLE: Angle Sensor - Assembly
SCALE: 2:1
DATE: 6 Apr 95
No. BE000215
Unless otherwise specified:
Dimensions are in inches
Tolerances on angles ± 0° 30'
Decimals .XX ± .03, .XXX ± .005
REV A
Mat'l: Alum
Heat Treat : No
DRAWN BY: A. P. Hilton
PROJECT: Actuator II
FILE NAME: be00215.dwg
RELEASE DATE: 6 Apr 95
APPROVAL:

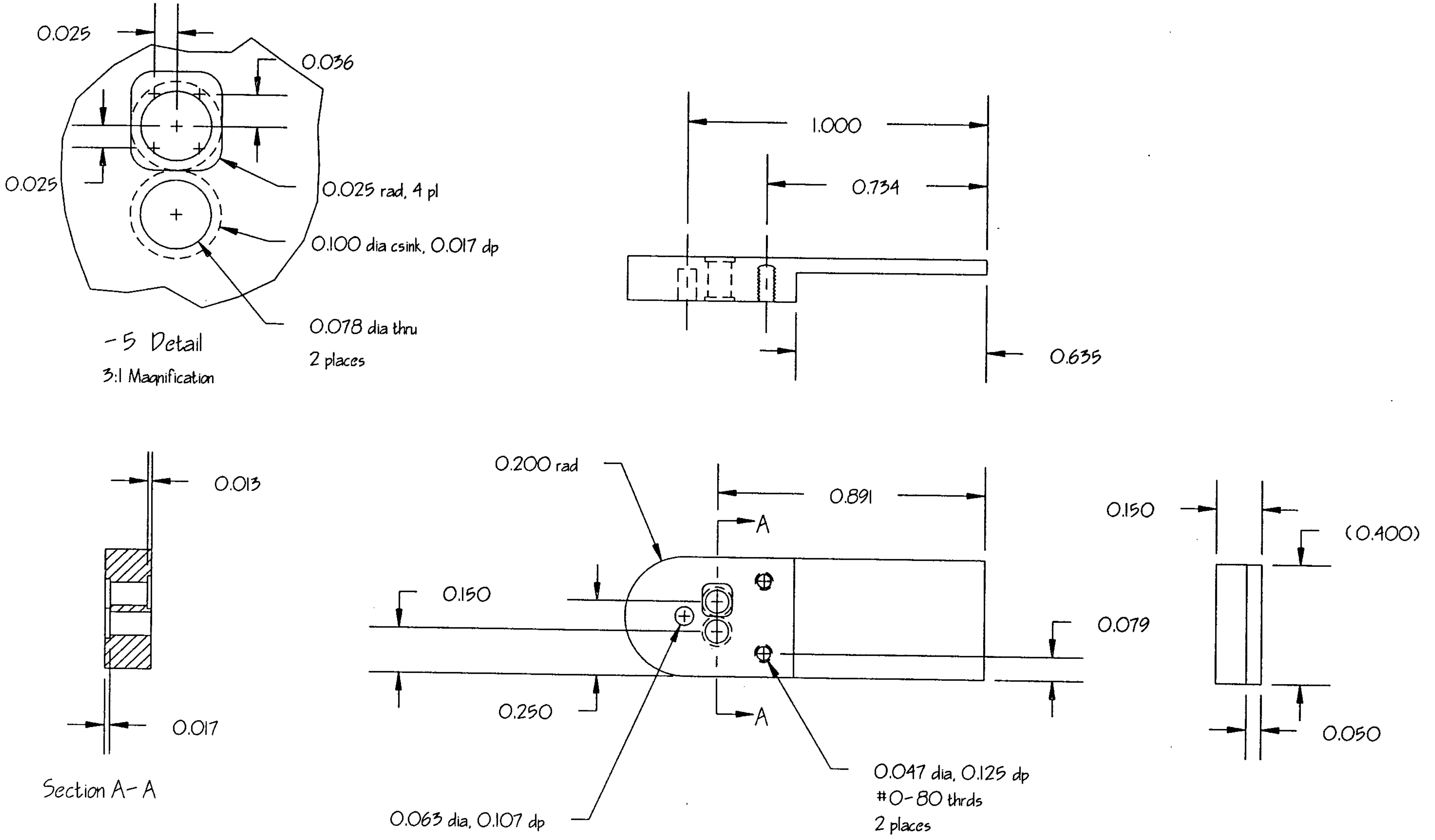

-3 Distal Section

Unless otherwise specified: Dimensions are in inches Tolerances on angles ± 0° 30' Decimals .XX ± .03, .XXX ± .005	REV A Matl: Alum Heat Treat : No	TITLE: Angle Sensor - Detail; Distal SCALE: 2:1 DATE: 3 Apr 95 DRAWN BY: A. P. Hilton PROJECT: Actuator II FILE NAME: be00216.dwg	No. BE000216 RELEASE DATE: 7 Apr 95 APPROVAL:

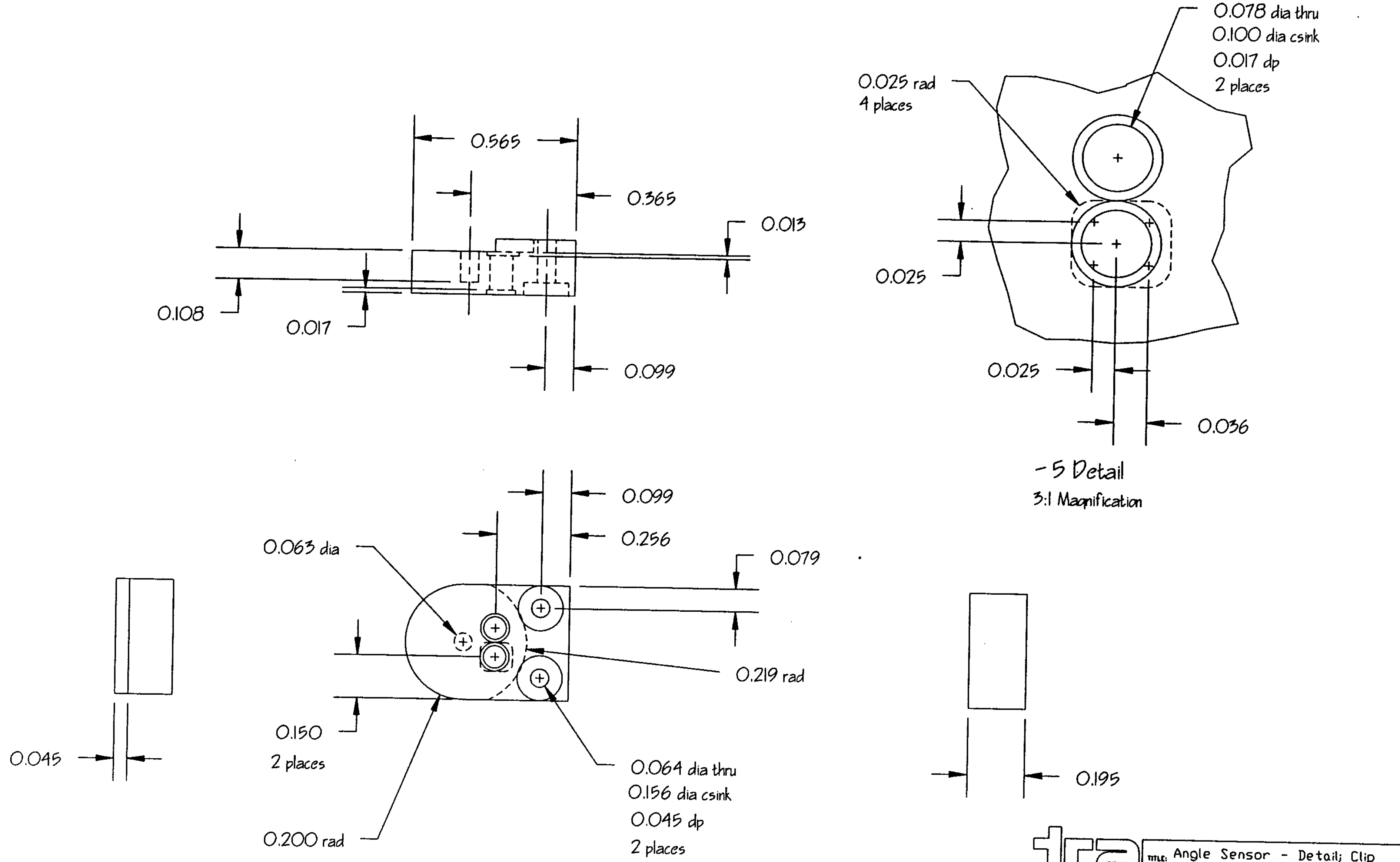

Unless otherwise specified:
Dimensions are in inches
Tolerances on angles ± 0° 30'
Decimals .XX ± .03, .XXX ± .005

REV A
Mat'l: Alum
Heat Treat : No

TITLE: Angle Sensor - Detail; Clip
SCALE: 2:1
DATE: 6 Apr 95
No. BE000217
DRAWN BY: A. P. Hilton
RELEASE DATE: 6 Apr 95
PROJECT: Actuator II
APPROVAL:
FILE NAME: be00217.dwg

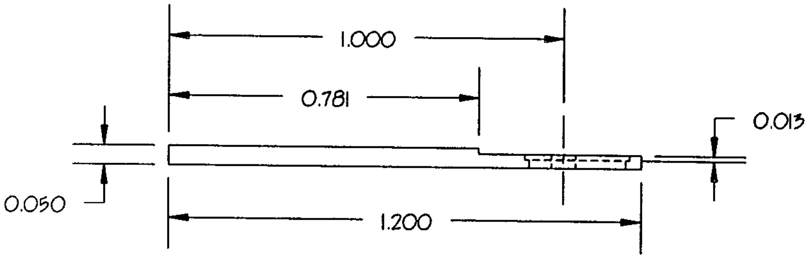

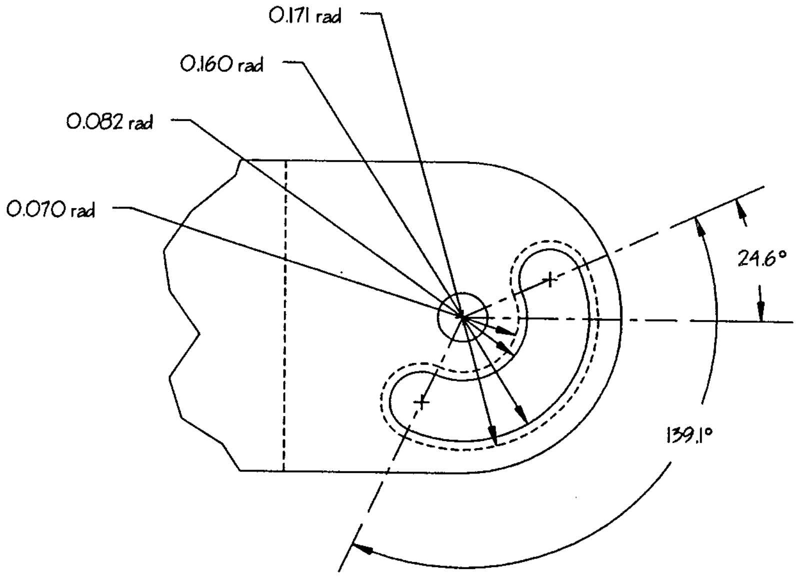

- 5 Detail
2:1 Magnification

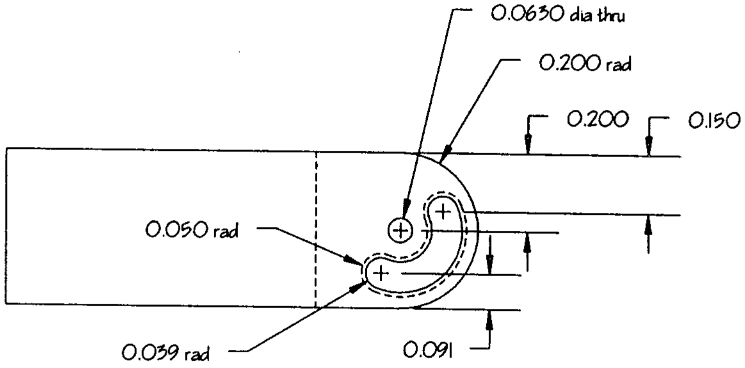

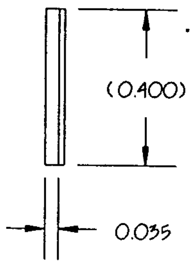

- 3 Proximal Section

Unless otherwise specified:
Dimensions are in inches
Tolerances on angles ± 0° 30'
Decimals .XX ± .03, .XXX ± .005

REV A
Matl: Alum
Heat Treat : No

TITLE: Angle Sensor - Detail; Proximal
SCALE: 2:1
DATE: 6 Apr 95
No. BE000218
DRAWN BY: A. P. Hilton
RELEASE DATE: 6 Apr 95
PROJECT: Actuator II
APPROVAL:
FILE NAME: be00218.dwg

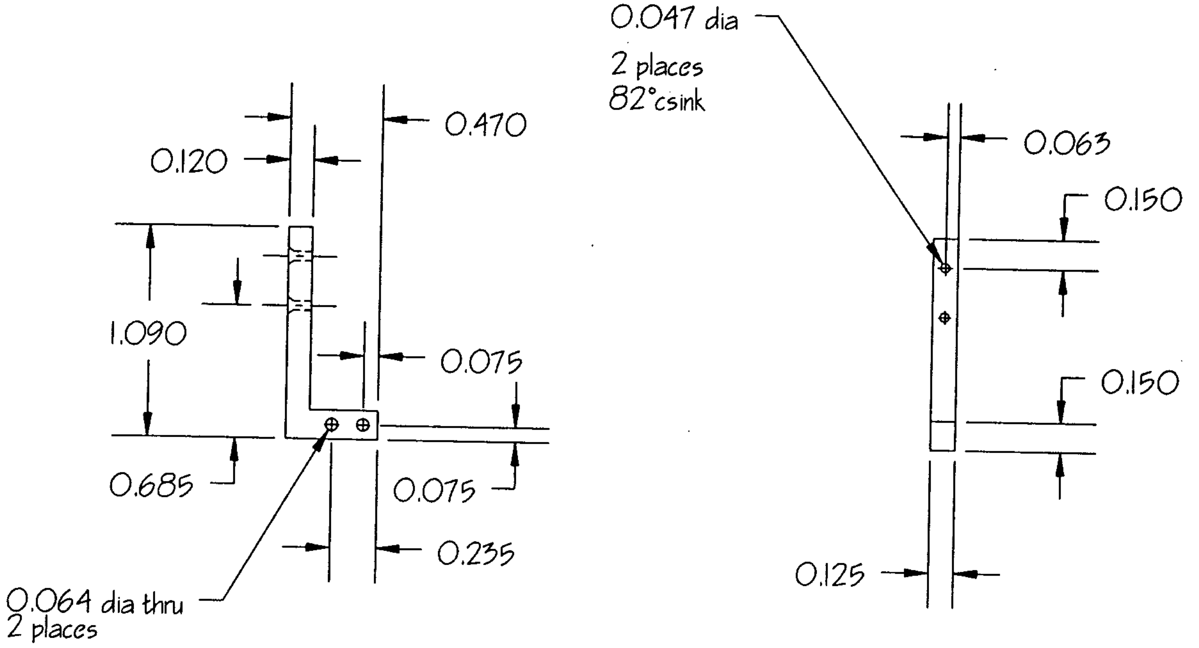

Unless otherwise specified:
Dimensions are in inches
Tolerances on angles ± 0° 30'
Decimals .XX ± .03, .XXX ± .005

REV B
Matl: Alum
Heat Treat.: No

TITLE: 'L' Angle - Motor Mount
SCALE: 1:1
DATE: 11 Apr 95
No. BE000219
DRAWN BY: A. P. Hilton
RELEASE DATE: 14 Apr 95
PROJECT: Actuator II
APPROVAL:
FILE NAME: be00219.dwg

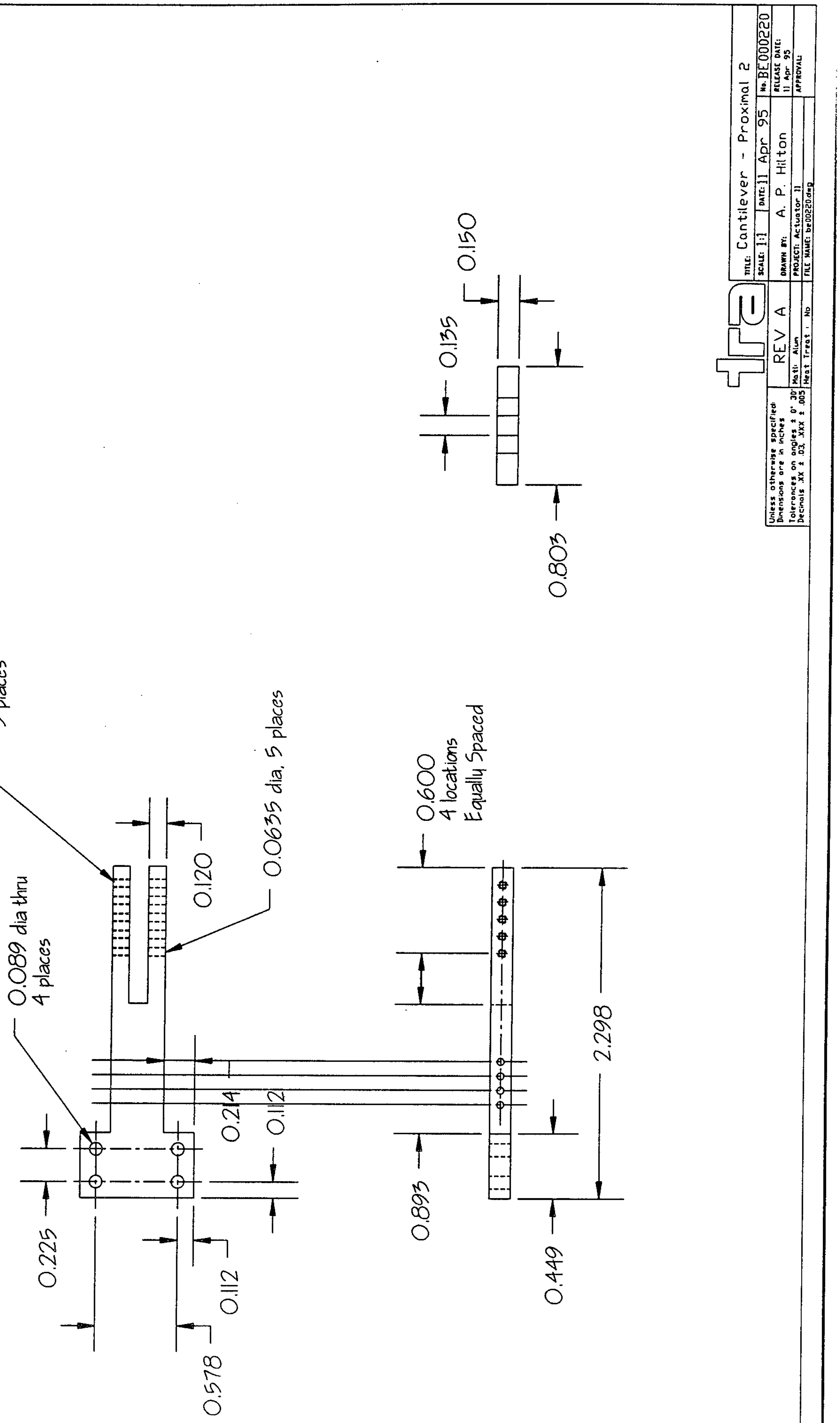
#0-80 thrd
5 places
0.089 dia thru
4 places
0.0635 dia, 5 places
0.120
0.600
4 locations
Equally Spaced
0.225
0.578
0.112
0.214
0.112
0.893
2.298
0.449
0.135
0.150
0.803
Unless otherwise specified:
Dimensions are in inches
Tolerances on angles ± 0° 30'
Decimals .XX ± .03, .XXX ± .005
TITLE: Cantilever - Proximal 2
SCALE: 1:1
DATE: 11 Apr 95
No. BE000220
DRAWN BY: A. P. Hilton
RELEASE DATE: 11 Apr 95
REV A
Mat'l: Alum
Heat Treat: No
PROJECT: Actuator II
FILE NAME: be00220.dwg
APPROVAL:

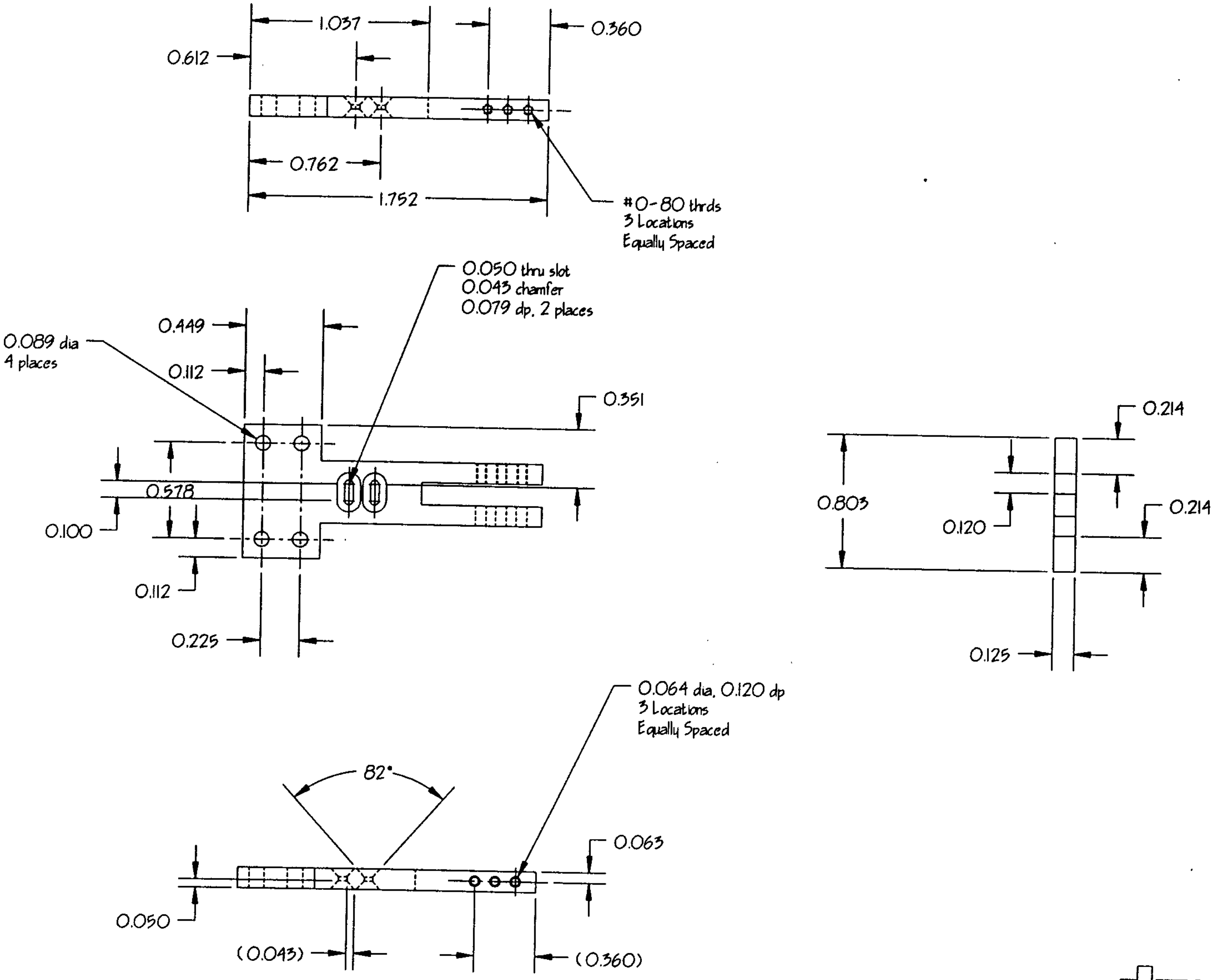

Unless otherwise specified:
Dimensions are in inches
Tolerances on angles ± 0° 30'
Decimals .XX ± .03, .XXX ± .005

REV A
Matl: Alum
Heat Treat : No

TITLE: Cantilever - Middle 2
SCALE: 1:1
DATE: 13 Apr 95
No. BE000222
DRAWN BY: A. P. Hilton
RELEASE DATE: 13 Apr 95
PROJECT: Actuator II
APPROVAL:
FILE NAME: be00222.dwg

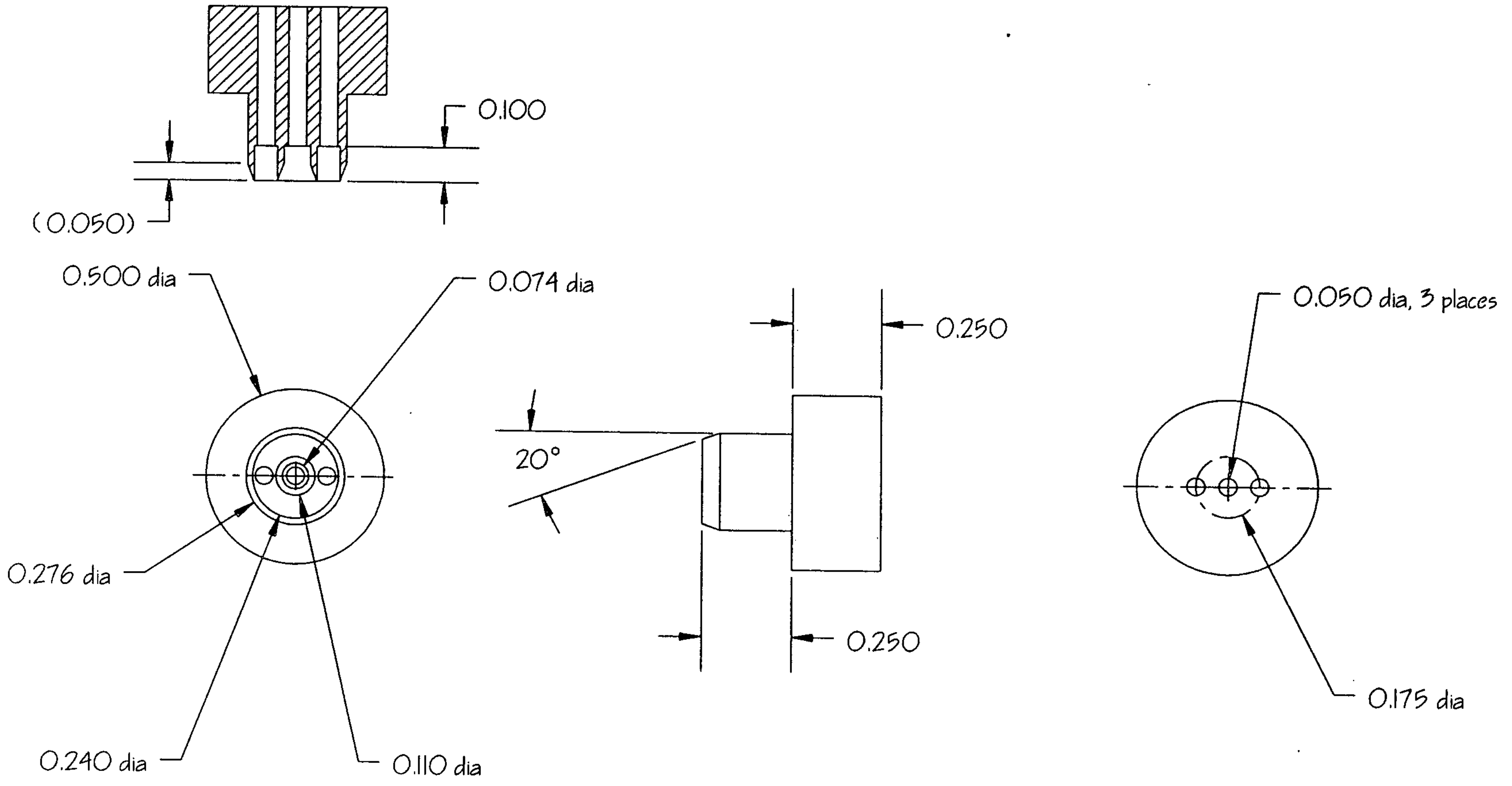

Unless otherwise specified:
Dimensions are in inches
Tolerances on angles ± 0° 30'
Decimals .XX ± .03, .XXX ± .005

REV A
Matl: tool steel
Heat Treat : No

TITLE: Punch - Teflon Washer
SCALE: 1:1
DATE: 14 Apr 95
No. BE000223
DRAWN BY: A. P. Hilton
RELEASE DATE: 14 Apr 95
PROJECT: Actuator II
FILE NAME: be00223.dwg
APPROVAL:

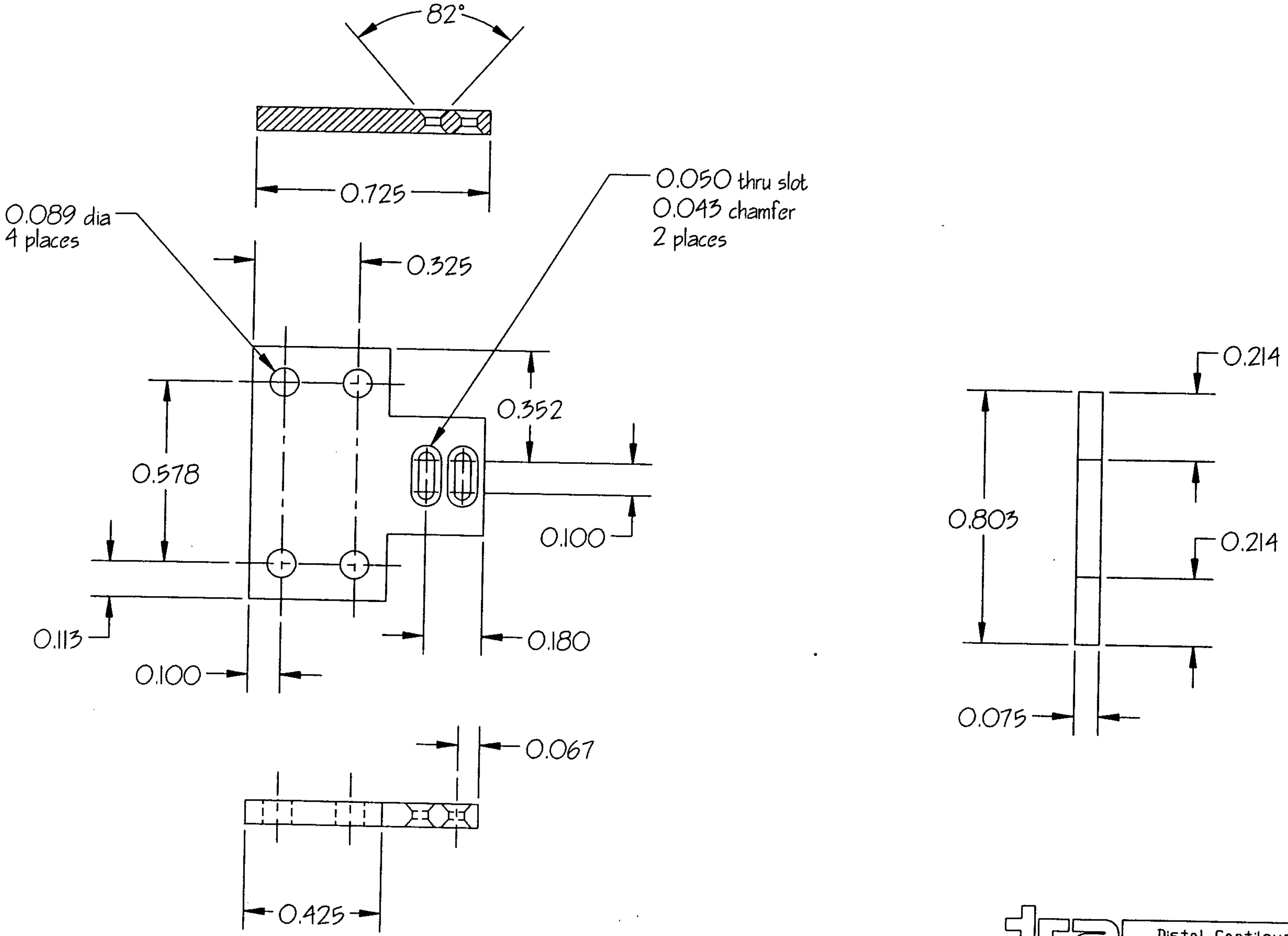

Unless otherwise specified: Dimensions are in inches Tolerances on angles ± 0° 30' Decimals .XX ± .03, .XXX ± .005	REV A Matl: Alum Heat Treat : No	TITLE: Distal Cantilever - Digit #2 SCALE: 2:1 DATE: 14 Apr 95 DRAWN BY: A. P. Hilton PROJECT: Actuator II FILE NAME: be00224.dwg	No. BE000224 RELEASE DATE: 14 Apr 95 APPROVAL:

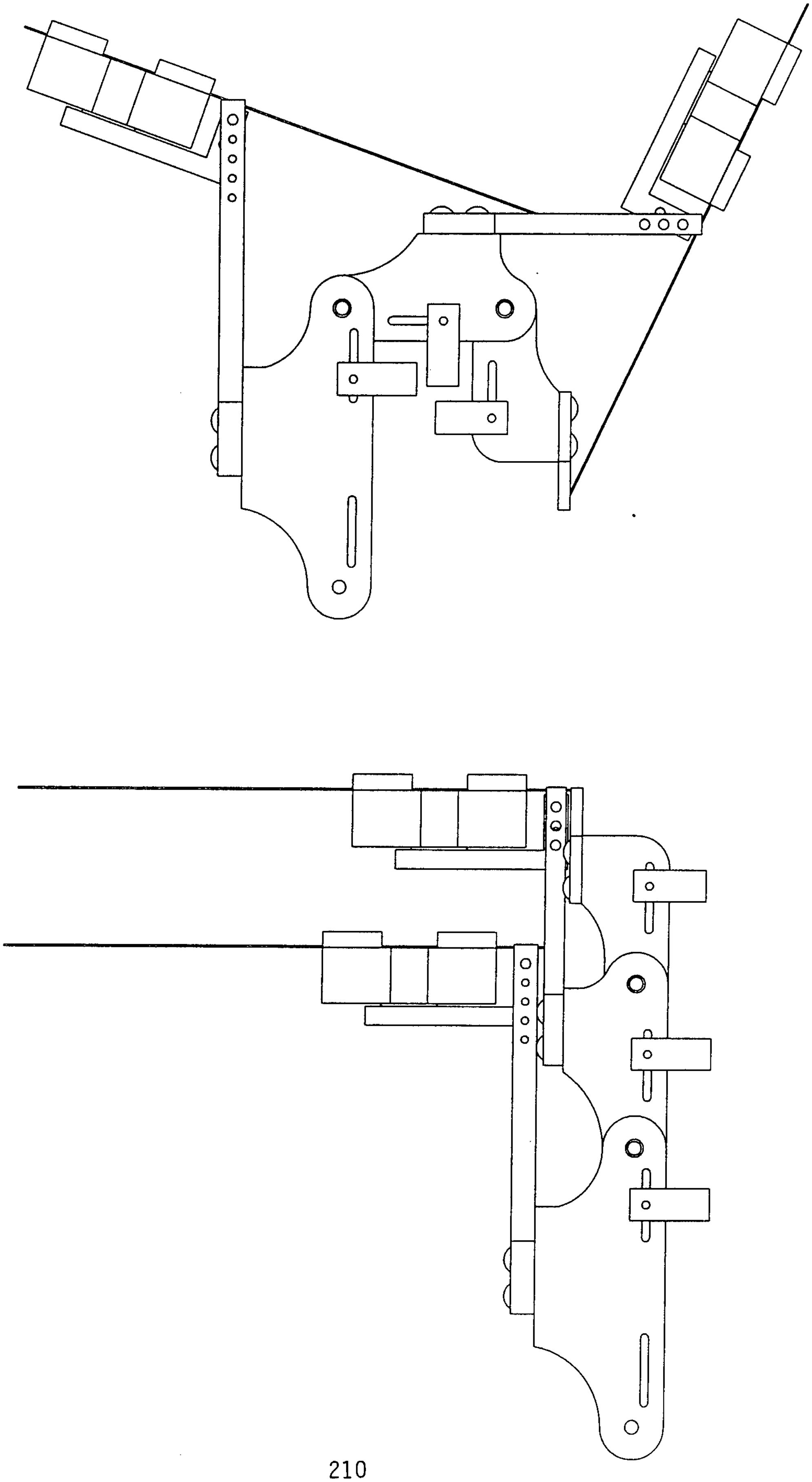

TITLE: Assembly - Digit 2; with Motors

SCALE: 1:1 | DATE: 20 Apr 95 | No. BE000225

DRAWN BY: A. P. Hilton

RELEASE DATE: 20 Apr 95

PROJECT: Actuator II

APPROVAL:

FILE NAME: be00225.dwg

REV B

Mat'l: XXX

Heat Treat : No

Unless otherwise specified:
Dimensions are in inches
Tolerances on angles ± 0° 30'
Decimals .XX ± .03, .XXX ± .005

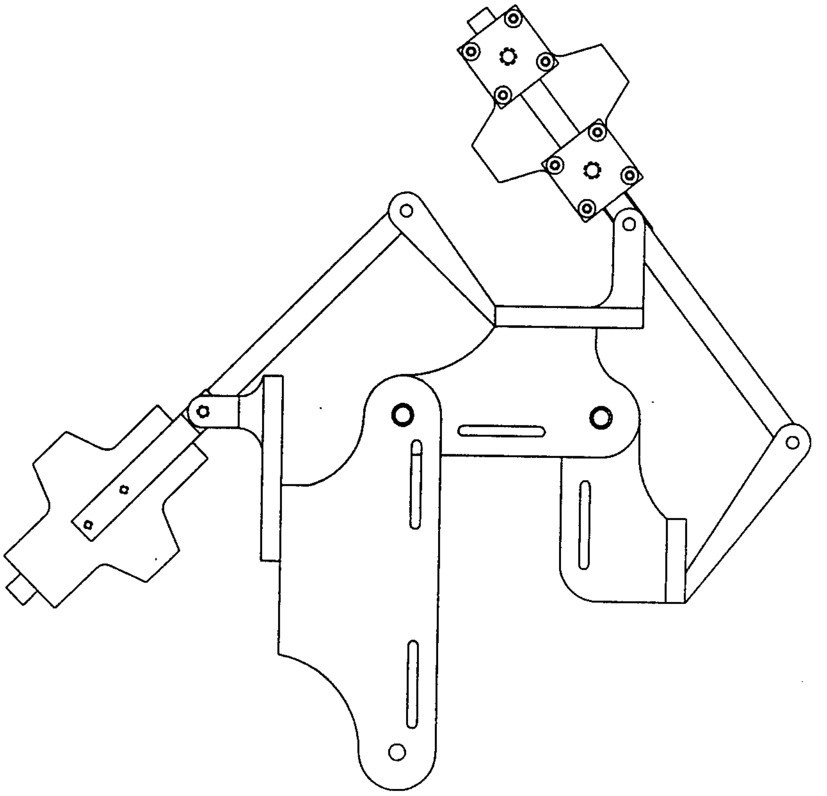

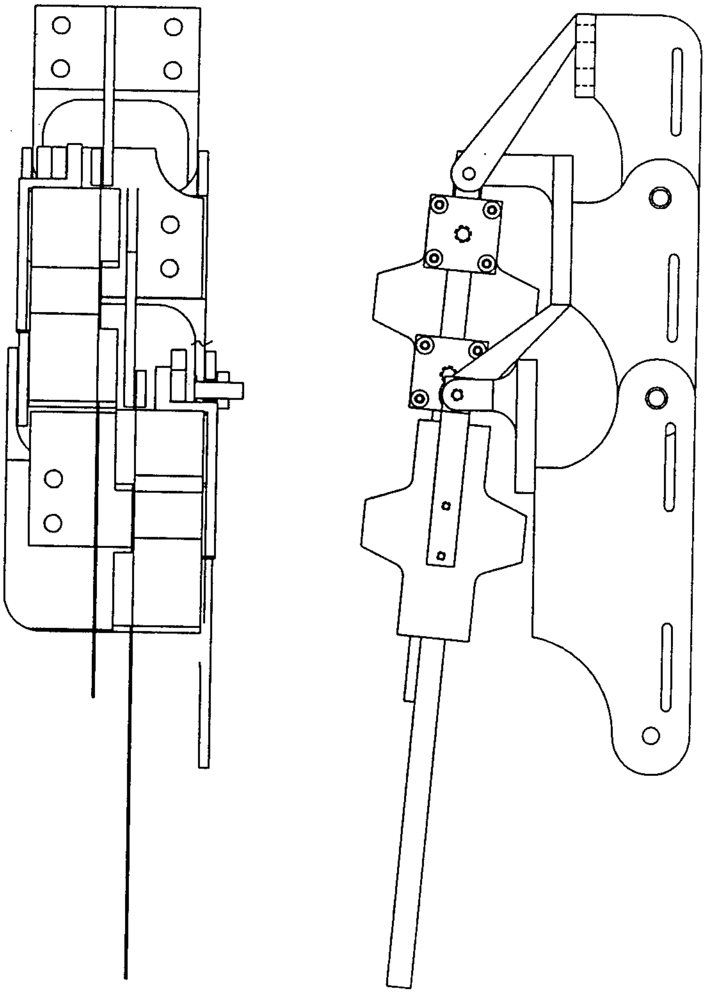

Unless otherwise specified:
Dimensions are in inches
Tolerances on angles ± 0° 30'
Decimals .XX ± .03, .XXX ± .005

tra

REV A

Mat'l: XXX
Heat Treat : No

TITLE: Assembly - Digit 2- 3rd Iteration
SCALE: 1:1
DATE: 24 Apr 95
No. BE000230
DRAWN BY: A. P. Hilton
RELEASE DATE: 24 Apr 95
PROJECT: Actuator II
APPROVAL:
FILE NAME: be00230.dwg

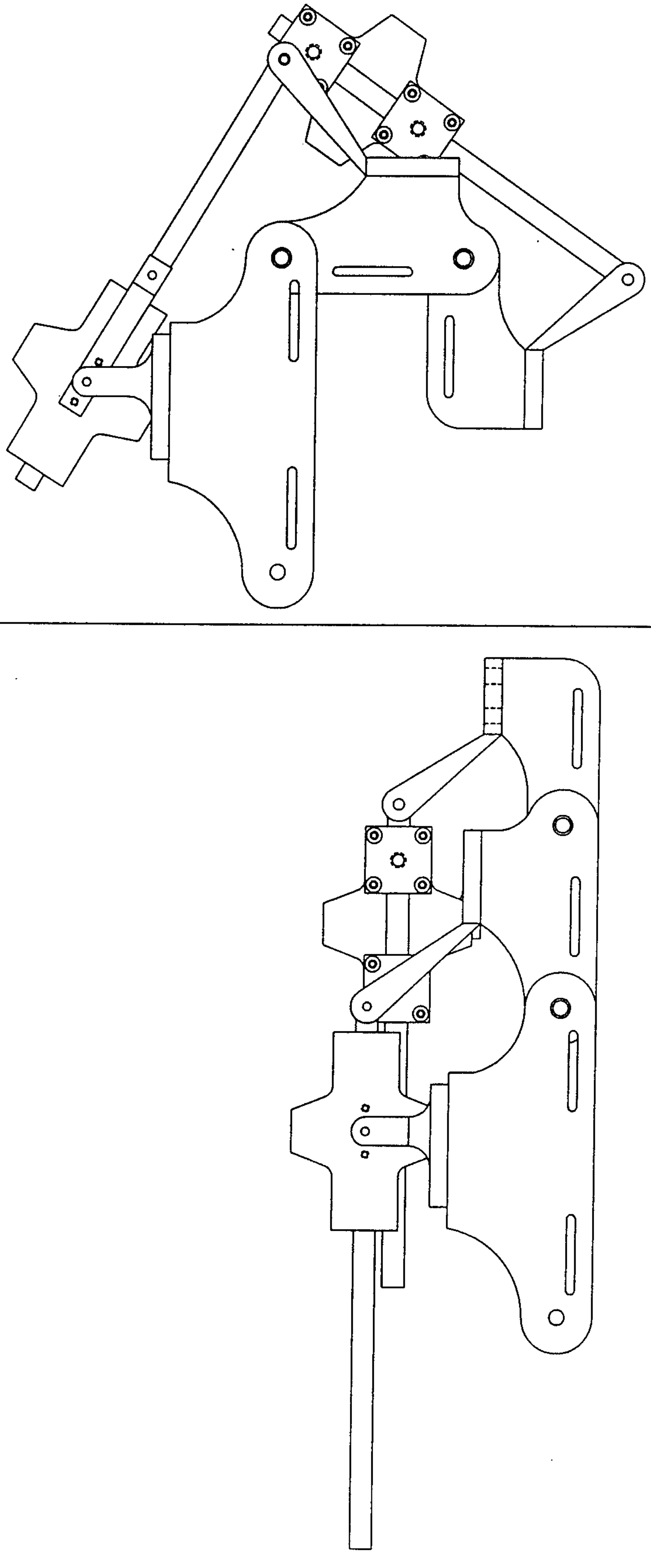

TITLE: Assembly - Digit 2- 4th Iteration
SCALE: 1:1
DATE: 28 Apr 95
No. BE000232
DRAWN BY: A. P. Hilton
RELEASE DATE: 28 Apr 95
PROJECT: Actuator II
APPROVAL:
FILE NAME: be00232.dwg
REV A
Mat'l: XXX
Heat Treat : No
Unless otherwise specified:
Dimensions are in inches
Tolerances on angles ± 0° 30'
Decimals .XX ± .03, .XXX ± .005

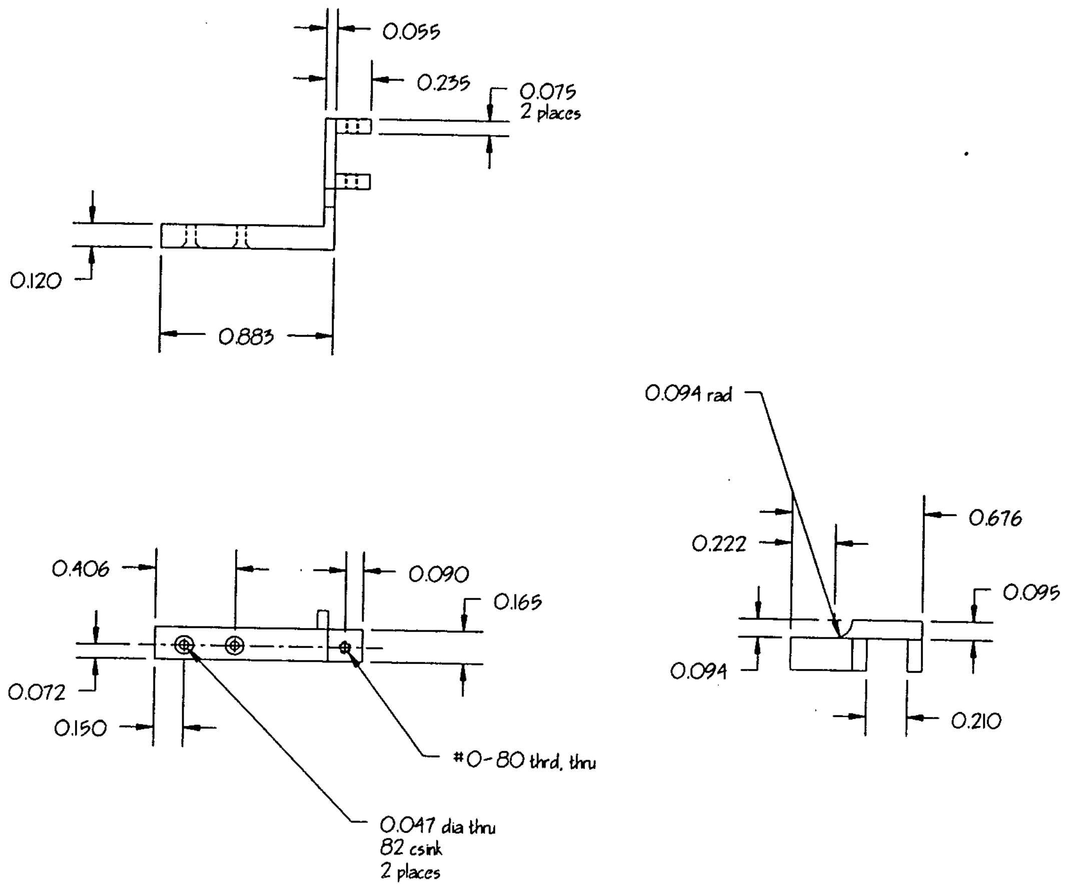

-3 - Proximal "F" Clip

tra

Unless otherwise specified:
Dimensions are in inches
Tolerances on angles ± 0° 30'
Decimals .XX ± .03, .XXX ± .005

REV A
Matl: Alum
Heat Treat : No

TITLE: Proximal "F" Clip
SCALE: 1:1
DATE: 21 Apr 95
DRAWN BY: A. P. Hilton
PROJECT: Actuator II
FILE NAME: be00227.dwg

No. BE000227
RELEASE DATE:
21 Apr 95
APPROVAL:

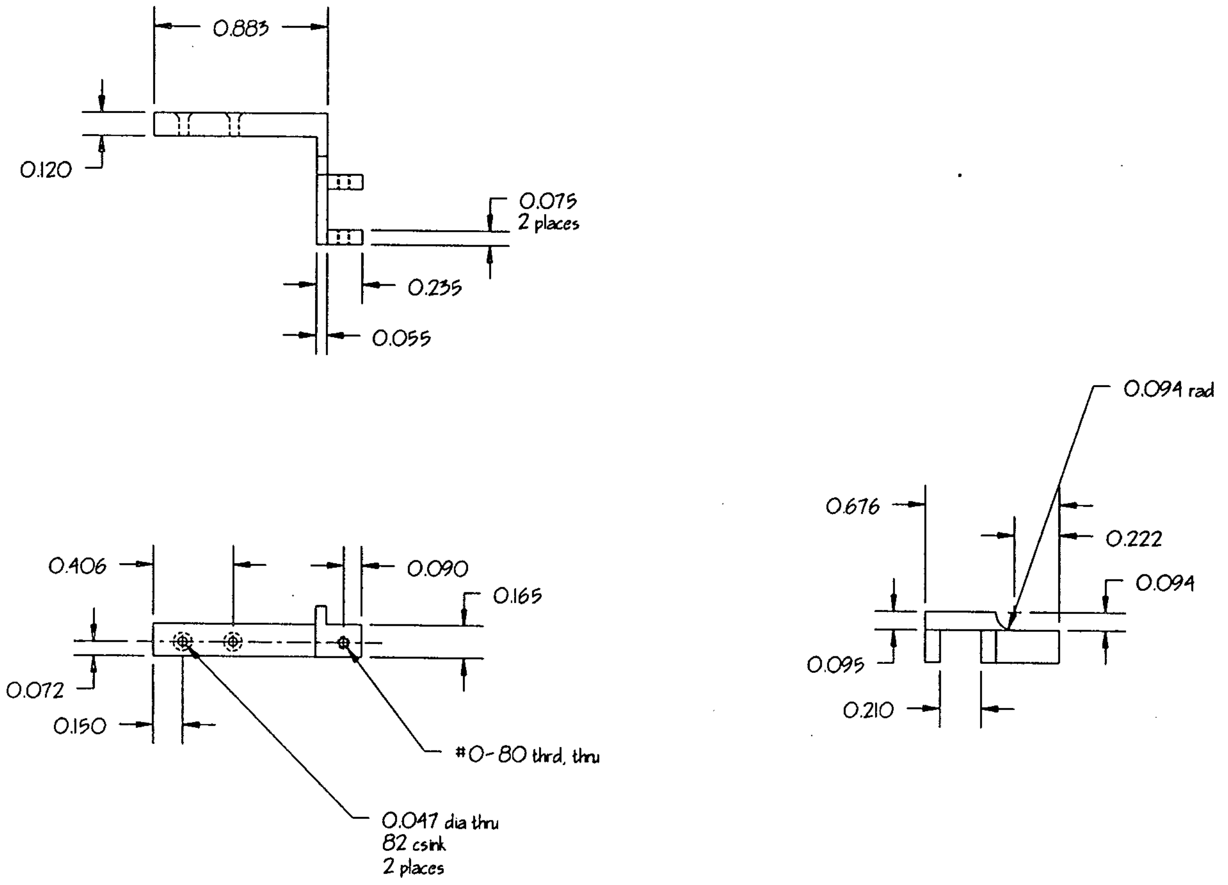

-3 - Middle "F" Clip

tra

TITLE: MIddle "F" Clip
SCALE: 1:1
DATE: 21 Apr 95
No. BE000228
Unless otherwise specified:
Dimensions are in inches
Tolerances on angles ± 0° 30'
Decimals .XX ± .03, .XXX ± .005
REV A
DRAWN BY: A. P. Hilton
RELEASE DATE: 21 Apr 95
Matl: Alum
PROJECT: Actuator II
APPROVAL:
Heat Treat : No
FILE NAME: be00228.dwg

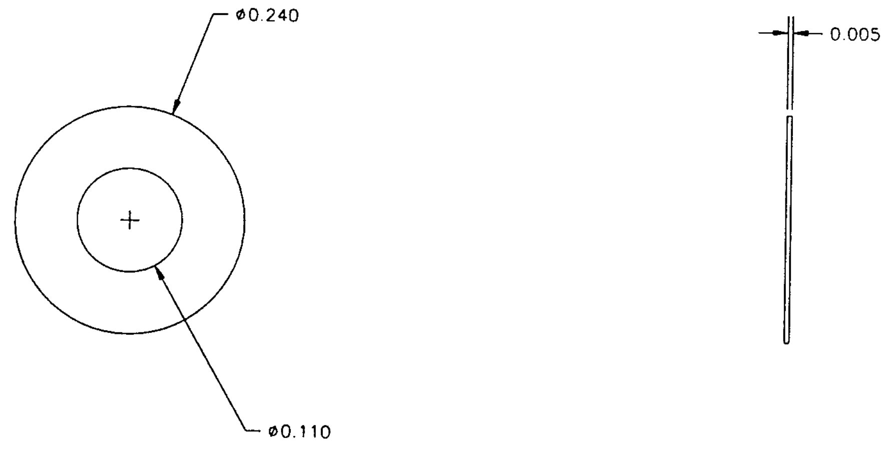

② Use 0.005" teflon sheet
Small Parts inc., Miami Lakes, FL 1-800-423-9009
Part No: A-VT-5

① Punch with BE000223

tra

TITLE: Washer, Motive Cell End Cap
SCALE: 10:1
DATE: 21 Aug 95
No. BE000264
Unless otherwise specified:
Dimensions are in inches
Tolerances on angles ± 0° 30'
Decimals .XX ± .03, .XXX ± .005
Rev A
DRAWN BY: A. P. Hilton
RELEASE DATE: 21 Aug 95
Matl:
PROJECT: Actuator II
APPROVAL:
Heat Treat:
FILE NAME: BE00264.dwg
C

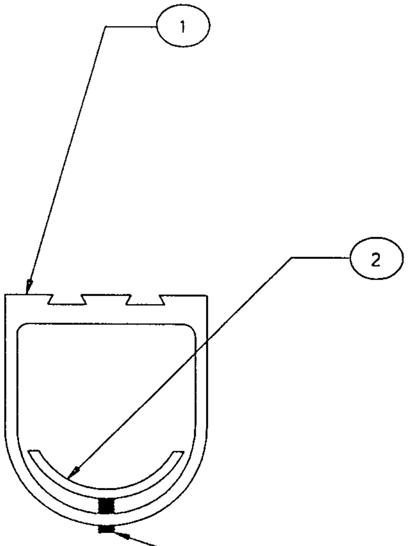

-1 Assembly

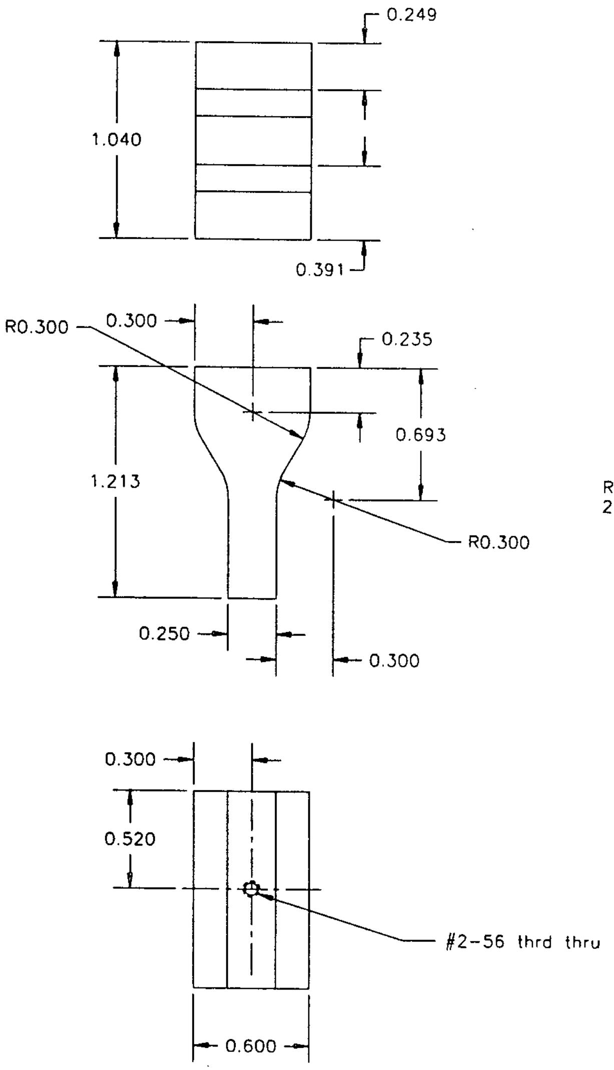

-3 Ring Detail

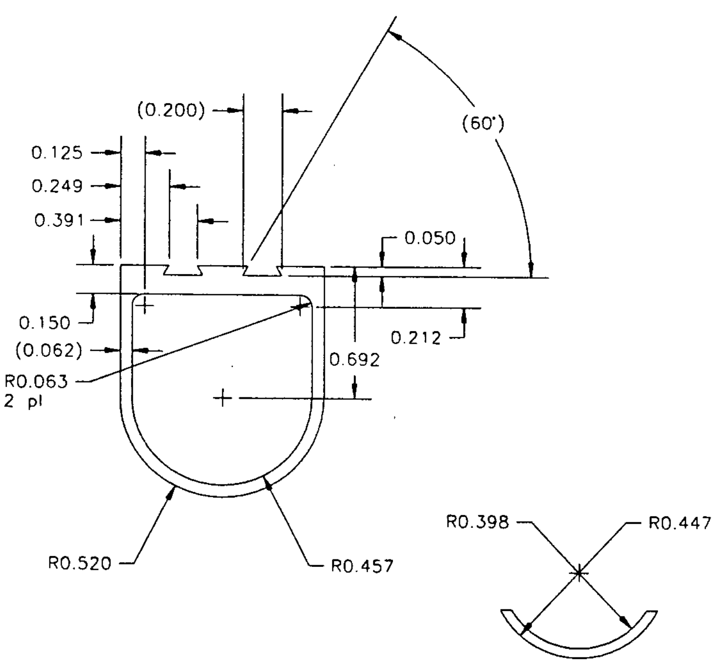

-5 Clamp Detail

①②

QTY REQD	ITEM NO.	PART NO.	DESCRIPTION	MAT'L/SPEC
1	5	XXX	XXX	---
1	4	XXX	XXX	---
1	3	SSAS-256-3	#2-56 x 3/16 set screw	---
1	2	BE000265-5	Adjustment Clamp	---
1	1	BE000265-3	Ring	---
1	---	BE000265	RING ASSEMBLY	---

PARTS LIST

② Fasteners of comparable spec's acceptable.
① Small Parts Inc., Miami Lakes, FL 1-800-220-4242

tra

TITLE: Ring Mount - PIP; Exoskeleton
SCALE: 2:1
DATE: 22 Aug 95
No. BE000265
DRAWN BY: A. P. Hilton
RELEASE DATE: 22 Aug 95
PROJECT: Actuator II
APPROVAL:
FILE NAME: BE00265.dwg
C

Unless otherwise specified:
Dimensions are in inches
Tolerances on angles ± 0° 30'
Decimals XX ± .03, XXX ± .005

Rev A
Matl: Delrin
Heat Treat:

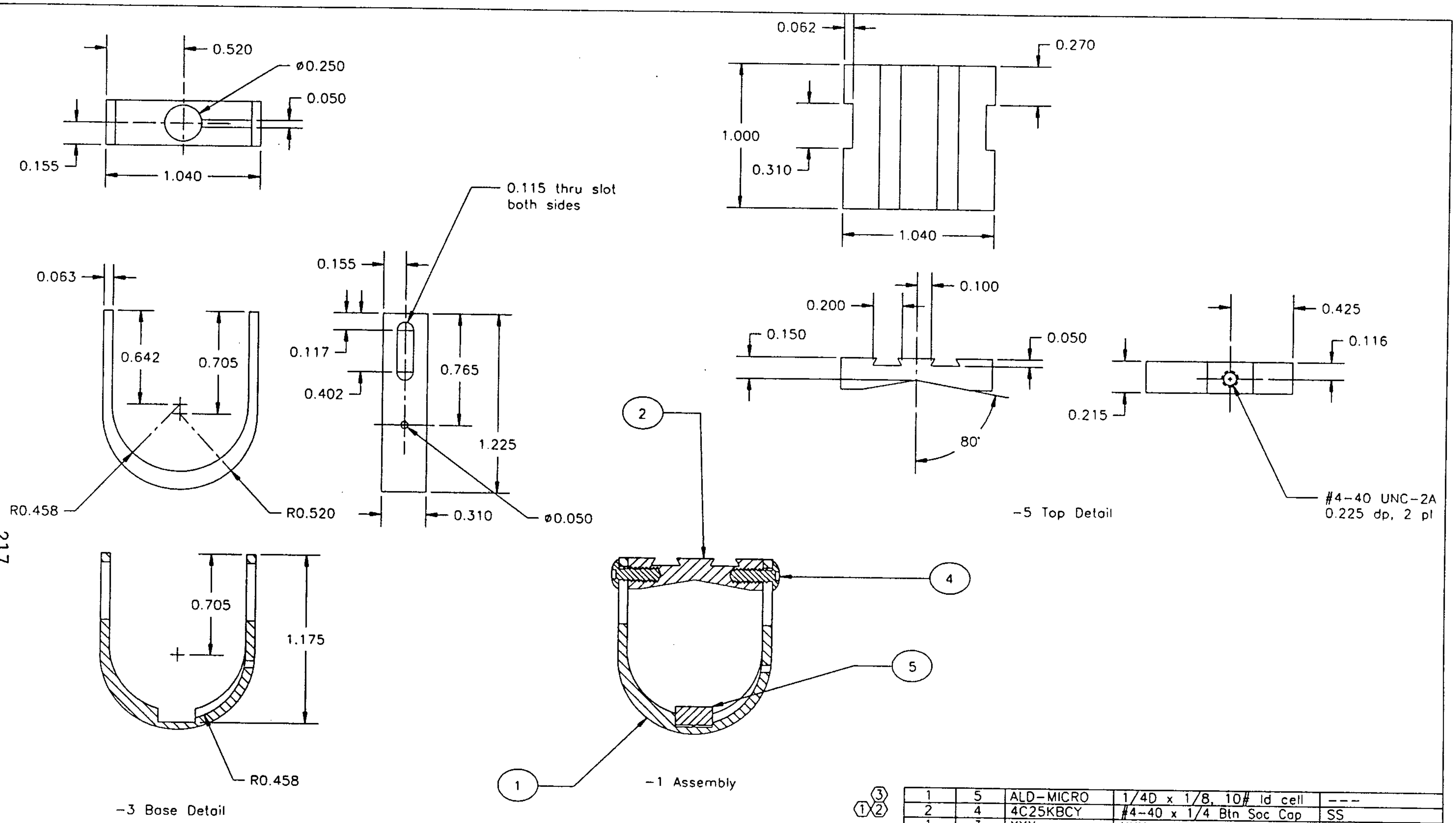

③ AL Design, Inc., 1411 Military Rd, Buffalo, NY 716-875-6240
② Fasteners of comparable spec's acceptable.
① ABABA Bolt Inc., El Cajon, CA (619) 440-1781

QTY REQD	ITEM NO.	PART NO.	DESCRIPTION	MAT'L/SPEC
1	5	ALD-MICRO ③	1/4D x 1/8, 10# ld cell	---
2	4	4C25KBCY ①②	#4-40 x 1/4 Btn Soc Cap	SS
1	3	XXX	XXX	---
1	2	BE000265-5	Ring Top	Delrin
1	1	BE000265-3	Ring Base	Delrin
1	---	BE000265	RING ASSEMBLY	---

PARTS LIST

TITLE: Ring Mount - PIP; Exoskeleton
SCALE: 2:1
DATE: 22 Aug 95
No. BE000265
DRAWN BY: A. P. Hilton
RELEASE DATE: 17 Oct 95
PROJECT: Actuator II
APPROVAL:
FILE NAME: BE00265d.dwg
C

Unless otherwise specified:
Dimensions are in inches
Tolerances on angles ± 0° 30'
Decimals .XX ± .03, .XXX ± .005

Rev D
Matl: Delrin
Heat Treat: N/A

①

NO.	REVISION	DATE	BY
3	length of top section	17 Oct 95	APH
2	two piece adjustable, load cell mount	14 Sep 95	APH
1	height, clamp pos, load cell mnt, strain relief	12 Sep 95	APH

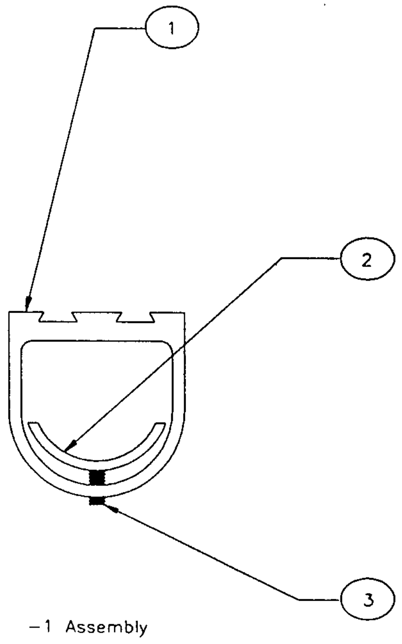

-1 Assembly

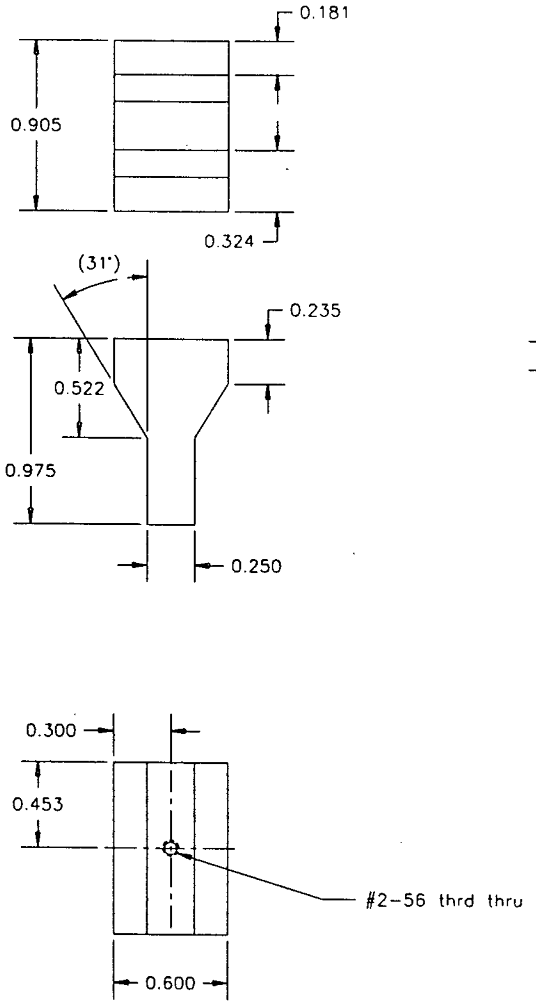

-3 Ring Detail

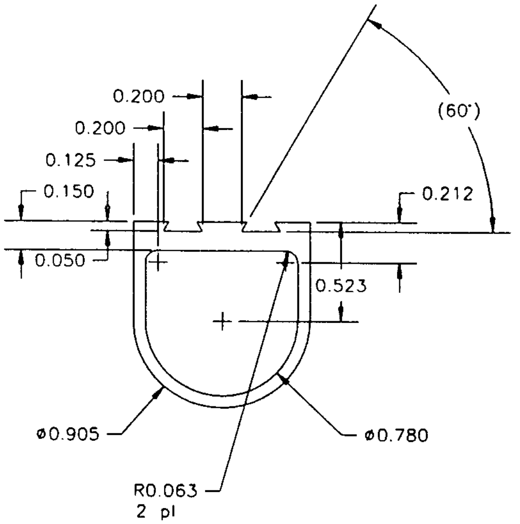

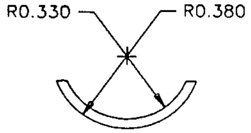

-5 Clamp Detail

⟨1⟩⟨2⟩

QTY REQD	ITEM NO.	PART NO.	DESCRIPTION	MAT'L/SPEC
1	5	XXX	XXX	---
1	4	XXX	XXX	---
1	3	SSAS-256-3	#2-56 x 3/16 set screw	---
1	2	BE000266-5	Adjustment Clamp	---
1	1	BE000266-3	Ring	---
1	---	BE000266	RING ASSEMBLY	---

PARTS LIST

⟨2⟩ Fasteners of comparable spec's acceptable.
⟨1⟩ Small Parts Inc., Miami Lakes, FL 1-800-220-4242

tra

Unless otherwise specified: Dimensions are in inches	Rev A	TITLE: Ring Mount - MIP; Exoskeleton	
		SCALE: 2:1 DATE: 23 Aug 95	No. BE000266
Tolerances on angles ± 0° 30' Decimals .XX ± .03, .XXX ± .005		DRAWN BY: A. P. Hilton	RELEASE DATE: 23 Aug 95
	Matl: Delrin	PROJECT: Actuator II	APPROVAL: C
	Heat Treat:	FILE NAME: BE00266.dwg	

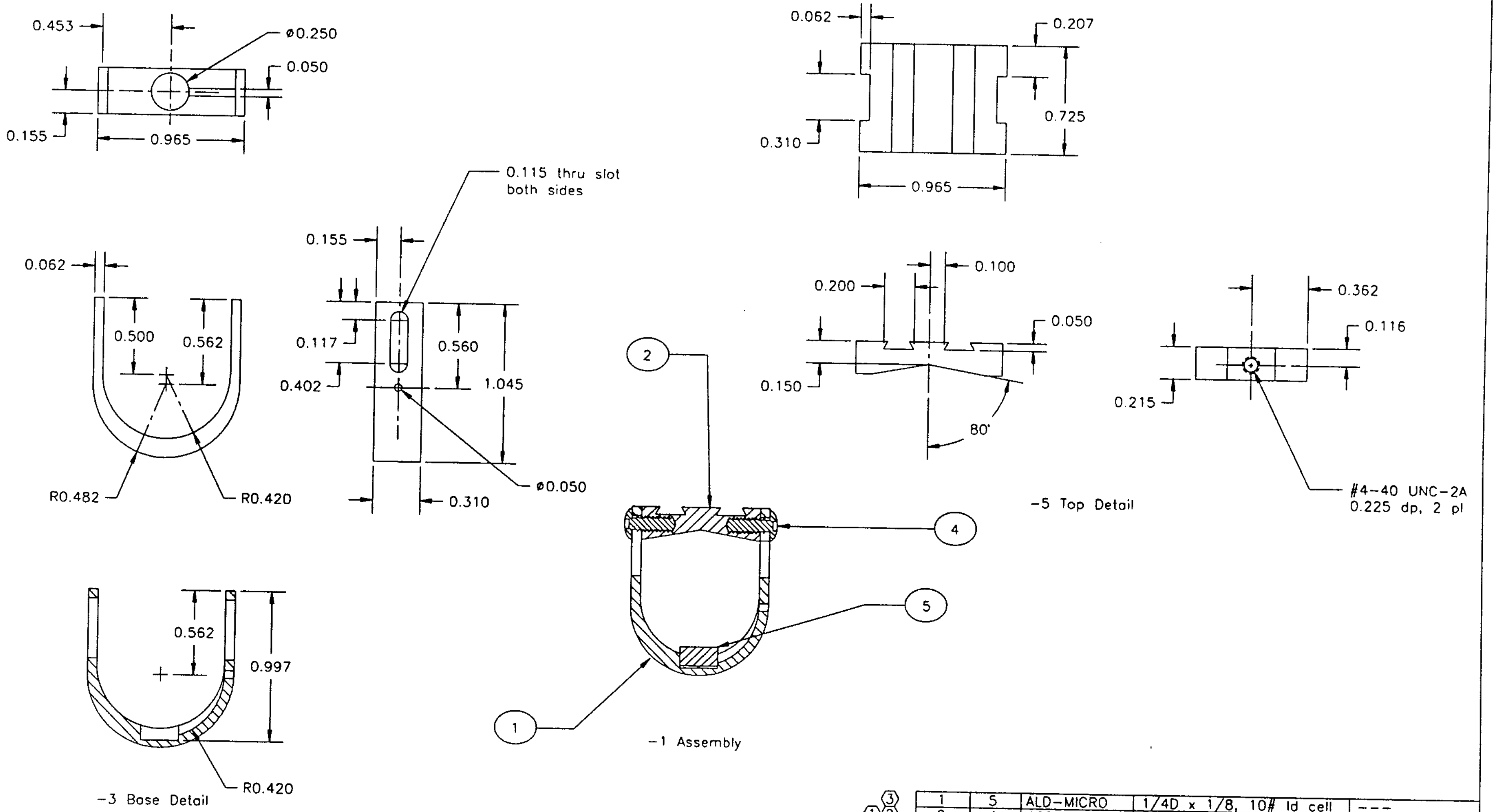

③ AL Design, Inc., 1411 Military Rd, Buffalo, NY 716-875-6240
② Fasteners of comparable spec's acceptable.
① ABABA Bolt Inc., El Cajon, CA (619) 440-1781

①②③

QTY REQD	ITEM NO.	PART NO.	DESCRIPTION	MAT'L/SPEC
1	5	ALD-MICRO	1/4D x 1/8, 10# ld cell	---
2	4	4C25KBCY	#4-40 x 1/4 Btn Soc Cap	SS
1	3	XXX	XXX	---
1	2	BE000266-5	Ring Top	Delrin
1	1	BE000266-3	Ring Base	Delrin
1	---	BE000266	RING ASSEMBLY	---

PARTS LIST

tra

TITLE: Ring Mount - MIP; Exoskeleton
SCALE: 2:1
DATE: 22 Aug 95
No. BE000266
DRAWN BY: A. P. Hilton
RELEASE DATE: 17 Oct 95
PROJECT: Actuator II
FILE NAME: BE00266d.dwg
APPROVAL:
C

Unless otherwise specified:
Dimensions are in inches
Tolerances on angles ± 0° 30'
Decimals .XX ± .03, .XXX ± .005

Rev D
Matl: Delrin
Heat Treat: N/A

NO.	REVISION	DATE	BY
3	length/width of top section, ring height & dia	17 Oct 95	APH
2	two piece adjustable, load cell mount	14 Sep 95	APH
1	height, clamp pos, load cell mnt, strain relief	12 Sep 95	APH

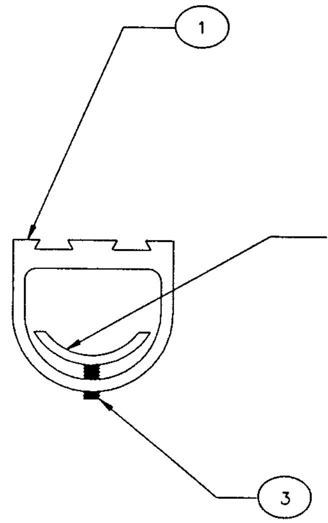

-1 Assembly

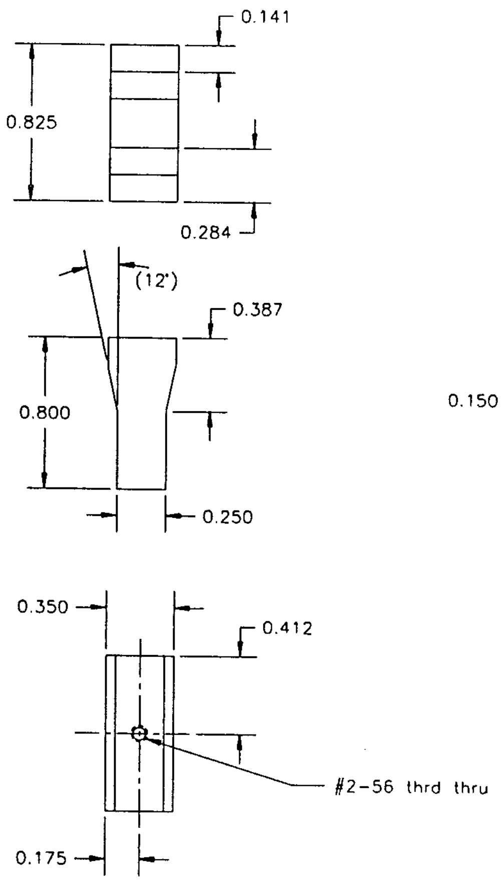

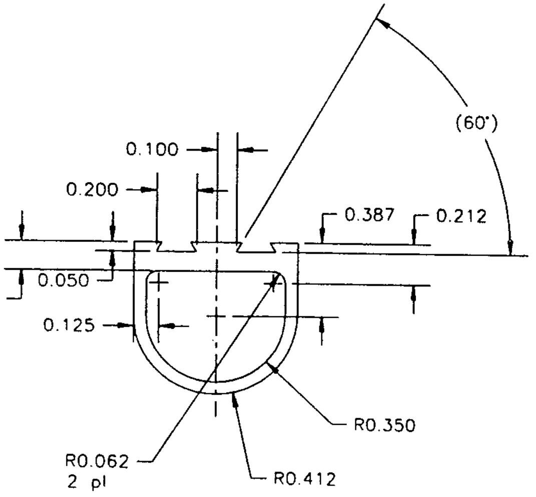

-3 Ring Detail

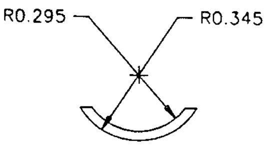

-5 Clamp Detail

⟨1⟩⟨2⟩

QTY REQD	ITEM NO.	PART NO.	DESCRIPTION	MAT'L/SPEC
1	5	XXX	XXX	---
1	4	XXX	XXX	---
1	3	SSAS-256-3	#2-56 x 3/16 set screw	---
1	2	BE000269-5	Adjustment Clamp	---
1	1	BE000269-3	Ring	---
1	---	BE000269	RING ASSEMBLY	---

PARTS LIST

② Fasteners of comparable spec's acceptable.
① Small Parts Inc., Miami Lakes, FL 1-800-220-4242

tra

TITLE: Ring Mount - DIP; Exoskeleton
SCALE: 2:1
DATE: 25 Aug 95
No. BE000269
DRAWN BY: A. P. Hilton
RELEASE DATE: 25 Aug 95
PROJECT: Actuator II
FILE NAME: BE00269.dwg
APPROVAL:
C

Unless otherwise specified:
Dimensions are in inches
Tolerances on angles ± 0° 30'
Decimals .XX ± .03, .XXX ± .005

Rev A
Matl: Delrin
Heat Treat:

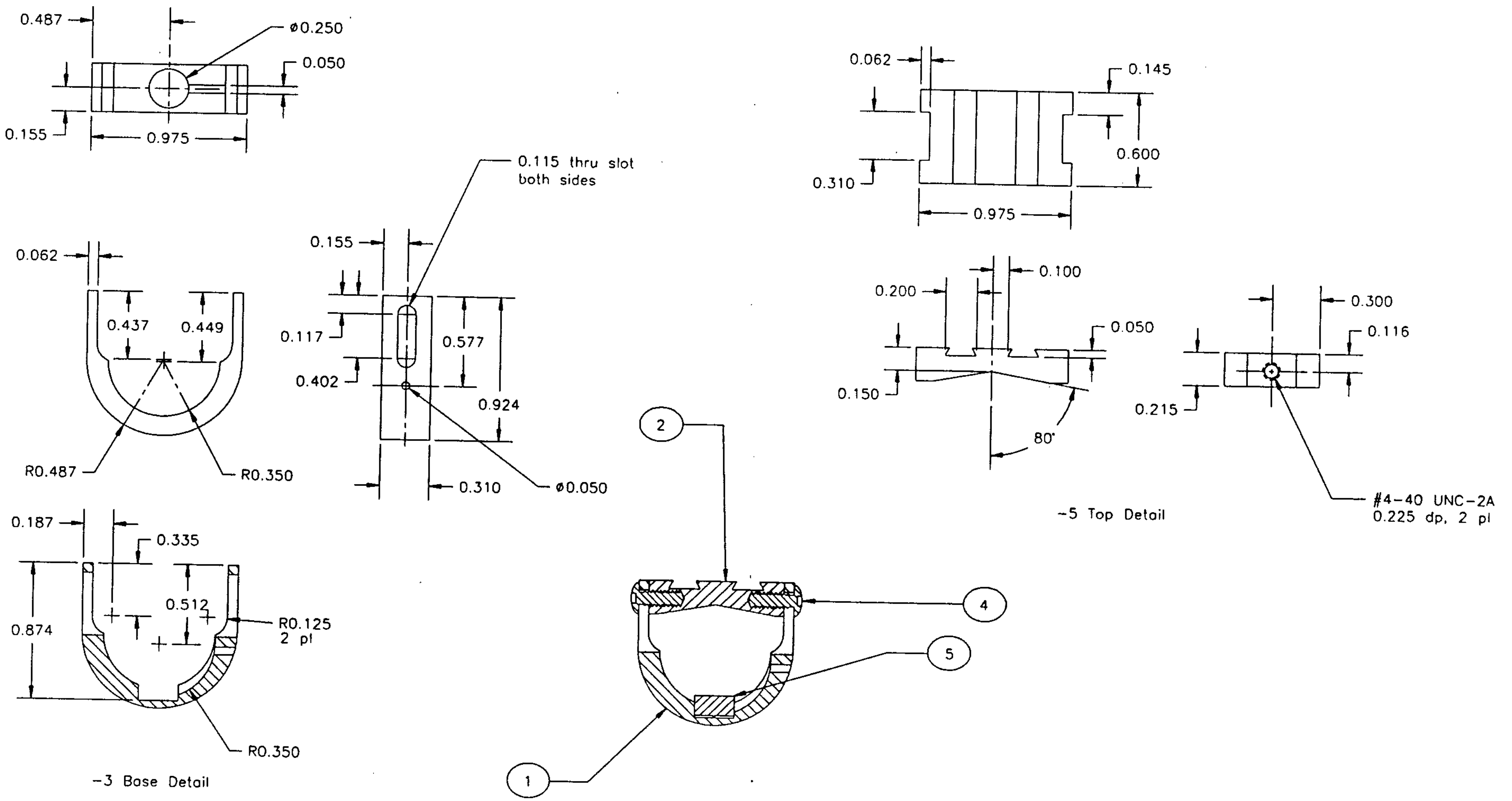

-3 Base Detail

-1 Assembly

-5 Top Detail

③ AL Design, Inc., 1411 Military Rd, Buffalo, NY 716-875-6240
② Fasteners of comparable spec's acceptable.
① ABABA Bolt Inc., El Cajon, CA (619) 440-1781

QTY REQD	ITEM NO.	PART NO.	DESCRIPTION	MAT'L/SPEC
1	5	ALD-MICRO ③	1/4D x 1/8, 10# ld cell	---
2	4	4C25KBCY ①②	#4-40 x 1/4 Btn Soc Cap	SS
1	3	XXX	XXX	---
1	2	BE000269-5	Ring Top	Delrin
1	1	BE000269-3	Ring Base	Delrin
1	---	BE000269	RING ASSEMBLY	---

PARTS LIST

tra

TITLE: Ring Mount - MIP; Exoskeleton			
SCALE: 2:1	DATE: 22 Aug 95	No. BE000269	
DRAWN BY: A. P. Hilton		RELEASE DATE: 17 Oct 95	
PROJECT: Actuator II		APPROVAL:	C
FILE NAME: BE00269d.dwg			

Unless otherwise specified:
Dimensions are in inches
Tolerances on angles ± 0° 30'
Decimals .XX ± .03, .XXX ± .005

Rev D
Matl: Delrin
Heat Treat: N/A

NO.	REVISION	DATE	BY
D	width and dia of ring	17 Oct 95	APH
C	two piece adjustable, load cell mount	14 Sep 95	APH
B	height, clamp pos, load cell mnt, strain relief	25 Aug 95	APH

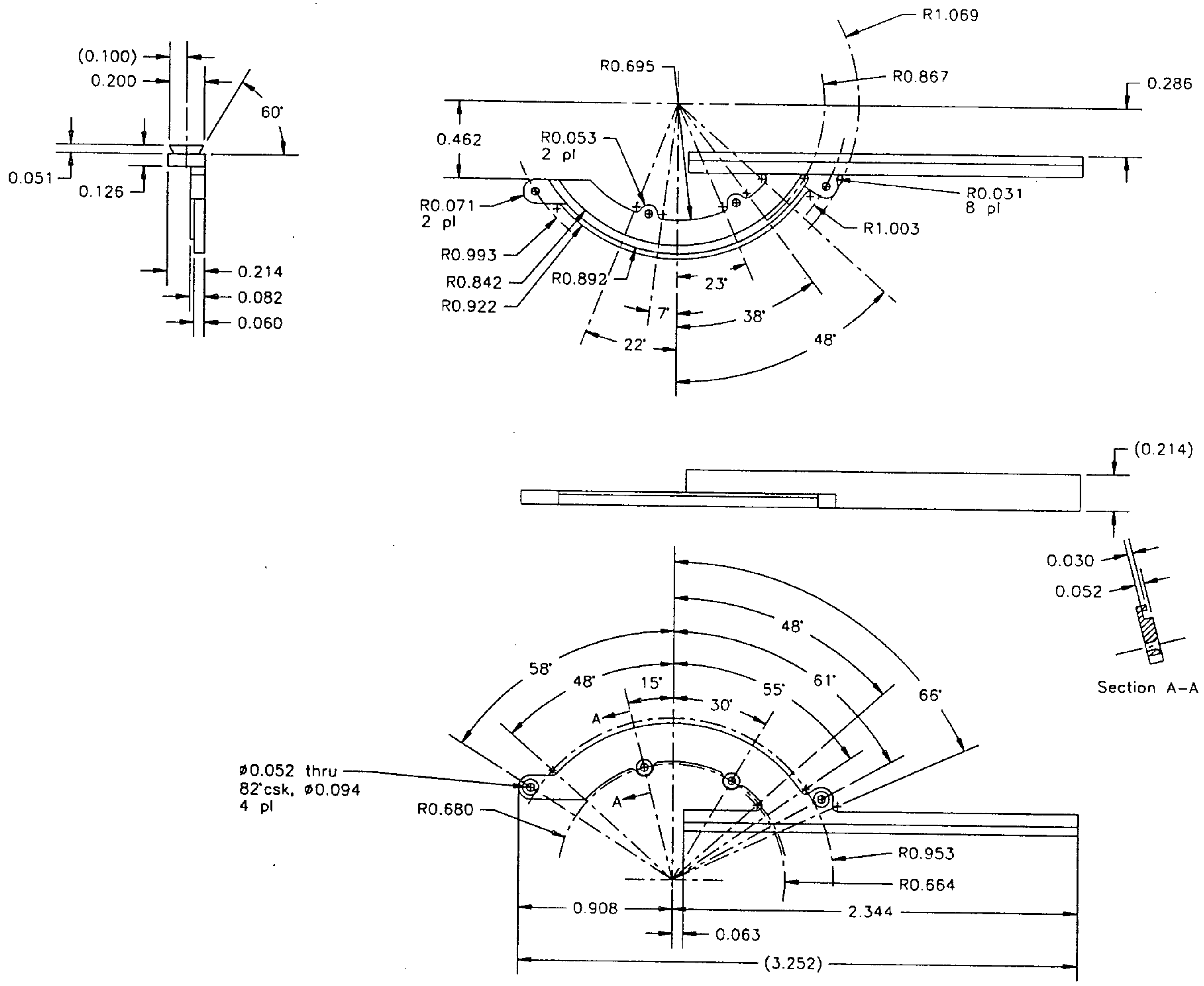

Unless otherwise specified: Dimensions are in inches Tolerances on angles ± 0° 30' Decimals .XX ± .03, .XXX ± .005	Rev A Matl: Delrin Heat Treat:

tra

TITLE: Base; SVJ (sliding virtual joint)
SCALE: 2:1
DATE: 31 Aug 95
No. BE000270
DRAWN BY: A. P. Hilton
RELEASE DATE: 6 Sep 95
PROJECT: Actuator II
APPROVAL:
FILE NAME: BE00270.dwg
C

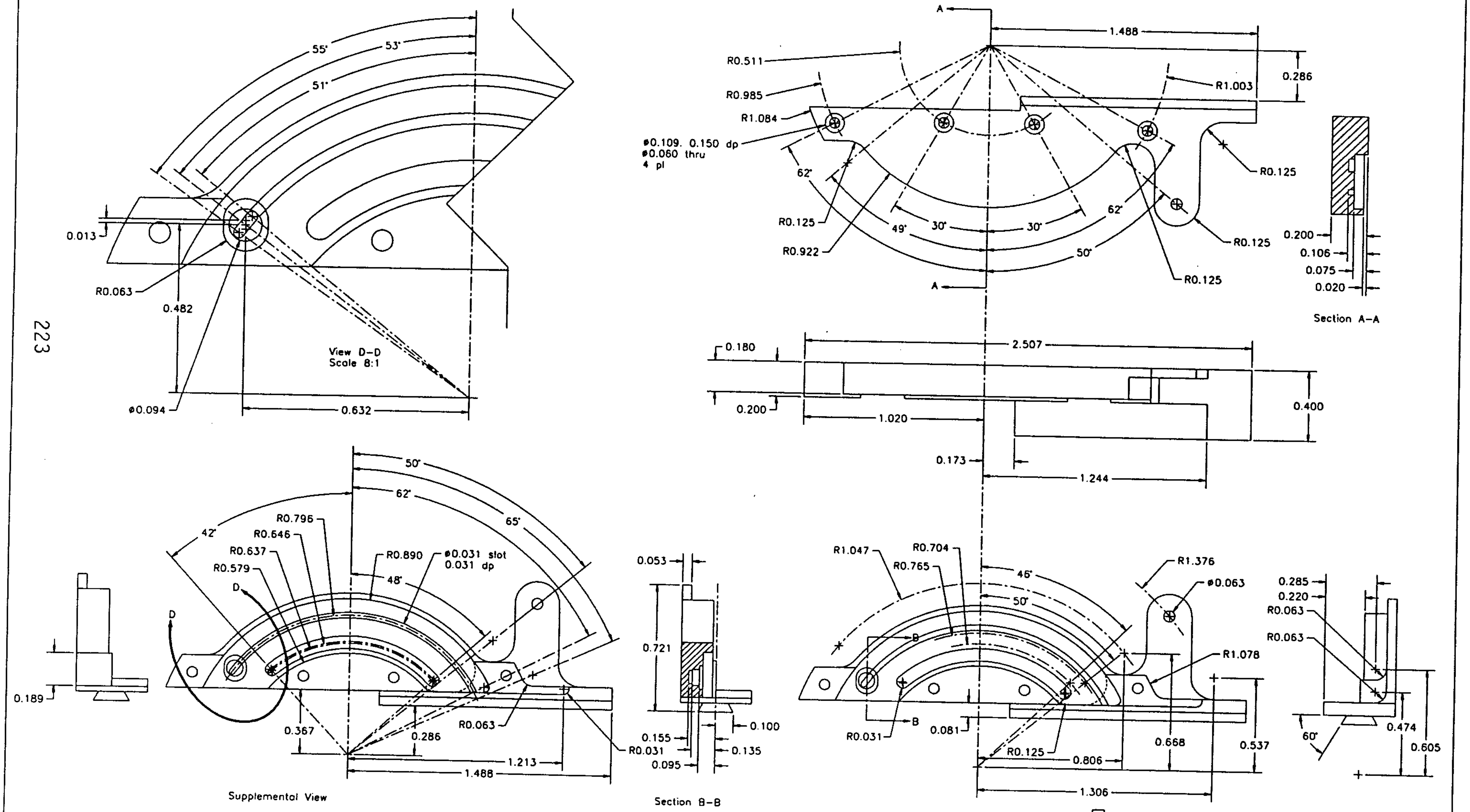

tra

TITLE: Base; SVJ (Sliding Virtual Joint)
SCALE: 4:1
DATE: 31 Aug 95
No. BE000270
DRAWN BY: A. P. Hilton
RELEASE DATE: 29 Sep 95
PROJECT: Actuator II
FILE NAME: BE00270c.dwg
APPROVAL:
DE
Rev C
Mat'l: Delrin
Heat Treat:

Unless otherwise specified:
Dimensions are in inches
Tolerances on angles ± 0° 30'
Decimals .XX ± .03, .XXX ± .005

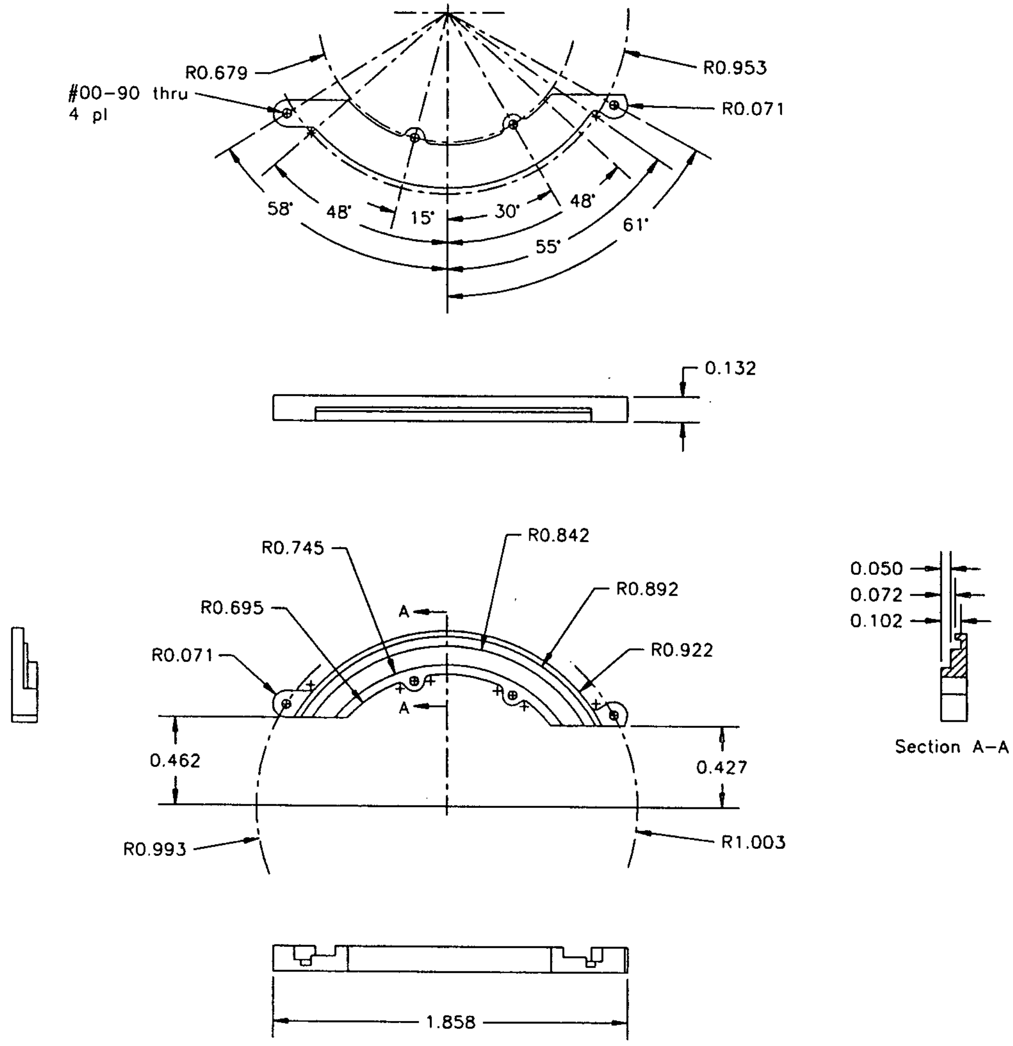

tra

Unless otherwise specified: Dimensions are in inches	Rev A	TITLE: Clamp; SVJ (sliding virtual joint)	
Tolerances on angles ± 0° 30' Decimals .XX ± .03, .XXX ± .005	Matl: Delrin	SCALE: 2:1 / DATE: 31 Aug 95	No. BE000271
	Heat Treat:	DRAWN BY: A. P. Hilton	RELEASE DATE: 5 Sep 95
		PROJECT: Actuator II	APPROVAL:
		FILE NAME: BE00271.dwg	C

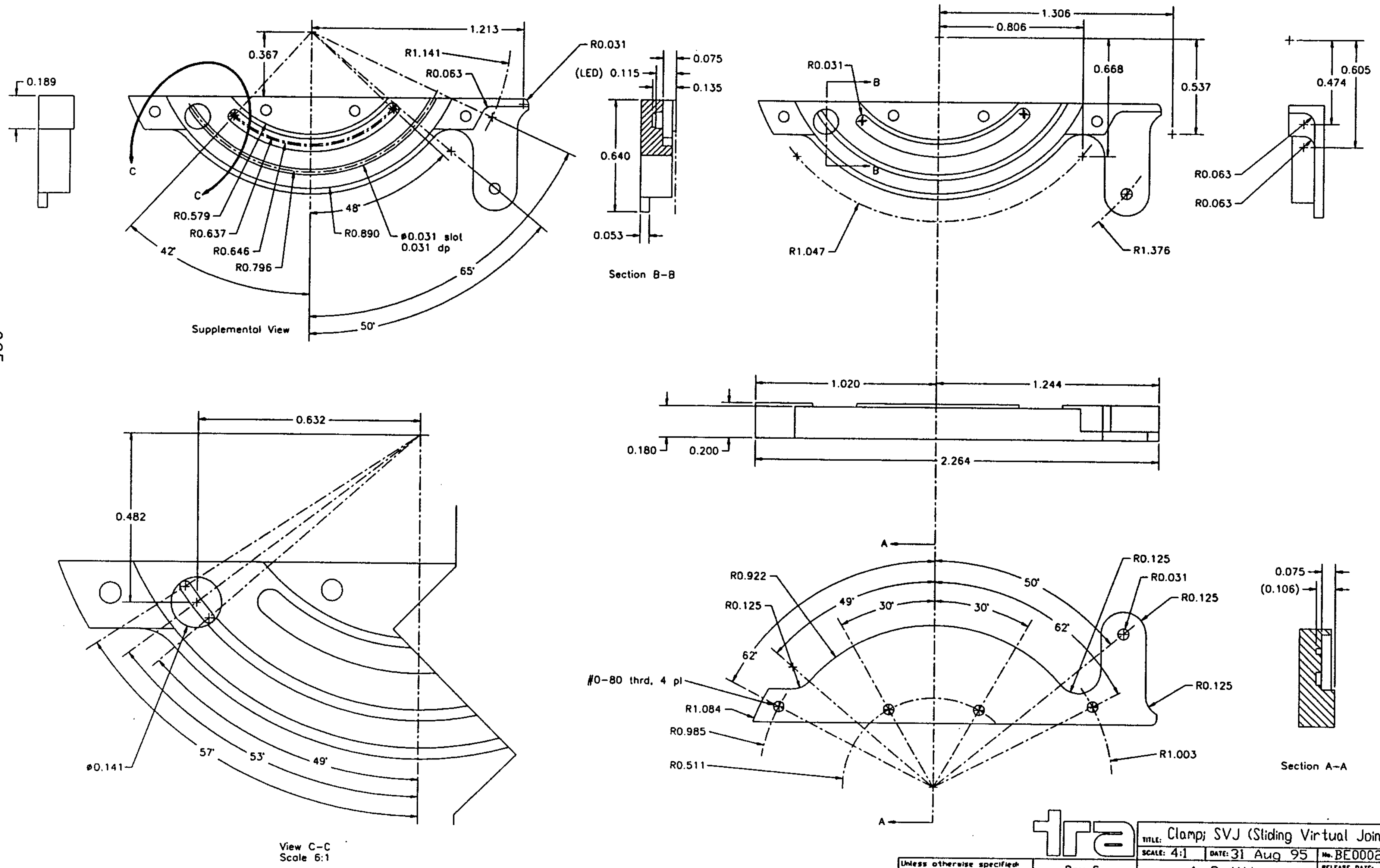

Unless otherwise specified:
Dimensions are in inches
Tolerances on angles ± 0° 30'
Decimals .XX ± .03, .XXX ± .005

		TITLE: Clamp; SVJ (Sliding Virtual Joint)	
		SCALE: 4:1 / DATE: 31 Aug 95	No. BE000271
	Rev C	DRAWN BY: A. P. Hilton	RELEASE DATE: 2 Oct 95
	Matl: Delrin	PROJECT: Actuator II	APPROVAL: DE
	Heat Treat:	FILE NAME: BE00271c.dwg	

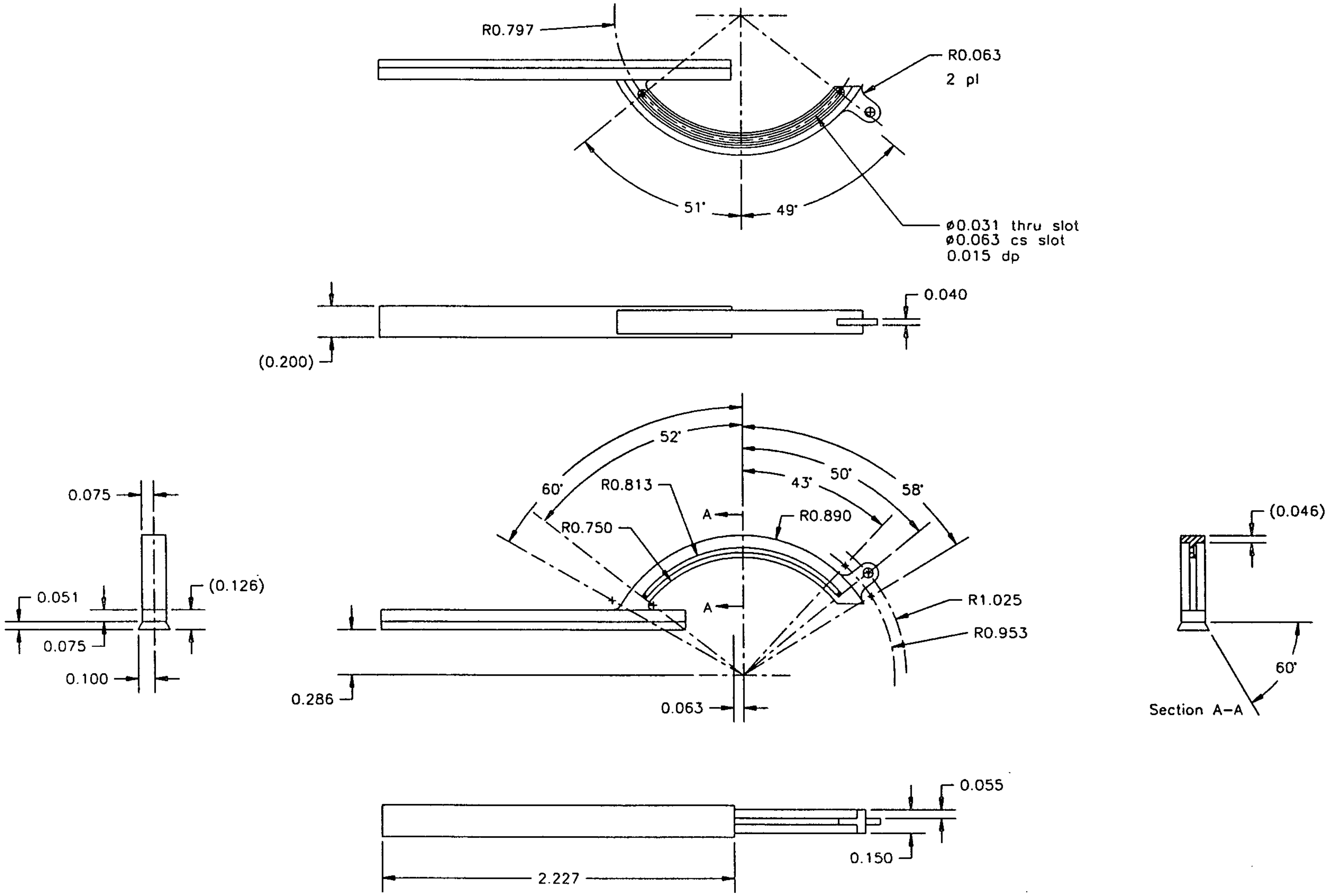

Unless otherwise specified: Dimensions are in inches Tolerances on angles ± 0° 30' Decimals .XX ± .03, .XXX ± .005	Rev A	TITLE: Male Insert; SVJ	
		SCALE: 2:1 DATE: 6 Sep 95	No. BE000272
		DRAWN BY: A. P. Hilton	RELEASE DATE: 7 Sep 95
	Matl: Delrin	PROJECT: Actuator II	APPROVAL:
	Heat Treat:	FILE NAME: BE00272.dwg	C

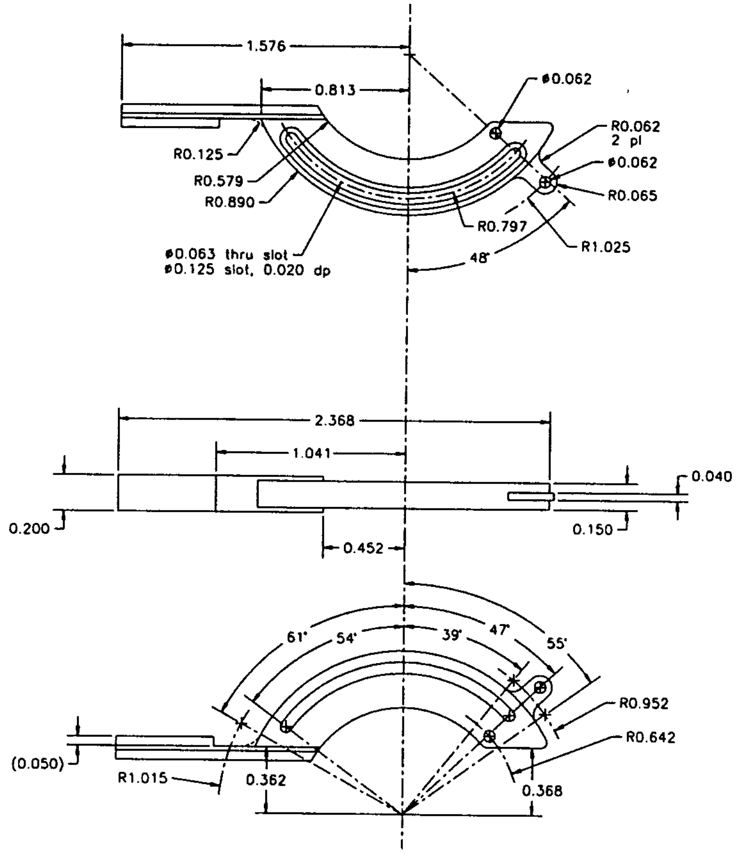

-3 Insert Detail

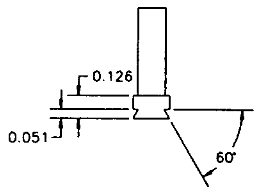

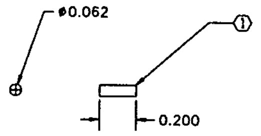

-5 Pin Detail

① Use Part #: DWX-1-4, Small Parts, Inc., Miami Lakes, FL

	tra	TITLE: Male Insert; SVJ	
Unless otherwise specified: Dimensions are in inches	Rev C	SCALE: 3:1 DATE: 6 Sep 95	No. BE000272
		DRAWN BY: A. P. Hilton	RELEASE DATE: 29 Sep 95
Tolerances on angles ± 0° 30' Decimals .XX ± .03, .XXX ± .005	Mat'l: Alum 7075-T6	PROJECT: Actuator II	APPROVAL:
	Heat Treat:	FILE NAME: BE00272c.dwg	D

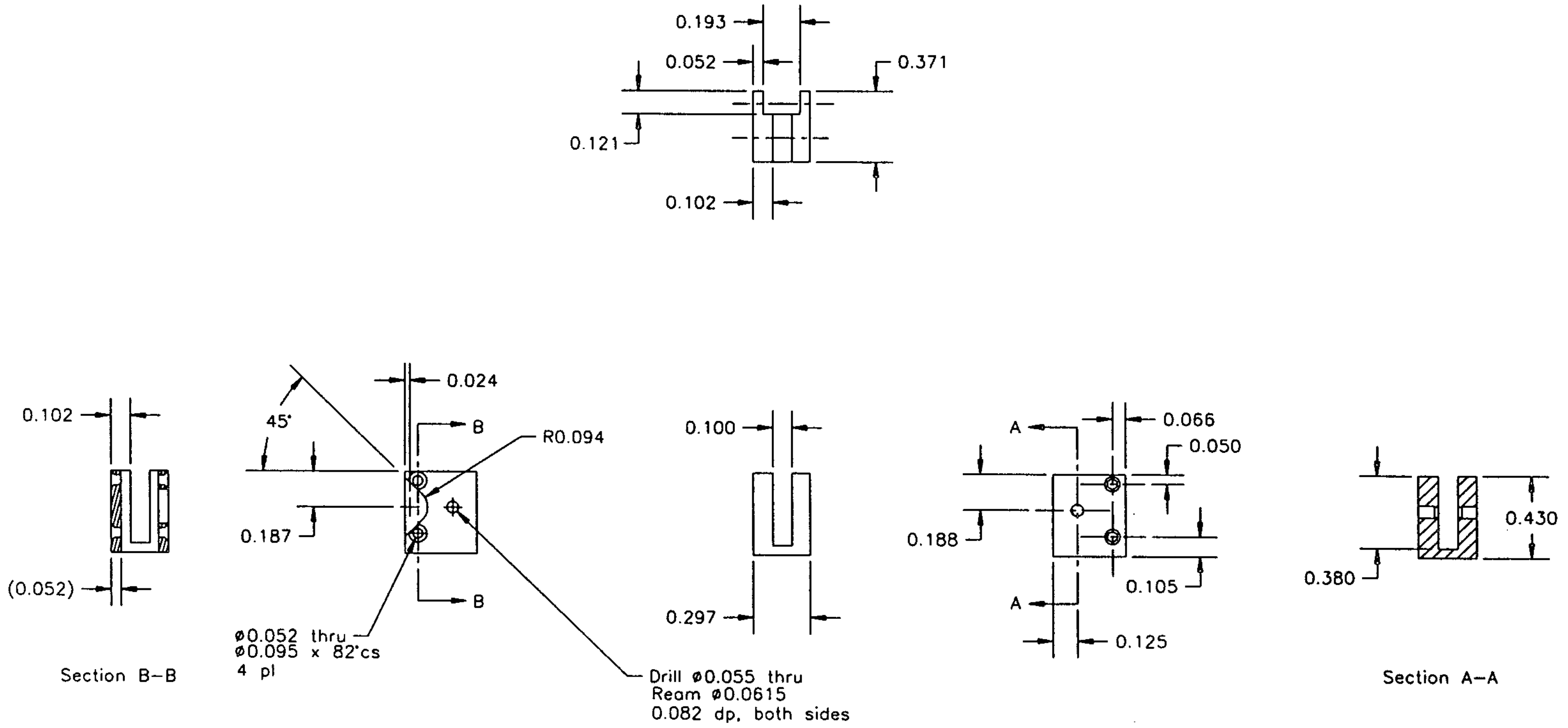

		TITLE: U-Clip; Motor Mount	
		SCALE: 2:1 | DATE: 22 Sep 95	No. BE000273
Unless otherwise specified: Dimensions are in inches	Rev A	DRAWN BY: A. P. Hilton	RELEASE DATE: 3 Oct 95
Tolerances on angles ± 0° 30' Decimals .XX ± .03, .XXX ± .005	Matl: 2011-T8 Alum Heat Treat:	PROJECT: Actuator II FILE NAME: BE00273.dwg	APPROVAL: C

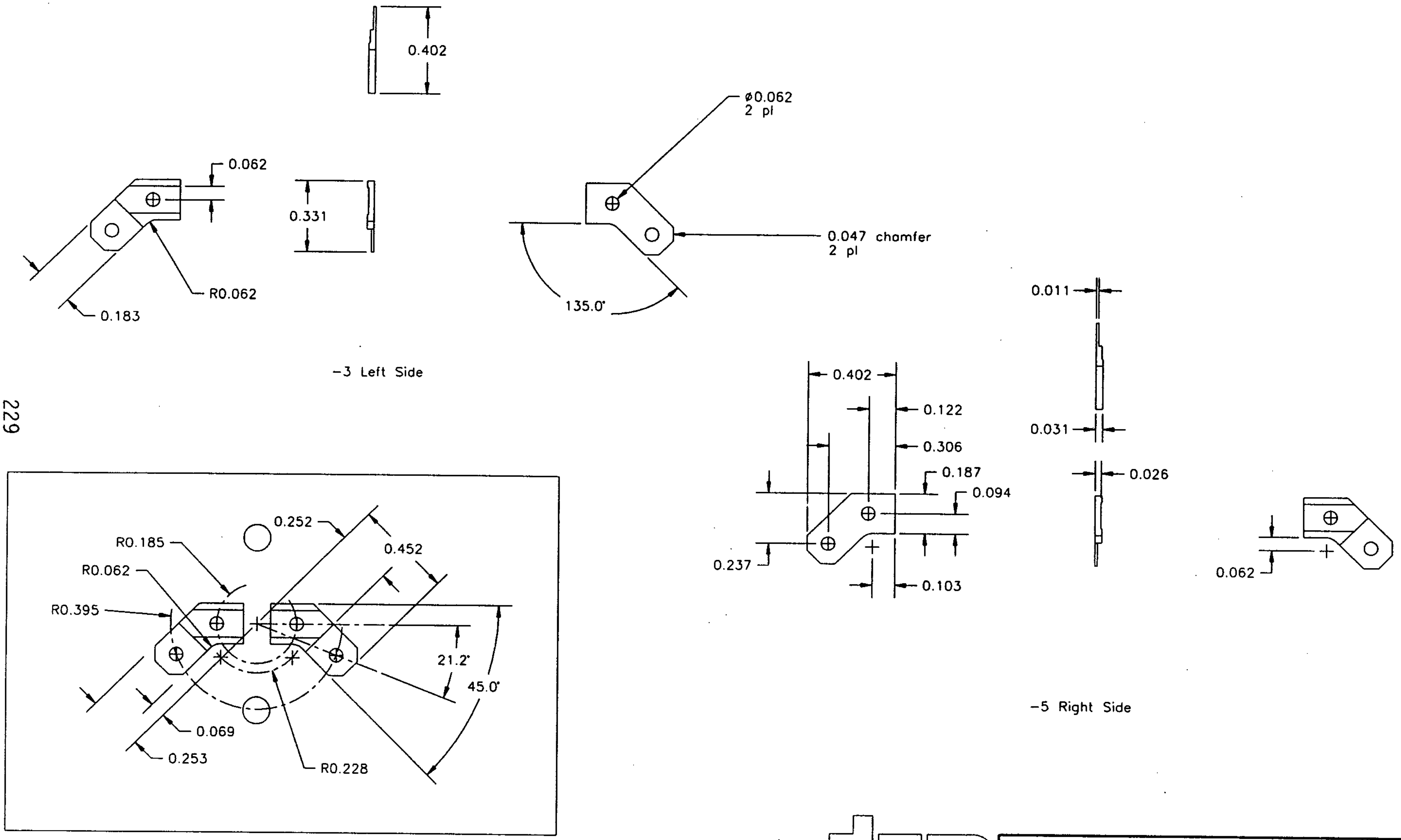

tra

		TITLE: Ribbon Clip	
		SCALE: 3:1 DATE: 25 Sep 95	No. BE000274
Unless otherwise specified: Dimensions are in inches	Rev A	DRAWN BY: A. P. Hilton	RELEASE DATE: 28 Sep 95
Tolerances on angles ± 0° 30' Decimals .XX ± .03, .XXX ± .001	Matl: 0.031 SS shim Heat Treat:	PROJECT: Actuator II FILE NAME: BE00274.dwg	APPROVAL: C

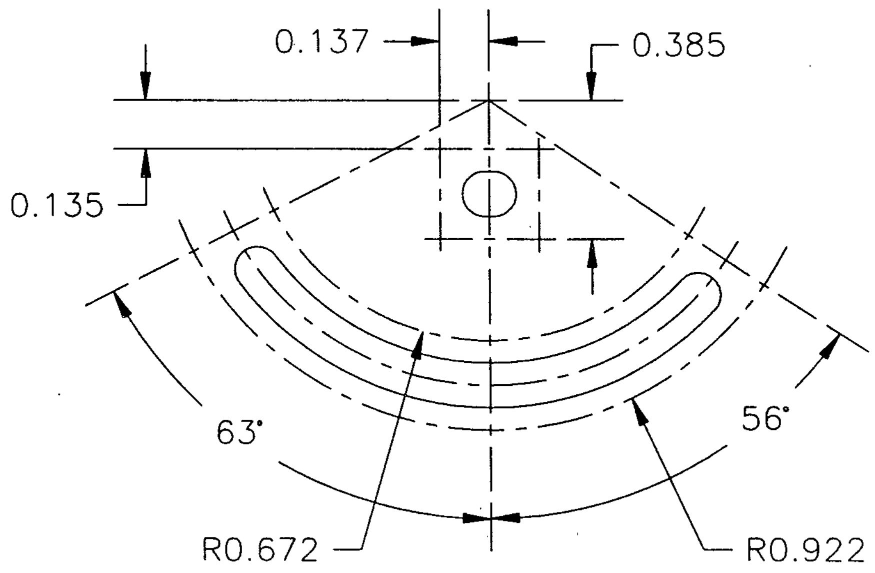

Use 0.125 end mill

Unless otherwise specified: Dimensions are in inches	Rev A	TITLE: Polaroid Film Sections; Angle Sensor	
		SCALE: 2:1 / DATE: 2 Oct 95	No. BE000276
		DRAWN BY: A. P. Hilton	RELEASE DATE: 2 Oct 95
Tolerances on angles ± 0° 30' Decimals .XX ± .03, .XXX ± .005	Matl: Heat Treat:	PROJECT: Actuator II FILE NAME: be00276.dwg	APPROVAL: A

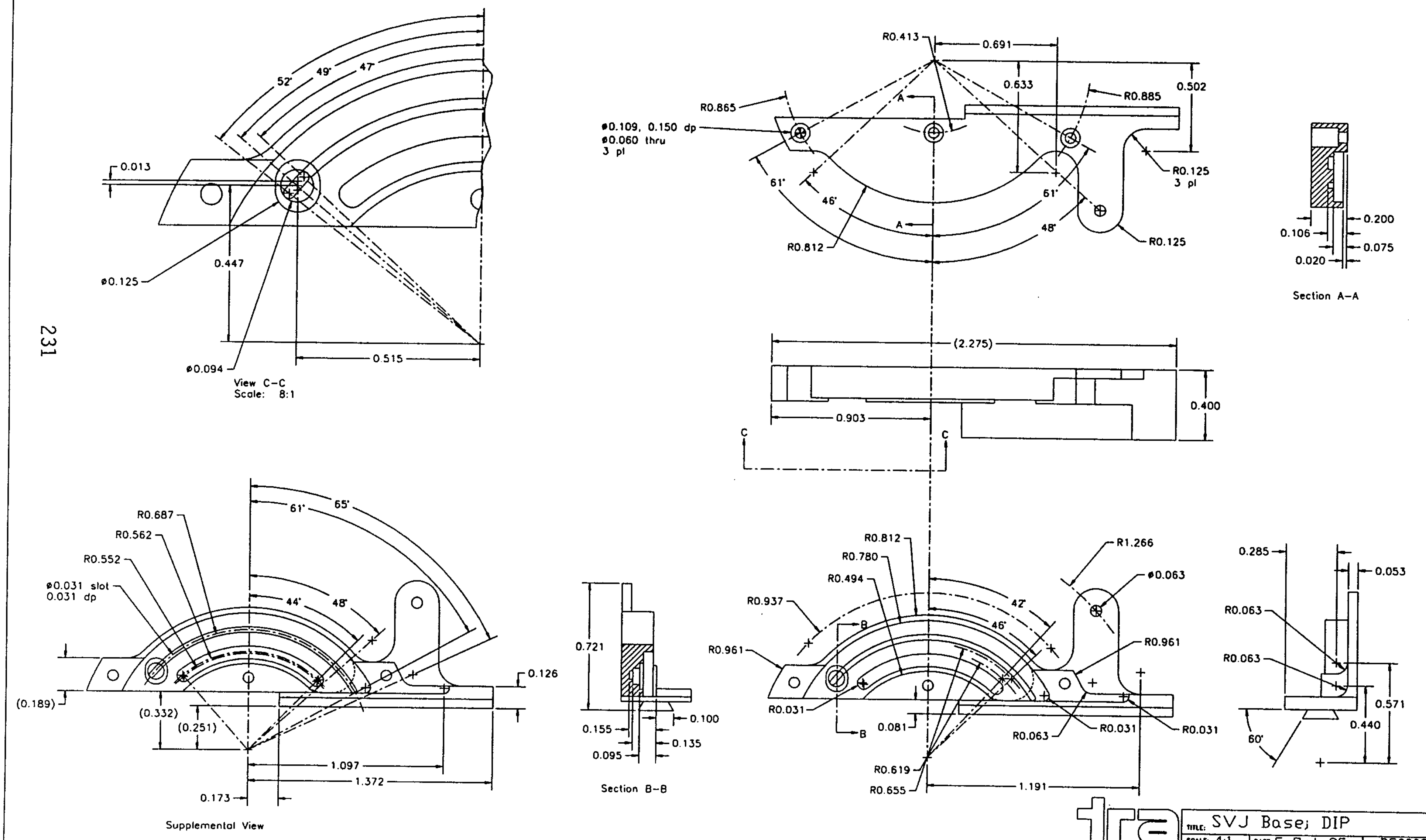

		TITLE: SVJ Base; DIP	
		SCALE: 4:1 DATE: 5 Oct 95	No. BE000277
Unless otherwise specified: Dimensions are in inches	Rev A	DRAWN BY: A. P. Hilton	RELEASE DATE: 5 Oct 95
Tolerances on angles ± 0° 30' Decimals .XX ± .03, .XXX ± .005	Matl: Delrin Heat Treat:	PROJECT: Actuator II FILE NAME: BE00277.dwg	APPROVAL: DE

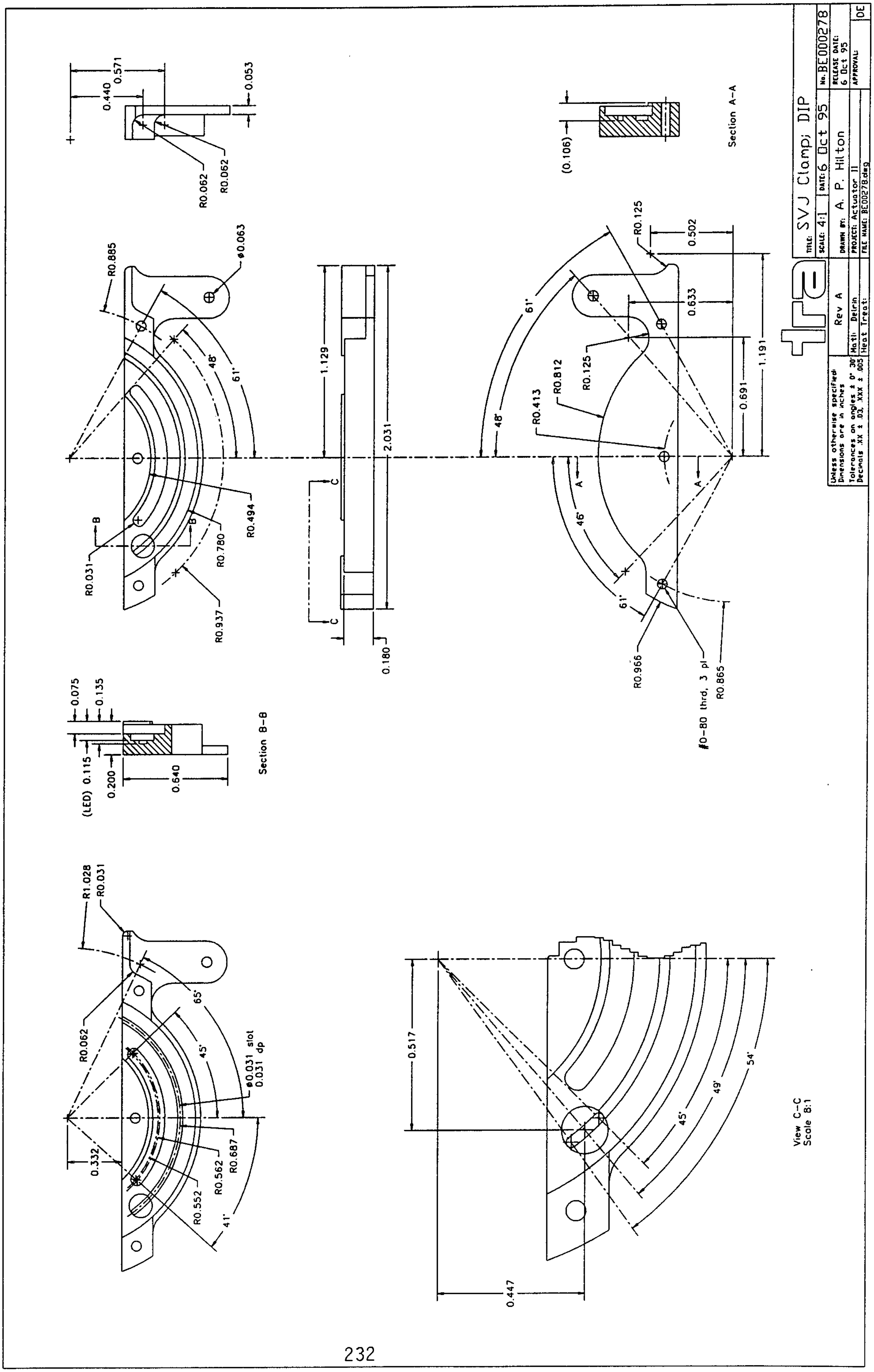
TITLE: SVJ Clamp; DIP
No. BE000278
SCALE: 4:1
DATE: 6 Oct 95
DRAWN BY: A. P. Hilton
PROJECT: Actuator II
FILE NAME: BE00278.dwg
RELEASE DATE: 6 Oct 95
APPROVAL:
DE
Rev A
Mat'l: Delrin
Heat Treat:
Unless otherwise specified: Dimensions are in inches
Tolerances on angles ± 0° 30'
Decimals .XX ± .03, .XXX ± .005
0.440
0.571
0.053
R0.062
R0.062
(0.106)
Section A-A
R0.885
⌀0.063
48°
61°
R0.494
R0.780
R0.031
R0.937
B
B
1.129
2.031
0.180
C
C
R0.125
0.502
0.633
1.191
0.691
61°
48°
R0.413
R0.812
R0.125
A
A
46°
61°
R0.966
#0-80 thrd, 3 pl
R0.865
0.075
0.135
(LED) 0.115
0.200
0.640
Section B-B
R1.028
R0.031
R0.062
65°
45°
⌀0.031 slot 0.031 dp
0.332
R0.552
R0.562
R0.687
41°
0.517
0.447
45°
49°
54°
View C-C
Scale 8:1

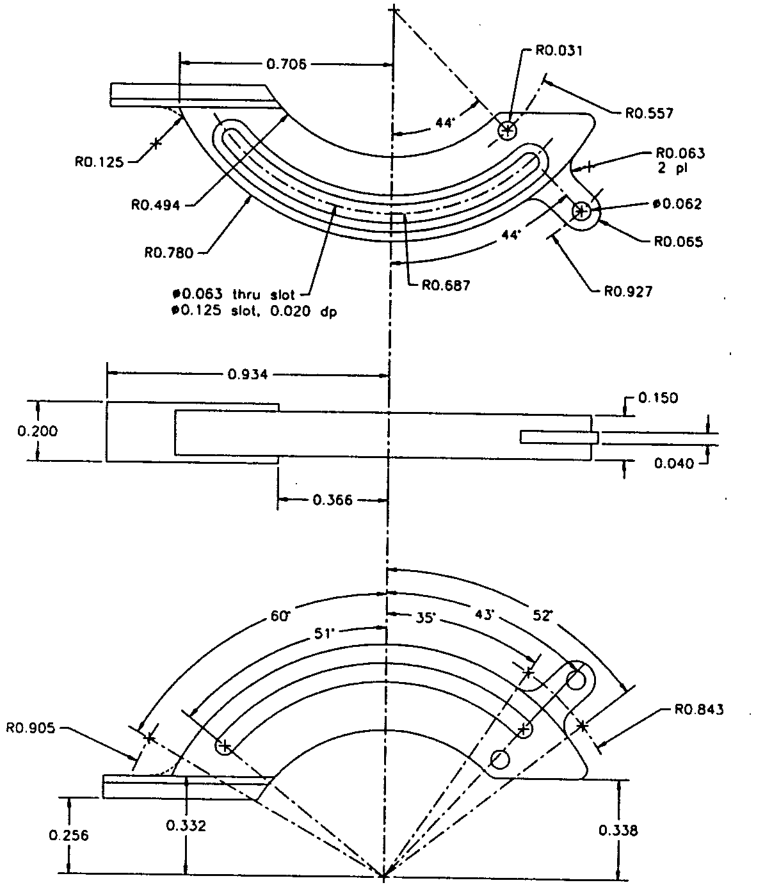

−3 Insert Detail

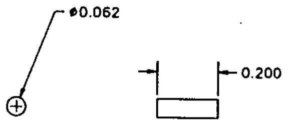

−5 Pin Detail

tra

TITLE: SVJ Male Insert, DIP
SCALE: 5:1
DATE: 6 Oct 95
No. BE000279
Unless otherwise specified:
Dimensions are in inches
Tolerances on angles ± 0° 30'
Decimals .XX ± .03, .XXX ± .005
Rev A
DRAWN BY: A. P. Hilton
RELEASE DATE: 6 Oct 95
Matl: Alum 7075-T6
PROJECT: Actuator II
APPROVAL:
DE
Heat Treat:
FILE NAME: BE00279.dwg

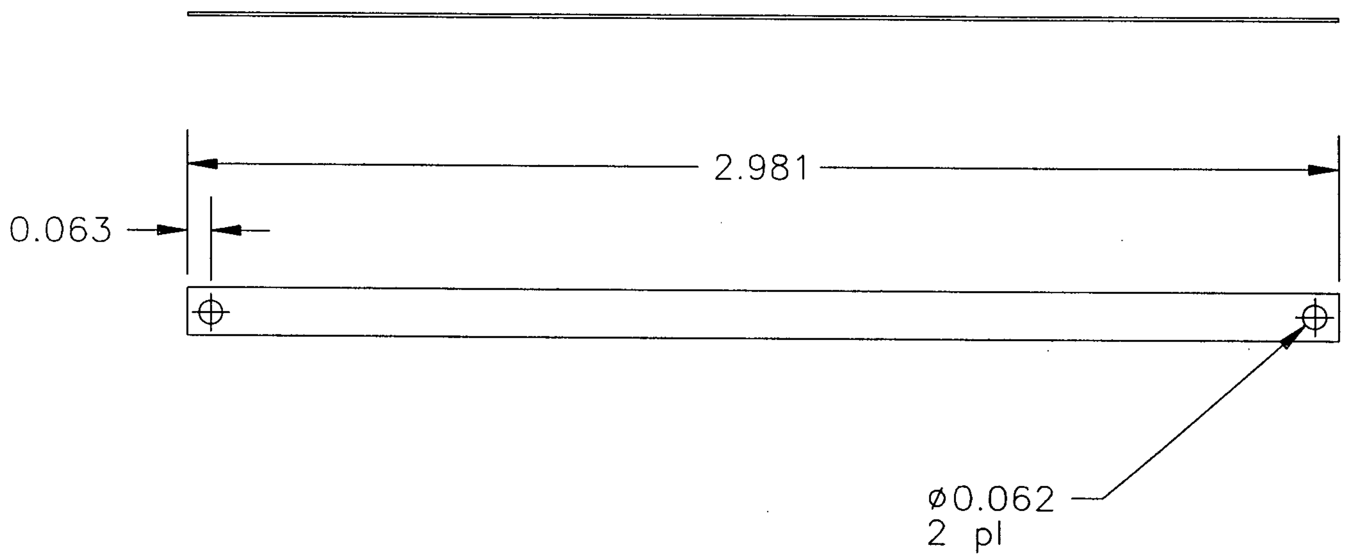

1 Use Starrett thickness gage gaps (0.009 x 0.125 x 6) as stock.

tra

TITLE: RIBBON-MIP; LINEAR MOTOR
SCALE: 2:1
DATE: 6 Oct 95
No. BE000280
Unless otherwise specified:
Dimensions are in inches
Tolerances on angles ± 0° 30'
Decimals .XX ± .03, .XXX ± .005
Rev A
DRAWN BY: A. P. Hilton
RELEASE DATE: 6 Oct 95
Matl:
PROJECT: Actuator II
APPROVAL:
Heat Treat:
FILE NAME: be00280.dwg
A

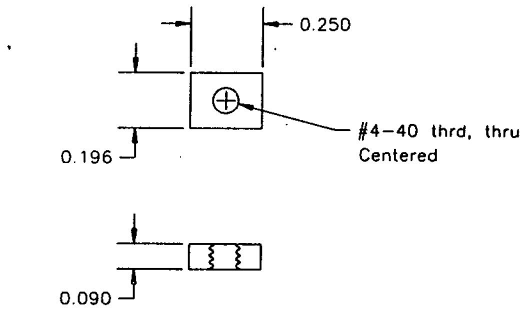

-7 Nut
Alum

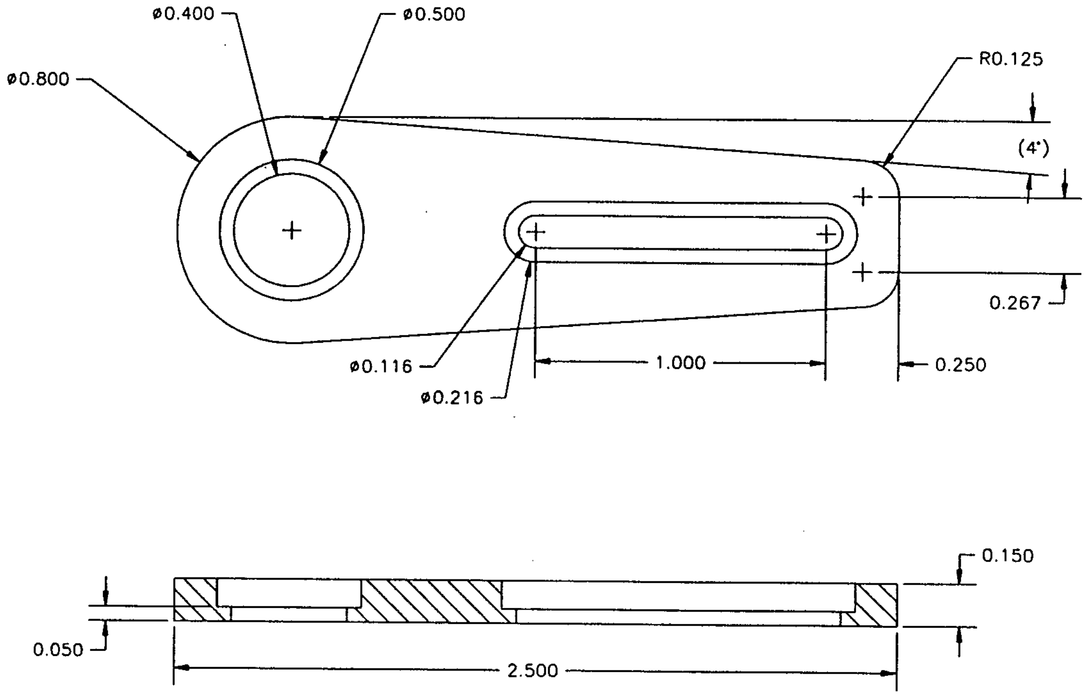

-3 PIP Joint
Alum

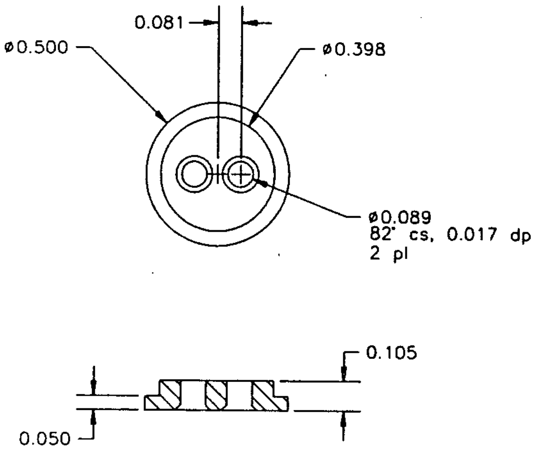

-5 Joint Center
Delrin

tra

		TITLE: PIP JOINT	
		SCALE: 3:1 DATE: 11 Oct 95	No. BE000281
Unless otherwise specified: Dimensions are in inches	Rev A	DRAWN BY: A. P. Hilton	RELEASE DATE: 12 Oct 95
Tolerances on angles ± 0° 30' Decimals .XX ± .03, .XXX ± .005	Matl: (noted)	PROJECT: Actuator II	APPROVAL: C
	Heat Treat:	FILE NAME: BE00281.dwg	

MOTIVE CELL

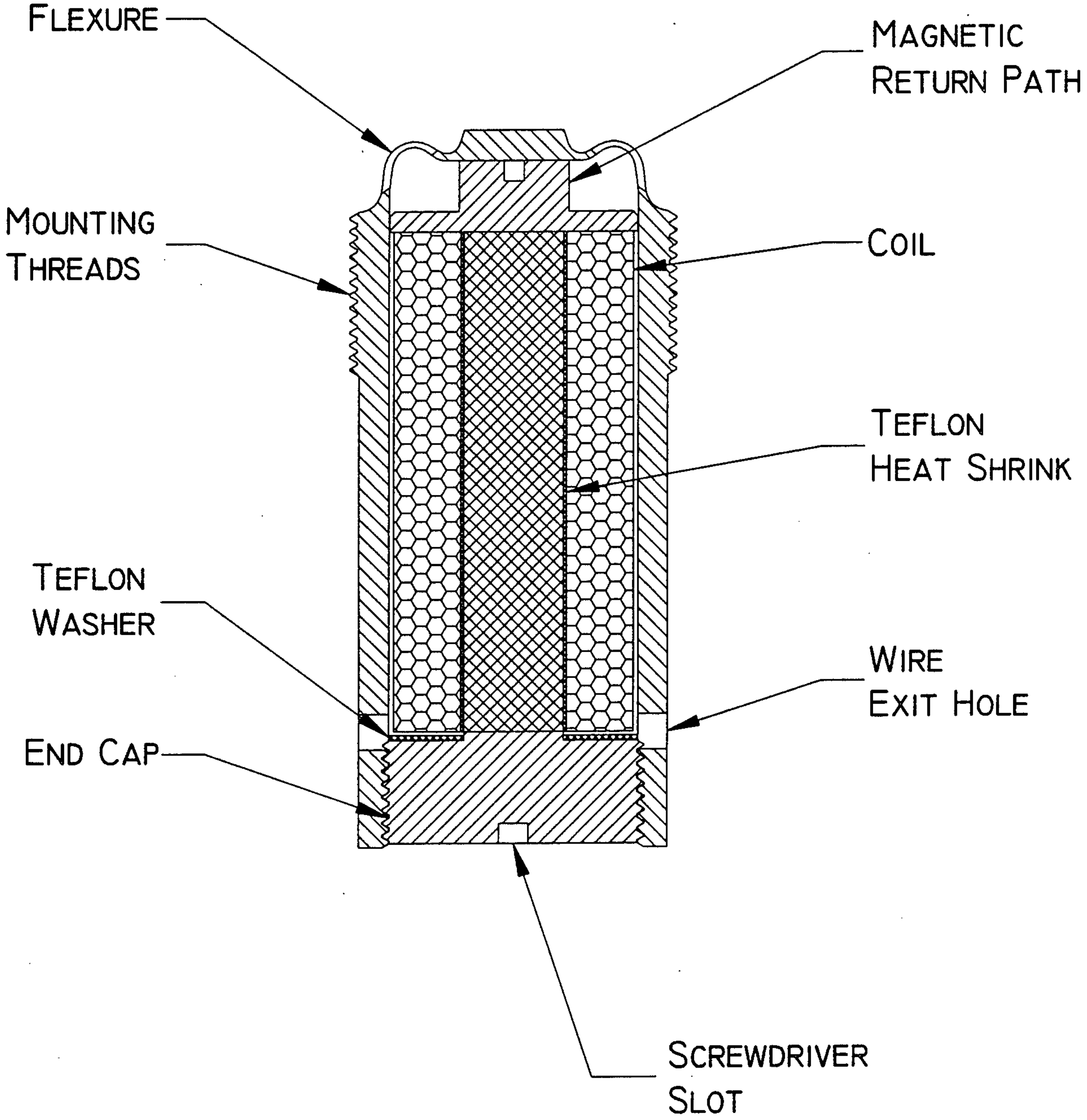
FLEXURE
MAGNETIC RETURN PATH
MOUNTING THREADS
COIL
TEFLON HEAT SHRINK
TEFLON WASHER
WIRE EXIT HOLE
END CAP
SCREWDRIVER SLOT

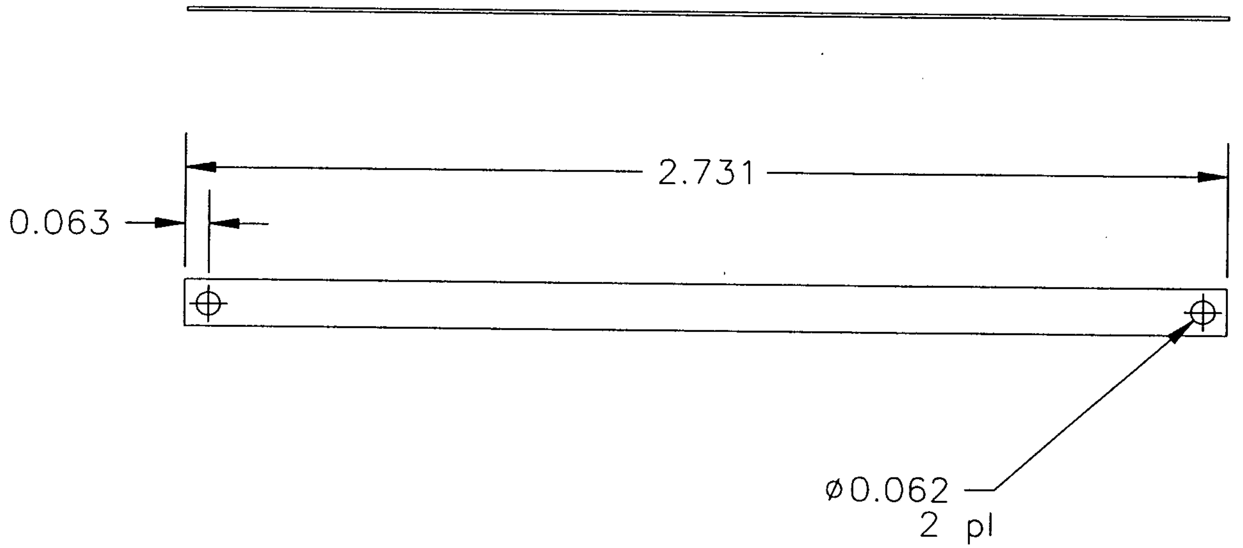

1 Use Starrett thickness gage gaps (0.009 x 0.125 x 6) as stock.

Unless otherwise specified:
Dimensions are in inches
Tolerances on angles ± 0° 30′
Decimals .XX ± .03, .XXX ± .005

Rev A

Matl:

Heat Treat:

TITLE: RIBBON-DIP; LINEAR MOTOR

SCALE: 2:1
DATE: 13 Oct 95
No. BE000282

DRAWN BY: A. P. Hilton

RELEASE DATE:
13 Oct 95

PROJECT: Actuator II

FILE NAME: be00282.dwg

APPROVAL:

A

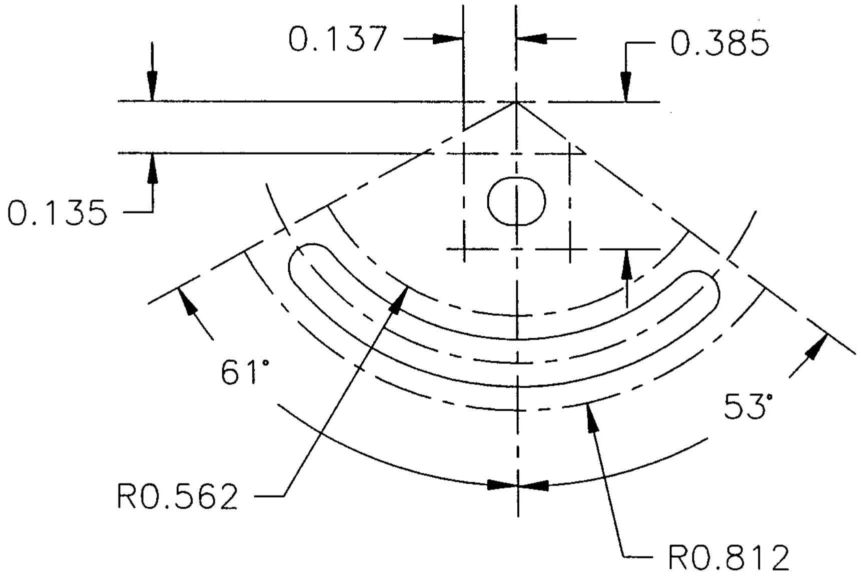

Use 0.125 end mill

tra

Unless otherwise specified: Dimensions are in inches Tolerances on angles ± 0° 30' Decimals .XX ± .03, .XXX ± .005	Rev A Matl: Heat Treat:	TITLE: Polaroid Film Sections; DIP SCALE: 2:1 DATE: 13 Oct 95 DRAWN BY: A. P. Hilton PROJECT: Actuator II FILE NAME: be00283.dwg	No. BE000283 RELEASE DATE: 13 Oct 95 APPROVAL: A

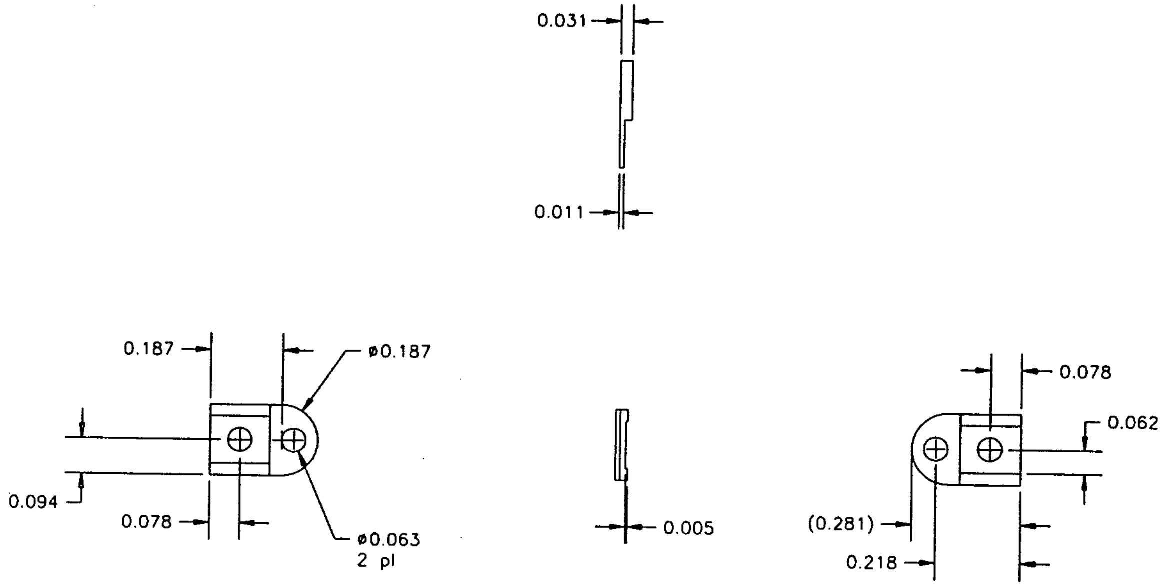

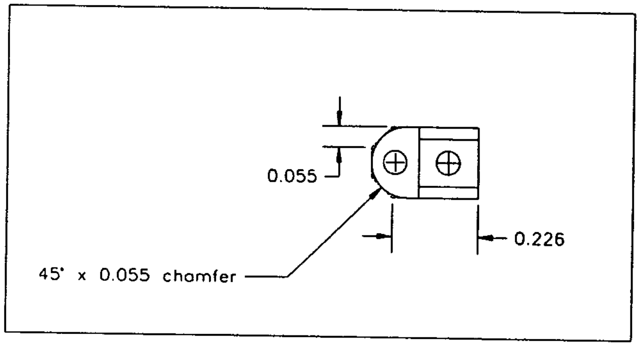

tra

TITLE: Ribbon Clip
SCALE: 4:1
DATE: 25 Sep 95
No. BE000274

Unless otherwise specified:
Dimensions are in inches
Tolerances on angles ± 0° 30'
Decimals .XX ± .03, .XXX ± .001

Rev C
Matl: 0.031 SS shim
Heat Treat:

DRAWN BY: A. P. Hilton
PROJECT: Actuator II
FILE NAME: BE00274c.dwg

RELEASE DATE:
24 Oct 95
APPROVAL:
C

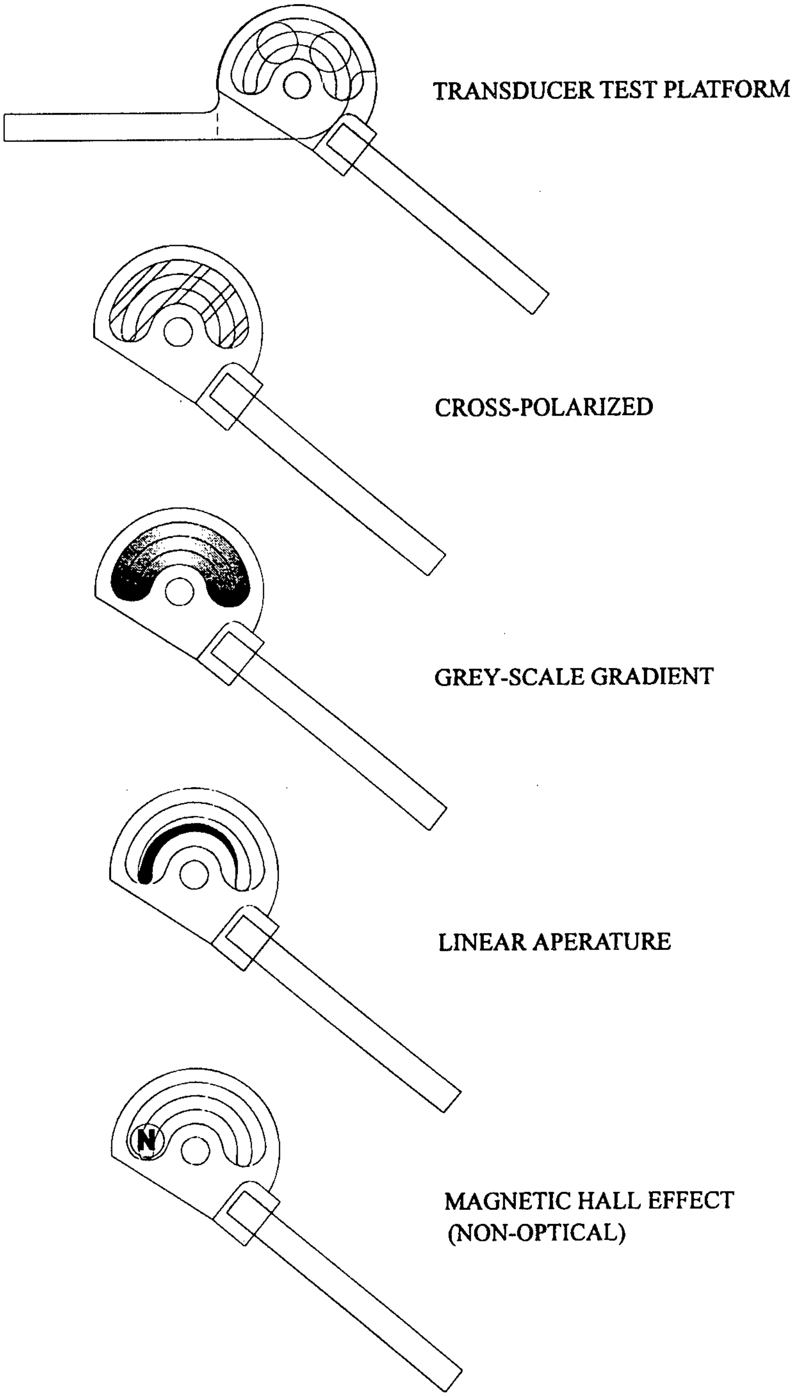

JOINT DISPLACEMENT TRANSDUCER OPTIONS

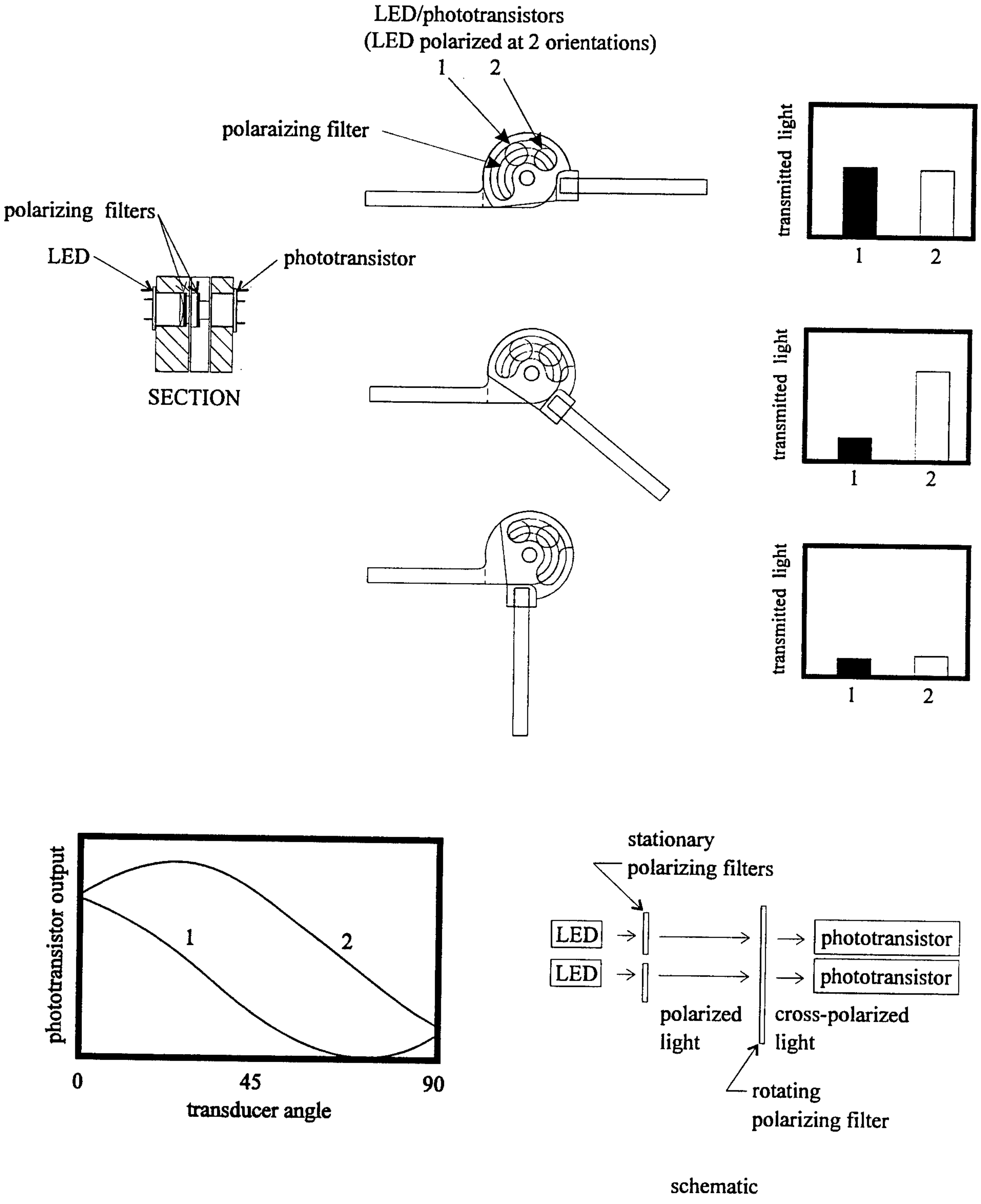

JOINT DISPLACEMENT TRANSDUCER TEST PLATFORM
PLOARIZED LIGHT CONFIGURATION

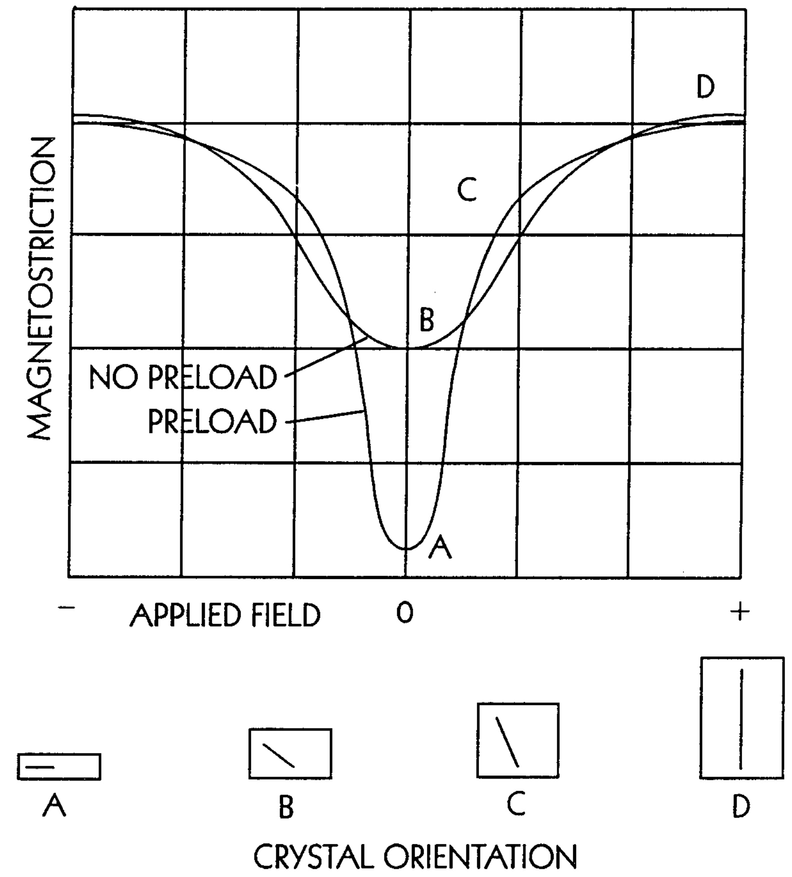
D
C
B
NO PRELOAD
PRELOAD
A
MAGNETOSTRICTION
−
APPLIED FIELD
0
+
A
B
C
D
CRYSTAL ORIENTATION

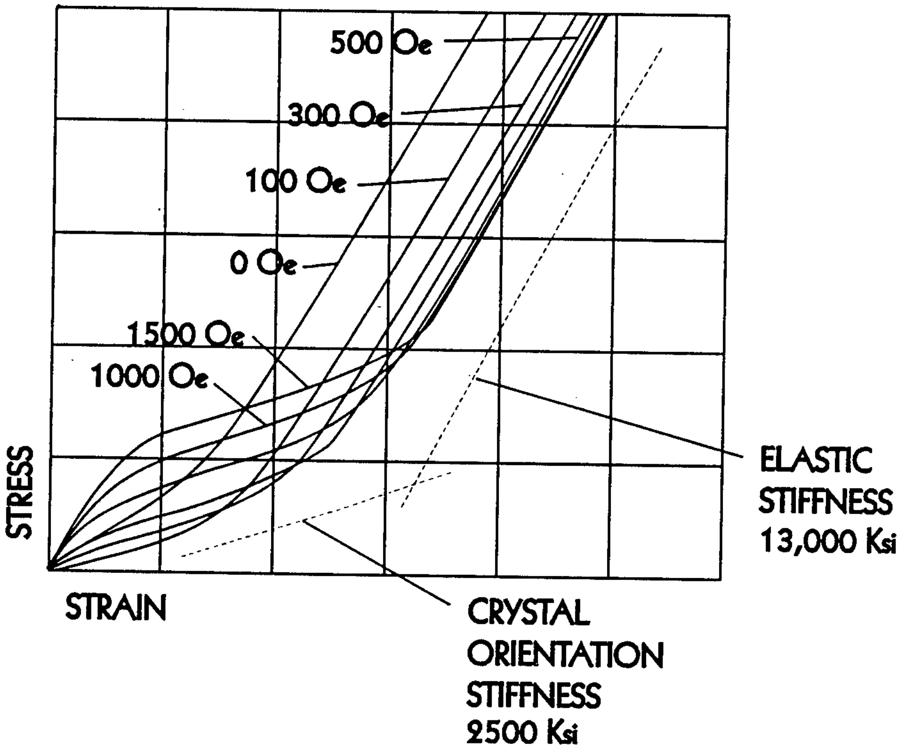
500 Oe
300 Oe
100 Oe
0 Oe
1500 Oe
1000 Oe
STRESS
STRAIN
ELASTIC STIFFNESS 13,000 Ksi
CRYSTAL ORIENTATION STIFFNESS 2500 Ksi

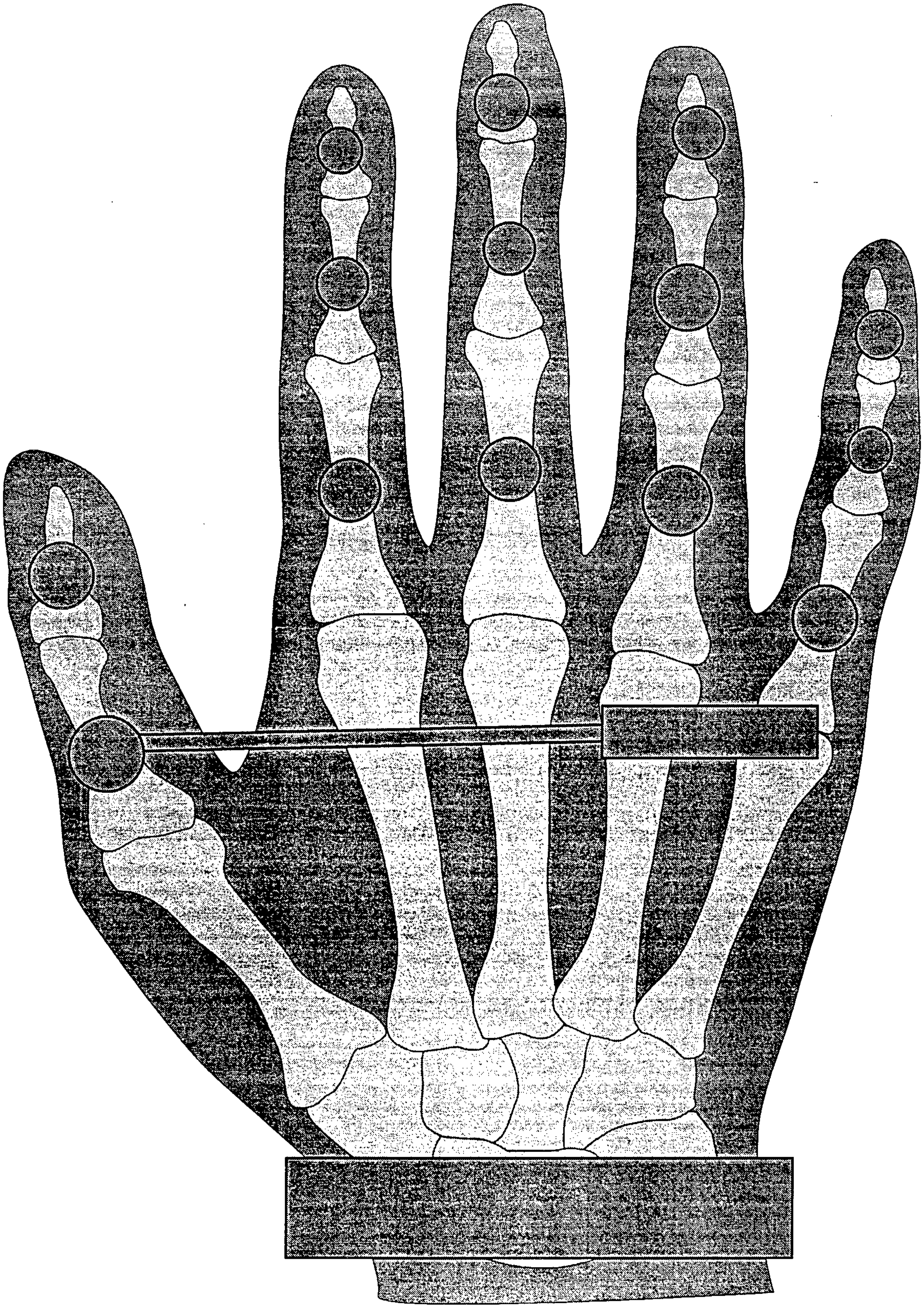

Average Digit Lengths

Digits I and II

Dimensions in mm

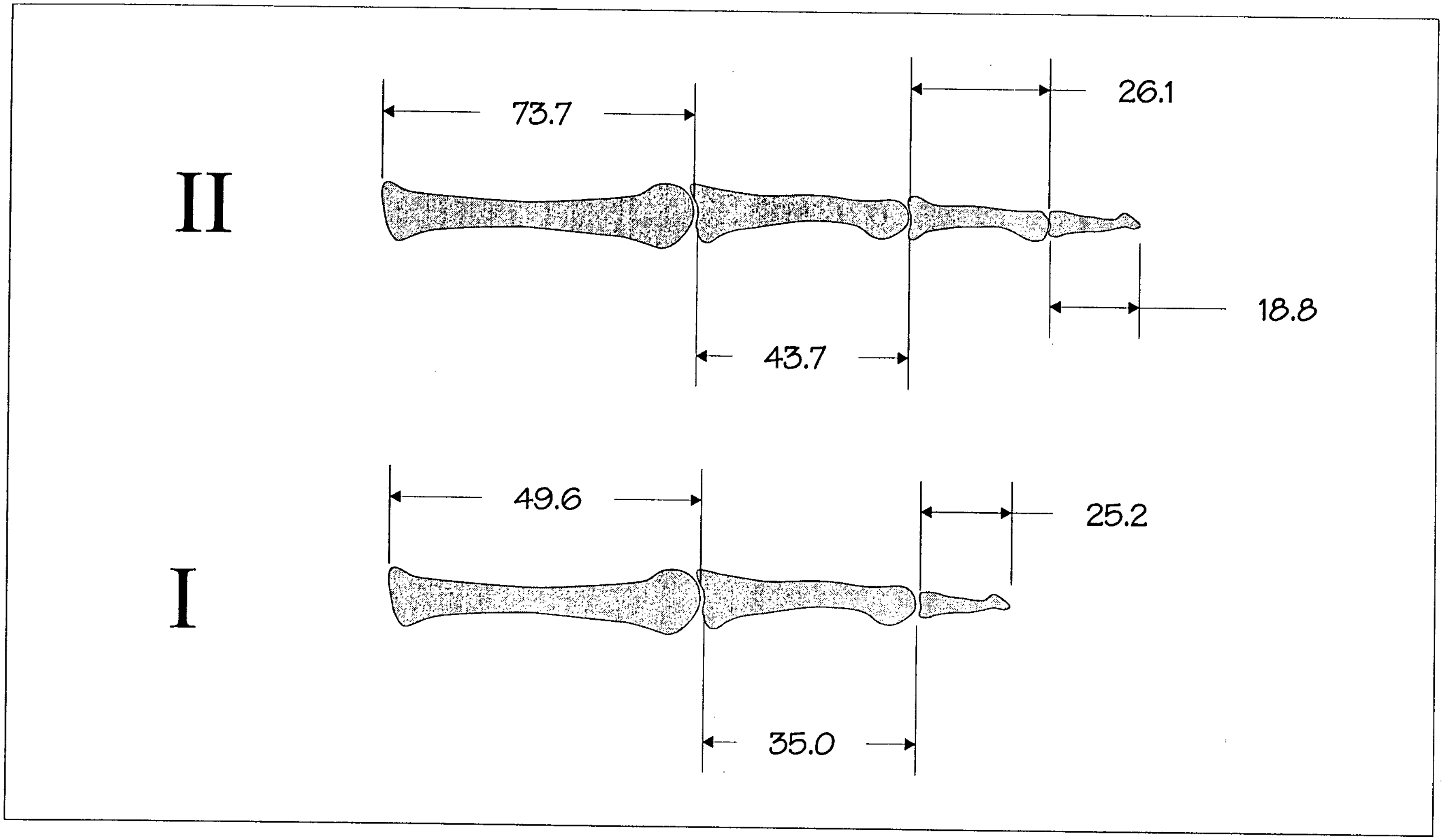

Poznanski A, "The Hand in Radiologic Diagnosis", *Second Edition*. W.B. Saunders Company, Philadelphia, pp 35-40, 1984.

◆ Appendix B ◆

Engineering Drawings - Electrical

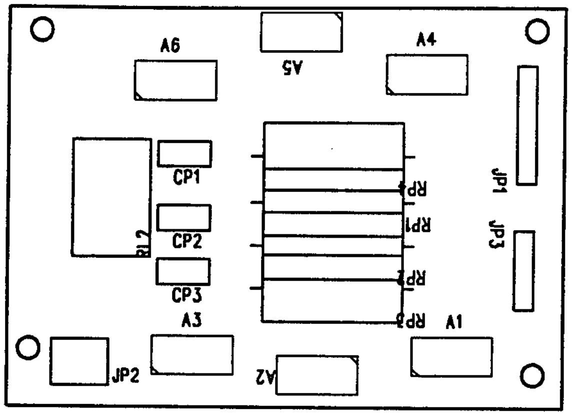
A6
A5
A4
CP1
CP2
CP3
RL2
RP4
RP1
RP2
RP3
JP1
JP3
A3
A1
JP2
A2

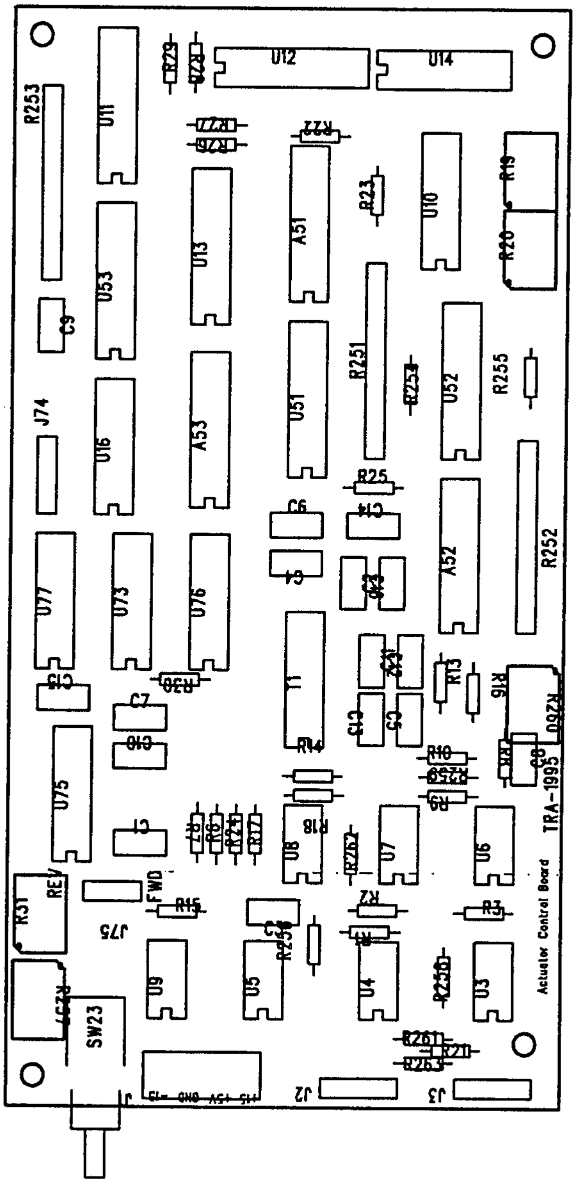
R29
R28
U12
U14
R253
U11
R27
R26
R22
R23
U10
R19
R20
U13
A51
U53
C9
R251
R254
U52
R255
U51
U16
A53
J74
R25
C6
C14
C4
C3
C43
A52
R252
U77
U73
U76
T1
C11
C12
R13
R16
R30
C15
C7
C10
C13
C5
R260
R14
R10
R259
R9
C8
U75
C1
R7
R6
R24
R17
R18
U8
R262
U7
U6
TRA-1995
REV
FWD
R31
R15
J75
C2
R258
R2
R1
R3
U9
U5
U4
R256
U3
Actuator Control Board
R257
SW23
R261
R21
R263
-15 GND +5V +15
J2
J3

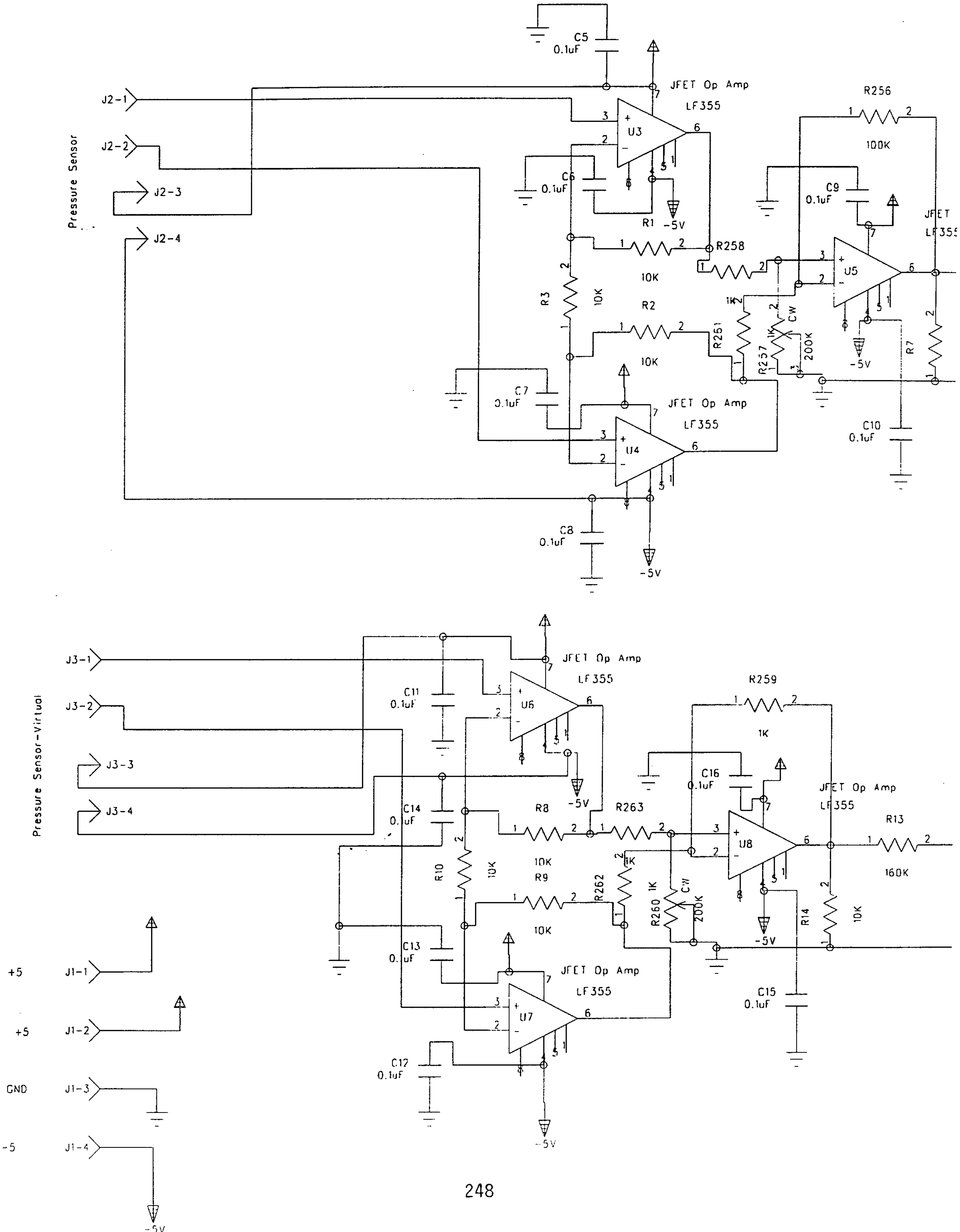
Pressure Sensor
J2-1
J2-2
J2-3
J2-4
C5
0.1uF
JFET Op Amp
LF355
U3
C6
0.1uF
R1
-5V
10K
R3
10K
R2
10K
R258
R251
1K
R257
1K
CW
200K
R256
100K
C9
0.1uF
JFET
LF355
U5
-5V
R7
C10
0.1uF
C7
0.1uF
JFET Op Amp
LF355
U4
C8
0.1uF
-5V
Pressure Sensor-Virtual
J3-1
J3-2
J3-3
J3-4
C11
0.1uF
JFET Op Amp
LF355
U6
-5V
C14
0.1uF
R8
10K
R263
R10
10K
R9
10K
R262
1K
R260
1K
CW
200K
R259
1K
C16
0.1uF
JFET Op Amp
LF355
U8
-5V
R13
160K
R14
10K
C15
0.1uF
C13
0.1uF
JFET Op Amp
LF355
U7
C12
0.1uF
-5V
+5
J1-1
+5
J1-2
GND
J1-3
-5
J1-4
-5V

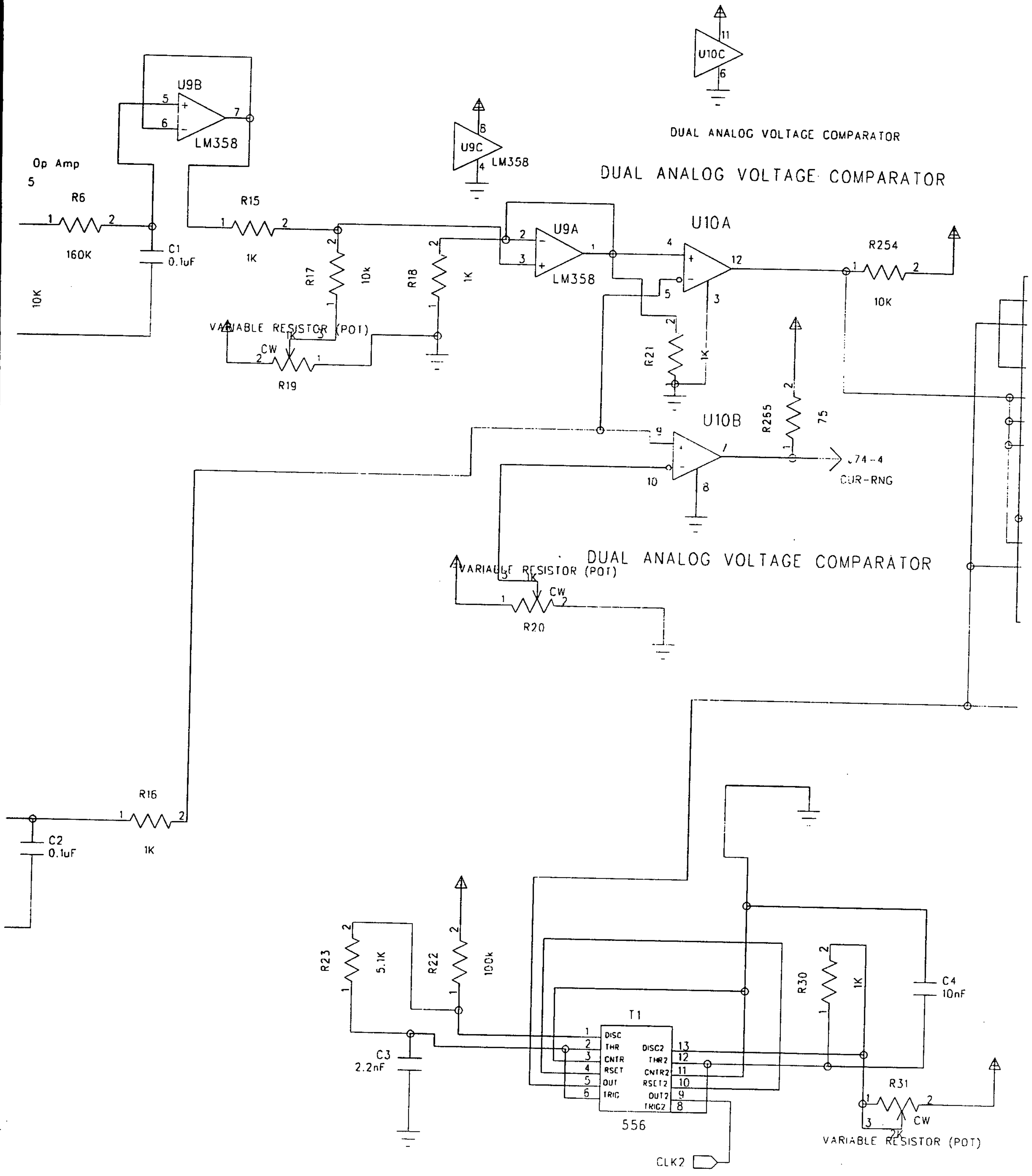
U10C
11
6
DUAL ANALOG VOLTAGE COMPARATOR
U9B
5
6
7
LM358
U9C
8
4
LM358
DUAL ANALOG VOLTAGE COMPARATOR
Op Amp
5
R6
160K
C1
0.1uF
10K
R15
1K
R17
10k
R18
1K
U9A
LM358
U10A
12
R254
10K
R21
1K
VARIABLE RESISTOR (POT)
1K
CW
R19
U10B
R255
75
J74-4
CUR-RNG
10
8
DUAL ANALOG VOLTAGE COMPARATOR
VARIABLE RESISTOR (POT)
1K
CW
R20
R16
1K
C2
0.1uF
R23
5.1K
R22
100k
C3
2.2nF
T1
DISC
THR
CNTR
RSET
OUT
TRIG
DISC2
THR2
CNTR2
RSET2
OUT2
TRIG2
556
R30
1K
C4
10nF
R31
2K
CW
VARIABLE RESISTOR (POT)
CLK2

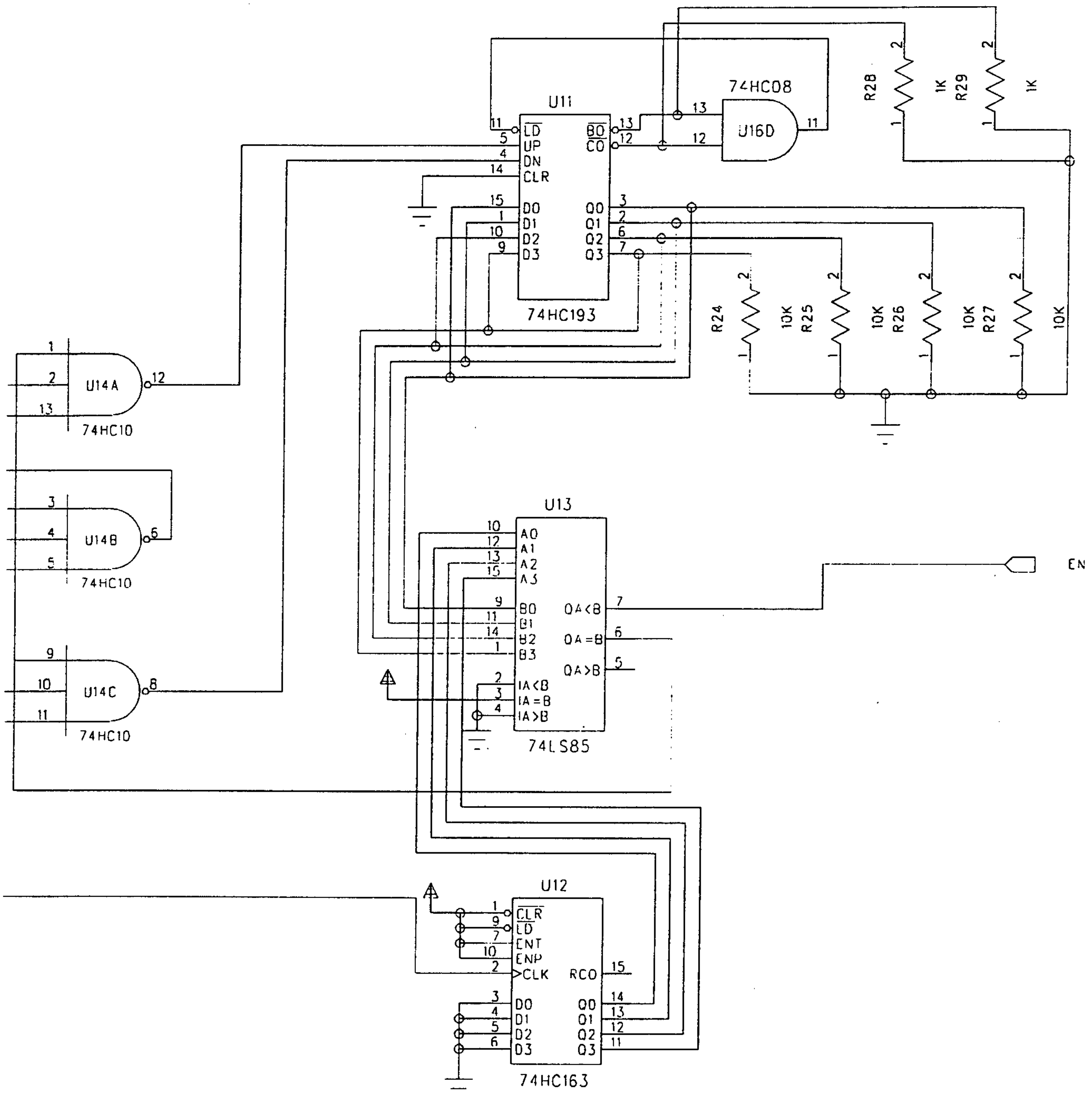
U11
74HC193
LD
UP
DN
CLR
D0
D1
D2
D3
BO
CO
Q0
Q1
Q2
Q3
74HC08
U16D
R28
1K
R29
1K
R24
10K
R25
10K
R26
10K
R27
10K
U14A
74HC10
U14B
74HC10
U14C
74HC10
U13
74LS85
A0
A1
A2
A3
B0
B1
B2
B3
IA<B
IA=B
IA>B
QA<B
QA=B
QA>B
EN
U12
74HC163
CLR
LD
ENT
ENP
CLK
RCO
D0
D1
D2
D3
Q0
Q1
Q2
Q3

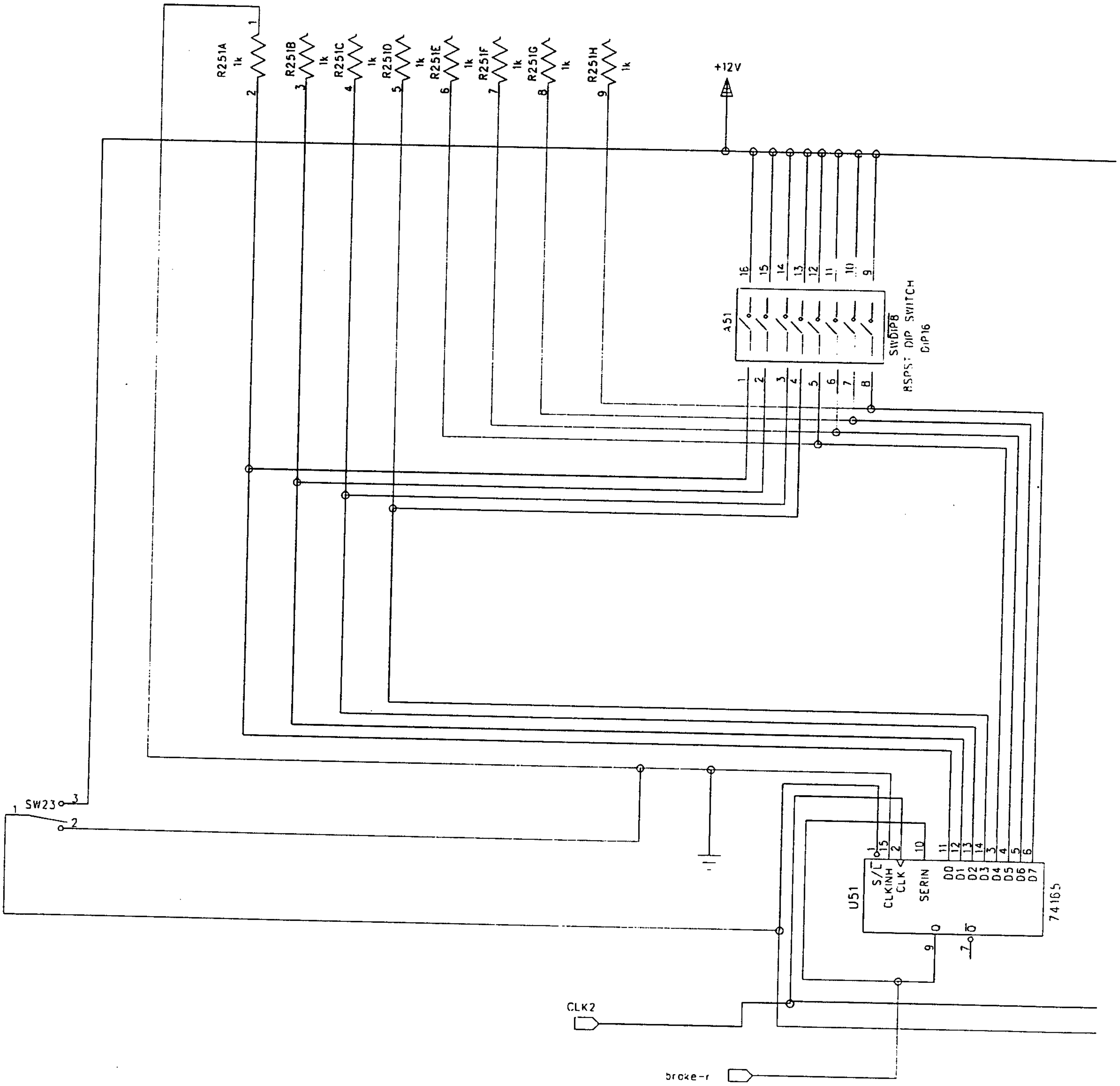
R251A
1k
R251B
1k
R251C
1k
R251D
1k
R251E
1k
R251F
1k
R251G
1k
R251H
1k
+12V
A51
SWDIP8
8SPST DIP SWITCH
DIP16
U51
S/L
CLKINH
CLK
SERIN
D0
D1
D2
D3
D4
D5
D6
D7
Q
Q̄
74165
SW23
CLK2
broke-r

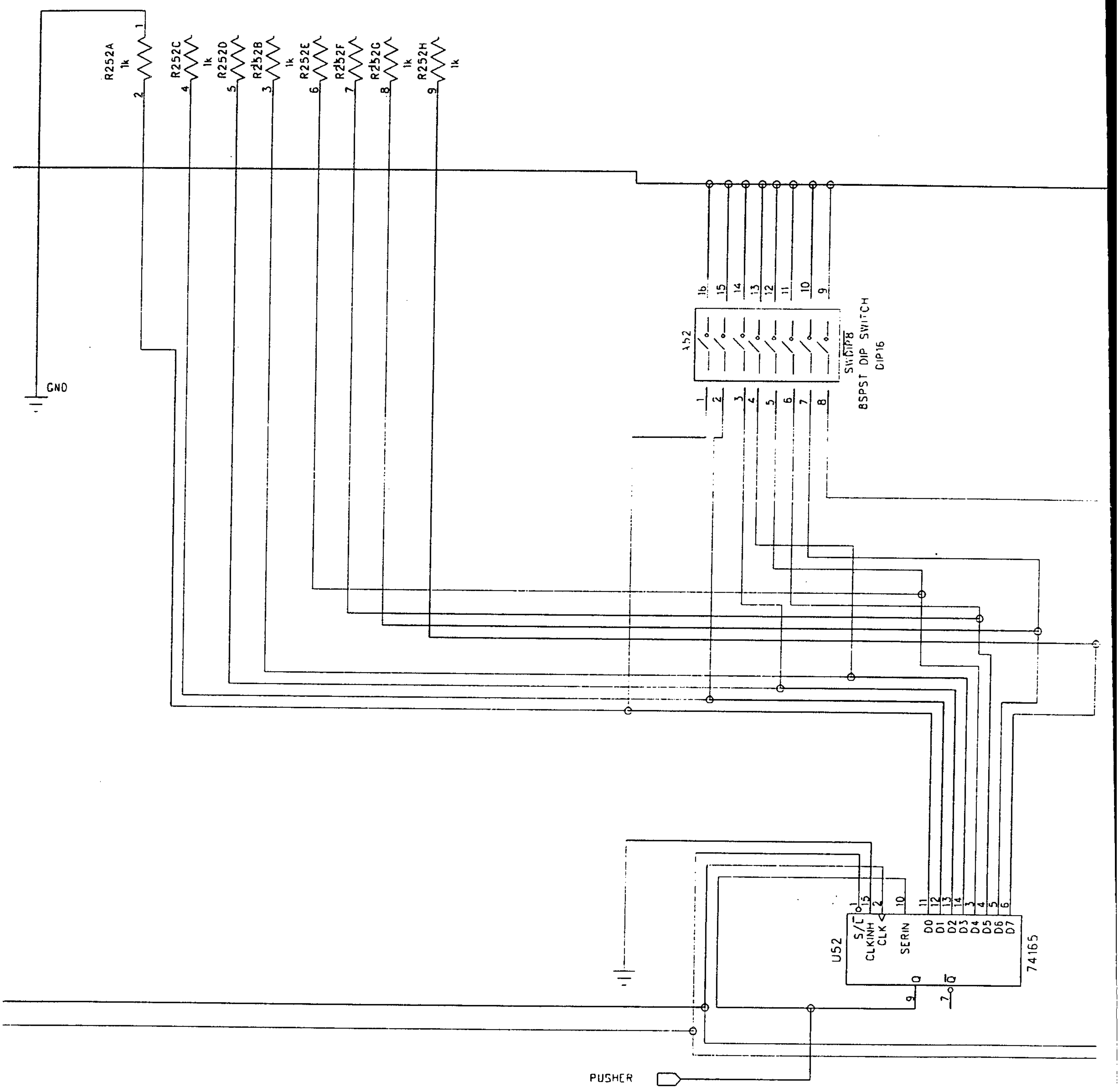
R252A
1k
R252C
1k
R252D
R252B
1k
R252E
R252F
R252G
1k
R252H
1k
GND
S52
SWDIP8
8SPST DIP SWITCH
DIP16
U52
S/L
CLKINH
CLK
SERIN
D0
D1
D2
D3
D4
D5
D6
D7
Q
Q̄
74165
PUSHER

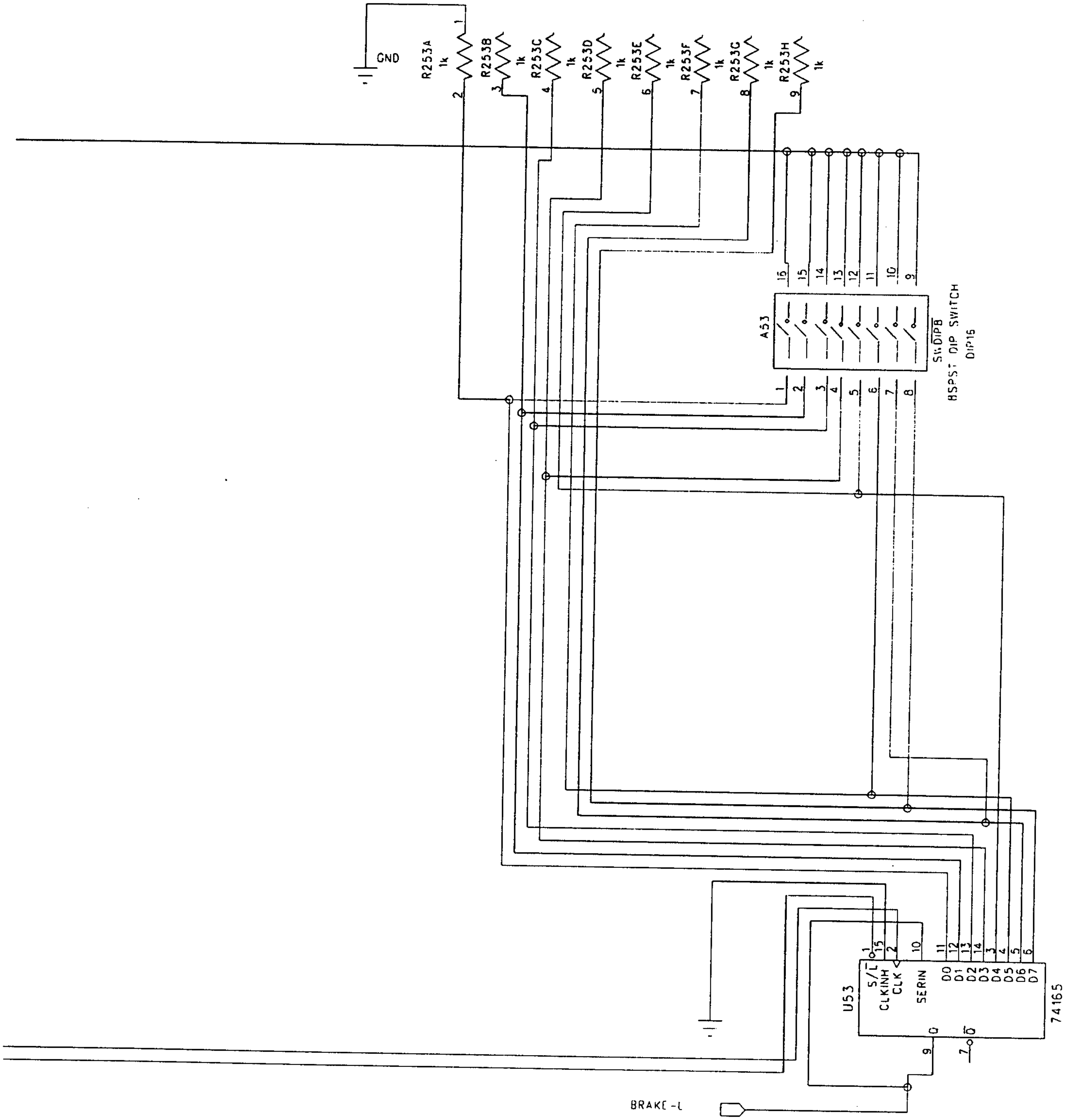
GND
R253A
1k
R253B
1k
R253C
1k
R253D
1k
R253E
1k
R253F
1k
R253G
1k
R253H
1k
A53
SWDIPB
8SPST DIP SWITCH
DIP16
U53
S/L
CLKINH
CLK
SERIN
D0
D1
D2
D3
D4
D5
D6
D7
Q
Q̄
74165
BRAKE-L

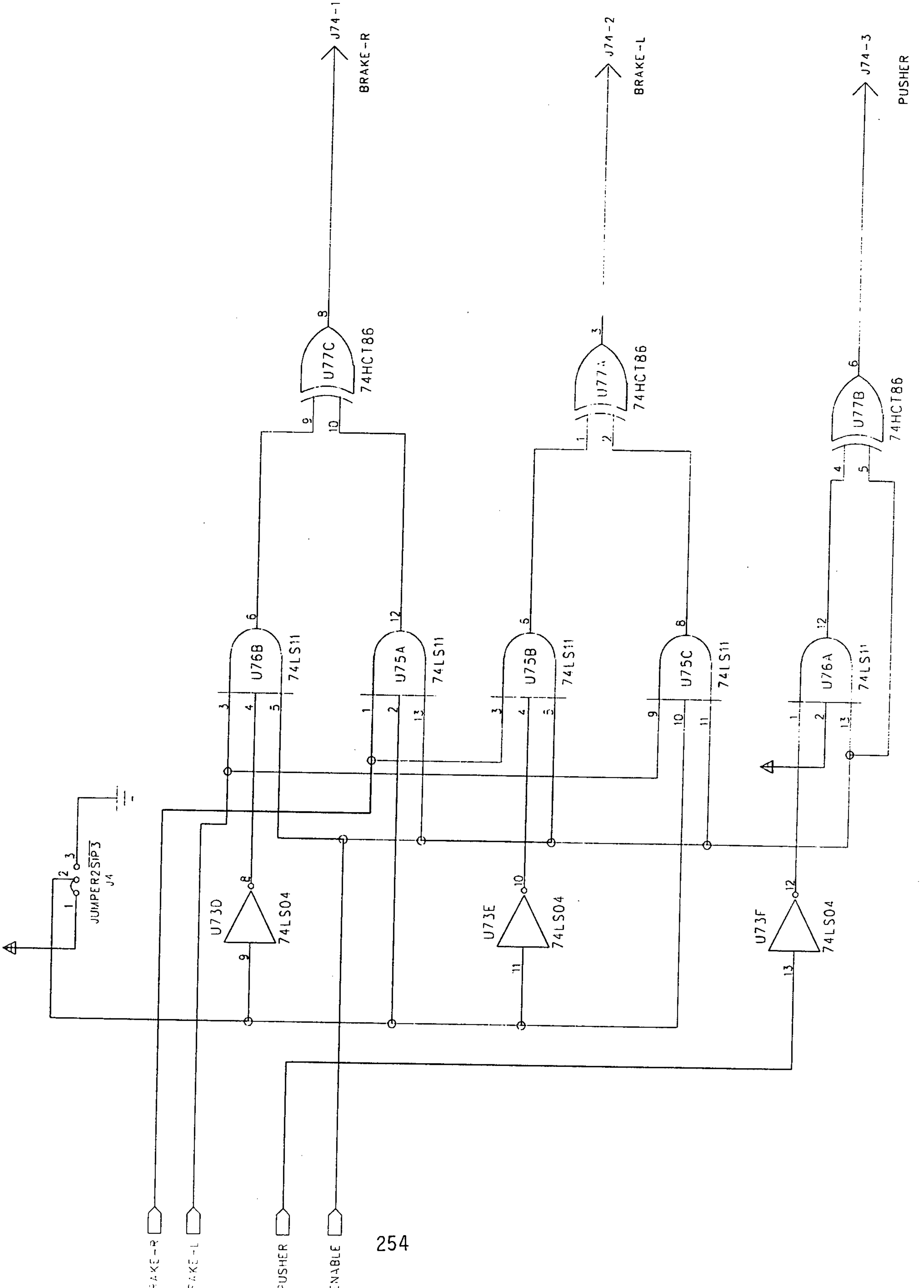

J74-1
BRAKE-R
J74-2
BRAKE-L
J74-3
PUSHER
U77C
74HCT86
U77A
74HCT86
U77B
74HCT86
U76B
74LS11
U75A
74LS11
U75B
74LS11
U75C
74LS11
U76A
74LS11
JUMPER2SIP3
J4
U73D
74LS04
U73E
74LS04
U73F
74LS04
RAKE-R
RAKE-L
USHER
NABLE

◆ Appendix C ◆

Software - Computer Programs

```
/*
*This graphical interface program will allow input of position information via
*an A/D interface card (PC30D-Cyberspace Research) and output force signals to
*be used by the TRA motors.  This interface is part of a closed loop system to
*simulate a force feedback exoskeleton.
*
*Program written by: Kristofer J. James
*Company written for: Technical Research Associates
*Date: September 25, 1995
*Version: 1.1
*
*Hardware requirements: 486CPU, VGA, PC30D (or similar) interface board, TRA angle *sensors, TRA motors,
and TRA designed interface electronics.
*
*************************************************************************** */

#include <conio.h>
#include <stdlib.h>
#include <math.h>
#include <graph.h>
#include <malloc.h>
#include <ctype.h>
#include <stddef.h>
#include "pc30.h"

#define ROTATE 0.000767

char far *buffer;            /* Buffer for image storage */
char far *xbuffer;           /* Buffer for image storage */
size_t imsize;
short square_pos[8]={400,5,410,12,420,20,430,27};     /* Position of squares for intial image capture (x,y) */
short square_size[4]={70,50,30,10};                    /* Parameter for square sizes */
long sx,sy,n=4,n_flag=0;                     /* sx,sy indicate position of animated square; n is a counter; n_flag indicates
if the square is being animated or not */
long cross_prod[4]={0,0,0,0},col_flag=0;        /* cross_prod stores the sign of the cross product for each square;
col_flag indicates if a collision with a smaller square has occured */
long cross_product;                          /* cross_product is the cross product between the finger segment and the cor-
ners of the square */


main()
{
   short x[4]={210,330,410,450};           /*xa, ya:position points a=phalange */
   short xt[3]={210,310,360};              /*xta, yta:thumb position points a=phalange */
   short y[4]={120,120,120,120};
   short yt[3]={220,220,220};
   int i,int_lvl=5,quit_flag=0;            /* int_lvl=interupt level of PC30 board */
   int ang_sample[9]={1,1,1,1,1,1,1,1,1};    /* Variables to record A/D values */
   double jang[4]={0.0,1.0,1.0,1.0};         /* index joint angles */
   double jangt[4]={0.0,1.0,1.0,1.0};        /* thumb joint angles */

   char key_hit;

   x[0]=210; y[0]=120;            /* X and Y offset */
```

```
xt[0]=210; yt[0]=220;          /* X and Y thumb offset */


initialize(x[0],y[0],xt[0],yt[0]);

do
{
      do
      {
      /* Index Finger */
        _setactivepage(0);
        _setvisualpage(1);
        for(i=0; i<3; i++)
                {
                phlang(i,x[i],y[i],x[i+1],y[i+1],9);
                }
        for(i=0; i<3; i++)
                {
                ad_in(i,&ang_sample[i]);
                /*Replace the line above with the appropriate command*/
                ang_sample[i]=ang_sample[i]-2047;
                jang[i+1]=jang[i]+((float)ang_sample[i])*ROTATE;
                x[i+1]=x[i]+((120/(i+1))*cos(jang[i+1]));
                y[i+1]=y[i]+((80/(i+1))*sin(jang[i+1]));
                phlang2(i,x[i],y[i],x[i+1],y[i+1],12);
                _setvisualpage(0);
                }

     /* Thumb */
/*
        for(i=0; i<2; i++)
                {
                phlangt(i,xt[i],yt[i],xt[i+1],yt[i+1],9);
                }

        for(i=0; i<2; i++)
                {
                ad_in(i+3,&ang_sample[i+3]);
                ang_sample[i+3]=2047;
                ang_sample[i+3]=ang_sample[i+3]-2047;
                jangt[i+1]=jangt[i]+((float)ang_sample[i+3])*ROTATE;
                xt[i+1]=xt[i]+((80/(i+1))*cos(jangt[i+1]));
                yt[i+1]=yt[i]-((80/(i+1))*sin(jangt[i+1]));
                phlangt(i,xt[i],yt[i],xt[i+1],yt[i+1],13);
                }
*/
     }while(!kbhit());
      _setactivepage(1);
      key_hit=getch();
      switch (key_hit)
      {
            case NULL:
            break;
```

```
                case 'q':
                quit_flag=1;
                break;

                case 'Q':
                quit_flag=1;
                break;

                case 27:
                quit_flag=1;
                break;

                case '0':
                if(n!=0 && n_flag!=0) break;
                n=0;
                if(n_flag!=0)
                {
                        _putimage(sx,sy,buffer,_GXOR);
                        n_flag=0;
                        break;
                }
                sx=250;sy=200;
                _putimage(sx,sy,buffer,_GXOR);
                n_flag=1;
                break;

/*          case '1':
                if(n!=1 && n_flag!=0) break;
                n=1;
                if(n_flag!=0)
                {
                        _putimage(sx,sy,buffer,_GXOR);
                        n_flag=0;
                        break;
                }
                sx=250;sy=200;
                _putimage(sx,sy,buffer,_GXOR);
                n_flag=1;
                break;

                case '2':
                if(n!=2 && n_flag!=0) break;
                n=2;
                if(n_flag!=0)
                {
                        _putimage(sx,sy,buffer,_GXOR);
                        n_flag=0;
                        break;
                }
                sx=250;sy=200;
                _putimage(sx,sy,buffer,_GXOR);
                n_flag=1;
                break;
                case '3':
                if(n!=3 && n_flag!=0) break;
                n=3;
                if(n_flag!=0)
                {
                        _putimage(sx,sy,buffer,_GXOR);
                        n_flag=0;
                        break;
                }
                sx=250;sy=200;
                _putimage(sx,sy,buffer,_GXOR);
                n_flag=1;
                break;
*/
                case 72:
                if(n_flag==1)
                {       _putimage(sx,sy,buffer,_GXOR);
                        sy=sy-5;
                        if(sy<=0) sy=0;
                        _putimage(sx,sy,buffer,_GXOR);
                }
                break;

                case 80:
                if(n_flag==1)
                {       _putimage(sx,sy,buffer,_GXOR);
                        sy=sy+5;
                        if(sy>=295) sy=295;
                        _putimage(sx,sy,buffer,_GXOR);
                }
                break;

                case 77:
                if(n_flag==1)
                {       _putimage(sx,sy,buffer,_GXOR);
                        sx=sx+5;
                        if(sx>=580) sx=580;
                        _putimage(sx,sy,buffer,_GXOR);
                }
                break;

                case 75:
                if(n_flag==1)
                {       _putimage(sx,sy,buffer,_GXOR);
                        sx=sx-5;
                        if(sx<=165) sx=165;
                        _putimage(sx,sy,buffer,_GXOR);
                }
                break;

                default:
                break;
    }
```

```
   }while(quit_flag==0);

   int_close();
   _ffree(buffer);
   _ffree(xbuffer);
   exit( !_setvideomode( _DEFAULTMODE ) );

}


initialize(int x,int y,int xt,int yt)
{
   int j=0,i=0,n=0;
   float m=0.0;
   short mode=_ERESCOLOR;
   unsigned char fill[8]={255,255,255,255,255,255,255,255};
   char dummy[10];

   while( !_setvideomode( mode ) )   /* Find a valid graphics mode   */
         mode--;
   if( mode == _TEXTMONO )
         exit( 1 );                  /* No graphics available     */

   /* Diagnostic of PC30 interface board */

   if(diag()==0) exit(0);     /* Check to make sure board is OK */
   set_type(3);               /* Notifying software of PC30D board */
   for(n=0; n<8; n++) set_gain(n,1);
   j = version();
   i = j/256;
   m = (float) j - i*256;
   m = i + m/100.0;
   printf("PC-30 Driver Version %5.2f\n", m);
   printf("***Press any key to continue***\n");
   getch();
   set_base(1792);   /* Sets base address of PC30 board to 700 hex */
   if (diag()==0){ printf("\aPC-30 found.\n");getch();}
         else if ((get_type() < found_30bc) || (get_type() == found_126))
           printf("\n PC-30B, PC-30C, PC-30D or PC-30PG required.");


   init();         /* Initialize PC30 interface board */
   _clearscreen(_GCLEARSCREEN);
   for(n=0; n<3; n++)
   {
     _setcolor(n+3);
     _setfillmask(fill);

_rectangle(_GFILLINTERIOR,square_pos[2*n],square_pos[2*n+1],square_pos[2*n]+square_size[n],square_pos[2
*n+1]+(square_size[n]*0.75));
   }
     n=0;
```

```
imsize=(size_t)_imagesize(square_pos[2*n]-1,(square_pos[2*n+1]-1),(square_pos[2*n]+square_size[n]+1),(square
_pos[2*n+1]+(0.75*square_size[n])+1));
    buffer=(char far *)_fmalloc(imsize);

_getimage((square_pos[2*n]-1),(square_pos[2*n+1]-1),(square_pos[2*n]+square_size[n]+1),(square_pos[2*n+1]+(
0.75*square_size[n])+1),buffer);


   for(n=0; n<2; n++)
   {
            _setactivepage(n);
            _setbkcolor(_LIGHTBLUE);
            _clearscreen( _GCLEARSCREEN );
            _setfillmask(fill);
            _setcolor(14);
            _moveto(x,y);
            _lineto(x-150,y);
            _lineto(xt,yt);
            _lineto(x,y);
            _floodfill(x-1,y+1,14);
            imsize=(size_t)_imagesize(59,119,211,221);
            xbuffer=(char far *)_fmalloc(imsize);
            _getimage(59,119,211,221,xbuffer);
            _clearscreen( _GCLEARSCREEN );
            _putimage(x-150,y,xbuffer,_GXOR);

   }

}

phlang(i,xref,yref,x1,y1,color)
{
  _setcolor(color);
  _moveto(xref,yref);
  _lineto(x1,y1);
}

phlang2(i,xref,yref,x1,y1,color)
{  long sx1=0,sy1=0,sxa,sya;
  int n2,n3;
  char on1='<',on2='-',on3='>';

  _setcolor(color);
  _moveto(xref,yref);
  _lineto(x1,y1);
  col_flag=0;

/* Cross products to check for collision--if all cross products have the same
sign, there is no collision */

         for (n3=2; n3>-1; n3=n3-1)
         {     sxa=sx+(n3*10);sya=sy+(n3*7.5);
                  for (n2=0; n2<4; n2++)
```

```
                        {     if(n2==0) sx1=sxa,sy1=sya;
                                if(n2==1) sx1=sxa+square_size[n3];
                                if(n2==2) sy1=sya+(square_size[n3]*0.75);
                                if(n2==3) sx1=sxa+square_size[n3],sy1=sya+(0.75*square_size[n3]);
                                cross_product=(((xref-x1)*(yref-sy1))-((yref-y1)*(xref-sx1)));
                                sx1=sxa;sy1=sya;
                                cross_prod[n2]=0;
                                if (cross_product<0) cross_prod[n2]=-1;
                                if (cross_product>0) cross_prod[n2]=1;
                        }
                        _setvisualpage(1);
                        if (col_flag==0 && (cross_prod[0]!=cross_prod[1] || cross_prod[1]!=cross_prod[2] ||
cross_prod[2]!=cross_prod[3]))
                        {     if(i==0)
                              {     if (cross_prod[1]<1 && cross_prod[2]>-1 && sya<y1 && x1>sxa &&
xref<sxa+square_size[n3] && yref<sya+(0.75*square_size[n3])) collision(n3,i);
                                          if (cross_prod[0]>-1 && cross_prod[3]<1 && sya<y1 &&
x1<sxa+square_size[n3] && xref>sxa && yref<sya+(0.75*square_size[n3])) collision(n3,i);
                              }
                              if(i==1)
                              {     if (cross_prod[1]<1 && cross_prod[2]>-1 && sya<y1 && x1>sxa &&
xref<sxa+square_size[n3] && yref<sya+(0.75*square_size[n3])) collision(n3,i);
                                          if (cross_prod[0]>-1 && cross_prod[3]<1 && sya<y1 &&
x1<sxa+square_size[n3] && xref>sxa && yref<sya+(0.75*square_size[n3])) collision(n3,i);
                              }
                              if(i==2)
                              {     if (cross_prod[1]<1 && cross_prod[2]>-1 && sya<y1 && x1>sxa &&
xref<sxa+square_size[n3] && yref<sya+(0.75*square_size[n3])) collision(n3,i);
                                          if (cross_prod[0]>-1 && cross_prod[3]<1 && sya<y1 &&
x1<sxa+square_size[n3] && xref>sxa && yref<sya+(0.75*square_size[n3])) collision(n3,i);
                              }
                        }
                        else
                        {     if(col_flag==0) da_out(i,2048);
                        }

            }

}

phlangt(i,xtref,ytref,xt1,yt1,color)
{
   _setcolor(color);
   _moveto(xtref,ytref);
   _lineto(xt1,yt1);

}

collision(int n3,int i)
{     int j=0;
         da_out(i,(int)((float)(n3+1)*-102.4)+2048);
         /* Replace the line above with the appropriate command. */
         col_flag=1;
}
```

BASAC PROGRAM TO CALCULATE COIL PARAMETERS

```
DECLARE SUB wirelength (wlen, ndia, drod, dwire, nlen)
DECLARE SUB printout ()
DECLARE SUB guagesize (guage!, dwire!, res)
CLS
SCREEN 9
'************** coil program ***********
'************* Allen P. Hilton *********
'************** June 1994 ************
pi = 3.141592654#
d = 2.0106E-08
'************** variables **************
'dwire = wire diameter
'drod = rod diameter
'idcoil = ID of coil
'odcoil = OD of coil
'lcoil = length of coil
'lrod = length of terfenol rod
'nlen = number of wire diameters that fit into length of coil
'ndia = number of wire diameters that fit into dia of coil
'turns = number of turns = (n-length)(n-dia)
'n = turns density = turns/length of coil
'wlen = length of wire
'rcoil = resistance of coil
'res = resistance of wire/length of wire
'H = magnetic field (Oe)
'I = current needed to achieve H
'Required voltage across coil
'S = strain of rod
'delta = change in length of rod
'guage = wire guage
'd = const 'T = prestress (equal to zero)

'******************** CASE ONE *******************
CLS
INPUT "Desired Magnetic Field (Oe) ", H
INPUT "Wire Guage ", guage
     CALL guagesize(guage, dwire, res)
     PRINT "OD of wire = "; dwire; "in"
INPUT "Length of Terfenol rod (in) ", lrod
     lcoil = lrod INPUT "Diameter of Terfenol rod (in) ", drod
INPUT "Max outer diameter of coil (in)", odcoil
```

BASAC PROGRAM TO CALCULATE COIL PARAMETERS

```
DECLARE SUB wirelength (wlen, ndia, drod, dwire, nlen)
DECLARE SUB printout ()
DECLARE SUB guagesize (guage!, dwire!, res)
CLS
SCREEN 9
'************** coil program ***********
'************* Allen P. Hilton *********
'**************  June 1994  ************
pi = 3.141592654#
d = 2.0106E-08
'************** variables **************
'dwire = wire diameter
'drod = rod diameter
'idcoil = ID of coil
'odcoil = OD of coil
'lcoil = length of coil
'lrod = length of terfenol rod
'nlen = number of wire diameters that fit into length of coil
'ndia = number of wire diameters that fit into dia of coil
'turns = number of turns = (n-length)(n-dia)
'n = turns density = turns/length of coil
'wlen = length of wire
'rcoil = resistance of coil
'res = resistance of wire/length of wire
'H = magnetic field (Oe)
'I = current needed to achieve H
'Required voltage across coil
'S = strain of rod
'delta = change in length of rod
'guage = wire guage
'd = const 'T = prestress (equal to zero)

'********************* CASE ONE ********************
CLS
INPUT "Desired Magnetic Field (Oe) ", H
INPUT "Wire Guage ", guage
    CALL guagesize(guage, dwire, res)
    PRINT "OD of wire = "; dwire; "in"
INPUT "Length of Terfenol rod (in) ", lrod
    lcoil = lrod INPUT "Diameter of Terfenol rod (in) ", drod
INPUT "Max outer diameter of coil (in)", odcoil
```

```
' ******** number of turns
nlen = CINT(lrod / dwire)
ndia = CINT(((odcoil - (drod + .01)) / 2) / dwire)
turns = nlen * ndia

'******** length of wire
CALL wirelength(wlen, ndia, drod, dwire, nlen)

'******* resistance of coil
rcoil = (wlen * res) / (12 * 1000)

'******** Current in coil to achieve mag field
n = turns / (lcoil * .0254)          '0.0254 is a conversion to meters
I = (H * 1000) / (n * 4 * pi)
voltage = I * rcoil

'******** Strain
S = d * (H * 1000 / (4 * pi)) delta = lrod * S
'PRINT S, delta
CALL printout
DO WHILE INKEY$ = "": LOOP
END

SUB guagesize (guage, dwire, res)
SELECT CASE guage
     CASE IS = 14
          dwire = .066
          res = 2.525
     CASE IS = 15
          dwire = .0589
          res = 3.184
     CASE IS = 16
          dwire = .0526
          res = 4.015
     CASE IS = 17
          dwire = .0471
          res = 5.063
     CASE IS = 18
          dwie = .042
         res = 6.384
     CASE IS = 19
          dwire = .0375
          res = 8.051
     CASE IS = 20
```

```
        dwire = .0336
        res = 10.15
    CASE IS = 21
        dwire = .03
        res = 12.8
    CASE IS = 22
        dwire = .0268
        res = 16.14
    CASE IS = 23
        dwire = .024
        res = 20.36
    CASE IS = 24
        dwire = .0215
        res = 25.67
    CASE IS = 25
        dwire = .0192
        res = 32.36
    CASE IS = 26
        dwire = .0171
        res = 40.81
    CASE IS = 27
        dwire = .0154
        res = 51.46
    CASE IS = 28
        dwire = .0138
        res = 64.89
    CASE IS = 29
        dwire = .0123
        res = 81.83
    CASE IS = 30
        dwire = .011
        res = 103.2
    CASE IS = 31
        dwire = .0098
        res = 130.1
    CASE IS = 32
        dwire = .0089
        res = 164.1
    CASE IS = 33
        dwire = .0079
        res = 206.9
    CASE IS = 34
        dwire = .007
        res = 260.9
        CASE IS = 35
            dwire = .0062
            res = 329!
        CASE IS = 36
            dwire = .0056
            res = 414.8
        CASE IS = 37
            dwire = .005
            res = 523.1
        CASE IS = 38
            dwire = .0044
            res = 659.6
        CASE IS = 39
            dwire = .0038
            res = 831.7
        CASE IS = 40
            dwire = .0034
            res = 1049!
        CASE ELSE
            PRINT "Guage size not in database ..."
    INPUT "Please input dia of wire + insulation in inches  ", dwire
    END SELECT
    END SUB


    SUB printout
    SHARED H, guage, dwire, lrod, drod, odcoil, lcoil, turns, n, wlen, rcoil
    SHARED I, voltage, S, delta
    CLS
    PRINT "Magnetic Field (H) = "; H; "Oe"
    PRINT "Wire Guage = "; guage
    PRINT "Wire Diameter (with insulation) "; dwire; "in"
    PRINT "Terfenol Rod Length = "; lrod; "in"
    PRINT "Terfenol Rod Diameter = "; drod; "in"
    PRINT "Coil OD = "; odcoil; "in"
    PRINT "Length of Coil = "; lcoil; "in"
    PRINT
    PRINT "Number of turns in Coil = "; turns
    PRINT "Turns Density = "; n; "turns/meter"
    PRINT "Length of Wire in Coil = "; wlen; "in"
    PRINT "Resistance of Coil = "; rcoil; "ohms"
    PRINT
    PRINT "Current Required for Magnetic Field = "; I; "amps"
    PRINT "Voltage Required to Achieve Current = "; voltage; "Volts"
```

```
PRINT "Strain Induced by Magnetic Field = "; (S * 1000); "ppm"
PRINT "Change in Terfenol Rod Length = "; delta; "in"
PRINT "New Terfenol Rod Length = "; (lrod + delta); "in"

END SUB


SUB wirelength (wlen, ndia, drod, dwire, nlen)
SHARED pi
'wlen = 0
FOR j = 2 TO (ndia * 2) STEP 2
     wlen = wlen + (((drod + .01) + (j * dwire)) * (pi * nlen))
NEXT j
PRINT wlen, ndia, drod, dwire, nlen
END SUB
```

◆ Appendix D ◆

User Manual

Terfenol-D
Force Feedback Handmaster
Prototype User's Manual

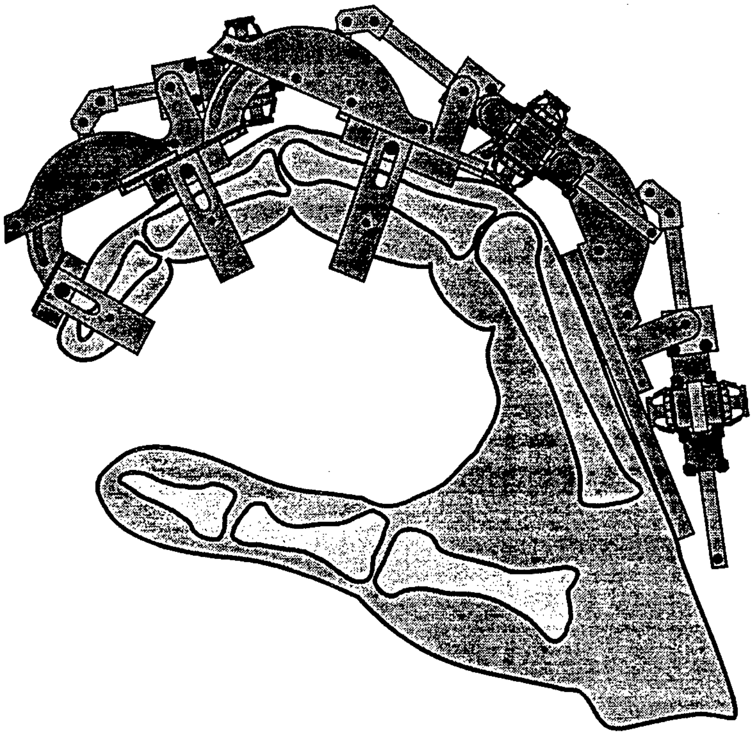

TECHNICAL RESEARCH ASSOCIATES, INC.
Salt Lake City, Utah 84106

*** NOTICE OF DISCLAIMER ***

To Whom It May Concern:

The Force Feedback Handmaster, with it's accompanying components, accessories, parts, materials, lubrications, coatings, mechanical drawings, electrical schematics, software, specifications, manuals, etc., is currently an engineering prototype. Consequently, there are no guarantees or warranties, either expressed or implied with the Force Feedback Handmaster or associated items. Furthermore, Technical Research Associates, Inc., will not be held responsible nor assume any liability for harm or injury.

This device has been designed and manufactured solely as an engineering prototype. All current instruments and associated items are for demonstration and evaluation purposes only. Sale of this device into interstate commerce is strictly prohibited until further notice.

TABLE OF CONTENTS

SECTION 1 - GENERAL DESCRIPTION

GENERAL FEATURES

The TRA Force Feedback Handmaster is a multi-dof (degree of freedom) exoskeleton hand for use in virtual reality and telerobotic environments. It combines force feedback, finger joint position sensing, and load sensing into one compact unit. This handmaster consists of five major components with unique features. They are as follows:

State of the art linear motor based on Terfenol-D

A state of the art linear motor that is based on the magnetostrictive material Terfenol-D is at the heart of the Force Feedback Handmaster. This motor is an inchworm based that consists of two brakes, a pusher, and drive shaft. It is small in size with high force and velocity. This makes it well suited to provide force feedback to the individual finger joints of the human hand.

Adjustable sliding virtual joints

The Terfenol-D based linear motors are mounted upon adjustable virtual joints that mount to the finger to track motion. The joints are made of delrin and high strength aluminum that provide a low friction contact surface. This allow the joint to move with little noticable drag.

Adjustable finger rings

The virtual joints are mounted upon adjustable finger rings that clamp onto the finger. They are adjustable for different finger sizes. The virtual joints mount in a dovetail track that permit the joints/rings to be positioned to fit a variety of finger sizes, and locked in place.

Novel angular position sensors

The virtual joints have an embedded novel angular position sensor. This sensor tracks the angular position of the joint over its full range of motion. This angular position sensor is based on the amount of light that passes through rotating polarizing films.

Load cells for force measurement

Embedded in the base of each adjustable finger ring is a load cell that measures the forces experienced by the Force Feedback Handmaster. This is a valuable component in the contol loop. It indicates the amount of force being applied by the linear motors to the fingers.

A schematic of the Force Feedback Handmaster system is illustrated below. Two power supplies are connected to the the electronic control case. The controler and power boards are securely mounted in the control case.

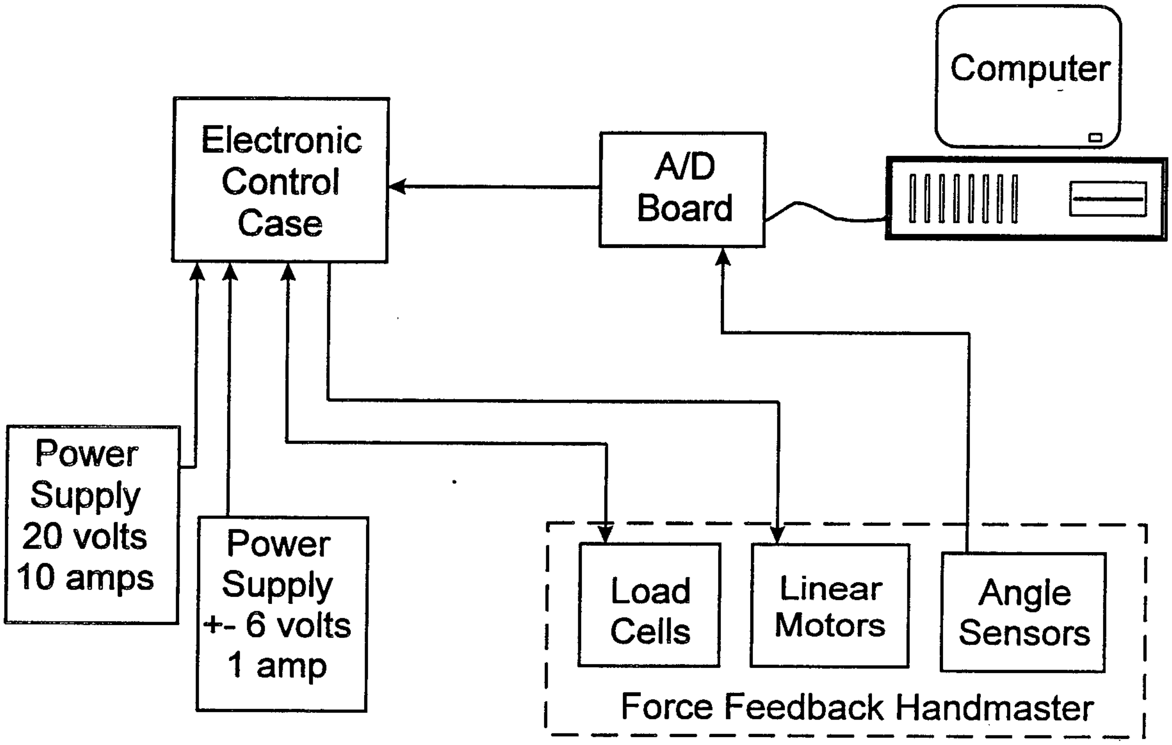
Computer
Electronic Control Case
A/D Board
Power Supply 20 volts 10 amps
Power Supply +- 6 volts 1 amp
Load Cells
Linear Motors
Angle Sensors
Force Feedback Handmaster

Figure 1: Schematic of Force Feedback Handmaster

The electronic control case is connected to the load cells, the linear motors, the angle sensors, and the computer A/D board.

The computer, A/D board, and power supplies are not included with the system.

Figure 2 is a detailed labeled sketch indicating part names and locations.

Terfenol–D
Force Feedback Handmaster

1 DIP (Virtual Distal Interphalangeal Joint)
2 PIP (Virtual Proximal Interphalangeal Joint)
3 MIP (Virtual Metacarpophalangeal Joint)
4 Distal Adjustable Finger Ring
5 Proximal Adjustable Finger Ring
6 Metacarpal Adjustable Finger Ring
7 Distal Finger Pad
8 Distal Joint Shaft
9 Angle Sensor Polarizing Film
10 Drive Shaft Clevis
11 Finger Height Adjustment Screw
12 Proximal Finger Pad
13 Load Cell Wire Feedthru
14 Load Cell Wire Feedthru
15 Finger Height Adjustment Screw
16 Drive Shaft
17 Motor Mount
18 Proximal Joint Shaft
19 Angle Sensor Polarizing Film
20 Linear Motor
21 Metacarpal Finger Pad
22 Drive Shaft Clevis
23 Load Cell Wire Feedthru
24 Finger Height Adjustment Screw
25 Drive Shaft
26 Motor Mount
27 Brake Pad Pressure Adjustment Cap
28 Linear Motor
29 Drive Shaft Clevis
30 Drive Shaft
31 Motor Mount Pin
32 Motor Mount
33 Linear Motor
34 Travel Stop
35 Metacarpal Segment
36 Angle Sensor Polarizing Film
37 MIP Joint Shaft
38 Location for Embedded Load Cell
39 Location for Embedded Load Cell
40 Location for Embedded Load Cell
41 Motor Mount Pin
42 Rotating Metacarpal Joint
43 MIP Finger Pad
44 Location for Set Screw to Lock the Virtual Joint to the Ring
45 Location for Set Screw to Lock the Virtual Joint to the Ring
46 Hand Clamp
47 Palm Pad
48 Adjustment Screw for Metacarpal Segments
49 Travel Stop

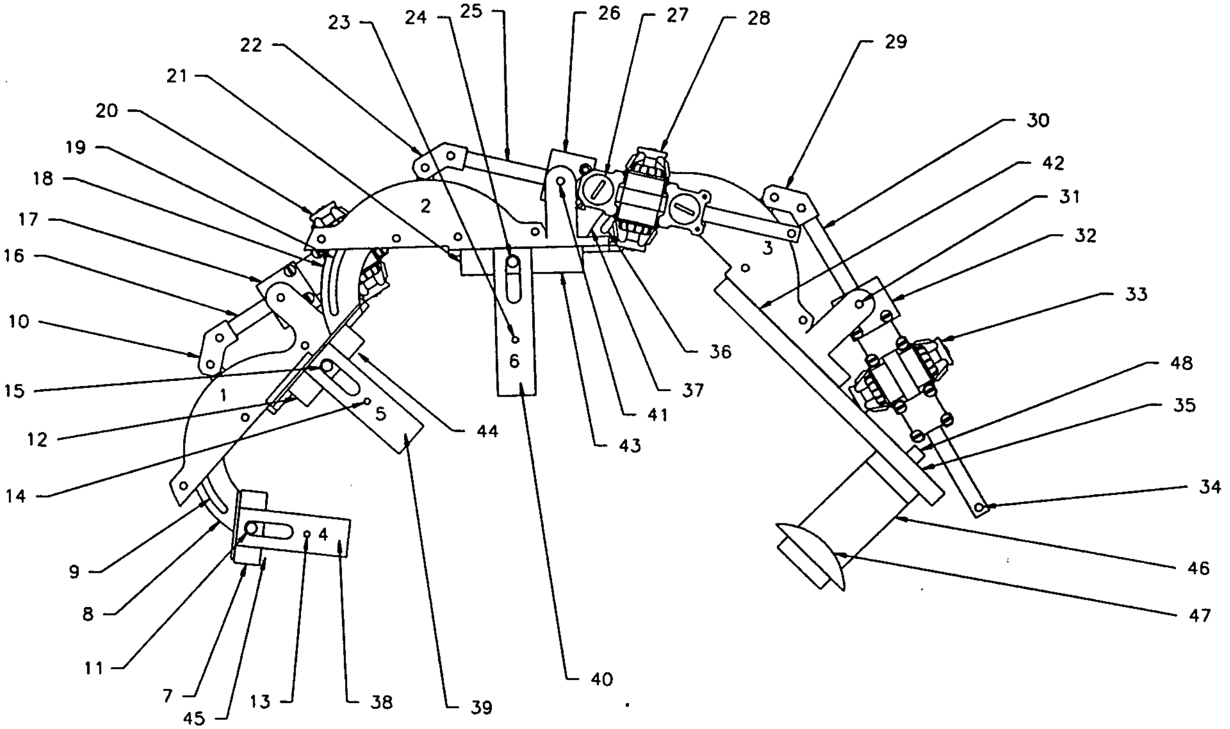

SECTION 2 - SOFTWARE

TRA SOFTWARE: FORCE FEEDBACK SIMULATION

The software is designed to read a signal from a TRA angle sensor and display a three segment finger. The angles between the adjacent segments will mimic the angle read by the TRA angle sensor. The TRA angle sensor outputs a voltage that is a function of its angular position. These signals are read by an analog-to-digital interface board and inputted into the software.

The screen will also display a square, movable object on the screen. The software will register any collision between the finger segments and the square. If contact is detected the system will output a virtual force signal (via a digital-to-analog interface board) to the TRA electronic control board. The level of the output signal will be determined by the depth the finger segment penetrates the square.

CONTROL KEYS FOR SOFTWARE:

Up Arrow: Moves the virtual object towards the top.
Down Arrow: Moves the virtual object towards the bottom.
Left Arrow: Moves the virtual object towards the left.
Right Arrow: Moves the virtual object towards the right.

0 (Zero): Activates/Deactivates the virtual object.

Esc or 'q': Quits the program.

USING DIFFERENT DATA ACQUISITION BOARDS:

There are two commands used in this program to read data from input A/D lines and produce signals from output D/A lines. These are **adin** and **daout** respectively. When using boards other than the PC-30D, these lines of code must be replaced with the command specific to the board used. The header file provided by the data interface board manufacturer will also have to replace the **#include "pc30.h"** in the program. The rest of the code is designed to run on reasonable equipped computer system.

SECTION 3 - BOARD ADJUSTMENTS

TRA CONTROLLER BOARD ADJUSTMENTS:

The controller boards are designed to be adjustable of several key functions. The DIP switches (A51, A52, A53) are used to control the phase timing between the brakes and the pusher. These have been set for maximum efficiency for the TRA motors.

Potentiometers R257 and R260 are used to adjust the CMRR (Common Mode Rejection Ratio) of the instrumentation amplifier circuits. Connect the inputs of an input channel (e.g. J2) to a load cell (with no load being placed on the transducer) and using an oscilliscope, monitor the voltage at R7 (the pin not connected to ground). Adjust R257 until the voltage reads approximately zero volts. Repeat with the second channel monitoring the voltage at R14 (again the pin not connected to ground) and adjust R260. Potentiometer R31 adjust the main timing sequence (i.e how much time for a full motor step) for the brakes and pusher. This has been set for maximum efficiency for the TRA motors. The threshold for the high/low current range is set by potentiometer R20. Adjusting this determines the force level which causes the relay to activate, allowing more current to flow to the pusher coil, hence increasing the force applied by the motor. The final adjustment, using R19, is the offset on the amplified load cell signal before comparing it to the virtual force signal.

SECTION 4 - HANDMASTER ADJUSTMENTS

THE MOTOR

The only thing to be adjusted on the Terfenol-D based linear motor is the brake pad pressure. The drive shaft is sandwiched between the brake pad and the flexure controlling the preload to the Terfenol-D in the brake. The adjustment can be seen in Figure 3 below.

Care and judgement must be used in adjusting this pressure since this same adjustment controls the preload to the Terfenol-D rod. By design, when the preload is 1000 psi, the pressure on the brake pad is at it's correct setting. If too much preload is applied and the motor is then energized, the Terfenol-D rod will fracture and will no longer function properly.

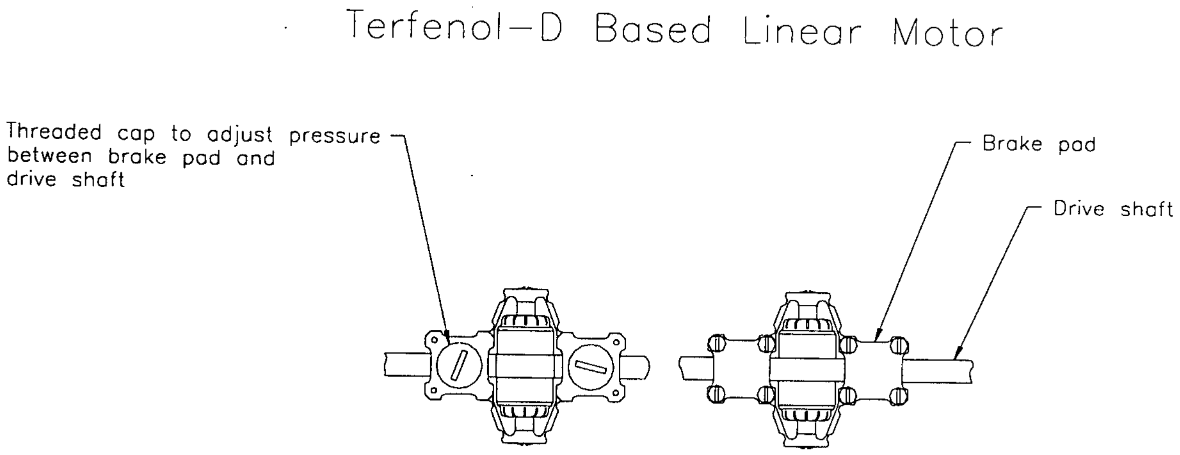
Terfenol-D Based Linear Motor
Threaded cap to adjust pressure between brake pad and drive shaft
Brake pad
Drive shaft

Figure 3: Adjustments on Terfenol-D based linear motor

VIRTUAL JOINT AND ADJUSTABLE FINGER RINGS

There are two adjustments that can be made to the virtual joint and finger rings. Both are on the finger rings and can be seen in Figure 4.

The virtual joint fits into a dovetail slot on top of the finger ring. It can be positioned by sliding it into the desired position and then locking it into place with the set screw located underneith the finger pad. This adjustment can be made without removing the ring and allows for different finger lengths.

The finger ring is adjustable to allow for different finger sizes. The top portion of the ring slides up and down in the adjustment slot and can be locked into place with the adjustment screw located on the side of the ring.

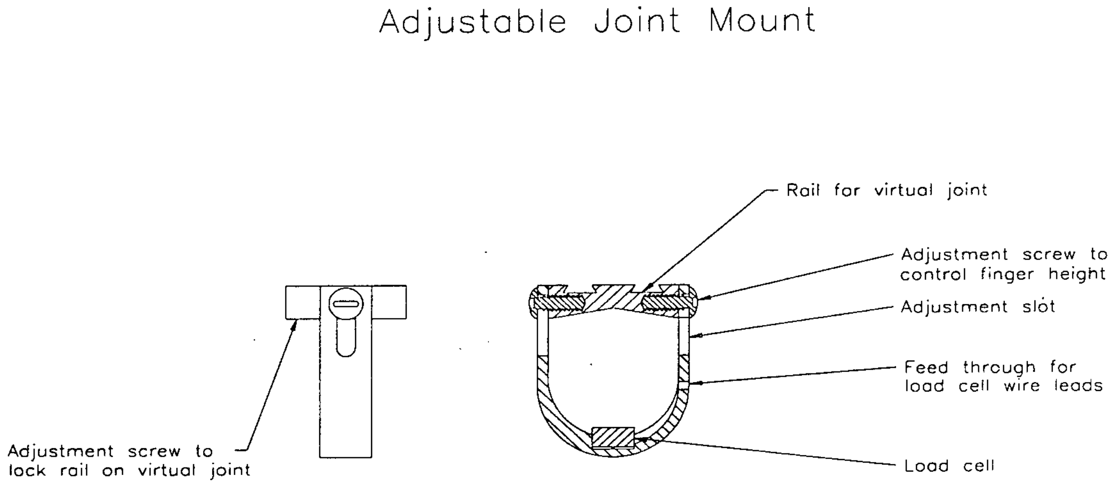
Adjustable Joint Mount
Rail for virtual joint
Adjustment screw to control finger height
Adjustment slot
Feed through for load cell wire leads
Load cell
Adjustment screw to lock rail on virtual joint

Figure 4: Adjustable Finger Joint Ring.

HAND MOUNT

The Force Feedback Handmaster clamps onto the hand and has two adjustments. The first controls the clamping thickness across the hand. This is adjusted by loosening the bolt/nut on the left side (assuming that the hand master is mounted upon the left hand) and adjusting the straps that go around the thumb and hand until the device feels comfortable.

The other adjustment is with the segments that correspond to the metacarpal bones of the hand. These need to be positioned such that the distal end is approximately over the MIP joint COR. This is accomplished by loosening the screw on the proximal end and sliding it into position.

DONNING THE HANDMASTER

It should be noted that the position of the virtual joint COR (center of rotation) relative to the actual COR of the finger is crucial. If the two COR's are not relatively close together, a torque is introduced inside the virtual joint and it significantly increases the friction of the joint. A suggested procedure for mounting the joints are as follows:

1. Place the finger into the adjustable finger rings and grossly position the joints.
2. Position the adjustable finger rings in approximately the middle of the finger segments and adjust them so that they clamp comfortably onto the finger segments.
3. Position the PIP virtual joint first by bending the finger approximatly 90° and positioning the virtual joint's COR over where you think the actual finger COR is.
4. Lock the virtual joint to the finger rings and flex the finger to verify the adjustment.
5. If the COR's are not positioned correctly, unlock the virtual joints and try again. (Minor positioning adjustments may be made to the finger rings and the virtual joints until the most comfortable position is located.)
6. Repeat steps 3-5 with the DIP and MIP joints.
7. Connect the straps around the thumb and tighten them until it feels comfortable.
8. Adjust the position of the segments that correspond to the metacarpal bones such that the distal ends are approximately over the MIP joint COR.

SECTION 5 - TROUBLESHOOTING

MOTORS RUNNING, BUT JOINTS NOT MOVING

The most probable problem is that the drive shaft (ribbon) is loose and needs to be tightened. The drive shaft is sandwiched between the brake pad and the flexure controlling the preload to the Terfenol-D in the brake. The adjustment can be seen in Figure 3.

Care and judgement must be used in adjusting this pressure since this same adjustment controls the preload to the Terfenol-D rod. By design, when the preload is 1000 psi, the pressure on the brake pad is at it's correct setting. If too much preload is applied and the motor is then energized, the Terfenol-D rod will fracture and will no longer function properly.

Another thing to check is the cleanliness of the drive shaft (ribbon). If it is dirty, or has dirt collected under the brake pad, then the motor will not function properly. If this is the problem, then remove the brake pads and carefully clean the underlying surfaces. Before replacing the brake pads, it is a good idea to lightly coat the drive shaft (ribbon) with a light weight lubricating oil.

JOINTS FEEL *STICKY* AND HARD TO MOVE

The problem is probably that the virtual joint COR (center of rotation) is not aligned with the actual finger joint COR. When this happens a torque is generated within the virtual joint and the friction force dramatically increases.

SECTION 6 - PRECAUTIONS

OVER-TIGHTENING OF THE THREADED CAPS

The only thing to be adjusted on the Terfenol-D based linear motor is the brake pad pressure. The drive shaft is sandwiched between the brake pad and the flexure controlling the preload to the Terfenol-D in the brake. The adjustment can be seen in Figure 3.

Care and judgement must be used in adjusting this pressure since this same adjustment controls the preload to the Terfenol-D rod. By design, when the preload is 1000 psi, the pressure on the brake pad is at it's correct setting. If too much preload is applied and the motor is then energized, the Terfenol-D rod will fracture and will no longer function properly.

OVERLOADING THE LOAD CELLS

The load cells are rated at 10 lbs and can be damaged if excessive loads are applied.

SECTION 7 - MAINTENANCE

1. Clean the polarizing film on the angle sensors with a lent free lens cloth.
2. Perodically place a small amount of light weight lubricating oil on drive shaft (ribbon).

☆ U.S. GOVERNMENT PRINTING OFFICE: 1996- 752-150